



**University of
Nottingham**

UK | CHINA | MALAYSIA

Non-equilibrium dynamics of bulk-deterministic cellular automata

Joseph W. P. Wilkinson

Thesis submitted to the University of Nottingham
for the degree of Doctor of Philosophy

**Supervised by Prof. Juan P. Garrahan
and Prof. Igor Lesanovsky**

*To William and Peter, whom without,
this would not have been possible.*

Abstract

In this thesis we study simple one-dimensional nonequilibrium many-body systems, namely, reversible cellular automata (RCA). These are discrete time lattice models exhibiting emergent collective excitations—solitons—that move with fixed velocities and that interact via pairwise scattering. In particular, we study the attractively interacting Rule 201 RCA and noninteracting Rule 150 RCA which, together with the extensively studied repulsively interacting Rule 54 RCA constitute arguably the simplest one-dimensional microscopic physical models of strongly interacting and asymptotically freely propagating particles, to investigate interacting nonequilibrium many-body dynamics.

After a brief literature review of the field, we present the first publication-style chapter which considers the Rule 201 RCA. Here, we study the stationary or steady state properties of systems with periodic, deterministic, and stochastic boundary conditions. We demonstrate that, despite the complexities of the model, specifically, a reducible state space and nontrivial topological vacuum, the model exhibits a simple and intuitive quasiparticle interpretation, reminiscent of the simpler Rule 54 RCA. This enables us to obtain exact expressions for the steady states in terms of a highly versatile matrix product state (MPS) representation that takes an instructive generalized Gibbs ensemble form.

In the second publication-style chapter, we study the Rule 150 RCA. Due to its simplicity, originating from the noninteracting dynamics, we are able to obtain many exact results relating to its dynamics. To start, we generalize the MPS ansatz used to study the Rule 201 RCA, and find its exact steady state distribution for identical boundary conditions. We proceed to extend the MPS ansatz further and obtain a class of eigenvectors that form the dominant decay modes of the Markov propagator. Following this, we postulate a conjecture for the complete spectrum, which is in perfect agreement with numerics obtained via exact diagonalization of computationally tractable system sizes, providing access to the full relaxation dynamics. From here, we further utilise the ansatz to investigate the large deviation statistics and obtain exact expressions for its scaled cumulant generating function and rate function, which demonstrate the existence of a dynamical first order phase transition.

The third and final publication-style chapter focuses on the exact dynamical large deviations statistics of the Rule 201 RCA. Specifically, we employ the methods introduced to study the large deviations of the Rule 54 RCA and show that they fail here to provide any insight into the atypical dynamical behaviour of the Rule 201 RCA. We suggest that this is due to the restrictions imposed by the local dynamical rules, which limits the support of the local observables. In spite of this, we explicitly derived an exact analytic expression for the dominant eigenvalue of the tilted Markov propagator, from which several large deviation statistics can be obtained.

Acknowledgements

Firstly, I would like to express my deepest gratitude and utmost admiration towards my supervisors Juan Garrahan and Igor Lesanovsky, whose unwavering support, insightful guidance, and boundless knowledge over the past four years has been truly invaluable. In the moments when one feels completely lost or utterly overwhelmed by the vastness of academia, their seemingly limitless enthusiasm and wonderfully childlike fascination for physics never failed to remind me of why I love what I do. Their trusting supervision and unyielding faith in my capabilities, no matter how misguided or antithetical to my own beliefs, provided me with the necessary freedoms to learn and develop as an academic, and gave me the confidence and motivation to achieve, what at times, felt impossible. I am truly privileged to have had the opportunity to work with them both.

To all of my collaborators, in particular, Katja Klobas and Tomaž Prosen, I would like to sincerely thank you for all of the illuminating discussions that were had, and perceptive suggestions that were made, during our time working together over the course of my PhD. I look forward to many more interesting conversations in the future.

To the members of the Condensed Matter Theory group here at the University of Nottingham, I thank you for the lunches, coffees, chats, and talks which made the years I spent in the group much more interesting and enjoyable. Most notably, I would like to significantly thank my fellow PhD students, and now close friends, Ellie Frampton, Matt Jessop, Gary McCormack, Ciarán McDonnell, Grace Morley, Jemma Needham, Maike Ostmann, and Dominic Rose for all of their ridiculous humour, unquestionable support, and loving care these past few years. You have made this experience truly unforgettable.

To my lifelong friends beyond the realms of academia, your unending support and peerless encouragement throughout this tumultuous period of my life has been indispensable. I am extremely fortunate to have each and every one of you astonishing people in my life and I cannot thank you all enough for always being there when I needed you most. I want to especially thank my closest friends, Jaime Grant and Ishbel Monckton, and my ex-partner, Elizabeth Harrison. Without your love, I would not be here, so from the bottom of my heart, thank you.

Lastly, I want to thank my entire family for their enduring support over the past four years, particularly, my mother Sarah, my brother Harry, my sisters Pearl and Hannah, my grandfathers William, Peter, and Alan, and my grandmothers Jane and Anne. I cannot articulate how truly appreciative I am of your unconditional love and the immeasurable belief you have always had in me, as it has irrefutably led me to where I am today.

List of Publications

This thesis contains research that has been the subject of several papers either published or in preparation. Here, we list these papers and their corresponding chapters.

Chapter 2

Exact solution of the Floquet-PXP cellular automaton, **J. W. P. Wilkinson**, K. Klobas, T. Prosen, J. P. Garrahan, Phys. Rev. E, **102**, 062107 (2020).

Chapter 3

Exact solution of the “Rule 150” reversible cellular automaton, **J. W. P. Wilkinson**, T. Prosen, J. P. Garrahan, Phys. Rev. E, **105**, 034124 (2022).

Chapter 4

Exact large deviation statistics of ultralocal observables for the boundary driven “Rule 201” reversible cellular automaton, **J. W. P. Wilkinson**, J. P. Garrahan, in preparation.

Contents

| | |
|--|------------|
| Abstract | i |
| Acknowledgements | ii |
| List of Publications | iii |
| 1 Introduction | 1 |
| 1.1 A brief history of statistical mechanics | 2 |
| 1.2 Exactly solvable models | 3 |
| 1.3 Nonequilibrium many-body systems | 6 |
| 1.4 Rule 54 reversible cellular automaton | 8 |
| 1.5 Thesis motivations and outline | 10 |
| 2 Exact nonequilibrium steady state of the Rule 201 RCA | 12 |
| 3 Exact nonequilibrium dynamics and large deviations statistics of the Rule 150 RCA | 13 |
| 4 Exact large deviations statistics of the Rule 201 RCA | 14 |
| 5 Conclusion | 15 |
| Bibliography | 17 |

Chapter 1

Introduction

Equilibrium is a concept ubiquitous in nature which has profound implications in myriad disciplines, including astronomy [1–3], biology [4–8], chemistry [9–12], economics [13–17], geology [18–20], mathematics [21–25], philosophy [26–28], political science [29–31], and sociology [32, 33], as well as numerous fields of physics. Indeed, equilibrium states are of critical importance in physics, since their existence is fundamentally intertwined with the foundational principles of statistical mechanics [34–37]. Specifically, via the postulate of *a priori* probabilities [38, 39] and, more generally, by the principle of maximum entropy [40, 41]. Moreover, understanding such states is expected to have direct implications on technological advancements in a variety of fields, with notable applications in quantum computation, including the efficient storage and transfer of energy and information, leading to the development of revolutionary quantum based technologies [42–44]. It is, therefore, crucial that we understand how to describe these states within physical systems.

Despite its diverse applicability throughout these varied branches of science, equilibrium is unanimously understood as a state of balance between opposing or competing forces, actions, or influences. Equilibrium is, therefore, intimately related to the notion of *time reversibility*, in particular, of the elementary processes governing the time evolution of the system which, from a physical perspective, can be understood in terms of the principle of detailed balance, whose foundations rely on, and are implied by, the principle of microscopic reversibility [45, 46]. For a system to be in an equilibrium state, however, requires macroscopic time reversibility, which is only possible if there is no dissipation or loss of information [47]. Since almost all physical systems found in nature are time irreversible, that is, they are constantly changing in time and are *not* in equilibrium, it is of paramount importance to study systems out of and far from equilibrium. This, therefore, immediately necessitates the definition of a nonequilibrium state, which is instead intrinsically related to the notion of *time irreversibility*, a distinction made explicit by the concept of entropy and the second law of thermodynamics [48].

Naturally, this leads us to ask perhaps one of the most historically relevant questions in statistical mechanics [49, 50], namely, that of *equilibration*; that is, if a system is in some initial state, will it eventually equilibrate, and if so, what are the processes and associated time-scales characterizing this equilibration? In classical systems, one typically invokes heuristic arguments relating

to *ergodicity* and dynamical chaos [51–54]. More precisely, one effectively assumes that the vast majority of microscopic states in the phase space have nearly identical macroscopic properties and so the system is almost surely in, or will go to, a macroscopic state characterized by these properties. Similarly, in (isolated) quantum systems, these concepts regarding relaxation are encapsulated by the *eigenstate thermalization hypothesis* (ETH). The ETH is closely connected to the quantum nature of chaos and the property of quantum ergodicity (i.e., the quantum origins of classical chaos) and relies on key insights of the quantum chaos conjecture, which asserts that in the classical limit, the spectrum of the Hamiltonian of a generic quantum system is distributed randomly and thus behaves as a random matrix [55, 56]. In essence, the ETH states that for an arbitrary initial state, the expectation value of an observable ultimately approaches the value predicted by statistical mechanics (i.e., the microcanonical ensemble), and exhibits only small fluctuations around this value [57–59]. This assumption implicitly relies on two conditions: that the leading contributions originate from the diagonal matrix elements, which vary smoothly as functions of the energy; and that the subleading corrections from the off-diagonal matrix elements are exponentially small in the system size and are distributed randomly. In spite of these remarkably intuitive ideas, obtaining a mathematically rigorous understanding of these processes still remains an exceptionally difficult task.

1.1 A brief history of statistical mechanics

While work towards a proper understanding of equilibration can conceptually be dated back to the 18th and early 19th century, when Euler and Bernoulli introduced the foundations of hydrodynamics [60, 61] and Fourier his law of heat conduction [62], perhaps a more appropriate place to start is with the inception of *statistical mechanics* [34–37]. Initially formulated in the late 19th century, predominantly by the pioneering physicists Maxwell, Gibbs, and Boltzmann [50, 63–66], statistical mechanics was originally introduced as a mathematical framework that applied statistical methods and probability theory to the field of thermodynamics, specifically, the kinetic theory of gases [67–72]. In particular, statistical mechanics was able to explain the physical behaviour of the macroscopic properties of a thermodynamic system, such as its temperature, pressure, and volume, in terms of the microscopic properties of its constituent particles. Using the statistical ensemble formalism, it was shown that the information encoding the probabilistic fluctuations or deviations of these microscopic properties about their mean values, which manifest in terms of the macroscopic properties of the system, could be obtained from the knowledge of only a few fundamental properties, such as the entropy and free energy. This remarkable ability to accurately describe the behaviour of many-body systems, based on the information of only a few key observables is truly profound, and often underappreciated, despite its extensive applicability far beyond classical equilibrium thermodynamics, for example, to quantum mechanical [57, 73–78] and nonequilibrium many-body systems [79–84].

In contrast to the outstanding success of statistical mechanics within the

domain of equilibrium states, in general, much less is known about nonequilibrium states. This is primarily due to the conceptual challenges introduced by the irreversible dynamics, since in nonequilibrium statistical mechanics, one is not only interested in stationary fluctuations, such as those in equilibrium, but also in dynamical fluctuations far from equilibrium. Consequently, a more general theory is necessarily required to describe such processes. Efforts towards obtaining such a mathematical framework were initially made alongside the developments of hydrodynamics [60, 61, 85, 86] and equilibrium statistical mechanics [49, 50, 65], however, perhaps the first notable excursions into the realm of nonequilibrium were those taken to develop the *fluctuation-dissipation relation* [87–89]. Originally introduced in the 1900s by Einstein to explain Brownian motion [90–92] and later in the 1920s by Nyquist to describe Johnson noise [93, 94], these relations quantify the relationship between the response of system to the presence of an external perturbation and the internal fluctuations of the system in the absence of the perturbation [88]. In the 1950s, these results were extended to general dissipative systems by Callen and Welton [95], and were later systematically generalized by Green and Kubo in their seminal papers deriving the Green-Kubo relations [96–98] and the foundations of *linear response theory* [83]. In addition to this progress, substantial developments were made to the theory of nonequilibrium statistical mechanics independently prior to this in the 1930s by Onsager with his groundbreaking papers on irreversible processes which derived the celebrated Onsager reciprocal relations [99–101]. While all of these results offered invaluable insight into the understanding of nonequilibrium states, they were all limited due to the necessary requirement of equilibrium or thermal fluctuations of Gaussian form [102, 103]. Indeed, it was not until the 1990s that a completely general nonequilibrium fluctuation theorem was conjectured, based on numerical evidence, by Evans, Cohen, and Morriss [104] and later rigorously derived by Gallavotti and Cohen [105] (see Ref. [106] for a review). This was explicitly shown to directly imply the aforementioned Green-Kubo fluctuation-dissipation relations [107] and led to the discovery of several fundamentally important relations in statistical mechanical, including the Jarzynski equality [108, 109] and Crooks equation [110].

1.2 Exactly solvable models

In spite of the remarkable progress made in understanding the complex dynamical behaviour of systems far from equilibrium, the question of whether a system will equilibrate, and if so by what means and over what timescales, remains firmly open. To ascertain further insight into how to answer this in full generality, we must necessarily study simpler models. A typical simplification made, that has proven invaluable in providing meaningful quantitative results in many branches of physics, is to consider *one-dimensional* systems [111–113]. The principal benefit of studying such models is that they are dramatically easier to solve due to the exponential decrease in the dimensionality of the state space. Indeed, computationally this allows one to simulate one-dimensional lattice systems of much larger size and, therefore, study quantum

many-body phenomena, albeit in one-dimension, without significant finite size effects. Moreover, since most physically interesting and accessible states (e.g., ground states and lowly excited states of local gapped quantum many-body systems) obey the area law for entanglement [114–116], this implies that the states can be numerically approximated exceptionally well using tensor networks and their dynamical properties can, therefore, be modelled utilising the recently developed efficient tensor network methods and algorithms [117–124].

Notwithstanding the substantial advancements in computational techniques, perhaps the most significant benefit of studying one-dimensional systems, at least from the perspective of a theoretical physicist, is the ability to exactly solve models of interacting many-body systems, often referred to as *integrable systems* [125, 126]. Integrability is a property of dynamical systems that possess a sufficient set of conserved quantities, that is, independent and mutually commuting integrals of motion, such that the dynamical behaviour of the system is completely described by a subset of degrees of freedom of the state space. Interest in integrable systems was revived in the late 1960s with the numerical discovery of strongly stable localized collective excitations, termed *solitons*, in the computational simulation of the Korteweg-de Vries (KdV) equation by Zabusky and Kruskal [127]. This work explained the puzzling earlier work of Fermi, Pasta, Ulam, and Tsingou [128] by arguing that the soliton solutions of the KdV equation, which broke ergodicity, were the origin of the quasiperiodicity in the experiment. This led to the development of the *inverse scattering transform* method by Gardner, Greene, Kruskal, and Muira, which facilitated the derivation of an analytical solution to the Korteweg-de Vries equation [129], and was later extended to exactly solve many other nonlinear partial differential equations, including, the nonlinear Schrödinger equation [130], sine-Gordon equation [131, 132], and Toda lattice [133, 134]. One-dimensional integrable systems were, however, studied earlier in a different context, the most notable example being the renowned Heisenberg spin chain model, originally introduced to study magnetism in quantum many-body systems [135]. The isotropic (XXX) Heisenberg model was exactly solved in the early 1930s by Bethe [136], using the celebrated *Bethe ansatz*, a method which was later used to solve numerous other one-dimensional integrable systems, such as, the anisotropic (XXZ) Heisenberg model [137], the bosonic Lieb-Liniger model [138, 139], and the fermionic Hubbard model [140]. Soon after in the 1960s, seminal work by Yang and Yang generalised many of these prior results using the Bethe ansatz (which is now known as the *coordinate Bethe ansatz*), and most notably, obtained their thermodynamics, providing the basis for the *thermodynamic Bethe ansatz* [141]. Later, in the 1970s, the notion of quantum integrability was formulated in the context of quantum field theories [142] under the powerful framework introduced by Fadeev of the *quantum inverse scattering method* [143–147]. The quantum inverse scattering method arose as a result of the unification of the Bethe ansatz and inverse scattering transform, with the quantization of the Lax representation of the latter allowing the former to be written in a more general form, namely, the *algebraic Bethe ansatz* [148, 149].

A hallmark feature of integrable systems is that they exhibit an extensive number of *conserved quantities*, which is in contrast to generic systems

(i.e., nonintegrable or chaotic systems), that usually only have an intensive number of conserved quantities, such as energy, charge, and particle number. The importance of these conserved quantities cannot be understated, since they characterize the dynamical behaviour of the system, due to the fact that quantities that are not conserved decay rapidly due to collisions and contribute negligibly to the dynamics, even after a short time [150]. Therefore, understanding how these quantities evolve in time is of the utmost significance. A particularly important case is in the limit of infinite time, whereby the state of a generic system is expected to approach a time invariant probability distribution, namely, the stationary or *steady state*. Here, the statistical ensemble describing the probability distribution over the possible states is the Gibbs ensemble [65]. For integrable systems, this notion must be extended to generalized Gibbs ensembles [151–155], which can be intuitively understood as generalizations of the aforementioned Gibbs ensembles, with an extensive, instead of an intensive, number of chemical potential and particle number conjugate pairs associated to the local or quasilocally conserved quantities. Conceptually, this generalization is easy to understand, and indeed, one may be tempted to assume that the question of finding the steady states of integrable systems is answered. However, despite this physical intuition, the exercise of explicitly identifying the operators associated to the conserved quantities is especially nontrivial, and even for the simplest nontrivial interacting integrable quantum many-body systems, the exact formulation of the generalized Gibbs ensembles has only recently been determined [156, 157].

In recent decades, integrable quantum many-body systems have proven an indispensable platform for studying nonequilibrium physics [142, 158–160]. In particular, *quantum quenches* have proven to be an ideal environment for investigating nonequilibrium phenomena, including transport, equilibration, and localization, both in experimental [161–163] and theoretical [164–170] settings. Moreover, the theoretical study of quench protocols, specifically, inhomogeneous quenches [171], led to the development of an effective hydrodynamic theory describing the dynamics of integrable interacting systems, known as *generalized hydrodynamics* (GHD) [172, 173]. As it suggests, GHD is simply a generalization of hydrodynamics, that effectively developed from the crucial realization that extensivity, not chaos, is a sufficient and necessary condition for the emergence of a generic hydrodynamic description, which consequently implied the existence of a hydrodynamic theory for integrable (i.e., non-chaotic) systems. Similarly to hydrodynamics, in GHD the basic physical principle is the assumption of local thermodynamic relaxation, which states that in any given mesoscopic volume or “fluid cell”, one expects that, as a result of local relaxation, the system can be approximated as being in an ergodic state (i.e., a state invariant under time and space translation). By a generalization of the ergodic principle, in the thermodynamic limit, these states are locally described by a GGE characterized by an extensive number of chemical potentials associated to the conserved charges [154, 174, 175]. From this, one can derive continuity equations for the expectation values of the currents of the conserved charges and explicitly evaluate charge and current density profiles in steady states far from equilibrium [176, 177]. It is worth stressing that, much like statistical mechanics, GHD is extremely powerful since it does not

explicitly depend on the specifics of the model under consideration. Rather, it is a universal framework consisting of a set of strictly mathematical techniques that can be applied to nearly any physical system, irrespective of the natural laws or rules that system obeys. As such, the GHD formalism has already been considerably generalized, despite its recent inception (see Ref. [178] for a recent review and references therein, and Ref. [179] for a pedagogical survey).

A slightly older, yet equally (arguably more) powerful framework that has risen to prominence in recent decades is *large deviations theory* (LDT) [180]. Initiated in the 1930s by Cramér [181], and later in the 1970s formulated into a unified theory, predominantly by the pioneering work of Varadhan, Donsker, Freidlin, and Wentzell [182–187], LDT fundamentally concerns itself with the statistics of asymptotic probability distributions. The foundational result of LDT is the so called *large deviation principle* (LDP), which states that in some asymptotic limit the probability distribution of a sequence of random variables can be approximated by a decaying exponential with an exponent determined by a scaled function known as the *rate function*. The significance of this result cannot be understated, particularly with respect to statistical mechanics [180]. Indeed, whilst originally introduced in mathematics, seminal work by Lanford and Ellis [188, 189] (see also the influential reviews by Oono, Ellis, and recently Touchette in Refs. [180, 190–192]) presented LDT as the proper mathematical framework in which problems of statistical mechanics can be formulated and solved efficiently and, if need be, rigorously [180]. Nonetheless, in spite of these profound developments in statistical mechanics, there still exists no completely established or rigorous framework to study nonequilibrium states.

1.3 Nonequilibrium many-body systems

An extensively studied class of nonequilibrium many-body problems are *constrained systems* [193]. These are stochastic models of interacting particles that exhibit constraints within the definitions of either their statics or dynamics. Typical examples of the former class are covering and packing problems, such as fully packed polymer coverings [194–197], where only certain configurations are allowed. Here, the aim is to cover an n -dimensional lattice with k -site particles called polymers in such a way that some quantity, typically the energy, is extremalized subject to certain constraints, such as that the lattice must be perfectly covered (i.e., every site is covered by exactly one polymer). In the latter class, the paradigmatic examples are *kinetically constrained models* (KCM) [198–215], which are systems whose dynamical rules are such that transitions between configurations occur with rates determined by a certain local condition, namely, the kinetic constraint. KCM were originally introduced in the 1960s to model the slow cooperative relaxation dynamics of classical glasses and study the glass transition problem (see [214] for a recent review and references therein), however, have since been generalized to address a variety of problems in nonequilibrium physics, including transport decoupling phenomena near critical points [216], slow relaxation and many-body localization of nonthermal systems [217, 218], atypical thermalization and quantum many-body scars [219–221], and ergodicity breaking phase transitions [222].

Simplistically, KCM can be understood as interacting particle systems (IPS) with explicit constraints in the definitions of their dynamics [52]. These systems are of interest due to the fact that they often exhibit unexpected complex dynamical behaviour at the macroscopic scale, despite possessing usually trivial microscopic dynamical rules. Generally speaking, KCM are either conservative or nonconservative (see, e.g., Ref. [212]). The former class are often modelled as lattice gases, with binary degrees of freedom corresponding to occupation functions on each site of the lattice, with dynamical rules that conserve the total occupation number of the system. The paradigmatic example is the widely studied class of nonequilibrium models known as *exclusion processes* (see Ref. [223] for a review): stochastic models of particles that hop between sites of a one-dimensional lattice, which are generally considered default models for studying transport phenomena. In all of these models, each site is either “empty” or “occupied” by a particle, which can jump to a neighbouring site with some probability if and only if that site is “empty”. Of particular note is the *asymmetric simple exclusion process*, first introduced in a physical context in the 1970s [51] and later generalized and extensively studied throughout the 1990s, which was of significant interest due to its solvability that facilitated the derivation of numerous important exact results [223–233]. In the latter class, namely, nonconservative KCM, the underlying conservation laws that restrict the dynamics are relaxed. Here, the dominant family of models are those of the Fredrickson-Andersen (FA) kind [234–237], often referred to more generally as *facilitated spin models* (see Ref. [212] and references therein), since the motion of sites is facilitated by neighbouring sites that are often interpreted as spins. The quintessential example is the “one-spin facilitated” FA model [198] for which the state of a site changes if any of its nearest neighbours are occupied.

The dynamics of KCM when studying glassy systems are described by continuous time Markov processes consisting of a sequence of constrained particle jumps or facilitated spin flips. That is, KCM are simple lattice models for studying *continuous time* stochastic and deterministic processes. For many problems in nonequilibrium many-body physics, however, it is often beneficial and sometimes necessary to consider *discrete time* processes due to the simplifications that they provide (see, e.g., Refs. [125, 126, 214]), including classical systems exhibiting complex cooperative dynamical behaviour, for which the discrete counterparts to KCM and, more generally, IPS are known as *cellular automata* (CA). CA were initially conceptualized by Ulam and von Neumann in the 1940s [238, 239], however, were not studied broadly until later in the 1970s with the inception of Conway’s Game of Life [240, 241]. In the 1980s, CA were rigorously formalized by the mathematical and computer science communities [242], most notably by Wolfram in his formative papers that systematically studied and completely classified *elementary cellular automata* [243–245]. These are classical one-dimensional two-state lattice systems with discrete time evolution governed by a deterministic local update rule, whereby the updated state of the site depends only on the current states of the site and its adjacent sites.

A closely related and intimately connected class of models to CA are systems with *circuit dynamics*. These are systems with dynamics defined on a discrete lattice in terms of “gates” corresponding to commuting local maps ap-

plied synchronously or periodically throughout the system. As such, they can be understood as a subclass of CA with global dynamics implemented by local gates in a circuit-like manner. Recently, systems with circuit dynamics have proven to be minimal sufficient tractable models for analysing nonequilibrium many-body phenomena, which are particularly difficult to analytically decipher using conventional mathematical and theoretical techniques [246–260], with notable examples being random and dual-unitary circuits. In quantum many-body physics, often one considers one-dimensional systems referred to as either “brickwork” *quantum circuits* or *Floquet systems*, due to the periodicity of the discrete dynamics where the local gates correspond to unitary transformations with finite support. Such periodically driven time-dependent systems can be straightforwardly understood as Suzuki-Trotter approximations [261–270] of one-dimensional continuous time spin chain models [271–274]. Indeed, systems with “Trotterized” time evolution are, in fact, veritable discrete time dynamical models, namely, *quantum cellular automata* [275–286]. Formally, quantum CA can be understood as quantum analogs to CA, which are generically classical, that is, with the state space and time evolution motivated by the principles of quantum mechanics. Brickwork quantum circuits then constitute a subclass of these quantum CA, whereby the global dynamics is performed by the periodic and staggered application of the local unitary gates (see, for example, Ref. [257] for a detail description).

In the past decade, both classical and quantum CA have garnered considerable interest due to their experimental realization, made possible by the significant technological advancements in the simulation and manipulation of microscopic systems [287–296]. This was predominantly driven by the recent generation of quantum simulators [297–302], based on gases of highly-excited, strongly-interacting Rydberg atoms [303–310]. Moreover, CA have gained significant interest in the mathematical and physical communities due to their applicability as idealized theoretical models to answer questions in quantum many-body and nonequilibrium physics. In particular, with respect to relaxation [218, 311–313], strong interactions [314], localization [217, 315, 316], entanglement growth [317–320], operator spreading [321–324], nonthermal eigenstates [220, 325, 326], nonergodicity [219, 327], chaos [253, 257, 328], and integrability [329–332].

1.4 Rule 54 reversible cellular automaton

In recent years, one model in particular, that relates to all the aforementioned fields of research, has attracted considerable research interest, specifically, the *Rule 54 reversible cellular automaton* (RCA54). Initially proposed in the 1990s by Bobenko [333], RCA54 is a discrete one-dimensional two-state lattice system that exhibits emergent interacting particle-like excitations, which can arguably be considered the simplest theoretical model to study interacting nonequilibrium many-body dynamics (for a review, see Ref. [334]). Interest in the model was revived recently by Prosen, who with Mejía-Monasterio obtained the exact NESS of the system with stochastic boundaries [335], and later reformulated it with Buča in terms of an MPS, which was generalized to richer boundaries to

facilitate the finding of the leading decay modes [336]. In the following years, many exact results were obtained for the classical model:

- Inoue *et al.* [337] found the exact NESS for completely general stochastic boundaries and realized the model was equivalent to the CA encoded ERCA250R of Takesue’s classification.
- Buča *et al.* [338] further generalized the MPS and derived methods to obtain the exact dynamical large deviation statistics and demonstrated that the dynamics occurs at the point of phase coexistence between competing active and inactive dynamical phases.
- Klobas *et al.* [339] constructed the exact time-dependent MPS representation for the time evolution of local observables, thus allowing the explicit transport properties of the model to be studied.
- Klobas *et al.* [340, 341] introduced a novel method to study the spatial evolution of so called “time states” and found an efficient way to encode multi-time correlation functions of local observables using MPS.
- Klobas *et al.* [342] extended the model to include multiple particle species and found explicit closed-form expressions for local conserved charges and provide an exact MPS form for the Gibbs state.

At a similar time the model was independently studied by Gopalakrishnan [318] in a quantum setting as a simple example of an interacting integrable model of quantum dynamics. Here, it was realized that RCA54 was equivalent to a discrete time deterministic version of the FA model, hence it is often referred to as the “one-spin facilitated” FA model or OR-FA model, since its update is exactly the logical OR function [198]. Soon after, several other exact results for the quantum model followed:

- Gopalakrishnan *et al.* [278] introduced a hydrodynamic description which allowed them to study the spreading of operators through the ballistic propagation of quasiparticles.
- Friedman *et al.* [329] generalized the model into a fully quantum interacting integrable Floquet model featuring emergent quasiparticle excitations by incorporating a Hamiltonian dispersion term and showed that it could be exactly diagonalized with the Bethe ansatz. The generalized thermodynamics and hydrodynamics then followed.
- Alba *et al.* [323, 324] studied operator entanglement via the time evolution of local quantum observables and provide an analytical upper bound on the rate of operator spreading for all local operators.
- Klobas *et al.* [312] investigated the nonequilibrium dynamics and derived the exact microscopic thermalization dynamics for a class of weakly entangled initial states via an analytic description of the global time evolution within finite subsystems.

- Gombor *et al.* [331] related classical and quantum CA to medium-range Hamiltonian models, and rigorously proved the Yang-Baxter integrability of various reversible CA, thus making important progress in strictly proving the integrability of RCA54.
- Klobas *et al.* [313] demonstrated, via inhomogeneous quantum quenches, that finite subsystems close to the boundary between the semi-infinite system halves relax to the NESS, namely the GGE, predicted by GHD.
- Klobas *et al.* [320] studied the entanglement dynamics generated by quantum quenches and derived exact expressions describing the asymptotic linear growth of all Rényi entropies in the thermodynamic limit.
- Lopez-Piqueres *et al.* [343] extended the generality of the model by introducing integrability-breaking perturbations that allowed for quasiparticle backscattering and subsequently analyzed the systems thermalization and diffusive hydrodynamics.

1.5 Thesis motivations and outline

The vast insight gained from studying reversible CA, particularly RCA54, has been astounding. However, with the naive ambition of attaining an overarching theoretical framework for nonequilibrium statistical mechanics, one would like to do better, or more precisely, be more general. This is exactly the motivation behind the work presented here; we propose two complementary reversible CA, specifically, the *Rule 150 reversible cellular automata* (RCA150) [344] and *Rule 201 reversible cellular automata* (RCA201) [345] which respectively correspond to non-interacting and attractively-interacting counterparts to the repulsively-interacting RCA54.

The research presented in this thesis, in the form of three publication-style chapters, contains results from two published papers [344, 345] and one paper in preparation. In light of the pedagogical formulations of these manuscripts, we forgo an unnecessary theoretical background chapter to introduce the models, and instead refer the readers directly to the aforementioned papers, which can be found in Chapters 2 and 3, respectively. The thesis is outlined as follows.

In [Chapter 2](#) we derive the steady states of RCA201 [345]. In particular, we generalize the mathematical techniques used to obtain the MPS via the so called *patch state ansatz* (PSA) and subsequently obtain an exact formulation for the NESS. Moreover, we discuss, in detail, the additional complications of the Rule 201 reversible cellular automaton, namely, the nontrivial topological structure of the vacuum on which the emergent quasiparticle excitations move and the fragmentation of the state space into kinetically constrained subspaces disconnected by the dynamics. Finally, we identify the local conserved charges and formulate the models partition function, which takes the form of a GGE.

[Chapter 3](#) is devoted to the noninteracting RCA150 [344] and consists of three key results. In the first main section, we similarly obtain the exact MPS representation of the NESS, via the PSA method introduced in Ref. [335] and generalized in Ref. [345]. We demonstrate that it likewise exhibits an intuitive generalized Gibbs form and identify the complete set of local conserved charges

corresponding to localized groups of noninteracting quasiparticles of the same species. In the second section, we employ the generalized ansatz presented in Ref. [336] and obtain explicit expressions for the decay modes. Furthermore, we present a conjecture for the complete spectrum of the Markov propagator (we confirm this numerically for computationally tractable system sizes and check it holds analytically by a simple counting procedure) and utilise to investigate the relaxation dynamics in the thermodynamic limit. Finally, in the third key section, we present the exact large deviation statistics, using the ansatz that was introduced in Ref. [338], via an explicit analytical formulation of the scaled cumulant generating function in terms of an MPS. We proceed to demonstrate that RCA150, like RCA54, exhibits a *dynamical first order phase transition*, but in contrast between two dynamically active phases, and additionally derive exact expressions for the first few cumulants.

The final publication-style chapter, **Chapter 4** deals with the large deviations of RCA201. We open the chapter by formally introducing the model and discuss, in detail, its dynamical properties and statistically important features. Following this, we expound on the construction of the MPS formulation of the NESS, which generalizes the analysis studied in Ref. [345] to richer boundaries, and is essential for the derivation of the exact large deviation statistics. From here, we proceed to the calculation of the main result of this chapter, explicitly, the dominant eigenvalue of the tilted propagator. We demonstrate that, due to the restrictions imposed by the ultralocal dynamics on the support of the local extensive observables, the current formulation of the theoretical methods used to extract the exact large deviation statistics, only facilitates a simple solution for the dominant eigenvalue and thus scaled cumulant generating function, that takes a linear response form. Despite this, we show that the corresponding dominant eigenvector displays an inhomogeneous generalized Gibbs form, in contrast to the homogeneous Gibbs form of the NESS.

In **Chapter 5**, we summarize our work and give some closing remarks and outlook for future research.

Chapter 2

Exact nonequilibrium steady state of the Rule 201 RCA

Exact solution of the Floquet-PXP cellular automatonJoseph W. P. Wilkinson ^{1,2,*},[†] Katja Klobas ^{3,*}, Tomaž Prosen,³ and Juan P. Garrahan^{1,2}¹*School of Physics and Astronomy, University of Nottingham, Nottingham NG7 2RD, United Kingdom*²*Centre for the Mathematics and Theoretical Physics of Quantum Non-equilibrium Systems, University of Nottingham, Nottingham NG7 2RD, United Kingdom*³*Department of Physics, Faculty of Mathematics and Physics, University of Ljubljana, SI-1000 Ljubljana, Slovenia*

(Received 8 July 2020; revised 28 October 2020; accepted 30 October 2020; published 3 December 2020)

We study the dynamics of a bulk deterministic Floquet model, the Rule 201 synchronous one-dimensional reversible cellular automaton (RCA201). The system corresponds to a deterministic, reversible, and discrete version of the PXP model, whereby a site flips only if both its nearest neighbors are unexcited. We show that the RCA201 (Floquet-PXP) model exhibits ballistic propagation of interacting quasiparticles—or solitons—corresponding to the domain walls between nontrivial threefold vacuum states. Starting from the quasiparticle picture, we find the exact matrix product state form of the nonequilibrium stationary state for a range of boundary conditions, including both periodic and stochastic. We discuss further implications of the integrability of the model.

DOI: [10.1103/PhysRevE.102.062107](https://doi.org/10.1103/PhysRevE.102.062107)**I. INTRODUCTION**

In this paper we study the dynamics of a deterministic reversible cellular automaton (RCA), the rule 201 RCA in the classification of Ref. [1] or alternatively the “Floquet-PXP” model (named so for reasons explained below). This is a lattice system with dynamics subject to a local kinetic constraint, whose evolution is defined in terms of a local update rule which can be coded in terms of a periodic circuit and that we show to be exactly solvable. We do this by constructing an algebraic cancellation structure which demonstrates the model’s integrability. This is therefore a problem that relates to three distinct areas of current research in condensed matter theory and statistical mechanics, namely, constrained dynamics, “Floquet” systems, and integrability.

Constrained systems are of interest because they often display rich collective behavior, most notably in their dynamics. Such systems have explicit constraints either in the definition of their state spaces or in their dynamical rules. A typical example of the latter class are fully packed dimer coverings of a lattice [2–5] where only certain configurations are allowed (i.e., those with no-overlapping dimers and no uncovered sites). Among the former class are kinetically constrained models (KCMs) [6–10], systems where dynamical rules are such that configurational changes can only occur if a certain local condition—the kinetic constraint—is satisfied. KCMs were originally introduced to model the slow cooperative dynamics of classical glasses (see, e.g., [9–11] for reviews). More recently they have been generalized to address questions in quantum nonequilibrium physics, including slow relaxation in the absence of disorder [12,13], as an effective description of strongly interacting

Rydberg atoms [14], and as systems displaying nonthermal eigenstates [15,16].

In systems like dimer coverings, transitions are only possible within the constrained space of states, implying constraints in the dynamics. Conversely, if in a KCM the kinetic constraint is strong enough, then a configurational subspace may become dynamically disconnected, thus becoming in effect a system with a constrained state space. The RCA201 (Floquet-PXP) model we consider here is of this kind: Dynamical rules imply the existence of certain locally conserved quantities, breaking the state space into constrained subspaces disconnected by the dynamics. In stochastic systems this is referred to as reducibility of the dynamics [9], a concept distinct from nonergodicity which corresponds to the inability to forget initial conditions in finite time within a connected component.

The second area of interest that our paper connects to are (brick-wall-like) circuit systems. By this we mean systems with space-time discrete dynamics defined in terms of local gates applied synchronously throughout the system. The set of all of these gates in space and over time forms the “circuit”. This has become a much studied problem in quantum many-body physics, where the gates correspond to unitary (or unitary and dissipative) transformations. Quantum circuits provide tractable models to study questions of entanglement, chaos, operator spreading, and localization [17–25]. Furthermore, when the sequence of applied gates is repeated periodically we refer to those as Floquet systems. The circuit platform is not only useful in unitary quantum many-body framework but also in classical deterministic systems of continuous [26] or discrete variables (RCAs) [27]. Moreover, so-called duality symmetries under the swap of space and time axes allow for remarkable advancements in analytic tractability [20,26,27].

Classically, the prototypical circuit models are cellular automata (CA) [28,29]. CAs can be both deterministic and

*These authors contributed equally to this work.

[†]Corresponding author: joseph.wilkinson@nottingham.ac.uk

stochastic. If deterministic, then they can either be reversible or not, where the former (RCA [1], see also Ref. [30]) can be considered as a model of classical many-body Hamiltonian (or symplectic) dynamics. The RCA201 (Floquet-PXP) is a deterministic RCA, closely related to the now much studied RCA54 (Floquet-FA) [27,31–41]. Just like the RCA54, the RCA201 (see detailed definitions below) is a one-dimensional lattice of binary variables with local three-site gates applied simultaneously to two halves (of even or odd indexed sites) of the lattice in two successive time steps. The repeated application of these makes the system a Floquet one. The local gate implements the kinetic constraint in this context. In the case of RCA54, the condition for a site to flip is identical to that of the classical Fredrickson-Andersen (FA) KCM [6,9,11]. For this reason RCA54 is sometimes called Floquet-FA [35–37]. In the case of RCA201, the local condition for spin flips coincides with that of the PXP model [14,15,42]. For this reason we call the RCA201 the Floquet-PXP model.

The third area to which our work here connects is that of integrable systems [43–45]. In particular, the RCA54 (Floquet-FA) was shown to be integrable [1,31], with elementary excitations corresponding to interacting localized quasiparticles (also referred to as *solitons* in our context). From this observation many results followed: the exact matrix product state (MPS) form of the steady-state distribution in the presence of stochastic reservoirs [31,32], the dominant decay modes [33], the exact large deviation statistics of dynamical observables [34], the explicit MPS representation of the complete time evolution of local observables [38], and the exact MPS representation of multitime correlations [39]. In this sense, the RCA54 is essentially a completely solved model, despite the fact that a highly versatile cubic algebraic cancellation mechanism put forward in Ref. [33] has not (yet) been related to more standard Yang-Baxter integrability structures. Here we show that the RCA201 (Floquet-PXP) is also integrable in the same sense as RCA54 and propose the corresponding algebraic cancellation scheme. There is, however, a remarkable difference, namely RCA201 has a topological structure of multiple vacua, and quasiparticles (connecting distinct vacuum states) which interact attractively (rather than repulsively as in the RCA54). As for the RCA54, our construction allows us to obtain a number of results for RCA201 (Floquet-PXP), like the exact MPS solution of its nonequilibrium stationary state (NESS) in a range of boundary conditions that we present here.

The paper is organized as follows. In Sec. II we introduce the model, discuss its kinematics and basic dynamics, in particular the definition of conserved quasiparticles. In Sec. III we consider dynamics under periodic boundary conditions, that is, when evolution is completely deterministic. The main result of that section is the exact NESS, in the form of a Gibbs state over the numbers of quasiparticles represented as an MPS. In Sec. IV we consider the case of stochastic boundaries, which can be obtained as a reduction of the periodic boundary case, and compute the exact MPS form of the corresponding NESS. In Sec. V we provide our conclusion and an outlook of future work.

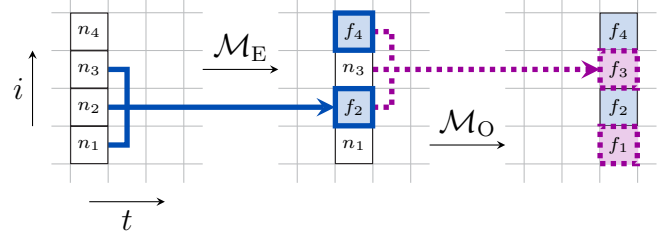


FIG. 1. Dynamical scheme. Evolution of four sites of the lattice under a full time step (i.e., consecutive even and odd time steps) of the deterministic dynamics. During the first time step, only the even sites are updated by the map \mathcal{M}_E whose action is denoted by blue (solid). Alternatively, in the second time step only odd sites are updated by \mathcal{M}_O , denoted by purple (dotted).

II. FLOQUET-PXP MODEL

A. Definition of the dynamics

We consider a system defined on a chain of even size N of binary variables $n_i \in \{0, 1\}$ on sites $i \in \{1, \dots, N\}$ which we refer to as being either *empty* or *occupied*. At discrete time t , the system is characterized by a configuration that we represent by a binary string,

$$\underline{n}^t \equiv (n_1^t, n_2^t, \dots, n_N^t) \in \{0, 1\}^{\times N}. \quad (1)$$

The site i at time t is referred to as empty (or unexcited) if $n_i^t = 0$ and occupied (or excited) if $n_i^t = 1$.

The dynamics of the system consists of two distinct time steps. In the first time step, $\underline{n}^t \rightarrow \underline{n}^{t+1}$, only the sites with even index are acted on by the local update rule (i.e., sites with odd index are left unchanged, that is, $n_{i+1}^{t+1} = n_{i+1}^t$ for even i). In contrast, during the second time step, $\underline{n}^{t+1} \rightarrow \underline{n}^{t+2}$, only the odd sites are updated and the even sites are left unchanged, $n_i^{t+2} = n_i^{t+1}$ for i even. This staggered dynamics is generated by the discrete space-time mapping,

$$\underline{n}^{t+1} = \begin{cases} \mathcal{M}_E(\underline{n}^t), & t = 0 \pmod{2}, \\ \mathcal{M}_O(\underline{n}^t), & t = 1 \pmod{2}, \end{cases} \quad (2)$$

where \mathcal{M}_E and \mathcal{M}_O are maps defined by local updates,

$$n_i^{t+1} = \begin{cases} f_i^t, & i+t = 0 \pmod{2}, \\ n_i^t, & i+t = 1 \pmod{2}, \end{cases} \quad (3)$$

with the shorthand notation,

$$f_i^t \equiv f(n_{i-1}^t, n_i^t, n_{i+1}^t), \quad (4)$$

denoting a local three-site update rule (or *gate*) acting on site i . One full step of time evolution (i.e., two consecutive time steps, $t \rightarrow t+2$) is then defined to be the successive application of the even and odd maps, \mathcal{M}_E and \mathcal{M}_O , respectively [see Eq. (2)],

$$\mathcal{M}(\underline{n}^t) \equiv \mathcal{M}_O(\mathcal{M}_E(\underline{n}^t)) = \underline{n}^{t+2}. \quad (5)$$

As the map \mathcal{M} is applied periodically, we call this a Floquet dynamics. A schematic representation of the discrete time evolution (5) is presented in Fig. 1.

In the bulk, $i \in \{2, \dots, N-1\}$, the discrete dynamics is given by the deterministic RCA rule 201 (RCA201)

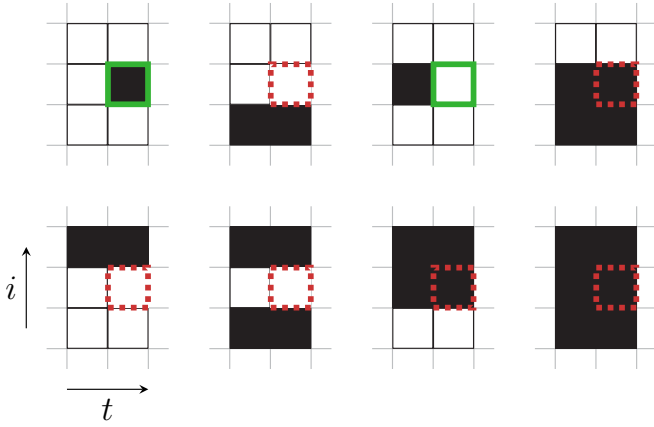


FIG. 2. Rule 201. Illustration of the action of the local gates implementing the deterministic RCA201 function (6). The white and black squares represent empty and occupied sites, respectively. In each of the diagrams, only the central site is updated; green (solid) and red (dotted) borders indicate whether the site has changed or not under the gate action.

function [1],

$$f_i^t = 1 + n_{i-1}^t + n_i^t + n_{i+1}^t + n_{i-1}^t n_{i+1}^t \pmod{2}. \quad (6)$$

A diagrammatic illustration of this local update rule is depicted in Fig. 2. This update rule can be thought of as a kinetic constraint: site i can only flip if both its nearest neighbors are empty (and it does so deterministically). In the KCM jargon it corresponds to the constraint of the “two-spin facilitated” Fredrickson-Andersen model [9]. This constraint is the same as that of the kinetic energy in the PXP model [14,15,42], and from it follows the alternative name of the RCA201 model.

Here and in the next section we will assume that the whole system is closed, of even size N , and has periodic boundary conditions (PBC). In later sections we generalize to other kinds of boundaries. PBC are imposed in the usual manner by identifying a pair of sites $n_0 \equiv n_N$ and $n_{N+1} \equiv n_1$. The dynamics for the sites at the left and right boundaries, $i \in \{1, N\}$, is then given by boundary functions equivalent to the RCA201 function (6),

$$f_1^t \equiv f(n_N^t, n_1^t, n_2^t), \quad f_N^t \equiv f(n_{N-1}^t, n_N^t, n_1^t). \quad (7)$$

B. Structure of the configuration space

The local dynamics generated by the RCA201 function (6) imposes a constraint on the system that derives from the spatial localization (immobility) of adjacent occupied sites within configurations, $\underline{n} = (\dots, 1, 1, \dots)$. Such pairs of excited sites are invariant under time evolution, as illustrated in Fig. 3. The kinetic constraint therefore makes the set of configurations $\mathbb{N} = \{0, 1\}^{\times N}$ reducible under the dynamics, that is, it becomes partitioned into disjoint subsets, or irreducible components, spanned by distinct subsets of dynamically connected configurations identified by the positions of pairs of adjacent occupied sites. The largest of these subsets, denoted by \mathbb{N}_0 , contains the configuration $\underline{n} = (0, 0, \dots, 0, 0)$ and is the unique subset of configurations that contain no adjacent occupied sites.

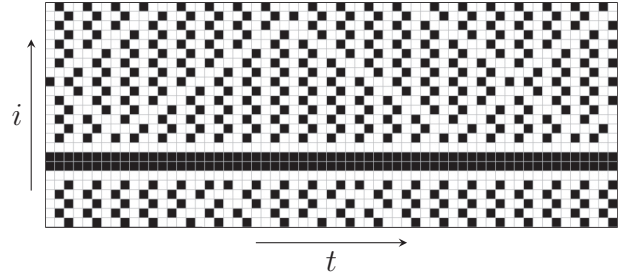


FIG. 3. RCA201 (Floquet-PXP) trajectory. A trajectory of the model with PBC illustrating the spatial localization of pairs of excited sites where only configurations at full time steps are shown (i.e., $\underline{n}^0, \underline{n}^2, \underline{n}^4, \dots$). In this trajectory there are two solitons that change direction under reflection with the localized pair (see Sec. IID for details on soliton reflection). Note also the distinct cycles of the vacua motifs. In the remainder of the paper we focus on the configurational sector with no pairs of excited neighbors.

It is straightforward to see that the cardinality of this subset grows exponentially according to a Fibonacci-like sequence known as the *Lucas sequence*,

$$|\mathbb{N}_0(N)| = L_N \sim \varphi^N, \quad (8)$$

where L_N is the N th Lucas number, defined by the recursion relation $L_N = L_{N-1} + L_{N-2}$ with $L_1 = 1$, $L_2 = 3$, and where $\varphi = (1 + \sqrt{5})/2$ is the golden ratio. To see this we first consider the set of configurations, denoted here by \mathbb{N}'_0 , of a *nonperiodic* system of size N with no adjacent occupied sites. Every configuration in this system with $n_N = 0$ can be obtained by appending 0 to the end of every configuration of a system with $N - 1$ sites, while every configuration with $n_N = 1$ can be obtained by appending 01 to the end of every configuration of a system with $N - 2$ sites. As such, the cardinality of the set \mathbb{N}'_0 satisfies the linear recursion relation

$$|\mathbb{N}'_0(N)| = |\mathbb{N}'_0(N-1)| + |\mathbb{N}'_0(N-2)|, \quad (9)$$

with $|\mathbb{N}'_0(1)| = 2$ and $|\mathbb{N}'_0(2)| = 3$. This is, of course, the celebrated Fibonacci recursion relation, and so we have

$$|\mathbb{N}'_0(N)| = F_{N+2}, \quad N > 0, \quad (10)$$

with F_N the N th Fibonacci number, defined by the relation $F_N = F_{N-1} + F_{N-2}$ with $F_1 = 1$ and $F_2 = 1$.

We now impose PBC on the system which equates to eliminating all configurations with $n_1 = n_N = 1$. This yields a set, denoted by \mathbb{N}_0 , whose cardinality is given by

$$|\mathbb{N}_0(N)| = |\mathbb{N}'_0(N)| - |\mathbb{N}'_0(N-4)|, \quad (11)$$

with $|\mathbb{N}_0(1)| = 1$ and $|\mathbb{N}_0(2)| = 3$. By substituting in the result from Eq. (10) and subsequently using the fundamental equation relating Fibonacci and Lucas numbers,

$$L_N = F_{N+1} + F_{N-1}, \quad (12)$$

it is trivial to see that this is exactly the Lucas recursion relation provided, $|\mathbb{N}_0(N)| = L_N$, $N > 0$. For simplicity, we shall focus the majority of our discussion on this subspace spanned by states with PBC whose configurations contain no adjacent occupied sites.

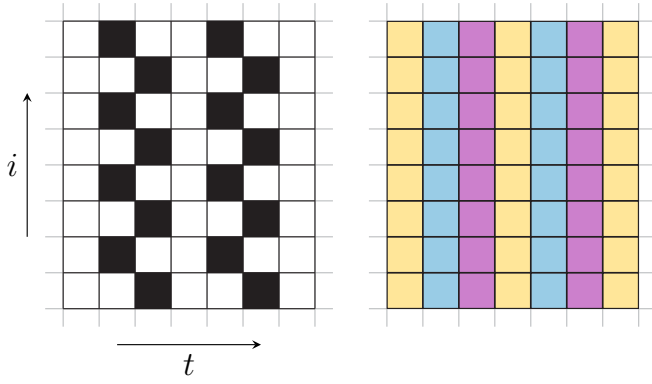


FIG. 4. Vacuum configurations. The three vacuum states are given by the spatial repetition of the motifs composed of all 0s, of alternating 0s and 1s with 1s on even sites, and alternating 0s and 1s with 1s on odd sites. In the absence of solitons, under the dynamics the three vacua repeat periodically with period three. In the panel on the right we represent the three vacuum states in orange (light gray) for the all 0s, blue (medium gray) for the 01s, and purple (dark gray) for the 10s, respectively.

C. Ballistic propagation of nontrivially interacting quasiparticles

The physical interpretation of the dynamics in the subspace with no adjacent occupied sites, induced by the deterministic RCA201 function (6), can be intuitively understood in terms of the ballistic propagation of interacting quasiparticles representing collective excitations on a nontrivial vacuum. Specifically, the vacuum is defined as a cycle of three distinct motifs, respectively composed of repeating 0s, alternating 0s and 1s (starting and ending with 0s on odd sites), and alternating 1s and 0s (starting and ending with 0s on even sites), as illustrated in Fig. 4. Indeed, it can be easily demonstrated that the configurations composed entirely of repeating these three distinct arrangements form a unique, invariant trajectory, which we refer to as the *vacuum* trajectory,

$$\begin{aligned} (0, 0, 0, 0, \dots, 0, 0) &\rightarrow (0, 1, 0, 1, \dots, 0, 1) \rightarrow \\ (1, 0, 1, 0, \dots, 1, 0) &\rightarrow (0, 0, 0, 0, \dots, 0, 0). \end{aligned} \quad (13)$$

Note that when presenting trajectories (e.g., Figs. 3–8) we only show configurations at *full time steps* (i.e., after the successive application of both the even and odd maps) such that, from left to right, the columns of the lattices correspond to the configurations $\underline{n}^t, \underline{n}^{t+2}, \underline{n}^{t+4}, \dots$, for t even.

The quasiparticles, pairs of adjacent empty sites at the interfaces between vacua, propagate with an effective velocity of $\pm \frac{1}{3}$ and interact via a scattering process which effectively triples their velocity to ± 1 for one time step (see Fig. 5). To distinguish the quasiparticles, we refer to them as either *positive* or *negative* depending on the sign of their velocity and denote their number within a configuration by the tuple,

$$Q_n \equiv (Q_n^+, Q_n^-), \quad (14)$$

where Q_n^\pm denotes the number of positive and negative quasiparticles, respectively, in the configuration \underline{n} .

The quasiparticles can be detected diagrammatically by observing four consecutive sites of the lattice. If the binary

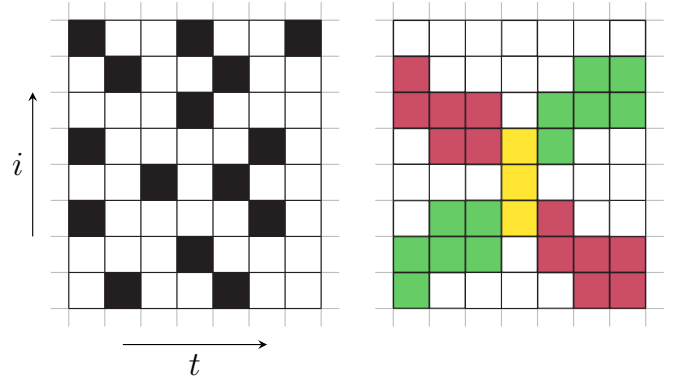


FIG. 5. Interacting quasiparticles. A fragment of a trajectory depicting the ballistic propagation and nontrivial interaction of opposing quasiparticles. On the right, green (medium gray) and red (dark gray) represent the locations of the positive and negative solitons, respectively, that is, they indicate the sites that straddle domain walls between distinct vacua (white). The collision is coloured in yellow (light gray). Notice the transient speeding up of both solitons, which emerge from the collision further away from their original trajectories.

string of these four adjacent sites reads either (0, 0, 0, 1), (1, 0, 0, 0), or (1, 0, 0, 1), then a quasiparticle is present, as succinctly detailed by the following tables:

$$\begin{array}{c|c|c|c||c} e & o & e & o & - \\ \hline 0 & 0 & 0 & 1 & - \\ 1 & 0 & 0 & 0 & - \\ 1 & 0 & 0 & 1 & + \end{array}, \quad \begin{array}{c|c|c|c||c} o & e & o & e & + \\ \hline 0 & 0 & 0 & 1 & + \\ 1 & 0 & 0 & 0 & + \\ 1 & 0 & 0 & 1 & - \end{array}, \quad (15)$$

where e or o denotes whether the adjacent sites indices are even or odd and + or – whether the quasiparticle present is positive or negative. Note that these tables are only associated with detecting quasiparticles on t even time steps. The corresponding tables for t odd time steps can be obtained by exchanging the quasiparticles, i.e., $+ \leftrightarrow -$. The quasiparticles can equivalently be identified by observing pairs of adjacent sites at the interfaces between vacua.

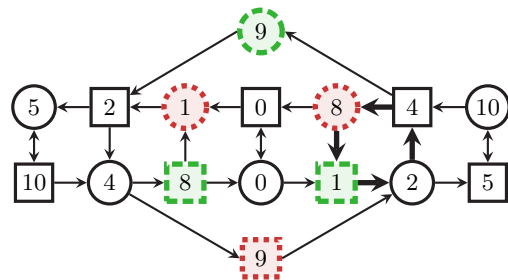


FIG. 6. Quasiparticle number constraint. Graph representation of the lattice illustrating the constraint (16) on the number of quasiparticles where, for readability, binary strings have been replaced by decimal integers [e.g., (0, 0, 1, 0) \equiv 2]. Vertices whose labels start on even and odd sites are represented by circles and squares with those denoting positive and negative quasiparticles in green (dashed) and red (dotted), respectively. Black arrows then denote the directed edges between them. The cycle corresponding to the configuration, $\underline{n} = (0, 1, 0, 0)$, is indicated by bold arrows as an example.

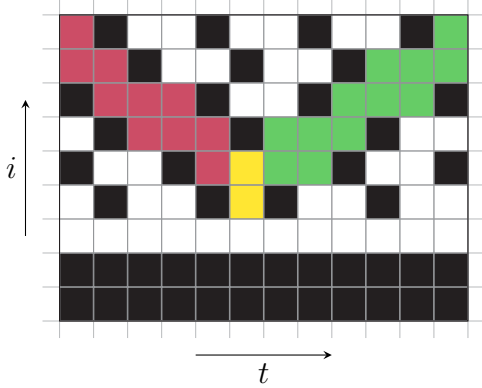


FIG. 7. Reflective boundaries. The action of the spatially localized neighboring excitations (i.e., reflective boundaries) on the propagation of a quasiparticle. The negative quasiparticle (red or dark gray) is *converted* into a positive quasiparticle (green or medium gray) on colliding with the boundary with the interaction (yellow or light gray) taking a similar form as that with an opposing quasiparticle, cf., Fig. 5 (here we have additionally colored the occupied (black) and empty (white) sites of the vacua to improve the presentation of the figure). Note that for closed systems with reflective boundaries, the number of each type of quasiparticle is no longer conserved; only the *total number* of quasiparticles is conserved.

Finally, we note that the numbers of positive and negative quasiparticles within any given configuration \underline{n} are constrained. Specifically, they must satisfy the following equality:

$$Q_n^+ - Q_n^- = 0 \pmod{3}. \quad (16)$$

To prove this, we introduce a graph representation for the lattice, as illustrated in Fig. 6. Specifically, we define a directed bipartite graph composed of two disjoint and independent sets of vertices, each identically labeled by binary strings of length four, and a set of directed edges between them. Here the vertices of the two vertex sets represent the binary strings of consecutive sites within the lattice starting on even and odd sites, respectively, and the directed edges the possible transitions between them as the lattice is positively translated. We can simplify the graph by contracting paths along the directed edges between vertices whose binary labels denote quasiparticles. From here, with a relabelling of the vertices to denote positive and negative quasiparticles, it is trivial to see that any cycle of the graph satisfies Eq. (16).

D. Adjacent excitations and quasiparticle reflection

As illustrated in Fig. 3, pairs of adjacent occupied sites within configurations [i.e., $\underline{n} = (\dots, 1, 1, \dots)$] are invariant to time evolution. That is, neighboring excitations are *spatially localized*. This kinetic constraint, imposed by the deterministic dynamics, induces a partitioning of the configuration space into disjoint subspaces spanned by subsets of configurations characterized by the locations of adjacent occupied sites. The set of configurations $\mathbb{N} = \{0, 1\}^{\times N}$ is therefore reducible under the dynamics. In Sec. II B, we showed that the dimension of the largest of these subspaces, spanned by the subset of configurations with no adjacent

excitations, denoted by \mathbb{N}_0 , grew exponentially according to the Lucas sequence (8). We can similarly show that the dimension of every other subspace, each spanned by a subset of configurations identified by the locations of its neighboring occupied sites, is given by

$$|\mathbb{N}_j(N)| = \prod_{k=1}^B F_{N_k}, \quad j > 0, \quad (17)$$

where B denotes the number of groups of adjacent sites (which we refer to as reflective boundaries for reasons discussed below) and $\{N_k\}$ the sizes of the subsystems between them. For example, for the subset of configurations of size $N = 16$ with localized excitations on sites n_1, n_2 and n_7, n_8, n_9 we have $B = 2$ giving two distinct subsystems of sizes $N_k \in \{4, 7\}$. The dimension of the subspace is then $|\mathbb{N}_j(16)| = F_4 F_7$. To see this, we note that we can consider each of the subsystems that occupy the sites between reflective boundaries as *independent* systems of size N_k with zeros on the first and last sites (the time invariance of the adjacent occupied sites immobilizes the neighboring empty sites, as shown in Fig. 3). We then recall that the dimension of a nonperiodic system of size N_k with zeros on the first and last sites (i.e., an effective system size of $N_k - 2$) is given by F_{N_k} , see Eq. (10). Given that each nonperiodic subsystem is independent, the dimension of the system of size N , spanned by the set of configurations with fixed adjacent occupied sites, is simply the product of the dimensionality of its constituent subsystems.

In terms of the quasiparticles, the localized excitations play the role of *reflective boundaries* as illustrated in Fig. 7. This affects both the systems statics and dynamics. First, the conservation of the numbers of positive and negative quasiparticles no longer holds. Instead, for systems with reflective boundaries, only the *total number* of quasiparticles is conserved. This can be seen by inspecting Fig. 7 and noting that the negative quasiparticle is *converted* to a positive quasiparticle on interacting with the localized excitations that constitute the reflective boundary. A similar reasoning then follows for every quasiparticle as it collides with the boundary. Second, the numbers of positive and negative quasiparticles are no longer constrained, that is, Eq. (16) need no longer be satisfied. To see this, consider the illustrative proof of the constraint (16) in Fig. 6. For systems with adjacent occupied sites, we need to introduce additional vertices to the graph representation of the lattice that correspond to the seven binary strings of length four with adjacent 1s [i.e., $(0, 0, 1, 1)$, $(0, 1, 1, 0)$, $(0, 1, 1, 1)$, $(1, 0, 1, 1)$, $(1, 1, 0, 0)$, $(1, 1, 1, 0)$, $(1, 1, 1, 1)$]. Doing so subsequently introduces multiple edges between the vertices that facilitate new cycles through the graph which violate the constraint (16). A further consequence of the introduction of adjacent occupied sites to the system is that the rules for identifying quasiparticles near the reflective boundaries are different from those outlined in (15). For example, if the sites adjacent to the boundary read $(1, 0, 0, 1)$, then this does not represent a quasiparticle (see Fig. 7) while it would in the bulk. This can be mitigated with respect to simple quasiparticle counting by neglecting the sites directly adjacent to the pairs of excitations (as quasiparticles cannot occupy these sites).

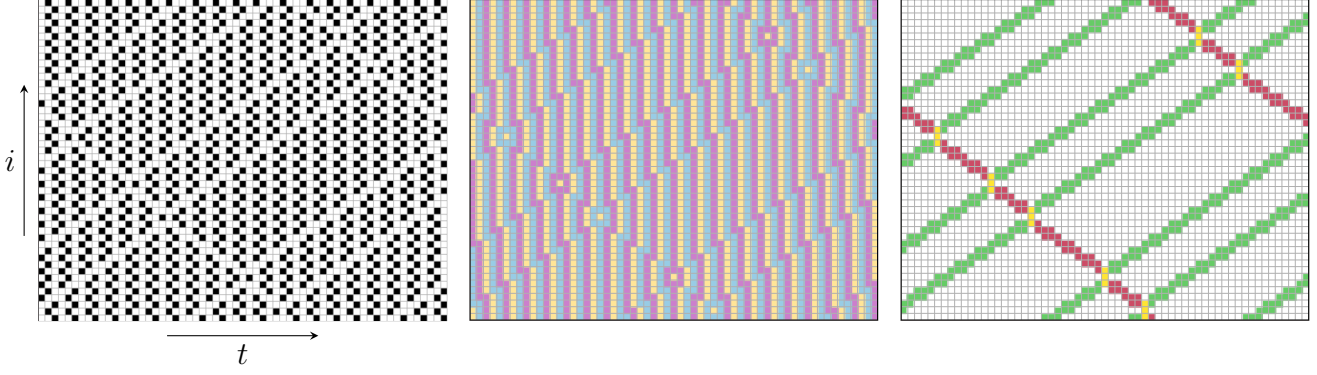


FIG. 8. Typical trajectory of the RCA201 (Floquet-PXP). A typical trajectory of the model in the subspace spanned by states with no adjacent occupied sites. The left panel represents the up and down sites as black and white, respectively. The middle panel shows the vacuum color scheme (see Fig. 4) while the right panel highlights the solitons (see Fig. 5). In this trajectory there are five solitons—four positive movers and one negative—that collide and wrap around the system due to the PBCs. Note that the location of the solitons coincides with domain walls between the vacuum states.

In the remainder of the paper we focus on the case without consecutive occupied sites for simplicity. Note that the discussion above enables us to (at least quantitatively) extend the results to any sector with fixed positions of excitation pairs.

III. EXACT STATIONARY STATE FOR PERIODIC BOUNDARY CONDITIONS

To study the macroscopic properties of the closed system we construct a class of macroscopic equilibrium states which we define as probability distributions over the set of configurations. For simplicity, we will restrict most of the discussion to the configuration sector without pairs of adjacent excited sites, in which case the numbers of both types of quasiparticles are conserved (being invariant, a cluster of two or more consecutive occupied sites acts as a reflective boundary for quasiparticles therefore changing their type but not their total number, see Fig. 3). In this sector the simplest class of steady states can be constructed by introducing two chemical potentials, μ^+ and μ^- , associated with numbers of positive and negative quasiparticles, respectively.

As we will demonstrate, such states can be expressed in two equivalent forms. We start with the *patch state ansatz* (PSA) formulation of the steady state, as introduced in Ref. [31]. The main advantage of the PSA formulation is the construction, which can be done in absence of knowledge of conserved quantities, by simply requiring the states to be stationary and at the same time exhibit short-range correlations. Equivalently, the steady states can be expressed in terms of MPS. They obey a similar cubic algebraic relation to the MPS form of the RCA54 steady states [33].

A. Macroscopic states and master equation

We start the discussion of stationary states by first introducing the necessary formalism. Each configuration of the system \underline{n} is associated with a probability $p_{\underline{n}}$, that satisfies the nonnegativity and normalization conditions,

$$p_{\underline{n}} \geq 0, \quad \sum_{\{\underline{n}\}} p_{\underline{n}} = 1. \quad (18)$$

Each probability distribution, given by the set of configurational probabilities $\{p_{\underline{n}}\}$, can be uniquely represented by a state vector,

$$\mathbf{p} = \sum_{\{\underline{n}\}} p_{\underline{n}} \bigotimes_{i=1}^N \mathbf{e}_{n_i}, \quad \mathbf{e}_n \equiv \begin{bmatrix} \delta_{n,0} \\ \delta_{n,1} \end{bmatrix}, \quad (19)$$

where \mathbf{e}_0 and \mathbf{e}_1 are the standard basis vectors of \mathbb{R}^2 and $\mathbf{p} \in (\mathbb{R}^2)^{\otimes N}$. The state space is then identified as a convex subset of the vector space $(\mathbb{R}^2)^{\otimes N}$.

The master equation describing the discrete time evolution of the system can be written as

$$\mathbf{p}^{t+1} = \begin{cases} \mathbf{M}_E \mathbf{p}^t, & t = 0 \pmod{2}, \\ \mathbf{M}_O \mathbf{p}^t, & t = 1 \pmod{2}, \end{cases} \quad (20)$$

where \mathbf{M}_E and \mathbf{M}_O are transition matrices associated with the even and odd time steps in (2), respectively,

$$\begin{aligned} \mathbf{M}_O &: p_{n_1 n_2 \dots n_{N-1} n_N} \mapsto p_{f_1 n_2 \dots f_{N-1} n_N}, \\ \mathbf{M}_E &: p_{n_1 n_2 \dots n_{N-1} n_N} \mapsto p_{n_1 f_2 \dots f_{N-1} n_N}. \end{aligned} \quad (21)$$

The one time-step propagators are equivalently given as products of local operators (gates),

$$\begin{aligned} \mathbf{M}_E &= \mathbf{U}_2 \mathbf{U}_4 \cdots \mathbf{U}_{N-2} \mathbf{U}_N, \\ \mathbf{M}_O &= \mathbf{U}_1 \mathbf{U}_3 \cdots \mathbf{U}_{N-3} \mathbf{U}_{N-1}, \end{aligned} \quad (22)$$

where for the bulk, $i \in \{2, \dots, N-1\}$,

$$\mathbf{U}_i = \mathbf{I}^{\otimes(i-2)} \otimes \mathbf{U} \otimes \mathbf{I}^{\otimes(N-i-1)}, \quad (23)$$

are matrices encoding the deterministic bulk function in (4) (with the subscript indicating on which site of the lattice the operator acts nontrivially), whereas for the boundaries, $i \in \{1, N\}$,

$$\begin{aligned} \mathbf{U}_1 &= \mathbf{I}^{\otimes N} + (\mathbf{X} - \mathbf{I}) \otimes \mathbf{P} \otimes \mathbf{I}^{\otimes(N-3)} \otimes \mathbf{P}, \\ \mathbf{U}_N &= \mathbf{I}^{\otimes N} + \mathbf{P} \otimes \mathbf{I}^{\otimes(N-3)} \otimes \mathbf{P} \otimes (\mathbf{X} - \mathbf{I}), \end{aligned} \quad (24)$$

are matrices encoding the left and right boundary functions, f_1^t and f_N^t , respectively. Here

$$\mathbf{U} = \mathbf{I}^{\otimes 3} + \mathbf{P} \otimes (\mathbf{X} - \mathbf{I}) \otimes \mathbf{P}, \quad (25)$$

is the 8×8 permutation matrix enacting the local time evolution rule of Eq. (6) on the vector space $(\mathbb{R}^2)^{\otimes 3}$,

$$\mathbf{U} = \begin{bmatrix} 0 & & & & & & & \\ & 1 & & & & & & \\ & & 1 & & & & & \\ 1 & & & 0 & & & & \\ & & & & 1 & & & \\ & & & & & 1 & & \\ & & & & & & 1 & \\ & & & & & & & 1 \end{bmatrix}, \quad (26)$$

with \mathbf{I} , \mathbf{P} , and \mathbf{X} the 2×2 identity, projector and Pauli-X matrices, respectively, acting on \mathbb{R}^2 ,

$$\mathbf{I} = \begin{bmatrix} 1 & 0 \\ 0 & 1 \end{bmatrix}, \quad \mathbf{P} = \begin{bmatrix} 1 & 0 \\ 0 & 0 \end{bmatrix}, \quad \mathbf{X} = \begin{bmatrix} 0 & 1 \\ 1 & 0 \end{bmatrix}. \quad (27)$$

B. Patch state ansatz formulation of Gibbs states

We require a stationary state \mathbf{p} to map into itself after a full time step composed of an even and odd time step, respectively,

$$\mathbf{p} = \mathbf{M}_O \mathbf{M}_E \mathbf{p}. \quad (28)$$

Due to the reversibility of the dynamics, $\mathbf{U}^{-1} = \mathbf{U}$, the stationarity condition can be equivalently recast as

$$\mathbf{M}_O \mathbf{p} = \mathbf{M}_E \mathbf{p}. \quad (29)$$

Similarly to the PSA introduced for RCA54 in Ref. [31], we propose the following form of the state \mathbf{p} :

$$p_{\underline{n}} \propto X_{n_1 n_2 n_3 n_4} X'_{n_2 n_3 n_4 n_5} X_{n_3 n_4 n_5 n_6} \cdots \\ \cdots X'_{n_{N-2} n_{N-1} n_N n_1} X_{n_{N-1} n_N n_1 n_2} X'_{n_N n_1 n_2 n_3}. \quad (30)$$

The values $X_{n_i n_{i+1} n_{i+2} n_{i+3}}$ are determined so that the stationarity condition in Eq. (29) is satisfied. Explicitly, for any configuration $\underline{n} = (n_1, n_2, n_3, \dots, n_N)$ the following equality has to hold:

$$X_{n_1 f_2 n_3 f_4} X'_{f_2 n_3 f_4 n_5} \cdots X'_{f_N n_1 f_2 n_3} = X_{f_1 n_2 f_3 n_4} X'_{n_2 f_3 n_4 f_5} \cdots X'_{n_N f_1 n_2 f_3}, \quad (31)$$

where we have used the notation $f_i = f(n_{i-1}, n_i, n_{i+1})$, as introduced in (4). Before solving the system of equations, we put all the components corresponding to configurations \underline{n} with pairs of consecutive 1s to 0 by requiring the following:

$$X_{11 n_1 n_2}^{(\prime)} = X_{n_1 11 n_2}^{(\prime)} = X_{n_1 n_2 11}^{(\prime)} = 0. \quad (32)$$

We are free to fix the normalization and therefore choose to set $X_{0000} X'_{0000} = 1$, which together with (31) implies

$$X_{0101} X'_{1010} = X_{1010} X'_{0101} = X_{0000} X'_{0000} = 1. \quad (33)$$

Additionally, we observe that the values $X_{n_1 n_2 n_3 n_4}^{(\prime)}$ are determined up to the following gauge transformation:

$$X_{n_1 n_2 n_3 n_4} \mapsto \alpha_{n_1 n_2 n_3} X_{n_1 n_2 n_3 n_4} \alpha_{n_2 n_3 n_4}^{-1}, \\ X'_{n_1 n_2 n_3 n_4} \mapsto \alpha'_{n_1 n_2 n_3} X'_{n_1 n_2 n_3 n_4} \alpha_{n_2 n_3 n_4}^{-1}, \quad (34)$$

which allows us to set $X_{0 n_1 n_2 n_3}^{(\prime)} = 1$ for all configurations of three sites belonging to the sector without pairs of 1s,

$$X_{0 n_1 n_2 n_3}^{(\prime)} = (1 - \delta_{n_1+n_2, 2})(1 - \delta_{n_2+n_3, 2}). \quad (35)$$

Combining the restriction to the relevant subspace (32) together with the choices of normalization (33) and gauge (35), and requiring stationarity (31) we obtain conditions for the remaining four components,

$$X_{1000} = X'_{1000} = X_{1001} X'_{1001}. \quad (36)$$

This condition exhibits the following two-parameter family of solutions:

$$X_{1001} = \frac{\omega^2}{\xi}, \quad X'_{1001} = \frac{\xi^2}{\omega}, \quad X_{1000} = X'_{1000} = \omega \xi, \quad (37)$$

with all the other components either being 0 [as given by (32)] or 1. The vector \mathbf{p} representing the steady state has to be normalizable, and therefore all its components have to be nonnegative, which restricts the values of the parameters ξ , ω to \mathbb{R}^+ .

At this point the choice of parametrization is arbitrary, but it can be straightforwardly demonstrated that the parameters ξ and ω are exponents of the chemical potentials μ^+ and μ^- corresponding to the numbers of positively and negatively moving quasiparticles, respectively. First, we use the gauge freedom to transform the tensors into an equivalent form,

$$\alpha_{000} = 1, \quad \alpha_{010} = \xi^{-1}, \quad \alpha_{001} = \alpha_{100} = \alpha_{101} = \omega^{-1}, \\ \alpha'_{n_1 n_2 n_3} = \alpha_{n_1 n_2 n_3} |_{\xi \leftrightarrow \omega}, \quad (38)$$

which by (34) implies

$$X_{0001} \mapsto \xi, \quad X_{1000} \mapsto \xi, \quad X_{1001} \mapsto \omega, \\ X'_{0001} \mapsto \omega, \quad X'_{1000} \mapsto \omega, \quad X'_{1001} \mapsto \xi, \quad (39)$$

while the other components either remain 0, cf., (32), or are mapped into 1. In a given configuration \underline{n} , the number of both types of quasiparticles can be determined by the count of subconfigurations (0,0,0,1), (1,0,0,0), and (1,0,0,1). Depending on the parity of the site indices where the subconfigurations are positioned, they correspond either to quasiparticles with positive or negative velocity, as summarized in (15). Therefore, the new values of $X_{n_1 n_2 n_3 n_4}^{(\prime)}$ imply that every component $p_{\underline{n}}$ of the stationary state \mathbf{p} is weighed as

$$p_{\underline{n}} \propto \xi^{Q_{\underline{n}}^+} \omega^{Q_{\underline{n}}^-}, \quad (40)$$

where $Q_{\underline{n}}^{\pm}$ are the numbers of positive and negative quasiparticles in a given configuration \underline{n} .

Since the requirement for stationarity is the invariance to evolution for two time steps (29) (i.e., an even and odd time step), we can define two versions of state, \mathbf{p} and \mathbf{p}' , corresponding to even and odd time steps respectively,

$$\mathbf{p}' = \mathbf{M}_E \mathbf{p}, \quad \mathbf{p} = \mathbf{M}_O \mathbf{p}'. \quad (41)$$

Together with the solution for \mathbf{p} , this condition implies that the odd-time version of the state takes the same form with the roles of $X_{n_1 n_2 n_3 n_4}$ and $X'_{n_1 n_2 n_3 n_4}$ reversed,

$$p'_{\underline{n}} \propto X'_{n_1 n_2 n_3 n_4} X_{n_2 n_3 n_4 n_5} X'_{n_3 n_4 n_5 n_6} \cdots \\ \cdots X_{n_{N-2} n_{N-1} n_N n_1} X'_{n_{N-1} n_N n_1 n_2} X_{n_N n_1 n_2 n_3}. \quad (42)$$

This parametrization of the steady state preserves the symmetry of the model: Shifting the state by one site (up or down) is the same as evolving it for one time step (half of the Floquet period).

C. Matrix product form of stationary states

Equivalently, the stationary states can be recast in the matrix product form,

$$\mathbf{p} = \frac{1}{Z} \text{tr}(\mathbf{V}_1 \mathbf{V}'_2 \mathbf{V}_3 \cdots \mathbf{V}_{N-1} \mathbf{V}'_N), \quad (43)$$

where $\mathbf{V}_i^{(l)}$ are vectors of matrices, corresponding to the physical site i , $\mathbf{V}^{(l)} = (V_0^{(l)}, V_1^{(l)})^T$, and Z is the normalization. Explicitly, the components $p_{\underline{n}}$ of the stationary state \mathbf{p} read

$$p_{\underline{n}} = \frac{1}{Z} \text{tr}(V_{n_1} V'_{n_2} V_{n_3} \cdots V_{n_{N-1}} V'_{n_N}). \quad (44)$$

To construct the MPS from the PSA, we introduce an eight-dimensional auxiliary space with each basis element labeled by a binary string $(m_1 m_2 m_3)$ and we define the 8×8 matrices $\tilde{V}_n^{(l)}$ with the entries given by the PSA values as

$$(\tilde{V}_n^{(l)})_{m_1 m_2 m_3}^{m'_1 m'_2 m'_3} = \delta_{m'_1, m_2} \delta_{m'_2, m_3} \delta_{m'_3, n} X_{m_1 m_2 m_3 n}^{(l)}, \quad (45)$$

where the strings in the superscript and the subscript are the binary representations of the row and column index, respectively. MPS consisting of these matrices are equivalent to the PSA steady states as introduced before,

$$\text{tr}(\tilde{V}_{n_1} \tilde{V}'_{n_2} \cdots \tilde{V}'_{n_N}) = X_{n_1 n_2 n_3 n_4} \cdots X'_{n_N n_1 n_2 n_3}. \quad (46)$$

The MPS can be simplified by introducing 4×8 and 8×4 auxiliary space matrices R and Q

$$R = \begin{bmatrix} 1 & & & 0 & & & & \\ & 1 & & & & 1 & & \\ & & 1 & & & & 0 & \\ & & & 0 & 1 & & & 0 \\ & & & & & & & \\ & & & & & & & \\ & & & & & & & \\ & & & & & & & \end{bmatrix}, \quad Q = \begin{bmatrix} 1 & & & & & & & \\ & 1 & & & & & & \\ & & 1 & & & & & \\ 0 & & & 0 & & & & \\ & & & & 1 & & & \\ & & & & & & & \\ & & & & & 0 & & \\ & & & & & & 0 & \\ & & & & & & & 0 \end{bmatrix}, \quad (47)$$

and noting that for any combination of n_1, n_2 , inserting QR between two consecutive matrices does not change the product,

$$\tilde{V}_{n_1} QR \tilde{V}'_{n_2} = \tilde{V}_{n_1} \tilde{V}'_{n_2}. \quad (48)$$

From here it follows that the MPS (43) composed of 4×4 matrices $V_n^{(l)}$, defined as $V_n^{(l)} = R \tilde{V}_n^{(l)} Q$, is equivalent to (46). Explicitly,

$$V_0 = \begin{bmatrix} 1 & 0 & 0 & \xi \\ 0 & 0 & 0 & 0 \\ 0 & 1 & 0 & 0 \\ 0 & 0 & 1 & 0 \end{bmatrix}, \quad V_1 = \begin{bmatrix} 0 & 0 & 0 & 0 \\ \xi & 0 & 1 & \omega \\ 0 & 0 & 0 & 0 \\ 0 & 0 & 0 & 0 \end{bmatrix}, \quad (49)$$

while the other pair of matrices is given by the exchange of parameters $\xi \leftrightarrow \omega$,

$$V'_n(\xi, \omega) = V_n(\omega, \xi). \quad (50)$$

The stationarity of the MPS is implied by the equivalence between the two representations. However, the MPS additionally exhibits an algebraic structure that allows us to explicitly demonstrate the stationarity without relying on the equivalence with the PSA. Matrices $V_n^{(l)}$ satisfy a cubic algebraic relation, analogous to [33],

$$\mathbf{U}_2(\mathbf{V}_1 \mathbf{V}'_2 \mathbf{V}_3 S) = \mathbf{V}_1 S \mathbf{V}_2 \mathbf{V}'_3, \quad (51)$$

which compactly encodes the following component-wise equalities:

$$V_{n_1} V'_{f(n_1, n_2, n_3)} V_{n_3} S = V_{n_1} S V_{n_2} V'_{n_3}. \quad (52)$$

We introduced the *delimiter matrix* S , defined as

$$S = \begin{bmatrix} \frac{\xi\omega}{\xi^2-\omega} & -\frac{\omega}{\xi^2-\omega} & 0 & \frac{\xi^2}{\xi^2-\omega} \\ 1 & 0 & 0 & \omega \\ 0 & 0 & 1 & 0 \\ -\frac{\omega}{\xi^2-\omega} & \frac{\xi}{\xi^2-\omega} & 0 & -\frac{\xi}{\xi^2-\omega} \end{bmatrix}. \quad (53)$$

The inverse of the delimiter matrix is given by exchanging the parameters,

$$S(\xi, \omega)^{-1} = S(\omega, \xi), \quad (54)$$

which immediately implies a *dual* relation similar to (51),

$$\mathbf{U}_2(\mathbf{V}'_1 \mathbf{V}_2 \mathbf{V}'_3 S^{-1}) = \mathbf{V}'_1 S^{-1} \mathbf{V}_2 \mathbf{V}'_3. \quad (55)$$

Note that in the cases $\xi = \omega^2$ or $\omega = \xi^2$, the matrices S and S^{-1} are not well defined; however, the products $V_n S$ and $V'_n S^{-1}$ have finite values in the limit $\xi \rightarrow \omega^2$ (or $\omega \rightarrow \xi^2$). Therefore the following discussion holds for any value of parameters. When $\xi = \omega = 1$, the stationary state becomes the maximum entropy state, where each allowed configuration is equally likely. In this case the MPS representation can be reduced to 2×2 matrices, as is explained in Appendix A.

The odd-time version of the state, \mathbf{p}' , has the same form as \mathbf{p} , but the parameters ξ and ω are exchanged (or, equivalently, \mathbf{V}' is replaced by \mathbf{V} and vice versa),

$$\mathbf{p}' = \frac{1}{Z} \text{tr}(\mathbf{V}'_1 \mathbf{V}_2 \mathbf{V}'_3 \cdots \mathbf{V}'_{N-1} \mathbf{V}_N). \quad (56)$$

The stationarity requirement (41) follows directly from relations (51) and (55). To prove the first of the stationarity conditions, we insert SS^{-1} between the matrices corresponding to the first and second sites and apply the local time-evolution operator \mathbf{U}_N using the three-site algebraic relation,

$$\begin{aligned} & \mathbf{M}_E \text{tr}(\mathbf{V}_1 \mathbf{V}'_2 \mathbf{V}_3 \cdots \mathbf{V}_{N-1} \mathbf{V}'_N) \\ &= \prod_{i=1}^{N/2} \mathbf{U}_{2i} \text{tr}(\mathbf{V}_{N-1} \mathbf{V}'_N \mathbf{V}_1 S S^{-1} \mathbf{V}'_2 \cdots \mathbf{V}_{N-3} \mathbf{V}'_{N-2}) \\ &= \prod_{i=1}^{N/2-1} \mathbf{U}_{2i} \text{tr}(\mathbf{V}'_1 S^{-1} \mathbf{V}'_2 \cdots \mathbf{V}_{N-3} \mathbf{V}'_{N-2} \mathbf{V}_{N-1} S \mathbf{V}_N). \end{aligned} \quad (57)$$

We keep applying local time-evolution operators $\mathbf{U}_{N-2}, \mathbf{U}_{N-4}, \dots$, one by one, each time moving the matrix S two sites to the

left as described by (51), until we are left with the following:

$$\begin{aligned} & \mathbf{U}_2 \text{tr}(\mathbf{V}'_1 S^{-1} \mathbf{V}'_2 \mathbf{V}'_3 S \mathbf{V}'_4 \cdots \mathbf{V}'_{N-1} \mathbf{V}'_N) \\ &= \text{tr}(\mathbf{V}'_1 \mathbf{V}'_2 \mathbf{V}'_3 S^{-1} S \mathbf{V}'_4 \cdots \mathbf{V}'_{N-1} \mathbf{V}'_N), \end{aligned} \quad (58)$$

where we used the dual relation in Eq. (55) together with $\mathbf{U}^{-1} = \mathbf{U}$. Thus we proved that the even time-evolution operator \mathbf{M}_E maps the state \mathbf{p} into its odd-time analog \mathbf{p}' . The second stationarity requirement (41) can be proved analogously.

D. Partition function

As demonstrated in Sec. III B, the stationary probabilities of configurations p_n are distributed according to the *grand-canonical ensemble*,

$$p_n = \frac{1}{Z} \exp(Q_n^+ \mu^+ + Q_n^- \mu^-), \quad (59)$$

with the chemical potentials corresponding to the numbers of positive and negative quasiparticles determined by the parameters

$$\xi = e^{\mu^+}, \quad \omega = e^{\mu^-}. \quad (60)$$

The partition function Z can therefore be given in two equivalent forms. The first one follows directly from the normalization condition of the MPS representation of the stationary state \mathbf{p} ,

$$Z = \sum_{\{n\}} \text{tr}(V_{n_1} V'_{n_2} V_{n_3} \cdots V'_{n_N}) \equiv \text{tr} T^{N/2}, \quad (61)$$

where we introduced the transfer matrix T as the sum of all products of matrices on two sites,

$$T = (V_0 + V_1)(V'_0 + V'_1) = \begin{bmatrix} 1 & 0 & \xi & \omega \\ \xi & 1 & \omega & \xi\omega \\ \omega & 0 & 1 & \xi \\ 0 & 1 & 0 & 0 \end{bmatrix}. \quad (62)$$

The second form of Z is defined as a weighted sum over the set of quasiparticle numbers,

$$Z = \sum_{\{n\}} \xi^{Q_n^+} \omega^{Q_n^-} = \sum_{\{Q\}} \Omega_Q \xi^{Q^+} \omega^{Q^-}, \quad (63)$$

where the entropic term Ω_Q , which counts the number of degenerate configurations with the same number of quasiparticles, takes the following combinatoric form:

$$\Omega_Q = \frac{1}{m_Q} \binom{\frac{1}{2}N - \frac{1}{3}Q^+ - \frac{2}{3}Q^-}{Q^+} \binom{\frac{1}{2}N - \frac{1}{3}Q^- - \frac{2}{3}Q^+}{Q^-}, \quad (64)$$

with m_Q the *time-averaged magnetization density* expressed in terms of the numbers of positive and negative quasiparticles as

$$m_Q = \frac{(\frac{1}{2}N - \frac{1}{3}Q^+ - \frac{2}{3}Q^-)(\frac{1}{2}N - \frac{1}{3}Q^- - \frac{2}{3}Q^+)}{\frac{1}{2}N(\frac{3}{2}N - 2Q^+ - 2Q^-)}. \quad (65)$$

A derivation of this is given in Appendix B. The set $\{Q\}$ above denotes the set of tuples of numbers of positive and negative quasiparticles that satisfy both the equality in Eq. (16), imposed by the even system size and PBC, and the following

inequalities that manifest from the finite effective size of the quasiparticles:

$$Q^\pm + 2Q^\mp \leq \frac{3}{2}N, \quad (66)$$

which is implicitly given by $\binom{n-k}{k} = 0$. To prove that the expression (64) really represents the entropic contribution, it suffices to show that the two forms of the partition sum [given by Eqs. (61) and (63)] coincide. The proof of equivalence is provided in Appendix C.

Alternatively, the inequalities of Eq. (66) can be understood directly from the quasiparticle picture. To begin, we recall that for any given configuration the difference between the numbers of positive and negative quasiparticles must satisfy Eq. (16), that is, it must be a multiple of three. This can be interpreted as a physical constraint on the system which requires the quasiparticles exist as either positive-negative pairs or positive-negative triples. The numbers of these pairs and triples, denoted by $Q^{(2)}$ and $Q^{(3)}$, respectively, are bounded by their effective size (i.e., the number of sites they occupy within a configuration). Inspecting the relevant cycles in Fig. 6 implies that these are at least four and eight sites, respectively, which imposes the following upper bound:

$$4Q^{(2)} + 8Q^{(3)} \leq N. \quad (67)$$

We now express these in terms of the numbers of positive and negative quasiparticles, where for $Q^\pm \geq Q^\mp$, we have

$$Q^{(2)} = Q^\mp, \quad Q^{(3)} = \frac{1}{3}(Q^\pm - Q^\mp). \quad (68)$$

A simple substitution then yields the inequalities outlined in Eq. (66).

In the limit of large N the expression for the partition function (63) can be written in terms of an integral over *quasiparticle densities*,

$$\rho^\pm = \frac{Q^\pm}{N}, \quad (69)$$

to read

$$Z = \int_0^1 d\rho^+ d\rho^- \exp(N\mathcal{F}(\rho^+, \rho^-)), \quad (70)$$

where \mathcal{F} is (minus) a free energy density with ‘‘energetic’’ terms, associated with the cost of each soliton species in terms of their chemical potential, and entropic terms from the counting of states,

$$\mathcal{F} = \mu^+ \rho^+ + \mu^- \rho^- + \mathcal{S}(\rho^+, \rho^-). \quad (71)$$

The entropy density \mathcal{S} is obtained from using the Stirling approximation in (64). It reads

$$\begin{aligned} \mathcal{S} &= -\rho^+ \ln \rho^+ \\ &+ \left(\frac{1}{2} - \frac{1}{3}\rho^+ - \frac{2}{3}\rho^-\right) \ln \left(\frac{1}{2} - \frac{1}{3}\rho^+ - \frac{2}{3}\rho^-\right) \\ &- \left(\frac{1}{2} - \frac{2}{3}\rho^- - \frac{4}{3}\rho^+\right) \ln \left(\frac{1}{2} - \frac{2}{3}\rho^- - \frac{4}{3}\rho^+\right) \\ &+ (\rho^+ \leftrightarrow \rho^-), \end{aligned} \quad (72)$$

and has the form of an entropy density of mixing of the quasiparticles subject to the constraints (16) and (67).

IV. EXACT STATIONARY STATE FOR STOCHASTIC BOUNDARY CONDITIONS

The RCA201 (Floquet-PXP) with PBC is fully deterministic. The integrability of the model implies that the dynamics is naturally decomposed into many different sectors, which makes the number of steady states of the closed system highly degenerate. In the absence of chaos, a way to make the dynamics ergodic is to impose stochastic boundary conditions (SBC) by considering a finite chain coupled to stochastic reservoirs on both ends, an approach similar to that of the RCA54, cf., Refs. [31–33]. With SBC the RCA201 (Floquet-PXP) becomes a stochastic model, and by ergodic we mean two things. First, all configurations are dynamically connected, that is, the relevant subspace is irreducible under the dynamics since quasiparticles can be created and destroyed at the boundaries. Note that this subspace is slightly larger than that of a similarly sized system with PBC as with SBC there is no restriction on the occupation of the first and last site which are no longer neighbors. The number of configurations in the subspace of interest is then the Fibonacci rather than the Lucas number (see Sec. II B). Second, the relaxation time (i.e., the time to forget a typical initial condition) is finite.

In this section we find a class of suitable stochastic boundary propagators to make the system relax to a unique NESS similar to the Gibbs state introduced in Sec. III. The starting point is the MPS form of the Gibbs state of a large system with periodic boundaries, which is used to express the probability distribution (i.e., state) of a finite subsection of the chain in the limit when the system size goes to infinity. The resulting probability distribution can be viewed as a NESS of the finite chain with the boundaries that stochastically inject and remove quasiparticles with rates that are compatible with the chemical potentials, μ^+ and μ^- , of the original Gibbs state.

A. State of a finite section of a larger system

We start with the closed system with periodic boundary conditions and length M that is assumed to be the equilibrium state given by spectral parameters ξ , ω , as introduced in Sec. III. By definition, the probabilities of configurations of a smaller section of the chain with length N are given by summing over the probabilities corresponding to the configurations $(n_1, n_2 \dots n_M)$ with the same first N bits,

$$p_{n_1 \dots n_N}^{(M)} = \sum_{n_{N+1} \dots n_M} Z^{-1} \text{tr}(V_{n_1} V'_{n_2} \dots V'_{n_M}). \quad (73)$$

Note that the superscript (M) refers to the length of the whole system and not the length of the section. Using T to denote the transfer matrix, as introduced in Eq. (62), the probability distribution $\mathbf{p}^{(M)}$ can be succinctly expressed as

$$\mathbf{p}^{(M)} = \frac{\text{tr}[\mathbf{V}_1 \mathbf{V}'_2 \dots \mathbf{V}'_N T^{(M-N)/2}]}{\text{tr} T^{M/2}}. \quad (74)$$

We define the state of the subsystem \mathbf{p} as the large system size limit of the distribution $\mathbf{p}^{(M)}$,

$$\mathbf{p} = \lim_{M \rightarrow \infty} \mathbf{p}^{(M)} = \frac{\langle l | \mathbf{V}_1 \mathbf{V}'_2 \dots \mathbf{V}'_N | r \rangle}{\lambda^{N/2} \langle l | r \rangle}, \quad (75)$$

where we introduced the parameter λ denoting the leading eigenvalue of the matrix T , and $\langle l |$ and $| r \rangle$ are the correspond-

ing left and right eigenvectors,

$$T | r \rangle = \lambda | r \rangle, \quad \langle l | T = \lambda \langle l|. \quad (76)$$

Explicitly, λ is the largest solution of the following quartic equation:

$$\lambda^4 - 3\lambda^3 + (3 - 2\xi\omega)\lambda^2 - (1 - \xi\omega)\lambda - (\xi^2 - \omega)(\omega^2 - \xi) = 0, \quad (77)$$

while the leading eigenvectors are implicitly given by parameters ξ , ω and the eigenvalue λ as

$$\langle l | = [(\lambda - 1)\xi + \omega^2] \begin{bmatrix} (\lambda - 1)\xi + \omega^2 \\ (\lambda - 1)^2 - \xi\omega \\ (\lambda - 1)\omega + \xi^2 \\ (\lambda - 1)[(\lambda - 1)^2 - \xi\omega] \end{bmatrix}^T, \quad (78)$$

and

$$| r \rangle = [(\lambda - 1)\omega + \xi^2] \begin{bmatrix} \lambda[(\lambda - 1)^2 - \xi\omega] \\ \lambda[(\lambda - 1)\xi + \omega^2] \\ \lambda(\lambda - 1)\omega - \xi\omega^2 + \xi^2 \\ (\lambda - 1)\xi + \omega^2 \end{bmatrix}, \quad (79)$$

where the nontrivial normalization prefactor is chosen to simplify the boundary equations in the next subsection. Note that the asymptotic form of the probability distribution (75) is valid as long as the leading eigenvalue λ is not degenerate, which is the case for all $\xi, \omega > 0$. The odd time-step version of the asymptotic distribution, \mathbf{p}' , takes the same form as \mathbf{p} with the exchanged roles of parameters ξ and ω . Explicitly,

$$\mathbf{p}' = \frac{\langle l' | \mathbf{V}'_1 \mathbf{V}_2 \dots \mathbf{V}_N | r' \rangle}{\lambda^{N/2} \langle l' | r' \rangle}, \quad (80)$$

where the vectors $\langle l' |$ and $| r' \rangle$ are defined as

$$\langle l'(\xi, \omega) | = \langle l(\omega, \xi) |, \quad | r'(\xi, \omega) \rangle = | r(\omega, \xi) \rangle, \quad (81)$$

and the leading eigenvalue λ is invariant under the exchange $\xi \leftrightarrow \omega$.

To avoid the cluttering of notation, we use the symbols \mathbf{p} , \mathbf{p}' to denote probability distributions on N sites, i.e., $\mathbf{p}^{(l)}$ are vectors from $(\mathbb{R}^2)^{\otimes N}$ with components $p_{n_1 n_2 n_3 \dots n_N}^{(l)}$. When we refer to probabilities of configurations of different lengths, we will always use the component-wise notation to avoid ambiguity. Note that values $p_{n_1 n_2 \dots n_k}^{(l)}$ take the form similar to (75) and (80) with N being replaced by k .

B. Compatible boundaries

The probability distribution of the section of the chain, \mathbf{p} , can be understood as the NESS of a boundary driven system. We assume the one time-step evolution operators to be deterministic in the bulk and stochastic at the boundaries. Explicitly, under the even time-step operator \mathbf{M}_E the sites $(1, 2, \dots, N - 4)$ change deterministically according to the time-evolution rule (6), while the evolution of

sites $(N-3, N-2, N-1, N)$ is given by a stochastic matrix \mathbf{R} ,

$$\mathbf{M}_E = \prod_{i=1}^{N/2-2} \mathbf{U}_{2i} \mathbf{R}_{N-3N-2N-1N}. \quad (82)$$

Similarly, in the odd time step, the evolution of sites $(5, 6, 7, \dots, N)$ is deterministic and the evolution of the first four sites $(1, 2, 3, 4)$ is encoded in the stochastic matrix \mathbf{L} ,

$$\mathbf{M}_O = \mathbf{L}_{1234} \prod_{i=2}^{N/2-1} \mathbf{U}_{2i+1}. \quad (83)$$

For the vectors \mathbf{p} and \mathbf{p}' to be understood as stationary states under the stochastic time evolution, the following conditions have to be satisfied:

$$\mathbf{M}_E \mathbf{p} = \mathbf{p}', \quad \mathbf{M}_O \mathbf{p}' = \mathbf{p}. \quad (84)$$

The stationarity condition is fulfilled when in addition to the bulk algebraic relations (51) and (55), the MPS introduced in (75) and (80) satisfies the appropriate boundary relations. Explicitly, \mathbf{p} is mapped into \mathbf{p}' under the even time-step evolution, when the following boundary equations hold:

$$\langle l | \mathbf{V}_1 S = \Gamma \langle l' | \mathbf{V}'_1, \quad (85)$$

$$\mathbf{R}_{1234} (\mathbf{V}_1 \mathbf{V}'_2 \mathbf{V}_3 \mathbf{V}'_4 | r') = \mathbf{V}_1 S \mathbf{V}'_2 \mathbf{V}_3 \mathbf{V}'_4 | r'.$$

Analogously, the second stationarity condition implies the following two boundary relations:

$$\mathbf{L}_{1234} (\langle l' | \mathbf{V}'_1 \mathbf{V}_2 \mathbf{V}'_3 \mathbf{V}_4) = \langle l | \mathbf{V}_1 \mathbf{V}'_2 \mathbf{V}_3 \mathbf{V}'_4 S^{-1}, \quad (86)$$

$$\mathbf{V}'_1 S^{-1} | r' = \frac{1}{\Gamma} \mathbf{V}'_1 | r,$$

where the scalar factor Γ is determined by the normalization of the MPS as

$$\Gamma = \frac{\langle l | r \rangle}{\langle l' | r' \rangle} = \frac{(\lambda - 1)\xi + \omega^2}{(\lambda - 1)\omega + \xi^2}. \quad (87)$$

The boundary propagators \mathbf{R} and \mathbf{L} are assumed to stochastically act only on the rightmost and leftmost sites respectively, while the other three sites change deterministically, according to the dynamical rule (6). Equivalently, we can imagine we temporarily introduce an additional site to the edge of the chain, in a state that depends on the configuration of the four sites, and update the site at the edge deterministically, as illustrated in Fig. 9. Explicitly, the matrix elements of \mathbf{R} and \mathbf{L} can be parametrized as

$$R_{n_1 n_2 n_3 n_4}^{n'_1 n'_2 n'_3 n'_4} = \delta_{n'_1, n_1} \delta_{n'_2, f_2} \delta_{n'_3, n_3} \sum_{n_5=0}^1 \delta_{n'_4, f_4} \phi_{n_1 n_2 n_3 n_4 n_5}^R, \quad (88)$$

$$L_{n_1 n_2 n_3 n_4}^{n'_1 n'_2 n'_3 n'_4} = \delta_{n'_2, n_2} \delta_{n'_3, f_3} \delta_{n'_4, n_4} \sum_{n_0=0}^1 \delta_{n'_1, f_1} \phi_{n_0 n_1 n_2 n_3 n_4}^L,$$

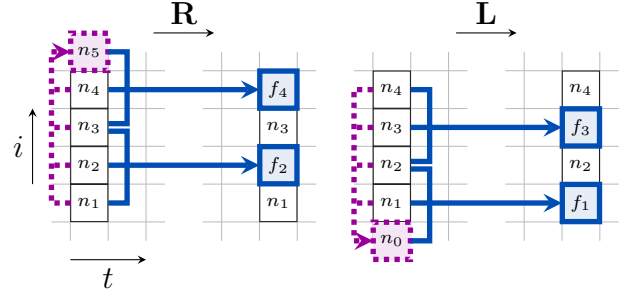


FIG. 9. Right and left boundary propagators. The action of \mathbf{R} is equivalent to introducing an additional *virtual* site on the top [purple (dotted) square], initialize it in the state that depends on the four sites preceding it, and then evolving the second and fourth site according to the deterministic rule 201 [blue (solid) arrows]. Similarly, the left boundary propagator \mathbf{L} can be reproduced by introducing a virtual site at the bottom, and then applying deterministic evolution.

where $\phi_{n_1 n_2 n_3 n_4 n_5}^R$ and $\phi_{n_0 n_1 n_2 n_3 n_4}^L$ can be interpreted as conditional probabilities of the virtual sites being n_5 and n_0 , respectively, if the configurations at the edge are $(n_1 n_2 n_3 n_4)$. Here we use the shorthand notation $f_i = f(n_{i-1}, n_i, n_{i+1})$, as introduced in (4). Additionally, the matrix elements in each column of \mathbf{R} and \mathbf{L} have to sum to unity, which for any four-site configuration $(n_1 n_2 n_3 n_4)$ implies

$$\sum_{n_5=0}^1 \phi_{n_1 n_2 n_3 n_4 n_5}^R = \sum_{n_0=0}^1 \phi_{n_0 n_1 n_2 n_3 n_4}^L = 1. \quad (89)$$

Applying the dynamical rule (6) to the ansatz (88) while taking into account the normalization condition (89), it immediately follows that for any combination of n_1, n_2, n_3, n_4 the following holds:

$$R_{n_1 n_2 n_3 n_4}^{n_1 n_2 n_3 n_4} = L_{n_1 n_2 n_3 n_4}^{n_1 n_2 n_3 n_4} = 1. \quad (90)$$

Furthermore, we note that the steady state is restricted to the subspace without pairs of 1s, therefore we can without loss of generality set

$$R_{1100}^{1100} = R_{1101}^{1101} = L_{0011}^{0011} = L_{1011}^{1011} = 1. \quad (91)$$

After reducing the number of parameters, we are left with three nondeterministic 2×2 blocks per boundary propagator, each one of them given by two parameters, either $(\phi_{n_1 n_2 n_3 01}^R, \phi_{n_1 n_2 n_3 11}^R)$ or $(\phi_{10 n_1 n_2 n_3}^L, \phi_{11 n_1 n_2 n_3}^L)$, with the fixed configuration (n_1, n_2, n_3) . Plugging the ansatz into boundary equations (85) reduces the number of parameters to one per block. Explicitly,

$$\phi_{00001}^R = \frac{\omega[(\lambda - 1)\omega + \xi^2]}{\lambda[(\lambda - 1)\xi + \omega^2]} + \theta_1^R, \quad \phi_{00011}^R = \frac{(\lambda - 1)\xi + \omega^2}{\xi[(\lambda - 1)^2 - \xi\omega]} \theta_1^R, \quad \phi_{01001}^R = \frac{\xi[(\lambda - 1)\omega + \xi^2]}{\lambda(\lambda - 1)[(\lambda - 1)^2 - \xi\omega]} + \theta_2^R,$$

$$\phi_{01011}^R = (\lambda - 1)\theta_2^R, \quad \phi_{10001}^R = \frac{\omega[(\lambda - 1)\omega + \xi^2]}{\lambda[(\lambda - 1)\xi + \omega^2]} + \theta_3^R, \quad \phi_{10011}^R = \frac{\xi[(\lambda - 1)\xi + \omega^2]}{\omega[(\lambda - 1)^2 - \xi\omega]} \theta_3^R, \quad (92)$$

where $\theta_{1,2,3}^R$ are the free parameters corresponding to the three nondeterministic blocks. Analogously, introducing the left-boundary coefficients $\theta_{1,2,3}^L$, the solution to (86) is given by

$$\begin{aligned}\phi_{10000}^L &= \frac{\xi[(\lambda-1)\xi + \omega^2]}{\lambda[(\lambda-1)\omega + \xi^2]} + \theta_1^L, & \phi_{11000}^L &= \frac{(\lambda-1)\omega + \xi^2}{\omega[(\lambda-1)^2 - \xi\omega]} \theta_1^L, & \phi_{10010}^L &= \frac{\omega[(\lambda-1)\xi + \omega^2]}{\lambda(\lambda-1)[(\lambda-1)^2 - \xi\omega]} + \theta_2^L, \\ \phi_{11010}^L &= (\lambda-1)\theta_2^L, & \phi_{10001}^L &= \frac{\xi[(\lambda-1)\xi + \omega^2]}{\lambda[(\lambda-1)\omega + \xi^2]} + \theta_3^L, & \phi_{11001}^L &= \frac{\omega[(\lambda-1)\omega + \xi^2]}{\xi[(\lambda-1)^2 - \xi\omega]} \theta_3^L.\end{aligned}\quad (93)$$

Equations (92) and (93) provide the most general form of the boundary propagators \mathbf{R} and \mathbf{L} , for which the asymptotic state introduced in the previous subsection is the fixed point. Note that the parameters $\theta_{1,2,3}^{R/L}$ are not completely arbitrary, since all the matrix elements of the stochastic boundary matrices should be between 0 and 1.

A particularly convenient choice of parametrization is to set $\theta_{1,2,3}^{R/L} = 0$. In this case the stochastic blocks can be summarized by

$$\begin{aligned}\phi_{n_1 n_2 n_3 n_4 n_5}^R &= \frac{p_{n_1 n_2 n_3 n_4 n_5 0} + p_{n_1 n_2 n_3 n_4 n_5 1}}{p_{n_1 n_2 n_3 n_4}}, \\ \phi_{n_0 n_1 n_2 n_3 n_4}^L &= \frac{p'_{0 n_0 n_1 n_2 n_3 n_4} + p'_{1 n_0 n_1 n_2 n_3 n_4}}{p'_{n_1 n_2 n_3 n_4}}.\end{aligned}\quad (94)$$

This is reminiscent of the situation observed in RCA54 (see, e.g., Ref. [39]): If the four spins at the edge are in the configuration $(n_1 n_2 n_3 n_4)$, then the probability of finding the virtual site to the right (or left) in the state n_5 (or n_0) is the same as the conditional Gibbs probability of observing the five-site configuration, given the knowledge of the state of the first four sites. The construction proves that the equilibrium distribution of finite configurations can be equivalently understood as a steady state of a boundary-driven system. Note that this does not apply to *dynamics*. Starting with a configuration on a finite subsection of the periodic lattice, while assuming a random distribution elsewhere (as described in Sec. IV A), evolving it in time and at the end averaging over all the sites outside of the finite subsection we started with, will give us a different distribution compared to taking the same initial configuration and evolving it with the stochastic boundaries.

The construction in this section represents a class of nontrivial boundary propagators, for which the NESS is particularly simple. Generalizing boundary vectors to encode the information about the sites close to the boundary (similarly to the situation considered in Refs. [33,34]), might provide a richer family of stochastic boundary propagators with nontrivial NESS. However, this is beyond the scope of this paper and the full classification of all possible solvable (or integrable) boundaries remains an open question.

V. CONCLUSIONS

In this paper we have studied in detail the dynamics of the RCA201 (Floquet-PXP) model, a classical deterministic reversible cellular automaton. This model is to the classical PXP model (or one-dimensional two-spin facilitated FA model) what the RCA54 is to the classical stochastic FA

model: a deterministic lattice system with periodic circuit-dynamics with the same kinetic constraint of the corresponding KCM. The study of these RCAs thus allows us to extend our understanding of the consequences of constraints to dynamics.

We have shown that the RCA201 (Floquet-PXP) model is integrable. Its dynamics is fully determined by conserved quasiparticles that propagate ballistically and interact via collisions. As usual, integrability implies that many properties of the model can be investigated exactly. Most notably, we have calculated the exact nonequilibrium stationary state, which takes the form of a low bond dimension MPS, under both periodic and stochastic boundary conditions. The methods we applied are similar to those employed to solve the RCA54 model. Note, however, that the RCA201 is a slightly more complicated model. In particular, the stricter kinetic constraint forces the dynamics to be always strictly out of equilibrium due to the underlying period three cycling of its threefold vacua (which implies the existence of probability currents under all conditions).

Our work here opens the door for obtaining several other exact results for the dynamics of the RCA201 (Floquet-PXP) model, just like it was done recently for the RCA54. We anticipate the following: (i) the exact large deviation statistics of trajectory observables, cf., Ref. [34]; (ii) the exact MPS form of the “time state”, that is, the probability vector that encodes all time-correlators that are local in space, cf., Ref. [39]; (iii) construction of the MPS representation for the time evolution of local observables and the explicit solutions of the dynamical correlation functions and quench dynamics, cf., Ref. [38]; and (iv) the properties of the dual system to the RCA201 where propagation is in the space rather than time direction, and the consequences of this duality, cf., Ref. [27]. We hope to report on some of these in the near future.

Note added. Recently, we became aware of Ref. [46], which also considers the RCA201 (Floquet-PXP) model. While focusing mostly on its quantum generalization, Ref. [46] makes several observations about the classical RCA201 (Floquet-PXP) model, notably its integrability due to the conserved quasiparticles, that coincide with the ones we make also here (we refer the reader specifically to Appendix A of Ref. [46]). In our paper here, however, we prove exactly these and various other results.

ACKNOWLEDGMENTS

J.W.P.W. and J.P.G. acknowledge support of The Leverhulme Trust through Grant No. RPG-2018-181. K.K. and T.P. acknowledge support from the European Research Council

(ERC) under Advanced Grant No. 694544–OMNES and the Program No. P1-0402 of Slovenian Research Agency.

APPENDIX A: MPS FOR MAXIMUM ENTROPY STATE

When $\xi = \omega = 1$ the MPS representation simplifies. In particular, it can be equivalently expressed as

$$\text{tr}(\mathbf{V}_1 \mathbf{V}'_2 \cdots \mathbf{V}'_N) |_{\xi, \omega \rightarrow 1} = \text{tr}(\mathbf{W}_1 \mathbf{W}_2 \cdots \mathbf{W}_N), \quad (\text{A1})$$

where W_0 and W_1 are the following 2×2 matrices:

$$W_0 = \begin{bmatrix} 1 & 1 \\ 0 & 0 \end{bmatrix}, \quad W_1 = \begin{bmatrix} 0 & 0 \\ 1 & 0 \end{bmatrix}. \quad (\text{A2})$$

To see that the two representations are equivalent, we first introduce 4×2 and 2×4 matrices Q and R ,

$$Q = \begin{bmatrix} 1 & 0 & 1 & 1 \\ 0 & 1 & 0 & 0 \end{bmatrix}, \quad R = \begin{bmatrix} 1 & 0 \\ 0 & 1 \\ 1 & 0 \\ -1 & 0 \end{bmatrix}, \quad (\text{A3})$$

that map $V_n^{(l)}$ into a set of 2×2 matrices $\{W_n\}_{n=0,1}$,

$$W_n = Q V_n R |_{\xi, \omega \rightarrow 1} = Q V_n' R |_{\xi, \omega \rightarrow 1}. \quad (\text{A4})$$

Therefore, to prove the equivalence, we have to show that the matrix product RQ can be inserted between every pair of matrices on the left-hand side of (A1). This follows from the following two relations that hold for any three-site configuration (n_1, n_2, n_3) :

$$\begin{aligned} V_{n_1} V_{n_2}' R Q V_{n_3} |_{\xi, \omega \rightarrow 1} &= V_{n_1} V_{n_2}' V_{n_3} |_{\xi, \omega \rightarrow 1}, \\ V_{n_1} R Q V_{n_2}' R Q V_{n_3} |_{\xi, \omega \rightarrow 1} &= V_{n_1} R Q V_{n_2}' V_{n_3} |_{\xi, \omega \rightarrow 1}, \end{aligned} \quad (\text{A5})$$

and the cyclic property of trace.

The stationarity of the right-hand side of Eq. (A1) can be directly demonstrated by an analog of the three-site algebraic relation (51), which in this case trivializes,

$$\mathbf{U}(\mathbf{W}_1 \mathbf{W}_2 \mathbf{W}_3) = \mathbf{W}_1 \mathbf{W}_2 \mathbf{W}_3. \quad (\text{A6})$$

The reduced MPS can be understood as the *maximum entropy state* in the restricted sector: every configuration is equally likely, as long as there are no pairs of consecutive 1s.

APPENDIX B: DERIVATION OF THE TIME-AVERAGED MAGNETIZATION DENSITY

For systems of finite size, the PBC ensure that the trajectories are *periodic*, that is, they can be written as distinct time-ordered subsets of configurations, referred to as orbits. We can therefore generally define the time-averaged magnetization density of a trajectory as the space- and time-averaged sum over the sites of its orbit,

$$m = \frac{1}{Nl} \sum_{i=1}^N \sum_{t=0}^{l-1} n_i^{2t}, \quad (\text{B1})$$

where l denotes the cardinality of the orbit (i.e., the periodic length of the trajectory). It can be easily verified that in this form the time-averaged magnetization density depends explicitly on the microscopic properties of the configurations due to its dependence on the length of the trajectory. To formulate an expression for m of the form given in (65) therefore requires

we derive some trajectory-invariant or *characteristic* length, denoted by l_Q , that is dependent only on the system size and numbers of positive and negative quasiparticles.

With a little work, it can be demonstrated that the orbits of the system can be partitioned into distinct subsets characterized by their numbers of positive and negative quasiparticles. The sizes of the orbits of these subsets are compactly detailed in the following table:

| $Q^{(2)}$ | $Q^{(3)}$ | $F = 0$ | $F \neq 0$ |
|-----------|-----------|----------------|--|
| 0 | 0 | 3 | – |
| 0 | k | 4 | $\frac{3}{2}N$ |
| j | 0 | 2 | $\frac{3}{2}N - 2Q^+ - 2Q^-$ |
| j | k | $\frac{1}{2}N$ | $\frac{1}{2}N(\frac{3}{2}N - 2Q^+ - 2Q^-)$ |

where $j, k > 0$ are arbitrary positive integers. Here we introduce the *quasiparticle filling factor* F , defined by

$$F = 4Q^{(2)} + 8Q^{(3)} \pmod{N}, \quad (\text{B3})$$

with $Q^{(2)}$ and $Q^{(3)}$ the numbers of pairs and triples of quasiparticles, respectively, as defined in (68). Based on these observations we postulate the following form for the trajectory-invariant length:

$$l_Q = \frac{1}{2}N \left(\frac{3}{2}N - 2Q^+ - 2Q^- \right), \quad (\text{B4})$$

which depends explicitly on the macroscopic properties of the model but also divides the size of every class of orbit detailed in (B2). This then allows us to write the time-averaged magnetization density as

$$m_Q = \frac{1}{Nl_Q} \sum_{i=1}^N \sum_{t=0}^{l_Q-1} n_i^{2t}. \quad (\text{B5})$$

We briefly remark here that the values in (B2) are the *maximum* sizes of the orbits as spatial symmetries of the configurations (e.g., translational symmetries explicitly dependent on the positions of the quasiparticles or sites) facilitate orbits of fractional sizes. This is, however, irrelevant as the sizes of these orbits will also be divisors of the length l_Q .

We now separate the Nl_Q sites in (B5) into three distinct parts associated to the vacua, free quasiparticles and interactions. Here, by “free quasiparticles” and “interactions” we are explicitly referring to the sites in Fig. 5 colored green/red (medium or dark gray) and yellow (light gray), respectively, with the vacua corresponding to the sites colored white. Specifically, we have

$$Nl_Q = N_v + N_q + N_i, \quad (\text{B6})$$

where N_v , N_q , and N_i denote the number of vacua, free quasiparticle, and interaction sites, respectively. Considering first the sites associated to interactions, it follows directly from the properties of the trajectory-invariant length that there are exactly NQ^+Q^- interactions, that is, for a trajectory of length l_Q every positive quasiparticle interacts with every negative quasiparticle N times. Noting that the interactions between quasiparticles occupy three sites of the lattice then yields

$$N_i = 3NQ^+Q^-. \quad (\text{B7})$$

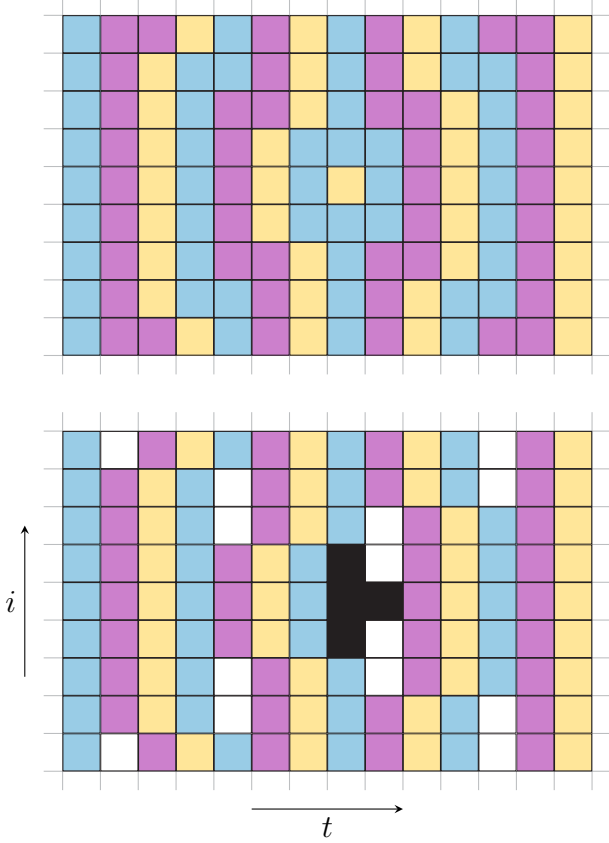


FIG. 10. Staggered vacuum configurations. A schematic comparing the vacua representation in Fig. 4 to the effective description of staggered vacuum configurations. On the bottom, sites of the vacuum are colored as in the scheme shown above with the remaining sites belonging to the effective free quasiparticles and the interactions respectively colored white and black for clarity. As per convention, only the configurations at even t time steps are shown.

Focusing now on the free quasiparticles, it follows trivially from the conservation laws that at each time step there are Q^+ positive and Q^- negative quasiparticles, respectively. Given that each occupies two sites of the lattice, we have

$$N_q = 2l_Q Q^+ + 2l_Q Q^- - 4N Q^+ Q^-, \quad (\text{B8})$$

where the final term prevents the double counting of interacting quasiparticles. Finally, we consider the vacua which is simply composed of the remaining sites,

$$N_v = Nl_Q - 2l_Q Q^+ - 2l_Q Q^- + N Q^+ Q^-. \quad (\text{B9})$$

We now map these sites to an effective vacuum description, similarly to that pictured in the middle diagram of Fig. 8, which is characterized by *staggered vacuum configurations*. By “staggered vacuum configurations”, we refer to sets of N sites staggered over adjacent time steps that are exactly the configurations of the vacuum trajectory detailed in Eq. (13), as illustrated in Fig. 10. In this new representation, the sites can again be separated into three parts,

$$Nl_Q = N'_v + N'_q + N'_i, \quad (\text{B10})$$

where N'_v denotes the number of sites associated to the staggered vacua configurations while N'_q and N'_i denote the

number of remaining sites that effectively correspond to free quasiparticles and interactions, respectively, as shown in Fig. 10. Considering first the number of effective quasiparticle sites, it is trivial to see that this is given by

$$N'_q = \frac{2}{3}l_Q Q^+ + \frac{2}{3}l_Q Q^- - \frac{4}{3}N Q^+ Q^-. \quad (\text{B11})$$

Similarly, the number of effective interacting quasiparticle sites can easily be demonstrated to be

$$N'_i = 4N Q^+ Q^-. \quad (\text{B12})$$

Finally, the number of staggered vacuum configurations is given by what remains, namely,

$$N'_v = Nl_Q - \frac{2}{3}l_Q Q^+ - \frac{2}{3}l_Q Q^- - \frac{8}{3}N Q^+ Q^-. \quad (\text{B13})$$

From here, we remark that the effective free quasiparticle sites are always 0, while a third of the staggered vacuum configuration sites and a quarter of the effective interaction sites are 1. The magnetization $M_Q = Nl_Q m_Q$ can therefore be expressed as

$$M_Q = \frac{1}{3}Nl_Q - \frac{2}{9}l_Q Q^+ - \frac{2}{9}l_Q Q^- + \frac{1}{9}N Q^+ Q^-. \quad (\text{B14})$$

Substituting in the characteristic length l_Q and dividing through by Nl_Q then yields the time-averaged magnetization density, as given in Eq. (65). We can interpret this result more intuitively by expressing m_Q as

$$m_Q = \frac{1}{3} - \frac{2}{9} \frac{Q^+ + Q^-}{N} + \frac{1}{9} \frac{Q^+ Q^-}{l_Q}. \quad (\text{B15})$$

Here the first term is the time-averaged magnetization density of the vacuum with the second and third terms representing the perturbations to this due to the quasiparticles and their interactions, respectively.

APPENDIX C: EQUIVALENCE OF THE TWO FORMS OF THE PARTITION SUM

To prove the equivalence of the partition functions in Eqs. (61) and (63), we first express the product of transfer matrices as a recursion relation of the form

$$T^K = T T^{K-1}, \quad (\text{C1})$$

with matrix elements, denoted by T_{jk}^K , given by

$$T_{jk}^K = \sum_{i=1}^4 T_{ji} T_{ik}^{K-1}, \quad (\text{C2})$$

where to ease the notation we introduce the parameter K , defined as $2K = N$. Substituting this parametrization into Eq. (61) admits the following expression for the partition function:

$$Z = \sum_{i=1}^4 T_{ii}^K. \quad (\text{C3})$$

Before searching for a solution to the system of equations in (C2), we note that there is significant redundancy in the components of the transfer matrix which we wish to eliminate. Indeed, one can show that the elements of T^K can be

succinctly written in terms of just four free recursive parameters,

$$\begin{aligned}
 T_{11}^K &= T_{22}^K, & T_{31}^K &= T_{12}^K + \omega T_{42}^K, \\
 T_{13}^K &= T_{32}^K + \xi T_{42}^K, & T_{33}^K &= T_{22}^K, \\
 T_{14}^K &= \xi T_{32}^K + \omega T_{42}^K, & T_{34}^K &= \xi T_{42}^K + \omega T_{12}^K, \\
 T_{21}^K &= T_{32}^K + \xi T_{42}^K + \omega T_{12}^K, & T_{41}^K &= T_{32}^K, \\
 T_{23}^K &= T_{12}^K + \xi T_{32}^K + \omega T_{42}^K, & T_{43}^K &= T_{12}^K, \\
 T_{24}^K &= \xi T_{12}^K + \omega T_{32}^K + \xi \omega T_{42}^K, & T_{44}^K &= T_{22}^K - T_{42}^K,
 \end{aligned} \quad (C4)$$

which reduces (C2) into the remaining four relations,

$$\begin{aligned}
 T_{12}^K &= T_{12}^{K-1} + \xi T_{32}^{K-1} + \omega T_{42}^{K-1}, \\
 T_{22}^K &= \xi T_{12}^{K-1} + T_{22}^{K-1} + \omega T_{32}^{K-1} + \xi \omega T_{42}^{K-1}, \\
 T_{32}^K &= \omega T_{12}^{K-1} + T_{32}^{K-1} + \xi T_{42}^{K-1}, \\
 T_{42}^K &= T_{22}^{K-1}.
 \end{aligned} \quad (C5)$$

Combining (C4) and (C5) provides an expression for the partition function in terms of one recursive parameter,

$$Z = 4T_{22}^K - T_{22}^{K-1}, \quad (C6)$$

which, using Eq. (C5), can be rewritten as a higher-order recurrence relation,

$$\begin{aligned}
 T_{22}^K &= 3T_{22}^{K-1} + (2\xi\omega - 3)T_{22}^{K-2} + (1 - \xi\omega)T_{22}^{K-3} \\
 &\quad + (\xi^3 + \omega^3 - \xi^2\omega^2 - \xi\omega)T_{22}^{K-4}.
 \end{aligned} \quad (C7)$$

To relate this expression for the partition function to Eq. (63) it suffices to find a combinatoric form for T_{22}^K ,

$$T_{22}^K = \sum_{\{Q\}} C_Q^K \xi^{Q^+} \omega^{Q^-}, \quad (C8)$$

where C_Q^K is some combinatoric factor to be determined and the set $\{Q\}$ the set of tuples of positive and negative quasiparticle numbers satisfying the constraints in Eqs. (16) and (66). With a little work, one can show that the combinatoric term is given by

$$C_Q^K = \binom{K - \frac{1}{3}Q^+ - \frac{2}{3}Q^-}{Q^+} \binom{K - \frac{1}{3}Q^- - \frac{2}{3}Q^+}{Q^-}. \quad (C9)$$

The partition function can then be rewritten as

$$Z = \sum_{\{Q\}} (4C_Q^K - C_Q^{K-1}) \xi^{Q^+} \omega^{Q^-}, \quad (C10)$$

where to combine summations we have used the property that the binomial coefficients vanish when Eq. (66) is not satisfied. Utilizing the binomial identity $\binom{n-1}{k} = \frac{n-k}{n} \binom{n}{k}$, we can express C_Q^{K-1} in terms of C_Q^K , specifically,

$$C_Q^{K-1} = \frac{(K - \frac{2}{3}Q^+ - \frac{4}{3}Q^-)(K - \frac{2}{3}Q^- - \frac{4}{3}Q^+)}{(K - \frac{1}{3}Q^+ - \frac{2}{3}Q^-)(K - \frac{1}{3}Q^- - \frac{2}{3}Q^+)} C_Q^K. \quad (C11)$$

From here, with a simple substitution, we immediately see that this expression for the partition function is exactly equivalent to that in Eq. (64), where the combinatorial coefficients follow directly as


$$4C_Q^K - C_Q^{K-1} = \frac{1}{m_Q} C_Q^K = \Omega_Q. \quad (C12)$$

-
- [1] A. Bobenko, M. Bordemann, C. Gunn, and U. Pinkall, On two integrable cellular automata, *Commun. Math. Phys.* **158**, 127 (1993).
- [2] M. E. Fisher, Statistical mechanics of dimers on a plane lattice, *Phys. Rev.* **124**, 1664 (1961).
- [3] C. L. Henley, The ‘‘coulomb phase’’ in frustrated systems, *Annu. Rev. Condens. Matter Phys.* **1**, 179 (2010).
- [4] R. Moessner and K. Raman, Quantum dimer models, in *Introduction to Frustrated Magnetism: Materials, Experiments, Theory*, edited by C. Lacroix, P. Mendels, and F. Mila (Springer Science & Business Media, New York, 2011), Vol. 164, Chap. 17, pp. 437–477.
- [5] J. T. Chalker, Spin liquids and frustrated magnetism, in *Topological Aspects of Condensed Matter Physics: Lecture Notes of the Les Houches Summer School*, edited by C. Chamon, M. O. Goerbig, R. Moessner, and L. F. Cugliandolo (Oxford University Press, Oxford, 2017), Vol. 103, Chap. 3, pp. 123–162.
- [6] G. H. Fredrickson and H. C. Andersen, Kinetic Ising Model of the Glass Transition, *Phys. Rev. Lett.* **53**, 1244 (1984).
- [7] R. G. Palmer, D. L. Stein, E. Abrahams, and P. W. Anderson, Models of Hierarchically Constrained Dynamics for Glassy Relaxation, *Phys. Rev. Lett.* **53**, 958 (1984).
- [8] J. Jäckle and S. Z. Eisinger, A hierarchically constrained kinetic ising model, *Z. Phys. B* **84**, 115 (1991).
- [9] F. Ritort and P. Sollich, Glassy dynamics of kinetically constrained models, *Adv. Phys.* **52**, 219 (2003).
- [10] J. P. Garrahan, P. Sollich, and C. Toninelli, Kinetically Constrained Models, in *Dynamical Heterogeneities in Glasses, Colloids, and Granular Media*, edited by L. Berthier, G. Biroli, J.-P. Bouchaud, L. Cipelletti, and W. van Saarloos, International Series of Monographs on Physics (Oxford University Press, Oxford, 2011), Chap. 10, pp. 341–366.
- [11] J. P. Garrahan, Aspects of non-equilibrium in classical and quantum systems: Slow relaxation and glasses, dynamical large deviations, quantum non-ergodicity, and open quantum dynamics, *Physica A* **504**, 130 (2018).
- [12] M. van Horssen, E. Levi, and J. P. Garrahan, Dynamics of many-body localization in a translation-invariant quantum glass model, *Phys. Rev. B* **92**, 100305(R) (2015).
- [13] Z. Lan, M. van Horssen, S. Powell, and J. P. Garrahan, Quantum Slow Relaxation and Metastability Due to Dynamical Constraints, *Phys. Rev. Lett.* **121**, 040603 (2018).
- [14] I. Lesanovsky, Many-Body Spin Interactions and the Ground State of a Dense Rydberg Lattice Gas, *Phys. Rev. Lett.* **106**, 025301 (2011).
- [15] C. J. Turner, A. A. Michailidis, D. A. Abanin, M. Serbyn, and Z. Papić, Weak ergodicity breaking from quantum many-body scars, *Nat. Phys.* **14**, 745 (2018).

- [16] N. Pancotti, G. Giudice, J. I. Cirac, J. P. Garrahan, and M. C. Bañuls, Quantum East Model: Localization, Nonthermal Eigenstates, and Slow Dynamics, *Phys. Rev. X* **10**, 021051 (2020).
- [17] A. Nahum, J. Ruhman, S. Vijay, and J. Haah, Quantum Entanglement Growth under Random Unitary Dynamics, *Phys. Rev. X* **7**, 031016 (2017).
- [18] A. Nahum, S. Vijay, and J. Haah, Operator Spreading in Random Unitary Circuits, *Phys. Rev. X* **8**, 021014 (2018).
- [19] A. Chan, A. De Luca, and J. T. Chalker, Solution of a Minimal Model for Many-Body Quantum Chaos, *Phys. Rev. X* **8**, 041019 (2018).
- [20] B. Bertini, P. Kos, and T. Prosen, Exact Correlation Functions for Dual-Unitary Lattice Models in $1+1$ Dimensions, *Phys. Rev. Lett.* **123**, 210601 (2019).
- [21] C. W. von Keyserlingk, T. Rakovszky, F. Pollmann, and S. L. Sondhi, Operator Hydrodynamics, OTOCs, and Entanglement Growth in Systems without Conservation Laws, *Phys. Rev. X* **8**, 021013 (2018).
- [22] T. Rakovszky, F. Pollmann, and C. W. von Keyserlingk, Diffusive Hydrodynamics of Out-of-Time-Ordered Correlators with Charge Conservation, *Phys. Rev. X* **8**, 031058 (2018).
- [23] C. Sünderhauf, D. Pérez-García, D. A. Huse, N. Schuch, and J. I. Cirac, Localization with random time-periodic quantum circuits, *Phys. Rev. B* **98**, 134204 (2018).
- [24] V. Khemani, A. Vishwanath, and D. A. Huse, Operator Spreading and the Emergence of Dissipative Hydrodynamics under Unitary Evolution with Conservation Laws, *Phys. Rev. X* **8**, 031057 (2018).
- [25] S. Pai, M. Pretko, and R. M. Nandkishore, Localization in Fractonic Random Circuits, *Phys. Rev. X* **9**, 021003 (2019).
- [26] Ž. Krajnik and T. Prosen, Kardar–parisi–zhang physics in integrable rotationally symmetric dynamics on discrete space–time lattice, *J. Stat. Phys.* **179**, 110 (2020).
- [27] K. Klobas and T. Prosen, Space-like dynamics in a reversible cellular automaton, *SciPost Phys. Core* **2**, 10 (2020).
- [28] S. Wolfram, Statistical mechanics of cellular automata, *Rev. Mod. Phys.* **55**, 601 (1983).
- [29] A. Ilachinski, *Cellular Automata: A Discrete Universe* (World Scientific, Singapore, 2001).
- [30] S. Takesue, Reversible Cellular Automata and Statistical Mechanics, *Phys. Rev. Lett.* **59**, 2499 (1987).
- [31] T. Prosen and C. Mejía-Monasterio, Integrability of a deterministic cellular automaton driven by stochastic boundaries, *J. Phys. A: Math. Theor.* **49**, 185003 (2016).
- [32] A. Inoue and S. Takesue, Two extensions of exact nonequilibrium steady states of a boundary-driven cellular automaton, *J. Phys. A: Math. Theor.* **51**, 425001 (2018).
- [33] T. Prosen and B. Buča, Exact matrix product decay modes of a boundary driven cellular automaton, *J. Phys. A: Math. Theor.* **50**, 395002 (2017).
- [34] B. Buča, J. P. Garrahan, T. Prosen, and M. Vanicat, Exact large deviation statistics and trajectory phase transition of a deterministic boundary driven cellular automaton, *Phys. Rev. E* **100**, 020103(R) (2019).
- [35] A. J. Friedman, S. Gopalakrishnan, and R. Vasseur, Integrable Many-Body Quantum Floquet-Thouless Pumps, *Phys. Rev. Lett.* **123**, 170603 (2019).
- [36] S. Gopalakrishnan, Operator growth and eigenstate entanglement in an interacting integrable floquet system, *Phys. Rev. B* **98**, 060302(R) (2018).
- [37] S. Gopalakrishnan, D. A. Huse, V. Khemani, and R. Vasseur, Hydrodynamics of operator spreading and quasiparticle diffusion in interacting integrable systems, *Phys. Rev. B* **98**, 220303(R) (2018).
- [38] K. Klobas, M. Medenjak, T. Prosen, and M. Vanicat, Time-dependent matrix product ansatz for interacting reversible dynamics, *Commun. Math. Phys.* **371**, 651 (2019).
- [39] K. Klobas, M. Vanicat, J. P. Garrahan, and T. Prosen, Matrix product state of multi-time correlations, *J. Phys. A: Math. Theor.* **53**, 335001 (2020).
- [40] V. Alba, J. Dubail, and M. Medenjak, Operator Entanglement in Interacting Integrable Quantum Systems: The Case of the Rule 54 Chain, *Phys. Rev. Lett.* **122**, 250603 (2019).
- [41] V. Alba, Diffusion and operator entanglement spreading, [arXiv:2006.02788](https://arxiv.org/abs/2006.02788).
- [42] P. Fendley, K. Sengupta, and S. Sachdev, Competing density-wave orders in a one-dimensional hard-boson model, *Phys. Rev. B* **69**, 075106 (2004).
- [43] V. E. Korepin, N. M. Bogoliubov, and A. G. Izergin, *Quantum Inverse Scattering Method and Correlation Functions*, Vol. 3 (Cambridge University Press, Cambridge, UK, 1997).
- [44] B. Sutherland, *Beautiful Models: 70 Years of Exactly Solved Quantum Many-body Problems* (World Scientific, Singapore, 2004).
- [45] R. J. Baxter, *Exactly Solved Models in Statistical Mechanics* (Elsevier, Amsterdam, 2016).
- [46] T. Iadecola and S. Vijay, Nonergodic quantum dynamics from deformations of classical cellular automata, *Phys. Rev. B* **102**, 180302 (2020).

Chapter 3

Exact nonequilibrium dynamics and large deviations statistics of the Rule 150 RCA

Exact solution of the “Rule 150” reversible cellular automatonJoseph W. P. Wilkinson ^{1,2,*}, Tomaž Prosen,³ and Juan P. Garrahan^{1,2}¹*School of Physics and Astronomy, University of Nottingham, Nottingham, NG7 2RD, United Kingdom*²*Centre for the Mathematics and Theoretical Physics of Quantum Non-equilibrium Systems, University of Nottingham, Nottingham, NG7 2RD, United Kingdom*³*Department of Physics, Faculty of Mathematics and Physics, University of Ljubljana, SI-1000 Ljubljana, Slovenia*

(Received 3 December 2021; accepted 18 February 2022; published 17 March 2022)

We study the dynamics and statistics of the Rule 150 reversible cellular automaton (RCA). This is a one-dimensional lattice system of binary variables with synchronous (Floquet) dynamics that corresponds to a bulk deterministic and reversible discretized version of the kinetically constrained “exclusive one-spin facilitated” (XOR) Fredrickson-Andersen (FA) model, where the local dynamics is restricted: A site flips if and only if its adjacent sites are in different states from each other. Similar to other RCA that have been recently studied, such as Rule 54 and Rule 201, the Rule 150 RCA is integrable, however, in contrast is noninteracting: The emergent quasiparticles, which are identified by the domain walls, behave as free fermions. This property allows us to solve the model by means of matrix product ansatz. In particular, we find the exact equilibrium and nonequilibrium stationary states for systems with closed (periodic) and open (stochastic) boundaries, respectively, resolve the full spectrum of the time evolution operator and, therefore, gain access to the relaxation dynamics, and obtain the exact large deviation statistics of dynamical observables in the long-time limit.

DOI: [10.1103/PhysRevE.105.034124](https://doi.org/10.1103/PhysRevE.105.034124)**I. INTRODUCTION**

In this paper we study the Rule 150 reversible cellular automaton (RCA) and solve many of its dynamical properties exactly. The model is defined on a one-dimensional lattice of sites of binary variables with deterministic and reversible discrete classical “circuit” dynamics. The naming of this RCA is due to the classification introduced in Ref. [1], according to the specific dynamical rule.

The Rule 150 RCA is similar in many respects to other recently studied RCA, specifically, Rule 54 [2–12] (for a review see Ref. [13]) and Rule 201 [14,15]: (i) its dynamics is defined in terms of local space and time reversible gates applied periodically (in this sense it can be thought of as a driven Floquet system); (ii) the local dynamical rules impose kinetic constraints similar to those of known stochastic kinetically constrained models (KCM [16–18]), particularly, variations of the Fredrickson-Andersen (FA) model: the “exclusive one-spin facilitated” FA (XOR-FA) model [19] in the case of Rule 150, and the “one-spin facilitated” FA (FA or OR-FA) [20] and “two-spin facilitated” FA (PXP or, simply, AND-FA) [21] models, respectively, for Rules 54 [5] and 201 [15]; and (iii) the Rule 150 RCA is integrable [22], but in contrast to Rules 54 and 201, its quasiparticles are noninteracting [8].

Properties (i) and (ii) mean that the Rule 150 RCA can alternatively be called the “Floquet-XOR-FA” model, as Rules 54 and 201 can, respectively, be called the Floquet-FA [7] and Floquet-PXP [15]. Property (iii) implies that we can readily solve the Rule 150 RCA exactly, whereby the noninteracting

nature of the emergent quasiparticles makes the solutions simpler than those for Rules 54 and 201. This is precisely what we do here using matrix product ansatz. We consider the cases for periodic boundary conditions, for which the overall dynamics is completely deterministic, and open boundary conditions, where the dynamics becomes stochastic at the boundaries. We find the exact stationary states, for systems both in and out of equilibrium, obtain closed expressions for the complete spectrum of the Markov operator generating time evolution and, subsequently, resolve the relaxation dynamics, and compute the exact large deviation statistics for long-time dynamical observables.

The study of RCA models like Rules 150, 54, and 201 relates to several other areas of interest. The first of these is slow dynamics due to physical constraints. Stochastic kinetically constrained models (KCM) [20,23–25] (for a detailed review, see Refs. [16–18]) are simple models for the kind of slow dynamically heterogeneous relaxation of classical glasses. Given that these RCA can be considered to be discrete, deterministic, and reversible counterparts to KCM, a natural question is to what extent they share features with those constrained models, for example, with the existence of phase transitions in their dynamical large deviations. This helps us to understand which properties are determined by kinetic constraints compared to those governed by the nature of the dynamics (e.g., stochastic versus deterministic and integrable versus ergodic). The second related area are “circuit” systems of the brick-wall type, where dynamics is defined in terms of local gates applied synchronously throughout the system. Recently, this has become a much studied problem in the fields of quantum many-body physics, where the gates correspond to either unitary or dissipative transformations, as the

*Corresponding author: joseph.wilkinson@nottingham.ac.uk

cellular automata can be used as tractable systems to address questions regarding, for example, entanglement growth, localization, operator spreading, chaos, and integrability [26–34]. In particular, circuit models exhibiting space-time duality are specially amenable to analytic solutions [10,29,35,36]. The third related area is that of quantum KCM for the exploration of issues associated to quantum relaxation, nonergodicity, and nonthermal eigenstates [37–40].

The main objective of this paper is to provide a clear, comprehensive, and self-contained study of the dynamics of the Rule 150 RCA. The simplicity of the model allows us to present numerous exact results (e.g., the stationary states, dynamical spectrum, and large deviations) which, for the more complex Rules 54 and 201, required several separate articles. In that sense, this current paper serves as an entry point for studying integrable RCA. The paper is organized as so. In Sec. II, we introduce the model and define the discrete dynamics. In Secs. III and IV, we find the exact solution for the stationary states under closed periodic and open stochastic boundary conditions. In Sec. V, we obtain exact analytic expressions for the entire spectrum of the stochastic time evolution operator and study the relaxation dynamics of the system in both the thermodynamic and long-time limits. Section VI then presents the exact dynamical large deviation statistics of space and time extensive observables, while Sec. VII provides our conclusions and several appendices contain miscellaneous other directly related results.

II. MODEL

In this section we introduce and define the model that we study throughout this paper.

A. Dynamics

We consider a system, defined on a (1 + 1)-dimensional discrete square space-time lattice of even size $2N$ of sites of binary variables. We identify the position in space of a site on the lattice by x , with $x = 1, 2, \dots, 2N$, and denote its associated value or state by $n_x = 0, 1$. At discrete time t , the configuration \underline{n}^t of the system is represented by a binary string,

$$\underline{n}^t \equiv (n_1^t, n_2^t, \dots, n_{2N}^t) \in \{0, 1\}^{2N}, \quad (1)$$

where the site x at time t is referred to as being *empty* (or unexcited) if $n_x^t = 0$ and *occupied* (or excited) if $n_x^t = 1$. We assume the system is initially closed and has periodic boundary conditions, imposed by setting $n_{x+2N}^t \equiv n_x^t$.

The time evolution of the system is defined in discrete time and consists of two distinct time steps. In the first, $\underline{n}^{2t} \rightarrow \underline{n}^{2t+1}$, referred to as the even time step, only sites with *even* index are updated, that is, sites with odd index are left unaltered, whereas in the second, $\underline{n}^{2t+1} \rightarrow \underline{n}^{2t+2}$, the odd time step, only sites with *odd* index are updated. A full step of time evolution, $\underline{n}^{2t} \rightarrow \underline{n}^{2t+2}$, is then defined by the composition of an even and odd time step, respectively. This discrete staggered dynamics is generated by the local space-time (or “parity” [41]) mapping,

$$n_x^{t+1} = \begin{cases} f_x^t, & x+t = 0 \pmod{2}, \\ n_x^t, & x+t = 1 \pmod{2}, \end{cases} \quad (2)$$

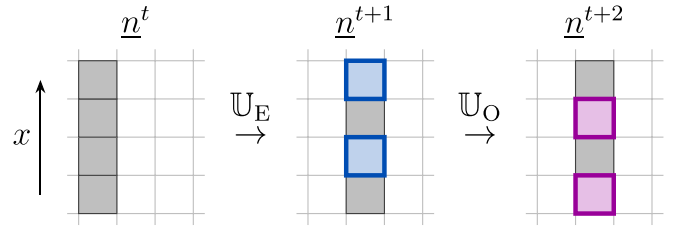


FIG. 1. Time evolution. Schematic representation of the discrete time evolution of $2N = 4$ sites of the lattice under one full step of time evolution (i.e., two successive time steps). In the first time step, referred to as the *even time step*, only the sites with even spatial indices x are updated, while during the second, the *odd time step*, only odd indexed sites are updated. Blue and purple borders indicate which sites have been updated by the local three-site function f_x^t in the even and odd time steps, respectively.

where we have introduced the shorthand notation,

$$f_x^t \equiv f(n_{x-1}^t, n_x^t, n_{x+1}^t), \quad (3)$$

to denote a three-site function acting on site x at time t . The dynamics is given by the discrete, deterministic, and reversible *Rule 150 reversible cellular automaton* (RCA), identified by the local update rule,

$$f_x^t = n_{x-1}^t + n_x^t + n_{x+1}^t \pmod{2}. \quad (4)$$

It is convenient to represent the time evolution of the lattice geometrically, as shown schematically in Fig. 1. It then follows that the local update rule in Eq. (4) can be expressed diagrammatically, as illustrated in Fig. 2, by representing the empty and occupied sites with white and black squares, respectively, where the squares on the left of each diagram correspond to the local subconfigurations of sites at time t , i.e., $(n_{x-1}^t, n_x^t, n_{x+1}^t)$, while the squares on the right are the same subset of sites at $t + 1$, that is, after the local update rule Eq. (4) acts on the triplet of sites, i.e., $(n_{x-1}^{t+1}, n_x^{t+1}, n_{x+1}^{t+1}) \equiv$

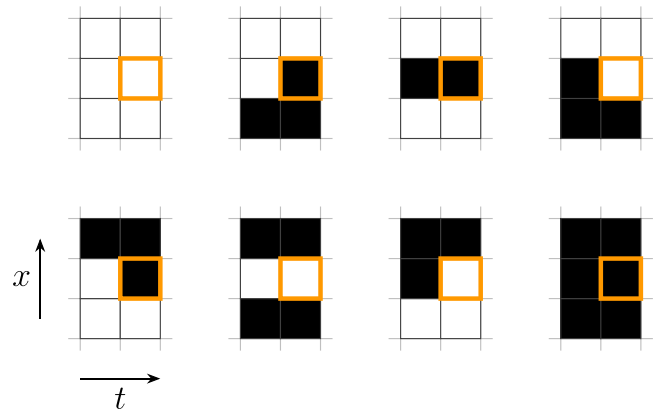


FIG. 2. Rule 150. Illustration of the Rule 150 cellular automaton, as defined in Eq. (4), where white and black squares represent empty and occupied sites, respectively. In each diagram, only the central site is updated by the local three-site update rule f_x^t , as indicated by the orange borders. Note also the discrete local symmetries of the model: spatial-inversion (“up-down”), time-reversal (“left-right”), and particle-hole (“black-white”).

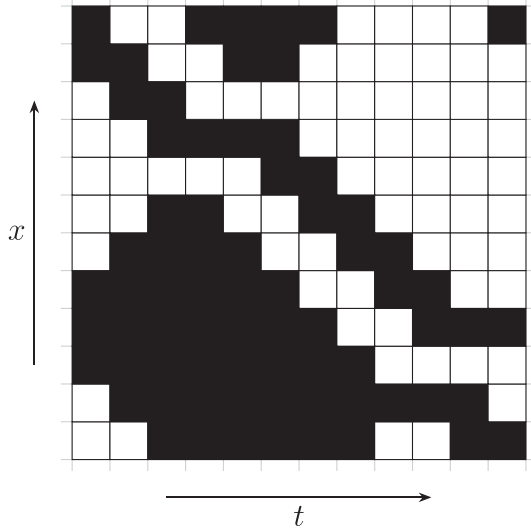


FIG. 3. Dynamics. An example of the discrete time evolution of a random initial configuration with periodic boundary conditions. We intuitively interpret the pairs of adjacent sites located at the interfaces between sets of empty and occupied sites (i.e., $\begin{smallmatrix} \blacksquare \\ \square \end{smallmatrix}$, $\begin{smallmatrix} \square \\ \blacksquare \end{smallmatrix}$) as up- and down-moving *quasiparticles* that are noninteracting and propagate ballistically with velocities of $v^\pm = \pm 1$, respectively. Notice that after colliding, the sites of the quasiparticles are exchanged (i.e., $\begin{smallmatrix} \blacksquare \\ \square \end{smallmatrix} \leftrightarrow \begin{smallmatrix} \square \\ \blacksquare \end{smallmatrix}$).

which conserves the parity of the number of excited sites. For more details on the symmetries, see Appendix A.

C. Quasiparticles

The graphical representation for the model introduced in Fig. 1 immediately offers an intuitive interpretation of the discrete dynamics in terms of up- and down-moving *quasiparticles* (see, e.g., Fig. 3), which propagate ballistically with constant velocities of $v^\pm = \pm 1$ and interact trivially without scattering. We can, therefore, interpret the model as a discretized *Fermi gas* (i.e., an ensemble of noninteracting fermions in discrete space and time). The quasiparticles, or *solitons*, are identified as pairs of adjacent sites located at the interfaces between sets of empty and occupied sites (i.e., the *domain walls*), as highlighted in Fig. 3. Specifically,

$$(0, 1) \equiv \begin{smallmatrix} \blacksquare \\ \square \end{smallmatrix}, \quad (1, 0) \equiv \begin{smallmatrix} \square \\ \blacksquare \end{smallmatrix}. \quad (22)$$

Whether a quasiparticle is *positive* (i.e., an up-mover) or *negative* (i.e., down-mover) depends explicitly on the parity of the sum of the space and time indices, as succinctly detailed by the following expression:

$$(n'_x, 1 - n'_x) \equiv \begin{cases} \text{negative,} & x + t = 0 \pmod{2}, \\ \text{positive,} & x + t = 1 \pmod{2}. \end{cases} \quad (23)$$

It then follows that quasiparticles only collide if they have opposite velocities. Specifically, the interactions between quasiparticles are necessarily *two-body*, involving exactly one up-mover and one down-mover, and are given by the partial overlap of the subconfigurations representing the positive and

negative quasiparticles. Explicitly,

$$(0, 1, 0) \equiv \begin{smallmatrix} \square \\ \blacksquare \\ \square \end{smallmatrix}, \quad (1, 0, 1) \equiv \begin{smallmatrix} \blacksquare \\ \square \\ \blacksquare \end{smallmatrix}. \quad (24)$$

The remaining sites between quasiparticles, namely, the subsets of empty and occupied sites,

$$\begin{matrix} \vdots \\ \vdots \\ \vdots \end{matrix} \begin{smallmatrix} \square \\ \square \\ \square \end{smallmatrix} \equiv (\dots, 0, 0, \dots), \quad \begin{matrix} \vdots \\ \vdots \\ \vdots \end{matrix} \begin{smallmatrix} \blacksquare \\ \blacksquare \\ \blacksquare \end{smallmatrix} \equiv (\dots, 1, 1, \dots), \quad (25)$$

are then collectively referred to as *vacua*.

Due to the even system size and periodic boundaries, the numbers of positive and negative quasiparticles in a configuration are *constrained* and, therefore, must satisfy the following identity:

$$N_n^+ - N_n^- = 0 \pmod{2}, \quad (26)$$

where N_n^+ and N_n^- count the total number of positive and negative quasiparticles, respectively, in the configuration \underline{n} . To prove this, we introduce a graph representation for the lattice and demonstrate that all closed walks, which correspond to the configurations, are composed of cycles that necessarily satisfy the physical constraint Eq. (26). The details of this proof are presented in Appendix B.

III. EQUILIBRIUM STATIONARY STATES FOR PERIODIC BOUNDARY CONDITIONS

A particularly interesting family of macroscopic states are those invariant under time evolution. In this section, we consider the *equilibrium stationary states* (ESS). The simplest class of ESS, as we will show, can be constructed by introducing a pair of chemical potentials associated to the quasiparticles of each species which are conjugate to the numbers of positive and negative quasiparticles that are conserved by the deterministic dynamics and periodic boundary conditions (PBC). We demonstrate that these stationary states correspond to *generalized Gibbs states*, which we show can be expressed in two equivalent forms. Namely, using a *patch state ansatz* (PSA) and as a *matrix product state* (MPS), as was done for Rule 54 in Refs. [2] and [4], respectively. The principal benefit of the PSA is in its intuitive construction, which only requires that the states be stationary and exhibit short-range correlations. Moreover, it facilitates a rigorous derivation for an efficient MPS representation of the state, which manifests a highly versatile algebraic structure that explicitly demonstrates the stationarity of the states without relying on the prior equivalence to the PSA.

A. Patch state ansatz

Given the staggering of the discrete time evolution, we require the stationary states to map into themselves after a full step of time evolution (i.e., a consecutive even and odd time step). Therefore, each ESS is associated to two vectors, \mathbf{p} and \mathbf{p}' , which correspond to the even and odd time steps,

respectively,

$$\mathbb{U}_E \mathbf{p} = \mathbf{p}', \quad \mathbb{U}_O \mathbf{p}' = \mathbf{p}. \quad (27)$$

For closed systems with period boundary conditions, the dynamics is reversible and so the conditions for time invariance Eq. (27) can be recast as

$$\mathbb{U}_E \mathbf{p} = \mathbb{U}_O \mathbf{p}. \quad (28)$$

We now propose the following patch state ansatz, similar to those introduced for Rule 54 [2] and Rule 201 [15], for the components p_n of the stationary state \mathbf{p} , that can be straightforwardly demonstrated to be the simplest ansatz of this form. Namely, the staggered product of $2N$ rank 2 tensors exhibiting short-range correlations,

$$p_n = \frac{1}{Z} (X_{n_1, n_2} Y_{n_2, n_3} \cdots X_{n_{2N-1}, n_{2N}} Y_{n_{2N}, n_1}), \quad (29)$$

where $X_{n_x, n_{x+1}}$ and $Y_{n_x, n_{x+1}}$ are the rank 2 tensors to be determined, and Z is the partition function given by the normalization.

To ensure that the stationarity condition Eq. (28) is satisfied, the following equality must hold for each and every configuration \underline{n} :

$$\begin{aligned} X_{n_1, f_2} Y_{f_2, n_3} \cdots X_{n_{2N-1}, f_{2N}} Y_{f_{2N}, n_1} \\ = X_{f_1, n_2} Y_{n_2, f_3} \cdots X_{f_{2N-1}, n_{2N}} Y_{n_{2N}, f_1}. \end{aligned} \quad (30)$$

For $N > 1$, this set of equations is highly degenerate and overdetermined, and simplifies to the following conditions for the scalar components:

$$X_{00} Y_{00} = X_{11} Y_{11}, \quad X_{01} Y_{10} = X_{10} Y_{01}. \quad (31)$$

We recall that the probabilities p_n are normalized by the partition function Z and so we are free to set $X_{00} Y_{00} = 1$ which, together with Eq. (31), implies

$$X_{00} Y_{00} = X_{11} Y_{11} = 1. \quad (32)$$

Furthermore, we note that the scalar components are determined up to the following gauge transformation:

$$\begin{aligned} X_{n_x, n_{x+1}} &\mapsto g_{n_x} X_{n_x, n_{x+1}} h_{n_{x+1}}^{-1}, \\ Y_{n_x, n_{x+1}} &\mapsto h_{n_x} Y_{n_x, n_{x+1}} g_{n_{x+1}}^{-1}, \end{aligned} \quad (33)$$

which, together with the normalization in Eq. (32), allows us to choose the following gauge,

$$X_{00} = Y_{00} = X_{01} = Y_{01} = 1. \quad (34)$$

Combining the solutions to the system of Eqs. (31) with the chosen normalization Eq. (32) and gauge Eq. (34) yields the following two-parameter family of solutions:

$$\begin{aligned} X_{00} &= 1, & Y_{00} &= 1, \\ X_{01} &= 1, & Y_{01} &= 1, \\ X_{10} &= \xi \omega, & Y_{10} &= \xi \omega, \\ X_{11} &= \frac{\omega}{\xi}, & Y_{11} &= \frac{\xi}{\omega}, \end{aligned} \quad (35)$$

where ξ and ω are *spectral parameters* which, due to the nonnegativity and normalizability of the probabilities p_n , are strictly positive (i.e., $\xi, \omega \in \mathbb{R}^+$).

The conditions for stationarity Eq. (27), together with the solutions Eq. (35) imply that \mathbf{p}' , that is, the stationary state

associated with the odd time step, takes on a form similar to \mathbf{p} , but with the patch tensors exchanged. Explicitly,

$$p'_n = \frac{1}{Z} (Y_{n_1, n_2} X_{n_2, n_3} \cdots Y_{n_{2N-1}, n_{2N}} X_{n_{2N}, n_1}). \quad (36)$$

We remark that interchanging the roles of the patch state tensors $X_{n_x, n_{x+1}} \leftrightarrow Y_{n_x, n_{x+1}}$ is equivalent to exchanging the spectral parameters $\xi \leftrightarrow \omega$, and, therefore the states $\mathbf{p} \leftrightarrow \mathbf{p}'$. Hence, the PSA preserves the symmetry of the model, specifically, shifting the state one site in space is equivalent to evolving the state one step in time.

B. Conserved charges

The parametrization chosen for the tensors in Eq. (35) is arbitrary. However, these solutions exhibit a physically intuitive form, whereby the spectral parameters ξ and ω can be expressed in terms of thermodynamic quantities,

$$\xi = \exp(-\mu^+), \quad \omega = \exp(-\mu^-), \quad (37)$$

with μ^\pm the chemical potentials associated to the positive and negative quasiparticles, respectively. To demonstrate this, we utilize the gauge freedom to transform the patch state tensor solutions into an equivalent form. Explicitly, we choose the gauge transformation

$$\begin{aligned} g_0 &= 1, & h_0 &= 1, \\ g_1 &= \frac{1}{\omega}, & h_1 &= \frac{1}{\xi}, \end{aligned} \quad (38)$$

which, by Eq. (35), yields

$$\begin{aligned} X_{00} &\mapsto 1, & Y_{00} &\mapsto 1, \\ X_{01} &\mapsto \xi, & Y_{01} &\mapsto \omega, \\ X_{10} &\mapsto \xi, & Y_{10} &\mapsto \omega, \\ X_{11} &\mapsto 1, & Y_{11} &\mapsto 1. \end{aligned} \quad (39)$$

It follows from Eq. (23) that the number of each species of quasiparticle within a configuration \underline{n} can be determined by the counts of the two site subconfigurations (0, 1) and (1, 0). Therefore, the newly parametrized solutions imply that the components p_n of the stationary states \mathbf{p} can be distributed according to a *grand canonical ensemble*,

$$p_n = \frac{1}{Z} \xi^{N_n^+} \omega^{N_n^-}, \quad (40)$$

where the numbers of positive and negative quasiparticles N_n^\pm in the configurations \underline{n} can be calculated directly by taking the logarithmic derivatives of the (unnormalized) probability components p_n of the PSA. Explicitly,

$$\begin{aligned} N_n^+ &= \frac{d}{d \ln \xi} \ln \prod_{x=1}^N X_{n_{2x-1}, n_{2x}}, \\ N_n^- &= \frac{d}{d \ln \omega} \ln \prod_{x=1}^N Y_{n_{2x}, n_{2x+1}}, \end{aligned} \quad (41)$$

TABLE I. Locally conserved charges. The number of locally conserved charges $\#_r$ with support r , obtained numerically by solving the sets of equations in Eq. (43) with rank r tensors.

| r | 2 | 3 | 4 | 5 | 6 | 7 | 8 | 9 |
|--------|---|---|---|---|---|---|----|----|
| $\#_r$ | 2 | 2 | 4 | 4 | 8 | 8 | 16 | 16 |

which can equivalently be written as extensive sums over the locally conserved charges as

$$N_n^+ = \sum_{x=1}^N \frac{d}{d\xi} X_{n_{2x-1}, n_{2x}}, \quad (42)$$

$$N_n^- = \sum_{x=1}^N \frac{d}{d\omega} Y_{n_{2x}, n_{2x+1}}.$$

It follows straightforwardly that the positive and negative quasiparticles are exactly the elementary local charges of the Floquet-XOR-FA model. Still, they do not represent a *complete* set of local charges. Indeed, it can be readily shown that PSA tensors with ranks $r > 2$ yield similarly conserved charges that correspond to localized groups of noninteracting quasiparticles of the same species. Solving an equivalent set of equations to Eq. (30), explicitly,

$$p_n = \frac{1}{Z} (X_{n_1, \dots, n_r} Y_{n_{2}, \dots, n_{r+1}} \cdots Y_{n_{2N}, \dots, n_{r-1}}), \quad (43)$$

we observe that the Floquet-XOR-FA model possesses an exponential number of locally conserved charges, as can be seen in Table I. We can then immediately deduce that the number of groups of noninteracting quasiparticles of the same species with support r , denoted by $\#_r$, reads

$$\#_r = 2 \sum_{k=1}^{\lfloor \frac{r}{2} \rfloor} \binom{\lfloor \frac{r}{2} \rfloor - 1}{k-1} = 2(2^{\lfloor \frac{r}{2} \rfloor - 1}) = 2^{\lfloor \frac{r}{2} \rfloor}, \quad (44)$$

where k counts the number of quasiparticles of the same species in the localized group with support r . Intuitively, this can be understood simply as following directly from the physical properties of the quasiparticles. Specifically, the expression for $\#_r$ counts the total number of ways of arranging k quasiparticles of the same species of size 2 on r sites for $k = 1, \dots, \lfloor \frac{r}{2} \rfloor$ for each species of quasiparticle.

C. Matrix product ansatz

As with Rules 54 [4] and 201 [15], the stationary states can equivalently be expressed in terms of *matrix product states*,

$$p_n = \frac{1}{Z} \text{Tr}(V_{n_1} W_{n_2} \cdots V_{n_{2N-1}} W_{n_{2N}}), \quad (45)$$

where V_{n_x} and W_{n_x} are matrices to be determined, and Z is the partition function. To efficiently derive the exact MPS construction and present the versatile algebraic cancellation scheme that explicitly demonstrates the stationarity of the states, it will prove convenient to introduce the following vectors of matrices, which correspond to the physical sites of the lattice,

$$\mathbf{V}_x = \begin{bmatrix} V_0 \\ V_1 \end{bmatrix}, \quad \mathbf{W}_x = \begin{bmatrix} W_0 \\ W_1 \end{bmatrix}. \quad (46)$$

Using these vectors of matrices, we can compactly rewrite the stationary state \mathbf{p} using *tensor product notation*,

$$\mathbf{p} = \frac{1}{Z} \text{Tr}[V_1 W_2 \cdots V_{2N-1} W_{2N}], \quad (47)$$

where the subscripts denote which elementary space \mathbb{R}^2 , i.e., which site x of the lattice, of the tensor product the vector is an element of. Formally, Eq. (47) reads

$$\mathbf{p} = \frac{1}{Z} \text{Tr}(V \otimes W \otimes \cdots \otimes V \otimes W); \quad (48)$$

however, we choose to use explicit notation with the site subscripts for clarity.

To exactly construct the MPS from the PSA, we introduce a two-dimensional *auxiliary space* which allows us to define V_{n_x} and W_{n_x} as 2×2 matrices, whose nonzero components are given by the PSA tensors,

$$[V_{n_x}]_{n_x, n_{x+1}} \equiv X_{n_x, n_{x+1}}, \quad (49)$$

$$[W_{n_x}]_{n_x, n_{x+1}} \equiv Y_{n_x, n_{x+1}},$$

which gives the following general class of 2×2 matrices,

$$V_0 = \begin{bmatrix} X_{00} & X_{01} \\ 0 & 0 \end{bmatrix}, \quad W_0 = \begin{bmatrix} Y_{00} & Y_{01} \\ 0 & 0 \end{bmatrix}, \quad (50)$$

$$V_1 = \begin{bmatrix} 0 & 0 \\ X_{10} & X_{11} \end{bmatrix}, \quad W_1 = \begin{bmatrix} 0 & 0 \\ Y_{10} & Y_{11} \end{bmatrix}.$$

Note that, by construction, Eq. (49) ensures equivalence between the MPS and PSA representations of the ESS,

$$\text{Tr}(V_{n_1} \cdots W_{n_{2N}}) \equiv X_{n_1, n_2} \cdots Y_{n_{2N}, n_1}. \quad (51)$$

Explicitly, the matrices V_{n_x} and W_{n_x} read

$$V_0 = \begin{bmatrix} 1 & \xi \\ 0 & 0 \end{bmatrix}, \quad W_0 = \begin{bmatrix} 1 & \omega \\ 0 & 0 \end{bmatrix}, \quad (52)$$

$$V_1 = \begin{bmatrix} 0 & 0 \\ \xi & 1 \end{bmatrix}, \quad W_1 = \begin{bmatrix} 0 & 0 \\ \omega & 1 \end{bmatrix}.$$

While the stationarity of the state \mathbf{p} is directly implied by the equivalence between the two representations, the MPS is unique in that it exhibits an algebraic structure that allows us to explicitly demonstrate the stationarity. Namely, the matrices satisfy a *cubic algebraic relation*,

$$U_x [V_{x-1} W_x V_{x+1} S] = V_{x-1} S V_x W_{x+1}, \quad (53)$$

which compactly encodes the matrix product identities,

$$V_{n_{x-1}} W_{f_x} V_{n_{x+1}} S = V_{n_{x-1}} S V_{n_x} W_{n_{x+1}}, \quad (54)$$

obtained by explicitly writing out the physical space vectors in terms of their auxiliary space matrices. Here, we have introduced the *delimiter matrix*,

$$S = \frac{1}{(1-s^-)(1+s^+)} \begin{bmatrix} 1 - \xi\omega & \omega - \xi \\ \omega - \xi & 1 - \xi\omega \end{bmatrix}, \quad (55)$$

which is defined by the bulk algebraic relations Eq. (54), with the parameters s^\pm equal to either of the spectral parameters (i.e., $s^+ = \xi$ or ω and $s^- = \xi$ or ω). We can easily demonstrate that the inverse of the delimiter matrix S is given by exchanging the spectral parameters,

$$S^{-1}(\xi, \omega) \equiv S(\omega, \xi). \quad (56)$$

Noticing that the MPS bulk matrices V_{n_x} and W_{n_x} are similarly given by an exchange of parameters,

$$W_{n_x}(\xi, \omega) = V_{n_x}(\omega, \xi), \quad (57)$$

immediately implies a *dual-relation*,

$$U_x[\mathbf{W}_{x-1}S^{-1}\mathbf{W}_xV_{x+1}] = \mathbf{W}_{x-1}V_x\mathbf{W}_{x+1}S^{-1}, \quad (58)$$

which explicitly encodes the following identities:

$$W_{n_{x-1}}S^{-1}W_{f_x}V_{n_{x+1}} = W_{n_{x-1}}V_{n_x}W_{n_{x+1}}S^{-1}. \quad (59)$$

Before setting s^\pm , we must consider the cases $\xi \rightarrow 1$ and $\omega \rightarrow 1$ where the delimiter matrix and its inverse are not well defined. However, we can trivially demonstrate that the matrix products $V_{n_x}S$ and $W_{n_x}S^{-1}$ are well defined and finite in the limits $\xi \rightarrow 1$ and $\omega \rightarrow 1$, respectively, if $s^- = \xi$. The following discussion, therefore, holds for all $\xi, \omega \in \mathbb{R}^+$, as required Eq. (9). From here, we are free to set $s^+ = \xi$ such that the matrix products trivialize,

$$V_{n_x}S = W_{n_x}, \quad W_{n_x}S^{-1} = V_{n_x}. \quad (60)$$

For the special case where $\xi = \omega = 1$, the states \mathbf{p} and \mathbf{p}' converge to the *maximum entropy state*: the state for which the probabilities of every configuration are equally likely. In this limit, the MPS representation for the ESS simplifies, as detailed in Appendix C.

Akin to the situation for the PSA, the stationary state \mathbf{p}' , corresponding to the odd time step, takes an identical form to the even time step stationary state \mathbf{p} , but with the spectral parameters exchanged $\xi \leftrightarrow \omega$ which equates to exchanging the physical space vectors $\mathbf{V}_x \leftrightarrow \mathbf{W}_x$,

$$\mathbf{p}' = \frac{1}{Z} \text{Tr}[\mathbf{W}_1\mathbf{V}_2 \cdots \mathbf{W}_{2N-1}\mathbf{V}_{2N}]. \quad (61)$$

Explicitly, the components p'_n of the ESS \mathbf{p}' read

$$p'_n = \frac{1}{Z} \text{Tr}(W_{n_1}V_{n_2} \cdots W_{n_{2N-1}}V_{n_{2N}}). \quad (62)$$

The stationarity conditions Eq. (27) then follow directly from the algebraic relations in Eqs. (53) and (58).

To prove the first of the conditions Eq. (27), we insert SS^{-1} between the matrices V_{n_1} and W_{n_2} and apply the local time evolution operator U_{2N} while utilizing Eq. (54),

$$\begin{aligned} \mathbb{U}_E \mathbf{p} &= U_2 \cdots U_{2N} \text{Tr}[V_1 S S^{-1} W_2 \cdots V_{2N-1} W_{2N}], \\ &= U_2 \cdots U_{2N-2} \text{Tr}[\mathbf{W}_1 S^{-1} \mathbf{W}_2 \cdots V_{2N-1} S V_{2N}]. \end{aligned} \quad (63)$$

We then continually apply the local time evolution operators U_x , in order, each shifting the delimiter matrix S two sites to the left, until we are left with the following:

$$\begin{aligned} \mathbb{U}_E \mathbf{p} &= U_2 \text{Tr}[\mathbf{W}_1 S^{-1} \mathbf{W}_2 V_3 S V_4 \cdots \mathbf{W}_{2N-1} V_{2N}], \\ &= \text{Tr}[\mathbf{W}_1 V_2 \mathbf{W}_3 S^{-1} S V_4 \cdots \mathbf{W}_{2N-1} V_{2N}], \end{aligned} \quad (64)$$

where, to obtain the second equality, we utilized the dual-relation in Eq. (58), together with the property that the time evolution operators are involutory (i.e., $U^2 = \mathbb{1}^{\otimes 3}$). Noting that extracting the product $S^{-1}S$ yields the ESS \mathbf{p}' proves the stationarity in Eq. (27). The second condition then follows directly from the first by taking advantage of Eqs. (56) and (57).

D. Partition function

As demonstrated in Sec. III A, the components of the stationary states p_n are distributed according to a simple grand canonical ensemble,

$$p_n = \frac{1}{Z} \exp(-\mu^+ N_n^+ - \mu^- N_n^-), \quad (65)$$

where the spectral parameters ξ and ω are given in terms of the chemical potentials μ^\pm associated to the numbers of quasiparticles N_n^\pm in the configuration \underline{n} Eq. (37). It then follows directly from the normalization of the MPS representation of the state \mathbf{p} , that the corresponding grand canonical partition function can be written as a sum over the trace of the product of the MPS auxiliary matrices. That is,

$$Z = \sum_n \text{Tr}(V_{n_1} W_{n_2} \cdots W_{n_{2N}}) \equiv \text{Tr}(T^N), \quad (66)$$

where, to obtain the second expression, we have used the linearity of the trace, and for ease of notation, introduced the *transfer matrix* T , defined as the sum of all products of auxiliary matrices on two adjacent sites,

$$T = (V_0 + V_1)(W_0 + W_1) = \begin{bmatrix} 1 + \xi\omega & \omega + \xi \\ \omega + \xi & 1 + \xi\omega \end{bmatrix}. \quad (67)$$

Similarly, it follows directly from the normalization of Eq. (40) that Z can equivalently be expressed explicitly in terms of a sum over the spectral parameters exponentiated by their respective quasiparticle numbers,

$$Z = \sum_n \xi^{N_n^+} \omega^{N_n^-} \equiv \sum_{N^\pm} \Omega(N, N^+, N^-) \xi^{N^+} \omega^{N^-}, \quad (68)$$

where, in the second expression, we have introduced the counting function Ω which counts the number of distinct configurations with N^+ positive and N^- negative quasiparticles. More precisely, Ω takes the following combinatoric form,

$$\Omega(N, N^+, N^-) = 2 \binom{N}{N^+} \binom{N}{N^-}. \quad (69)$$

Additionally, we have introduced the shorthand notation for the index of summation N^\pm to denote the set of pairs of numbers of positive and negative quasiparticles that satisfy the constraint Eq. (26), imposed by the even system size and PBC, and the following inequalities manifesting from the finite size of the quasiparticles,

$$0 \leq N^\pm \leq N, \quad (70)$$

which are implicitly given by the following binomial identity, $\binom{n < k}{k} = 0$. To prove that Eq. (69) really counts the total number of configurations of even size $2N$ with N^+ positive and N^- negative quasiparticles, it is sufficient to show that the two forms of the grand canonical partition function Eqs. (66) and (68) are equivalent. An explicit proof of this equivalence, as well as a qualitative derivation of the counting function from physical arguments, is given in Appendix D.

In the thermodynamic limit (i.e., $N \rightarrow \infty$), the expression for the grand canonical partition function in Eq. (68) can be rewritten in terms of an integral over the *densities* of positive and negative quasiparticles,

$$n^\pm \equiv \lim_{N \rightarrow \infty} \frac{N^\pm}{N}, \quad (71)$$

such that it reads

$$\mathcal{Z} \equiv \lim_{N \rightarrow \infty} Z = \int \int_0^1 dn^+ dn^- \exp(-N\mathcal{F}), \quad (72)$$

where \mathcal{F} can be interpreted as a *free energy density*. More precisely, the free energy density is defined as

$$\mathcal{F} = \mu^+ n^+ + \mu^- n^- - \mathcal{S}, \quad (73)$$

where the entropic term \mathcal{S} corresponds to an entropy density, which comes from the counting of degenerate configurations (i.e., states with equivalent numbers of positive and negative quasiparticles) and is obtained by applying the Stirling approximation to Eq. (69). Explicitly,

$$\begin{aligned} \mathcal{S} = & -[n^+ \ln n^+ + (1 - n^+) \ln(1 - n^+) \\ & + n^- \ln n^- + (1 - n^-) \ln(1 - n^-)], \end{aligned} \quad (74)$$

which has the form of an entropy density of mixing of the quasiparticles, subject to the constraints Eqs. (26) and (70).

IV. NONEQUILIBRIUM STATIONARY STATES FOR STOCHASTIC BOUNDARY CONDITIONS

As demonstrated in Sec. III, the dynamics of the model with PBC is entirely deterministic and reversible, and is *integrable* (i.e., the system exhibits conserved quantities, possesses an algebraic geometry, and is exactly solvable), which necessarily implies that the system is *nonergodic*. The configuration space is *reducible* under the dynamics and is composed of dynamically disconnected subspaces (i.e., the orbits, or *trajectories*, of the dynamical system). The number of ESS of the periodic system is, therefore, numerous and highly degenerate. To make the dynamics ergodic we impose stochastic boundary conditions (SBC) by considering a chain of finite size coupled to stochastic reservoirs that inject and eject quasiparticles, as was done for Rule 54 (see Refs. [2–4]) and Rule 201 (see Ref. [15]). We start by taking the MPS representation of the ESS for a system with PBC and use it to express the probability distribution of a finite subsection of the chain in the large system size, or *thermodynamic*, limit (i.e., $N \rightarrow \infty$). We demonstrate that the resulting state can be understood as a *nonequilibrium stationary state* (NESS) of the finite Markov chain with stochastic boundaries that create and destroy the quasiparticles with rates compatible with the chemical potentials μ^\pm of the Gibbs state in Sec III. We proceed to show that the generator of the dynamics (i.e., the Markov operator) is *irreducible* and *aperiodic*, which implies the uniqueness of the NESS, and the asymptotic approach toward it from any initial state. The dynamics is, therefore, *ergodic* and *mixing*.

A. Asymptotic states

We consider a closed system of even size $2M$ with PBC that is assumed to be in an ESS given by the parameters ξ and ω as in Sec. III. The stationary probabilities of a subsection of the chain of even length $2N \leq 2M$ are then given by summing over the probabilities corresponding to the configurations with the same $2N$ sites,

$$p_{n_1, \dots, n_{2N}}^{(2M)} = \sum_{n_{2N+1}, \dots, n_{2M}} \frac{1}{Z} \text{Tr}(V_{n_1} \cdots W_{n_{2M}}). \quad (75)$$

Utilizing the transfer matrix T , defined as the sum of all products of matrices on two adjacent sites [see Eq. (67)], the state vectors $\mathbf{p}^{(2M)}$ can be written succinctly as

$$\mathbf{p}^{(2M)} = \frac{\text{Tr}(V_1 W_2 \cdots V_{2N-1} W_{2N} T^{M-N})}{\text{Tr}(T^M)}. \quad (76)$$

We then define the state of the subsystem, of fixed even size $2N$, as the large system size limit (i.e., $M \rightarrow \infty$) of the probability distribution $\mathbf{p}^{(2M)}$,

$$\mathbf{p} \equiv \lim_{M \rightarrow \infty} \mathbf{p}^{(2M)} = \frac{\langle l | V_1 W_2 \cdots V_{2N-1} W_{2N} | r \rangle}{\chi^N \langle l | r \rangle}, \quad (77)$$

where \mathbf{p} denotes the *asymptotic probability distribution* of the open subsystem of size $2N$. Here, we have introduced χ which denotes the leading eigenvalue of T with $|r\rangle$ and $\langle l|$ the corresponding right and left eigenvectors,

$$T|r\rangle = \chi|r\rangle, \quad \langle l|T = \chi\langle l|. \quad (78)$$

Explicitly, the leading eigenvalue is given by

$$\chi = (1 + \xi)(1 + \omega), \quad (79)$$

while the associated right and left eigenvectors read

$$|r\rangle = r \begin{bmatrix} 1 \\ 1 \end{bmatrix}, \quad \langle l| = l[1 \quad 1], \quad (80)$$

where r and l are scalars determined by the normalization [n.b., the transfer matrix is *symmetric* (i.e., $T \equiv T^T$), so the leading right and left eigenvectors are equivalent up to an arbitrary scalar]. Note that the leading eigenvalue is the largest solution of the characteristic polynomial,

$$\chi^2 - 2(1 + \xi\omega)\chi + (1 - \xi^2)(1 - \omega^2) = 0, \quad (81)$$

which for $\xi, \omega \in \mathbb{R}^+$ is the only real root greater than 1.

We can similarly define the odd state \mathbf{p}' as the asymptotic form of the primed probability distribution, which takes the same form as \mathbf{p} , but with the spectral parameters exchanged (i.e., $\xi \leftrightarrow \omega$). In particular,

$$\mathbf{p}' = \frac{\langle l' | W_1 V_2 \cdots W_{2N-1} V_{2N} | r' \rangle}{\chi^N \langle l' | r' \rangle}, \quad (82)$$

where $|r'\rangle$ and $\langle l'|$ are the (leading) right and left eigenvectors of the primed transfer matrix $T'(\xi, \omega) = T(\omega, \xi)$, respectively, defined as

$$|r'(\xi, \omega)\rangle = |r(\omega, \xi)\rangle, \quad \langle l'(\xi, \omega)| = \langle l(\omega, \xi)|. \quad (83)$$

Explicitly,

$$|r'\rangle = r' \begin{bmatrix} 1 \\ 1 \end{bmatrix}, \quad \langle l'| = l'[1 \quad 1], \quad (84)$$

where $r'(\xi, \omega) = r(\omega, \xi)$ and $l'(\xi, \omega) = l(\omega, \xi)$. Note that the transfer matrix is invariant under the exchange of the parameters $\xi \leftrightarrow \omega$, namely, $T \equiv T'$ and, therefore, so are the leading eigenvalue and eigenvectors (similarly, up to an arbitrary scalar). We remark that the expressions for the asymptotic probability distributions, \mathbf{p} and \mathbf{p}' , hold for all finite subsections of the periodic chain that start at odd sites, at even and odd times, respectively. For the case where the first site of the subsection is even, we need to exchange the spectral parameters, which, as shown in Sec. III C, is equivalent to exchanging the physical space vectors $V_x \leftrightarrow W_x$.

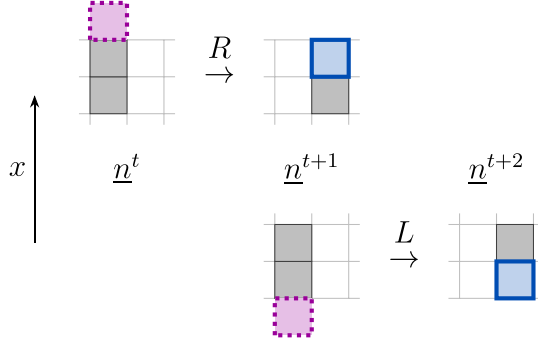


FIG. 4. Boundary propagators. The action of R and L can be understood by appending a *virtual site* to the edge of the lattice, whose state is dependent on the subconfiguration of the pair of adjacent sites, and then deterministically evolving the boundary site according to Eq. (4). Virtual sites are denoted by dotted purple, while updated sites are solid blue.

B. Compatible boundaries

Alternatively, the asymptotic probability distributions \mathbf{p} and \mathbf{p}' can be understood as the NESS of a boundary driven system whereby time evolution is deterministic in the bulk and stochastic at the boundaries. In particular, during the even time step, the sites $n_1, n_2, \dots, n_{2N-1}$ are updated deterministically by the bulk matrices U_x , while the site n_{2N} is updated stochastically by the *right boundary matrix* R_{2N} ,

$$\mathbb{M}_E = R_{2N} \prod_{x=1}^{N-1} U_{2x}. \quad (85)$$

Similarly, for the odd time step, the evolution of the sites n_2, n_3, \dots, n_{2N} is deterministic, while site n_1 is updated stochastically by the *left boundary matrix* L_1 ,

$$\mathbb{M}_O = L_1 \prod_{x=1}^{N-1} U_{2x+1}. \quad (86)$$

To ensure that only sites n_1 and n_{2N} are updated stochastically by L_1 and R_{2N} , the boundary matrices must satisfy the following compatibility conditions:

$$[L_1, U_3] = 0, \quad [R_{2N}, U_{2N-2}] = 0, \quad (87)$$

which are analogous to the conditions in Eq. (17). We can interpret the action of the boundary propagators equivalently, by imagining we temporarily append a *virtual site* to the edge of the lattice, in a state that depends on the configuration of the boundary site and its neighbor, and then updating the three sites deterministically according to Eq. (4), as demonstrated in Fig. 4. Explicitly, the components of the local boundary propagators R and L , which are given by

$$R_{2N} = \mathbb{1}^{\otimes(2N-2)} \otimes R, \quad L_1 = L \otimes \mathbb{1}^{\otimes(2N-2)}, \quad (88)$$

can be parametrized as

$$\begin{aligned} R_{(m_3, m_4), (n_3, n_4)} &= \sum_{n_5=0}^1 \delta_{m_3, n_3} \delta_{m_4, n_4} \phi_{n_3, n_4, n_5}, \\ L_{(m_1, m_2), (n_1, n_2)} &= \sum_{n_0=0}^1 \delta_{m_1, n_1} \delta_{m_2, n_2} \varphi_{n_0, n_1, n_2}, \end{aligned} \quad (89)$$

where, to improve readability, we have set $N = 2$ for R . The boundary matrices, therefore, read

$$\begin{aligned} R &= \begin{bmatrix} \phi_{000} & \phi_{011} & & \\ \phi_{001} & \phi_{010} & & \\ & \phi_{101} & \phi_{110} & \\ & \phi_{100} & \phi_{111} & \end{bmatrix}, \\ L &= \begin{bmatrix} \varphi_{000} & & \varphi_{110} & \\ \varphi_{101} & & \varphi_{011} & \\ \varphi_{100} & & \varphi_{010} & \\ & \varphi_{001} & & \varphi_{111} \end{bmatrix}, \end{aligned} \quad (90)$$

with the scalar quantities $\phi_{n_3, n_4, n_5}, \varphi_{n_0, n_1, n_2} \in (0, 1)$ the *conditional probabilities* of the virtual sites being n_5 and n_0 , respectively, given that the sites at the right and left boundaries are (n_3, n_4) and (n_1, n_2) . We can equivalently interpret the components of R and L as the conditional probabilities of either creating or destroying negative and positive quasiparticles at the boundaries, given the state of sites (n_3, n_4) and (n_1, n_2) , respectively. For example, ϕ_{001} can be understood to be the conditional probability of creating a negative quasiparticle at the right boundary given that the pair of sites $(n_3, n_4) = (0, 0)$, while φ_{110} is the conditional probability of destroying a negative quasiparticle, or equivalently not creating a positive quasiparticle, at the left boundary given that $(n_1, n_2) = (1, 0)$.

To ensure that the asymptotic probability distribution vectors \mathbf{p} and \mathbf{p}' are indeed stationary states under the stochastic time evolution, the conditions for stationarity in Eq. (27) must hold. Specifically,

$$\mathbb{M}_E \mathbf{p} = \mathbf{p}', \quad \mathbb{M}_O \mathbf{p}' = \mathbf{p}. \quad (91)$$

In addition to the bulk algebraic relations Eqs. (53) and (58), the probability states Eqs. (77) and (82) must also satisfy appropriate boundary relations to guarantee that Eq. (91) is met. In particular, for the even time step, the following boundary relations must hold:

$$\langle l | \mathbf{V}_1 \mathbf{S} = \frac{1}{\Gamma_R} \langle l' | \mathbf{W}_1, \quad (92)$$

$$R_{2N} [\mathbf{V}_{2N-1} \mathbf{W}_{2N} | r'] = \Gamma_R \mathbf{V}_{2N-1} \mathbf{S} \mathbf{V}_{2N} | r',$$

while for the odd time step, we have

$$\begin{aligned} L_1 [\langle l' | \mathbf{W}_1 \mathbf{V}_2] &= \Gamma_L \langle l | \mathbf{V}_1 \mathbf{W}_2 \mathbf{S}^{-1}, \\ \mathbf{W}_{2N} \mathbf{S}^{-1} | r' \rangle &= \frac{1}{\Gamma_L} \mathbf{W}_{2N} | r \rangle, \end{aligned} \quad (93)$$

where the scalar parameters Γ_R and Γ_L ensure the MPS is normalized and satisfies the fixed point condition Eq. (91). Immediately, we impose that the right and left boundary matrices must be *left stochastic*, more precisely, each and every column of R and L must sum to unity, implying

$$\sum_{n_5=0}^1 \phi_{n_3, n_4, n_5} = \sum_{n_0=0}^1 \varphi_{n_0, n_1, n_2} = 1, \quad (94)$$

which reduces the 4×4 stochastic matrices R and L to two nondeterministic 2×2 blocks of two parameters per boundary propagator.

Substituting the boundary ansatz Eq. (89) into the system of equations for the even time step Eq. (92) yields the following matrix product identities:

$$\langle l|V_{n_1}S = \frac{1}{\Gamma_R} \langle l'|W_{n_1}, \quad (95)$$

$$\sum_{n_5=0}^1 \phi_{n_3, f_4, n_5} V_{n_3} W_{f_4} |r\rangle = \Gamma_R V_{n_3} S V_{n_4} |r'\rangle, \quad (96)$$

where, for readability, we have again set $N = 2$. Solving separately these equations, while taking into account the normalization Eq. (94), returns the following expressions for the components of the right boundary propagator:

$$\begin{aligned} \phi_{001} &= \xi \theta_0, & \phi_{011} &= \frac{\xi - \omega}{\xi(1 + \omega)} + \theta_0, \\ \phi_{110} &= \xi \theta_1, & \phi_{100} &= \frac{\xi - \omega}{\xi(1 + \omega)} + \theta_1, \end{aligned} \quad (97)$$

where θ_0 and θ_1 are the free parameters corresponding to the two nondeterministic blocks of R_{2N} , with the boundary vector normalization given by

$$\frac{r}{r'} = \Gamma_R, \quad \frac{l}{l'} = \frac{1}{\Gamma_R}. \quad (98)$$

Similarly, substituting the ansatz Eq. (89) into the equations for the odd time step Eq. (93) gives the following identities:

$$\sum_{n_0=0}^1 \varphi_{n_0, f_1, n_2} \langle l'|W_{f_1} V_{n_2} = \Gamma_L \langle l|V_{n_1} W_{n_2} S^{-1}, \quad (99)$$

$$W_{n_{2N}} S^{-1} |r'\rangle = \frac{1}{\Gamma_L} W_{n_{2N}} |r\rangle, \quad (100)$$

which, after solving, return the following expressions for the left boundary propagator components:

$$\begin{aligned} \varphi_{100} &= \omega \vartheta_0, & \varphi_{110} &= \frac{\omega - \xi}{\omega(1 + \xi)} + \vartheta_0, \\ \varphi_{011} &= \omega \vartheta_1, & \varphi_{001} &= \frac{\omega - \xi}{\omega(1 + \xi)} + \vartheta_1, \end{aligned} \quad (101)$$

where ϑ_0 and ϑ_1 are the corresponding left boundary free parameters, with the normalization reading

$$\frac{r}{r'} = \Gamma_L \frac{1 + \xi}{1 + \omega}, \quad \frac{l}{l'} = \frac{1}{\Gamma_L} \frac{1 + \omega}{1 + \xi}. \quad (102)$$

Equating the expressions for the boundary parameters in Eqs. (98) and (102) then necessarily implies that

$$\frac{\Gamma_R}{\Gamma_L} = \frac{1 + \xi}{1 + \omega}. \quad (103)$$

At this point, we are free to choose specific values for the normalization parameters that satisfy Eq. (83) and set

$$\Gamma_R = 1, \quad \Gamma_L = \frac{1 + \omega}{1 + \xi}, \quad (104)$$

such that the right and left boundary vectors read

$$|r\rangle \equiv |r'\rangle = \begin{bmatrix} 1 \\ 1 \end{bmatrix}, \quad \langle l| \equiv \langle l'| = [1 \quad 1]. \quad (105)$$

The solutions in Eqs. (97) and (101) constitute the most general form for the boundary propagators R_{2N} and L_1 , where

the asymptotic probability distributions \mathbf{p} and \mathbf{p}' in Eqs. (77) and (82) are exactly the fixed points. Notice, however, that the stochastic parameters $\theta_0, \theta_1, \vartheta_0, \vartheta_1$ are not completely arbitrary as the elements of the boundary matrices must be appropriately bounded and the spectral parameters must be strictly nonnegative and equal at the right and left boundary. A particularly convenient choice for the parametrization is achieved by setting

$$\theta_0 \equiv \theta_1 = \frac{\omega}{\xi(1 + \omega)}, \quad \vartheta_0 \equiv \vartheta_1 = \frac{\xi}{\omega(1 + \xi)}, \quad (106)$$

as it facilitates the following summary for the conditional probabilities at the boundaries:

$$\begin{aligned} \phi_{n_3, n_4, n_5} &= \frac{p_{n_3, n_4, n_5, 0} + p_{n_3, n_4, n_5, 1}}{p_{n_3, n_4}}, \\ \varphi_{n_0, n_1, n_2} &= \frac{p'_{0, n_0, n_1, n_2} + p'_{1, n_0, n_1, n_2}}{p'_{n_1, n_2}}, \end{aligned} \quad (107)$$

which is comparable to the identities obtained for Rule 54 (see, e.g., Refs. [13,42]) and, similarly, for Rule 201 (see Ref. [15]). Explicitly, the probability of finding the virtual sites at the right and left boundaries in the states n_5 and n_0 , respectively, given that the pairs of adjacent spins are in the configurations (n_3, n_4) and (n_1, n_2) , that is ϕ_{n_3, n_4, n_5} and φ_{n_0, n_1, n_2} is equivalent to the conditional probability of finding the three sites in the configurations (n_3, n_4, n_5) and (n_0, n_1, n_2) , given the states of the sites (n_3, n_4) and (n_1, n_2) . The asymptotic distributions \mathbf{p} and \mathbf{p}' can then equally be interpreted as the nonequilibrium stationary states of a boundary driven system.

While the solutions in Eqs. (97) and (101) are general, they are not completely arbitrary. By this, we mean that the parameters $\theta_0, \theta_1, \vartheta_0, \vartheta_1$ cannot take arbitrary values, in particular, for given values of the spectral parameters $\xi, \omega \in \mathbb{R}^+$, the parameters $\theta_0, \theta_1, \vartheta_0, \vartheta_1$ must take values such that the conditional probabilities are appropriately bounded, namely, $\phi_{n_3, n_4, n_5}, \varphi_{n_0, n_1, n_2} \in (0, 1)$. Requiring this puts additional constraints on the boundary matrices R and L . Explicitly, it demands that the matrix elements ϕ_{n_3, n_4, n_5} and φ_{n_0, n_1, n_2} obey the particle-hole symmetry of the model (see Sec. II for details and Appendix E for a proof),

$$\begin{aligned} \phi_{n_3, n_4, n_5} &= \varphi_{1-n_3, 1-n_4, 1-n_5}, \\ \varphi_{n_0, n_1, n_2} &= \phi_{1-n_0, 1-n_1, 1-n_2}, \end{aligned} \quad (108)$$

which immediately implies the equivalence of the free parameters of the right and left boundaries,

$$\theta_0 = \theta_1, \quad \vartheta_0 = \vartheta_1. \quad (109)$$

To guarantee the consistency of the solutions in Eqs. (97) and (101) (i.e., the equivalence of the spectral parameters ξ and ω at the right and left boundaries), we eliminate the free parameters θ_0 and ϑ_0 by equating the expressions at the right and left boundaries, respectively, and subsequently solve for the spectral parameters which yields the following unique nontrivial solution:

$$\begin{aligned} \xi &= \frac{\phi_{001}(1 - \varphi_{110}) + (1 - \phi_{001})\varphi_{100}}{\phi_{011}(1 - \varphi_{100}) + (1 - \phi_{011})\varphi_{110}}, \\ \omega &= \frac{\varphi_{100}(1 - \phi_{011}) + (1 - \varphi_{100})\phi_{001}}{\varphi_{110}(1 - \phi_{001}) + (1 - \varphi_{110})\phi_{011}}, \end{aligned} \quad (110)$$

which can be easily verified to be appropriately bounded, that is, $\xi, \omega \in \mathbb{R}^+$ for any $\phi_{n_3, n_4, n_5}, \varphi_{n_0, n_1, n_2} \in (0, 1)$, as required. Remarkably, this solution is equivalent to that obtained by the parametrization introduced in Eq. (106). This can be proven straightforwardly by substituting the conditional probabilities Eq. (107) directly into the solutions for the spectral parameters Eq. (110).

C. Statistical independence

The asymptotic probability distributions Eqs. (77) and (82) admit a remarkable factorization property similar to that of Rule 54 [42]. In particular, the conditional probability of observing site $2N$ in the state n_{2N} , given the previous $2N - 1$ sites (n_1, \dots, n_{2N-1}) , depends only on the state of the last two sites (n_{2N-1}, n_{2N}) . Explicitly,

$$\begin{aligned} \frac{p_{n_1, \dots, n_{2N}}}{p_{n_1, \dots, n_{2N-1}}} &= \frac{p_{n_{2N-1}, n_{2N}}}{p_{n_{2N-1}}}, \\ \frac{p'_{n_1, \dots, n_{2N}}}{p'_{n_1, \dots, n_{2N-1}}} &= \frac{p'_{n_{2N-1}, n_{2N}}}{p'_{n_{2N-1}}}. \end{aligned} \quad (111)$$

Analogously, the conditional probability of finding site 1 in the state n_1 , given the next $2N - 1$ sites (n_2, \dots, n_{2N}) , depends only on sites (n_1, n_2) . Namely,

$$\begin{aligned} \frac{p_{n_1, \dots, n_{2N}}}{p_{n_2, \dots, n_{2N}}} &= \frac{p_{n_1, n_2}}{p_{n_2}}, \\ \frac{p'_{n_1, \dots, n_{2N}}}{p'_{n_2, \dots, n_{2N}}} &= \frac{p'_{n_1, n_2}}{p'_{n_2}}. \end{aligned} \quad (112)$$

An explicit proof of these equalities, which follow directly from the definitions of the MPS matrices V_{n_x} and W_{n_x} , as well as formal definitions of the asymptotic conditional probabilities are presented in Appendix F.

An important consequence of this factorization of the asymptotic conditional probabilities Eqs. (77) and (82) is the *statistical independence of quasiparticles*. Namely, in the stationary state, the probability of observing a quasiparticle at any given site of the lattice is the same at every site, independent of the positions of other quasiparticles. Let the conditional probability of encountering a positive or negative quasiparticle at any given pair of sites, given the state of either site, be denoted by p^+ and p^- , respectively. Then, in terms of the asymptotic probabilities, we can express these now well-defined quantities as

$$p^+ = \frac{p_{10}}{p_0} = \frac{p_{01}}{p_1} = \frac{p_{01}}{p_0} = \frac{p_{10}}{p_1} = \frac{\xi}{1 + \xi}, \quad (113)$$

$$p^- = \frac{p'_{01}}{p'_0} = \frac{p'_{10}}{p'_1} = \frac{p'_{10}}{p'_0} = \frac{p'_{01}}{p'_1} = \frac{\omega}{1 + \omega}, \quad (114)$$

which are identical to the expressions in Eq. (107) for the conditional probabilities of encountering quasiparticles at the left and right boundaries, respectively. In particular, let us denote the conditional probability of introducing a positive quasiparticle at the left boundary given the state of site n_0 by φ^+ , specifically,

$$\varphi^+ = \varphi_{100} = 1 - \varphi_{110}, \quad (115)$$

and that of a negative quasiparticle at the right boundary given n_{2N+1} by ϕ^- , that is,

$$\phi^- = \phi_{001} = 1 - \phi_{011}. \quad (116)$$

It then follows directly from Eq. (107) that

$$\varphi^+ = \frac{\xi}{1 + \xi} = p^+, \quad \phi^- = \frac{\omega}{1 + \omega} = p^-. \quad (117)$$

Note that the conditional probabilities p^+ and p^- provide an equivalent parametrization for the stationary states as their relation to the spectral parameters can be inverted. Explicitly,

$$\xi = \frac{p^+}{1 - p^+}, \quad \omega = \frac{p^-}{1 - p^-}. \quad (118)$$

In addition, p^+ and p^- exhibit a notable thermodynamic property, which is obtained by substituting the relations for the spectral parameters in Eq. (37), in terms of their associated chemical potentials, into Eqs. (113) and (114). Doing so yields

$$p^\pm = \frac{1}{\exp(\mu^\pm) + 1}, \quad (119)$$

which can be immediately identified as being exactly the *Fermi-Dirac distributions* of the quasiparticles.

D. Irreducibility and aperiodicity

To prove that the NESS Eq. (77) is unique and asymptotically approached from any initial state requires we show that the Markov operator \mathbb{M} is *irreducible* and *aperiodic* (cf. Theorem 1 in Ref. [2]). As per the Perron-Frobenius theorem [43], this amounts to demonstrating that, first, for any two basis states e_n and e_m (i.e., configurations \underline{n} and \underline{m}) there exists a nonnegative integer τ such that

$$e_m \cdot \mathbb{M}^\tau e_n > 0, \quad (120)$$

and, second, for the case where $e_m \equiv e_n$ that the greatest common divisor of the set of τ is unity.

To prove the irreducibility, we recall that the dynamics in the bulk is deterministic. Therefore, every positive and negative quasiparticle in the system propagates toward the right and left boundary, respectively. In contrast, the boundary dynamics is stochastic and so we are effectively free to choose the values of the sites n_1 and n_{2N} for every state between e_n and e_m . Now, consider the sequence of configurational states,

$$e_n^0 \rightarrow e_n^1 \rightarrow \dots \rightarrow e_n^{2\tau-1} \rightarrow e_n^{2\tau}, \quad (121)$$

connected by the Markov operator $e_n^{t+1} \cdot \mathbb{M} e_n^t > 0$ where $e_n^0 \equiv e_n$ and $e_n^{2\tau} \equiv e_m$, and with τ counting the number of *full time steps* between states e_n and e_m . For the first part of the sequence, we argue that we can set the values of the virtual sites n_0 and n_{2N+1} so that they *eject* each and every quasiparticle from the initial state e_n . Indeed, by recalling that the quasiparticles propagate ballistically with velocities of $v^\pm = \pm 1$ and interact trivially without scattering (i.e., are noninteracting), then after an integer number of full time steps $t_+ \leq 2N$ we are guaranteed to be in the vacuum state [i.e., either the state $(0, \dots, 0)$ or $(1, \dots, 1)$], irrespective of the initial state e_n . We do so with the following rules for the virtual sites,

$$n_0^t = n_1^{t-1}, \quad n_{2N+1}^t = n_{2N}^{t-1}. \quad (122)$$

For the second part of the sequence in Eq. (121), we need to show that we can set the values of the virtual sites such that the

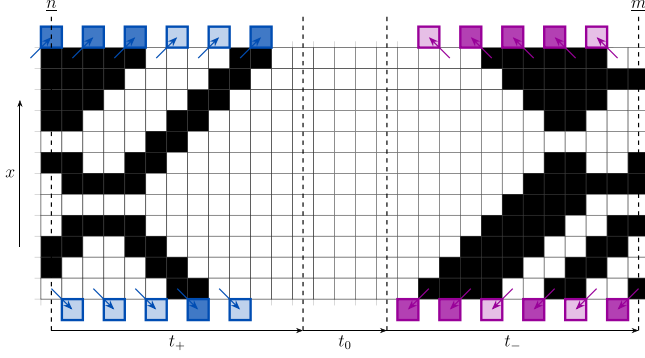


FIG. 5. Irreducibility and aperiodicity. Illustrative explanation of the idea of the proof of irreducibility and aperiodicity of the Markov operator \mathbb{M} . Each and every configuration is connected via a walk of at least $\tau = t_+ + t_0 + t_-$ time steps where t_+ , t_0 , and t_- denote the number of full time steps taken to reach the vacuum from $\mathbf{e}_n \equiv \mathbf{e}_n^0$, reach $\mathbf{e}_m \equiv \mathbf{e}_m^{2\tau}$ from the vacuum, and waited in the vacuum, respectively. In the example given, the states \mathbf{e}_n^0 and $\mathbf{e}_m^{2\tau}$ are connected in *at least* $\tau = 12$ full time steps. At the start of the walk (i.e., $t = 0, \dots, t_+$) the virtual sites, shown in blue, are set to causally *destroy* quasiparticles by taking the values of *past* boundary sites, specifically, with the rule $n'_0 = n_1^{t-1}$ and $n'_{2N+1} = n_{2N}^{t-1}$. In contrast, at the end of the walk (i.e., $t = t_+ + t_0, \dots, t_+ + t_0 + t_-$) the virtual sites, colored purple, are chosen to causally *create* quasiparticles by taking the values of *future* sites, that is, $n'_0 = n_1^{t+1}$ and $n'_{2N+1} = n_{2N}^{t+1}$. Consequently, there always exists an integer $\tau = t_+ + t_-$ such that $\mathbf{e}_m \cdot \mathbb{M}^\tau \mathbf{e}_n > 0$ for any arbitrary states \mathbf{e}_n and \mathbf{e}_m , hence, the Markov operator \mathbb{M} is irreducible. Finally, we consider the middle of the walk (i.e., $t = t_+, \dots, t_+ + t_0$) where the virtual sites take the values of *present* boundary sites, explicitly, $n'_0 = n'_1$ and $n'_{2N+1} = n'_{2N}$. This necessarily implies that the system can remain in either vacuum state for any integer number of full time steps $t_0 \in \mathbb{N}$ which guarantees that $\gcd(\{t_+ + t_0 + t_-\}) = 1$ and, therefore, proves that the Markov operator \mathbb{M} is aperiodic.

quasiparticles are *injected*, so that after an integer number of full time steps $t_- \leq 2N$ we obtain the state \mathbf{e}_m . To achieve this we exploit the *time reversibility* of the bulk dynamics and site freedom of the boundaries to get to the vacuum state from the final state \mathbf{e}_m , but with time evolution inverted. In particular, we apply the following rules:

$$n'_0 = n_1^{t+1}, \quad n'_{2N+1} = n_{2N}^{t+1}. \quad (123)$$

Due to the nonnegativity of the Markov matrix elements, and the sequence that connects the initial and final states \mathbf{e}_n and \mathbf{e}_m in $\tau = t_+ + t_- \leq 4N$ full time steps, we have that $\mathbf{e}_m \cdot \mathbb{M}^\tau \mathbf{e}_n$ is nonvanishing for any arbitrary states \mathbf{e}_n and \mathbf{e}_m , thus, proving the irreducibility of \mathbb{M} .

To show the aperiodicity, we recall that we are free to remain in either vacuum state for an indefinite number of full time steps t_0 . Consequently, τ can take any integer value in the closed interval $[t_+ + t_-, t_+ + t_0 + t_-]$ which implies that the greatest common divisor of the set of τ has to be unity. That is,

$$\gcd(\{t_+ + t_0 + t_-\}) = 1, \quad (124)$$

for $t_0 \in \mathbb{N}$. This, therefore, proves the aperiodicity of \mathbb{M} . For an illustrative explanation of the proof see Fig. 5.

V. SPECTRUM AND RELAXATION DYNAMICS

In Sec. IV, we demonstrated that the deterministic and reversible dynamics with PBC could be made ergodic by considering a finite subsection of the chain in the infinite size limit, which effectively imposed SBC. The resulting state could then be understood as a NESS. In this section we generalize the results above to study the *full relaxation dynamics* of the model, that is, to resolve the spectrum of the Markov operator \mathbb{M} . As was observed in Refs. [2,4], we find that the spectrum is composed of *orbitals*, that is, subsets of the set of eigenvalues which are roots of simple polynomial factors of the characteristic polynomial of the Markov operator \mathbb{M} , as illustrated in Fig. 6. We show that the eigenvectors of the simplest orbital, that we refer to as the *zereth orbital*, which contains the NESS derived in Sec. IV and a triplet of decay modes whose associated eigenvalues are size invariant, can be expressed explicitly in terms of an MPS similar to that of the stationary states \mathbf{p} and \mathbf{p}' in Sec. IV A. We then propose a conjecture for the Bethe-like equations for the entire spectrum (i.e., the distinct eigenvalues and the corresponding degeneracies), which follows directly as a consequence of the consistency conditions imposed, and that generalizes the expressions for the NESS. In addition, we study the thermodynamic limit and demonstrate that the leading decay modes, that is, the eigenvectors of the Markov operator \mathbb{M} associated to the eigenvalues with the largest real parts not equal to unity, that characterize the spectral gap and determine the relaxation rate of the system in the asymptotic limit, scale with $1/N$.

A. Markov operator

We are interested in obtaining exact analytic solutions to the eigenvalue equation for the Markov operator,

$$\mathbb{M}\mathbf{p} = \Lambda\mathbf{p}, \quad (125)$$

which we can conveniently separate into a pair of coupled linear equations for the even and odd time steps,

$$\mathbb{M}_E\mathbf{p} = \Lambda_R\mathbf{p}', \quad \mathbb{M}_O\mathbf{p}' = \Lambda_L\mathbf{p}, \quad (126)$$

with the eigenvalue of the Markov operator \mathbb{M} factorizing as $\Lambda = \Lambda_L\Lambda_R$. Here, the stochastic matrices \mathbb{M}_E and \mathbb{M}_O are defined as in Eqs. (85) and (86), respectively, however, for simplicity and without loss of generality, we assume that the constraints imposed on the boundary matrices R and L , by the normalization Eq. (94) and symmetry Eq. (108), apply implicitly, such that we have

$$R = \begin{bmatrix} 1 - \alpha & \beta & & \\ \alpha & 1 - \beta & & \\ & & 1 - \beta & \alpha \\ & & \beta & 1 - \alpha \end{bmatrix}, \quad (127)$$

$$L = \begin{bmatrix} 1 - \gamma & & \delta & \\ \gamma & 1 - \delta & & \\ & & 1 - \delta & \gamma \\ & & \delta & 1 - \gamma \end{bmatrix},$$

where $\alpha, \beta, \gamma, \delta \in (0, 1)$ are boundary driving parameters (i.e., conditional probabilities) that determine the rate at which the quasiparticles are either created or destroyed. For example, α and δ , respectively, denote the conditional probability that

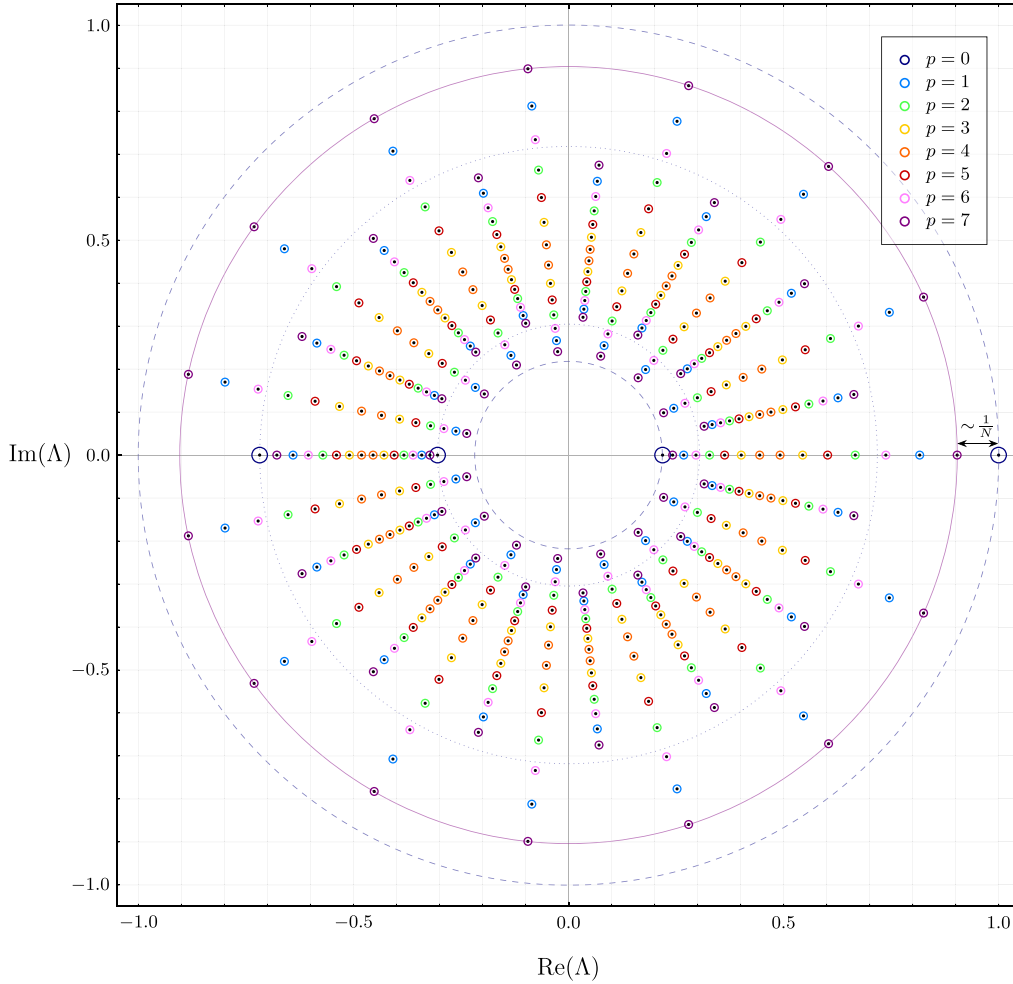


FIG. 6. Orbitals. Spectrum of the Markov operator \mathbb{M} for a system of even size $2N = 16$ with $\alpha = 3/5$, $\beta = 7/8$, $\gamma = 8/9$, and $\delta = 4/7$. The black dots mark the numerical solutions computed by exact diagonalization. The colored circles (see legend) then denote the analytic results for the orbital p eigenvalues Λ obtained from the conjectured expressions Eq. (166). The dark blue circles represent the roots λ of the quadratic characteristic polynomials Eq. (148), which are precisely the eigenvalues of the zeroth orbital. The dashed blue curves denote the circles with radii $r = 1$ and $r = |\mu|$ which, together with the dotted blue curves of radii $r = |\eta \pm \sqrt{\eta^2 - \mu}|$, bound the sets of eigenvalues generated by the momentum parameter z Eq. (164). In the thermodynamic limit $N \rightarrow \infty$, the purple curve, which corresponds to the algebraic curve bounding the eigenvalues of the orbital associated to the leading decay modes, converges to the unit circle, where the spectral gap that characterizes the relaxation dynamics of the system scales with $1/N$.

a negative quasiparticle is injected at the right boundary and ejected at the left boundary.

It can be straightforwardly demonstrated that solving the eigenvalue Eq. (125) provides access to the full relaxation dynamics of the model, as the probability for a given state \mathbf{p}' at time t can be written explicitly in terms of the eigenvalues Λ_j and corresponding eigenvectors \mathbf{p}_j . In particular, we can write

$$\mathbf{p}' = \sum_{j=0}^{2^{2N}-1} c_j \Lambda_j^t \mathbf{p}_j, \quad (128)$$

where c_j are coefficients that depend on the initial state. In Sec. IV D, we proved that the Markov operator \mathbb{M} is *irreducible* and *aperiodic* for arbitrary nontrivial driving parameters $0 < \alpha, \beta, \gamma, \delta < 1$. The Perron-Frobenius theorem [43], therefore, guarantees that the unique eigenvector \mathbf{p}_0 , associated to the eigenvalue $\Lambda_0 = 1$, namely, the NESS, does

not decay in time while the eigenvectors \mathbf{p}_j for $j > 0$ exponentially decay as their associated eigenvalues are bounded within the unit circle by $|\Lambda_j| < 1$. We refer to these eigenvectors as *decay modes* as they encode the time evolution of any initial state toward the NESS in the asymptotic limit.

B. Decay modes

We begin by presenting the ansatz for the eigenvectors of the zeroth orbital of the Markov operator \mathbb{M} , in terms of a simple staggered MPS which reads

$$\mathbf{p} = \langle L | V_1 W_2 \cdots V_{2N-1} W_{2N} | R \rangle, \quad (129)$$

$$\mathbf{p}' = \langle L' | W_1 V_2 \cdots W_{2N-1} V_{2N} | R' \rangle, \quad (130)$$

where V_x and W_x are the vectors of matrices Eq. (46) that we showed satisfy the bulk algebraic relations Eqs. (53) and (58). To ensure that the states \mathbf{p} and \mathbf{p}' in Eqs. (129) and

(130) satisfy the coupled eigenvalue equations in Eq. (126), we additionally require that the following modified boundary algebraic relations hold for the row vectors $\langle L|$ and $\langle L'|$, and column vectors $|R\rangle$ and $|R'\rangle$,

$$\langle L|V_1S = \langle L'|W_1, \quad (131)$$

$$R_{2N}[V_{2N-1}W_{2N}|R] = \Lambda_R V_{2N-1}S V_{2N}|R', \quad (132)$$

$$L_1[\langle L'|W_1V_2] = \Lambda_L \langle L|V_1W_2S^{-1}, \quad (133)$$

$$W_{2N}S^{-1}|R'\rangle = W_{2N}|R\rangle, \quad (134)$$

where S is the delimiter matrix Eq. (55) and S^{-1} its inverse. We can readily verify that these algebraic relations solve the staggered eigenvalue Eqs. (126) by substituting the ansatz into either of the equations and applying the appropriate relations to transform $\mathbf{p} \leftrightarrow \mathbf{p}'$. In particular, to obtain \mathbf{p} from \mathbf{p}' , we first write out $\mathbb{M}_O\mathbf{p}'$ in terms of the matrix product Eq. (86) and ansatz Eq. (130). Applying the operator L_1 and utilizing the boundary relation Eq. (133), we introduce the delimiter matrix inverse S^{-1} on the left, as well as the parameter Λ_L . We then repeatedly apply U_x to the odd sites of the chain (i.e., sites $n_3, n_5, \dots, n_{2N-1}$) using the bulk relation Eq. (58), which shifts S^{-1} to the right, two sites at a time. Finally, we eliminate S^{-1} with Eq. (134) to yield $\Lambda_L\mathbf{p}$. The other condition for the even time step then follows analogously. As an example, we consider the transformation $\mathbf{p} \rightarrow \mathbf{p}'$ for $N = 3$,

$$\begin{aligned} \mathbb{M}_E\mathbf{p} &= U_2U_4R_6\langle L|V_1W_2V_3W_4V_5W_6|R\rangle \\ &= \Lambda_R U_2U_4\langle L|V_1W_2V_3W_4V_5SV_6|R'\rangle \\ &= \Lambda_R U_2\langle L|V_1W_2V_3SV_4W_5V_6|R'\rangle \\ &= \Lambda_R \langle L|V_1SV_2W_3V_4W_5V_6|R'\rangle \\ &= \Lambda_R \langle L'|W_1V_2W_3V_4W_5V_6|R'\rangle \\ &= \Lambda_R\mathbf{p}'. \end{aligned} \quad (135)$$

Solving separately the equations for the right boundary Eqs. (132) and (134), we obtain the following pair of solutions, identical up to a sign, for the spectral parameters:

$$\xi = \sigma \frac{\Lambda_R - (1 - \alpha)}{\beta}, \quad (136)$$

$$\omega = \sigma \frac{\Lambda_R(1 - \beta) - (1 - \alpha - \beta)}{\Lambda_R\beta}, \quad (137)$$

with $\sigma = \pm 1$ and associated right boundary vectors,

$$|R\rangle = r \begin{bmatrix} 1 \\ \sigma \end{bmatrix}, \quad |R'\rangle = r \frac{1 + \sigma\omega}{1 + \sigma\xi} \begin{bmatrix} 1 \\ \sigma \end{bmatrix}, \quad (138)$$

where r is a scalar that determines the normalization of the solutions of the right boundary. Similarly solving the left boundary Eqs. (131) and (133) then returns an equivalent pair of solutions for the spectral parameters,

$$\xi = \tau \frac{\Lambda_L(1 - \delta) - (1 - \gamma - \delta)}{\Lambda_L\delta}, \quad (139)$$

$$\omega = \tau \frac{\Lambda_L - (1 - \gamma)}{\delta}, \quad (140)$$

with $\tau = \pm 1$ and left boundary vectors,

$$\langle L| = l[1 \quad \tau], \quad \langle L'| = l[1 \quad \tau], \quad (141)$$

with l the corresponding scalar determining the normalization of the left boundary solutions. To obtain solutions that are consistent with the results in Secs. III and IV, we choose to set

$$r = \frac{1}{1 + \sigma\omega}, \quad l = 1, \quad (142)$$

such that the components p_n of the eigenvectors \mathbf{p} of the Markov operator \mathbb{M} take a form reminiscent of the grand canonical ensemble Eq. (40). Specifically,

$$p_n = \tau^{n_1} \xi^{N_n^+} \omega^{N_n^-}, \quad (143)$$

where τ corresponds to the choice of solutions for the left boundary Eqs. (139), (140), and (141).

To guarantee that the solutions at the boundaries that were obtained independently of each other are consistent necessarily requires that we demand that the expressions for the spectral parameters ξ in Eqs. (136) and (139) and ω in Eqs. (137) and (140) are, respectively, equal. Notice, however, that the signs of the solutions at the right and left boundaries are independent and, therefore, pairwise equating all possible combinations of expressions for the spectral parameters ξ and ω returns a doubly degenerate closed pair of equations for the eigenvalue parameters Λ_R and Λ_L that we interpret as *Bethe equations*, imposed by the consistency conditions at the boundaries. Explicitly,

$$\frac{\Lambda_R - (1 - \alpha)}{\beta} = \tau \frac{\Lambda_L(1 - \delta) - (1 - \gamma - \delta)}{\Lambda_L\delta}, \quad (144)$$

$$\frac{\Lambda_L - (1 - \gamma)}{\delta} = \tau \frac{\Lambda_R(1 - \beta) - (1 - \alpha - \beta)}{\Lambda_R\beta}, \quad (145)$$

where, for simplicity, we have taken the positive solutions at the right boundary. Eliminating either Λ_R or Λ_L using the eigenvalue $\Lambda = \Lambda_L\Lambda_R$ and subsequently solving yields the following quadratic characteristic polynomial:

$$\Lambda^2 - (1 + \mu - \nu + \tau\nu)\Lambda + \mu = 0, \quad (146)$$

where, for readability, we have introduced the coefficients $\mu \in (-1, 1)$ and $\nu \in (0, 2)$, which are defined by

$$\mu = (1 - \alpha - \beta)(1 - \gamma - \delta), \quad \nu = \alpha\delta + \beta\gamma. \quad (147)$$

It follows straightforwardly that as Eq. (146) is a pair of quadratic equations it has, in general, four distinct roots that can be written succinctly as

$$\Lambda = 1, \mu, \eta \pm \sqrt{\eta^2 - \mu}, \quad (148)$$

where the coefficient $\eta \in (-1, 1)$ is given by

$$\eta = \frac{1 + \mu - 2\nu}{2}. \quad (149)$$

Clearly, $\Lambda \equiv \Lambda_0 = 1$ is always guaranteed to be a solution with the corresponding eigenvector being the NESS. The remaining solutions $\Lambda \equiv \Lambda_j$ for $j \neq 0$ then correspond to three decay modes whose eigenvalues are independent of the system size, that is, they are *size invariant*. We refer to this set of four eigenvalues as the *zeroth orbital*.

C. Quasiparticle excitations

Despite the fact that we are unable to find an explicit MPS expression for eigenvectors of the Markov operator \mathbb{M} beyond the zeroth orbital, exact numerical diagonalization for small systems suggest that the remaining eigenvalues also organize

into orbitals, see Fig. 6. This is similar to what occurs in Rule 54 [4], with the number of orbitals scaling linearly with the size of the system and the degeneracy of the eigenvalues increasing exponentially with the orbital level.

Using these observations, together with similar conjectures as in Ref. [4], we are able to construct exact analytic forms for the Bethe equations [cf. Eqs. (144) and (145)] that completely reproduce the entire spectrum of the Markov operator \mathbb{M} . To start, we introduce some additional parameters required for the conjecture, specifically, the nonnegative integer p that counts the orbital level, $z \in \mathbb{C}$ which we interpret as the momentum associated to quasiparticle excitations of the NESS, which in turn is intuitively understood as the vacuum state of the Markovian dynamics, and $A_{\pm} \in \mathbb{C}$, a pair of complex amplitudes associated to the operators that create the aforementioned quasiparticle excitations.

Having introduced the necessary prerequisites, we now postulate the following generalized expressions for ξ and ω at the right boundary [cf. Eqs. (136) and (137)],

$$\xi = \sigma \frac{\Lambda_R - z(1 - \alpha)}{z\beta}, \quad (150)$$

$$\omega = \sigma \frac{\Lambda_R(1 - \beta) - z(1 - \alpha - \beta)}{\Lambda_R\beta}, \quad (151)$$

while at the left boundary [cf. Eqs. (139) and (140)],

$$\xi = \tau \frac{\Lambda_L(1 - \delta) - z(1 - \gamma - \delta)}{\Lambda_L\delta}, \quad (152)$$

$$\omega = \tau \frac{\Lambda_L - z(1 - \gamma)}{z\delta}, \quad (153)$$

where $\sigma, \tau = \pm 1$. In addition, we require that the pair of amplitude parameters A_{\pm} satisfy the following identities at the right and left boundary, respectively,

$$\frac{A_+}{A_-} = \frac{\Lambda_R^{2p} z^{2N-1}}{z^{2p}(1 - \alpha - \beta)^p}, \quad (154)$$

$$\frac{A_-}{A_+} = \frac{\Lambda_L^{2p}}{z^{2p}(1 - \gamma - \delta)^p}. \quad (155)$$

Imposing the consistency condition, i.e., demanding that the expressions for the spectral parameters ξ and ω , and amplitude parameters A_+ and A_- are pairwise equivalent then returns the following closed set of generalized Bethe equations for Λ_R , Λ_L , and z ,

$$\frac{\Lambda_R - z(1 - \alpha)}{z\beta} = \tau \frac{\Lambda_L(1 - \delta) - z(1 - \gamma - \delta)}{\Lambda_L\delta}, \quad (156)$$

$$\frac{\Lambda_L - z(1 - \gamma)}{z\delta} = \tau \frac{\Lambda_R(1 - \beta) - z(1 - \alpha - \beta)}{\Lambda_R\beta}, \quad (157)$$

$$\frac{\Lambda_R^{2p} z^{2N-1}}{z^{2p}(1 - \alpha - \beta)^p} = \frac{z^{2p}(1 - \gamma - \delta)^p}{\Lambda_L^{2p}}, \quad (158)$$

where, as for the zeroth orbital, the \pm signs are obtained by equating expressions for the spectral parameters with positive signs for the right boundary with both solutions of the left boundary. Replacing either Λ_R or Λ_L with the eigenvalue $\Lambda = \Lambda_L\Lambda_R$ and eventually solving transforms the set of equations into a pair of identities for Λ and z . The first, which reads

$$\Lambda^2 - (1 + \mu - \nu + \tau\nu)\Lambda z^2 + \mu z^4 = 0, \quad (159)$$

can be interpreted as a *nonequilibrium dispersion relation* that connects the eigenvalues and momentum parameter and can be straightforwardly shown to be a direct generalization of the quadratic characteristic polynomial in Eq. (146), for which $z = 1$. The second identity,

$$\Lambda^{2p} z^{2N-4p-1} - \mu^p = 0, \quad (160)$$

can, instead, be understood as a *momentum conservation relation*. Indeed, remarking that the solution to Eq. (159) can be compactly written as

$$\Lambda = \lambda z^2, \quad (161)$$

where we have introduced the parameter λ , which can be straightforwardly demonstrated to be equivalent to the Λ in Eq. (148) (i.e., the eigenvalues of the zeroth orbital),

$$\lambda = 1, \mu, \eta \pm \sqrt{\eta^2 - \mu}, \quad (162)$$

then allows us to rewrite Eq. (160) as

$$z^{2N-1} = \frac{\mu^p}{\lambda^{2p}}. \quad (163)$$

Therefore, for a given orbital p and arbitrary parameters $\alpha, \beta, \gamma, \delta$, the magnitude of the momentum z is conserved. Specifically, the solutions to the momentum conservation relation are the $2N - 1$ distinct roots, that read

$$z = \exp \left[\frac{p \ln \rho}{2N - 1} + i \left(\frac{p\phi + 2\pi pq}{2N - 1} \right) \right], \quad (164)$$

where we have introduced the polar parameters,

$$\rho = \left| \frac{\mu}{\lambda^2} \right|, \quad \phi = \text{Arg} \left(\frac{\mu}{\lambda^2} \right), \quad (165)$$

with $q = 0, \dots, 2N - 2$. The eigenvalues then read

$$\Lambda = \exp \left[\ln \varrho + \frac{2p \ln \rho}{2N - 1} + i \left(\varphi + \frac{2p\phi + 2\pi pq}{2N - 1} \right) \right], \quad (166)$$

where, additionally, we have defined

$$\varrho = |\lambda|, \quad \varphi = \text{Arg}(\lambda), \quad (167)$$

with the orbital number $p = 0, \dots, N - 1$. We conjecture that the multivalued function Eq. (166) completely describes the entire spectrum of \mathbb{M} . Indeed, comparing the results calculated analytically with numerical values obtained by exact diagonalization of the Markov matrix \mathbb{M} for $N \leq 8$ we see perfect agreement as demonstrated in Fig. 6. In contrast to the typical Bethe ansatz [44], this conjecture implies that the entire spectrum is characterized by just one *universal* momentum parameter z , irrespective of the number of quasiparticle excitations (cf. Rule 54 [6,13]). This can be seen as following directly from the dispersion relation, in that each and every quasiparticle propagates with constant (group) velocity $v^{\pm} = \pm 1$ (i.e., each species is *nondispersive*).

Additionally, we present a conjecture for the associated degeneracy g of the eigenvalue Λ . Explicitly,

$$g = \sum_{d|D} \frac{d}{2N - 1} \sum_{d'|D'} \mu(d') \left(\frac{2N-1}{\frac{p}{dd'}} \right), \quad (168)$$

where $\mu(\cdot)$ denotes the Möbius function [45] and $j|k$ the set of positive integer divisors j of the integer k , with

$$D = \text{gcd}(2N - 1, p, q), \quad D' = \frac{\text{gcd}(2N - 1, p)}{q}, \quad (169)$$

where $\text{gcd}(\cdot)$ denotes the greatest common divisor. This conjecture can be confirmed numerically for small system sizes (see Appendix G for details).

D. Thermodynamic limit

In the thermodynamic limit $N \rightarrow \infty$, the series expansion of the momentum conservation relation Eq. (160), in the small parameter $1/N$, to leading order reads

$$z \simeq 1 + \frac{1}{N}z', \quad z' = \frac{p \ln \rho + i(p\phi + 2\pi pq)}{2}, \quad (170)$$

which immediately implies that, in the asymptotic limit, the momentum parameter z is given by

$$z(\kappa, \epsilon) = \exp(\epsilon \ln \rho + i\kappa), \quad (171)$$

where we have introduced the *momentum* $\kappa \in [0, 2\pi)$ and *decay* $\epsilon \in [0, \frac{1}{2})$, defined by

$$\kappa = \lim_{N \rightarrow \infty} \frac{p\phi + 2\pi pq}{2N - 1}, \quad \epsilon = \lim_{N \rightarrow \infty} \frac{p}{2N - 1}. \quad (172)$$

A direct consequence of this is that, in the limit $N \rightarrow \infty$, the eigenvalues of each and every orbital p converge to a set of algebraic curves, specifically, circles $\Lambda(\kappa, \epsilon)$, that are given by inserting Eq. (171) into Eq. (161). Explicitly,

$$\Lambda(\kappa, \epsilon) = \exp(\ln \rho + 2\epsilon \ln \rho + i\kappa). \quad (173)$$

$$|\text{Re}(\Lambda_1)| = \max_{\lambda, p} \left\{ \left| \exp \left[\frac{(2N - 2p - 1) \ln |\lambda| + 2p \ln \left| \frac{\mu}{\lambda} \right|}{2N - 1} \right] \cos \left[\frac{(2N - 2p - 1) \text{Arg}(\lambda) + 2p \text{Arg} \left(\frac{\mu}{\lambda} \right) + 2\pi pq}{2N - 1} \right] \right| \right\}, \quad (177)$$

for $\lambda \in \{1, \mu, \eta \pm \sqrt{\eta^2 - \mu}\}$ and $p \in \{1, \dots, N - 1\}$ where, to obtain the equality, we have used the properties of the logarithm, absolute value, and principle argument. From here, we remark that $|\lambda| \leq 1$ and $p \leq N - 1$, which imply that the first term of the exponential is nonpositive, and that $|\lambda| \geq |\mu|$ and $p \geq 1$, which similarly imply that the second term is nonpositive. Together, with the constraint that $|\mu| < 1$, these observations ensure that the exponent is strictly negative and must, therefore, be minimized to maximize the exponential. Similarly, the cosine function is maximized by minimizing the modulus of its argument, which, since $\mu \in \mathbb{R}$, $\lambda \in \mathbb{C}$, and $q \in \{0, \dots, 2N - 2\}$, can be achieved by setting $\lambda \in \mathbb{R}$ (i.e., $\lambda \in \{1, \mu\}$) and $q = 0$. For the case with $\lambda = 1$, it follows straightforwardly that $|\text{Re}(\Lambda_j)|$ is maximized by choosing $p = 1$ while for $\lambda = \mu$ it is maximized by selecting $p = N - 1$. Comparing both cases, and recalling that $|\mu| < 1$, we immediately realize that the leading decay modes are guaranteed to be in the orbital $p = N - 1$, with

$$\Lambda_1 = \exp \left(\frac{1}{2N - 1} \ln |\mu| \right), \quad (178)$$

for all $\alpha, \beta, \gamma, \delta \in (0, 1)$ and $N \in \mathbb{N}^+$.

While, naively, one would expect that the boundaries would become irrelevant in the thermodynamic limit and, therefore, force each and every eigenvalue to collapse onto the unit circle, as was the case for the closed system with periodic boundaries, this does not happen here. Instead, we observe that the eigenvalues distribute themselves over an infinite set

Writing the series expansion of the eigenvalue Λ as

$$\Lambda \simeq \rho \left(1 - \frac{1}{N} \Lambda' \right), \quad (174)$$

and substituting into the nonequilibrium dispersion relation Eq. (159), we obtain

$$\Lambda' = -2z', \quad (175)$$

which is consistent with the interpretation of the dynamics in terms of the ballistic propagation of quasiparticles.

In the long-time limit, the asymptotic relaxation rate of the system is determined by the leading decay mode, defined as the eigenvector \mathbf{p}_1 of the Markov operator \mathbb{M} , associated to the eigenvalue Λ_1 satisfying

$$|\text{Re}(\Lambda_1)| = \max_{j>0} (|\text{Re}(\Lambda_j)|), \quad (176)$$

that is, the eigenvalue with the largest real part not equal to unity. In contrast to Rule 54 (see, e.g., Refs. [2,4,13]), the leading decay modes, that determine the spectral gap of the Markov operator \mathbb{M} , are associated to eigenvalues with orbital number $p = N - 1$, as opposed to $p = 1$. To prove this, we begin by rewriting the condition Eq. (176) as

of circles $\Lambda(\kappa, \epsilon)$, that are parametrized radially by ϵ and angularly by κ ,

$$\lim_{N \rightarrow \infty} |\Lambda| = |\mu|^{2\epsilon} |\lambda|^{1-4\epsilon}, \quad \lim_{N \rightarrow \infty} \text{Arg}(\Lambda) = \kappa, \quad (179)$$

for $\epsilon \in [0, \frac{1}{2})$ and $\kappa \in [0, 2\pi)$, which then implies that the thermodynamic $N \rightarrow \infty$ and long-time $t \rightarrow \infty$ limits are *distinct* (i.e., the stationary state $\mathbf{p} \equiv \mathbf{p}_0$ is the only state in the asymptotic time limit for any even system size $2N$, but with the time taken to reach it increasing with N).

E. Observables and correlations

We now consider computing observables in the NESS. To do so, we define the partition function for the open system out of equilibrium as we did for the closed system with periodic boundaries, namely, via normalization of the MPS probabilities,

$$Z = \sum_n p_n = \sum_n \langle L | V_{n_1} \cdots W_{n_{2N}} | R \rangle = \langle L | T^N | R \rangle, \quad (180)$$

which, using the transfer matrix eigenvalue equation, can be simplified to

$$Z = \chi^N \langle L | R \rangle = 2(1 + \xi)^N (1 + \omega)^{N-1}. \quad (181)$$

The average density function for the NESS is

$$\langle n_x \rangle = \frac{1}{Z} \sum_n n_x p_{n_1, \dots, n_{2N}}. \quad (182)$$

A direct computation shows that we can rewrite this as

$$\begin{aligned}\langle n_{2x} \rangle &= \frac{1}{Z} \langle L | T^{x-1} V D_{2x} T^{N-x} | R \rangle, \\ \langle n_{2x-1} \rangle &= \frac{1}{Z} \langle L | T^{x-1} D_{2x-1} W T^{N-x} | R \rangle,\end{aligned}\quad (183)$$

where we have introduced the site density operator,

$$D_x = \begin{cases} W_1, & x = 0 \pmod{2}, \\ V_1, & x = 1 \pmod{2}, \end{cases}\quad (184)$$

with the shorthand notations,

$$V \equiv V_0 + V_1, \quad W \equiv W_0 + W_1.\quad (185)$$

$$\left\langle \prod_j n_{2x_j - y_j} \right\rangle = \frac{1}{Z} \sum_n \left(\prod_j n_{2x_j - y_j} \right) p_{n_1, \dots, n_{2N}} = \frac{1}{Z} \langle L | \prod_j (T^{x_j - x_{j-1} - 1} V^{1-y_j} D_{2x_j - y_j} W^{y_j}) T^{N-x_k} | R \rangle.\quad (187)$$

Specifically, the two-point correlator, for example, for sites $2x_1 - 1$ and $2x_2$, reads

$$\langle n_{2x_1-1} n_{2x_2} \rangle = \frac{\langle L | D_{2x_1-1} T^{x_2-x_1} D_{2x_2} | R \rangle}{\chi^{x_2-x_1+1} \langle L | R \rangle}.\quad (188)$$

Defining the connected correlation,

$$C_{x_1, x_2} = \langle n_{x_1} n_{x_2} \rangle - \langle n_{x_1} \rangle \langle n_{x_2} \rangle,\quad (189)$$

$$C_{2x_1-y_1, 2x_2-y_2} = \frac{\langle L_1 | V^{1-y_1} D_{2x_1-y_1} W^{y_1} | R_2 \rangle \langle L_2 | V^{1-y_2} D_{2x_2-y_2} W^{y_2} | R_1 \rangle}{\chi_1 \chi_2} \left(\frac{\chi_2}{\chi_1} \right)^{x_2-x_1}.\quad (192)$$

As expected, the correlation function depends only on the distance between the sites and decays exponentially as

$$C_{2x_1-y_1, 2x_2-y_2} \sim \exp\left(-\frac{|x_2 - x_1|}{\ell}\right),\quad (193)$$

with correlation length ℓ

$$\ell = \ln \left| \frac{\chi_1}{\chi_2} \right|.\quad (194)$$

Finally, we consider the ensemble average quasiparticle current in the nonequilibrium stationary state, defined as the difference between the densities of the quasiparticles. Explicitly, the density of positive quasiparticles $j^+ \equiv j_x^+$, which is independent of site x in the NESS, is given by

$$j^+ = \frac{1}{Z} \sum_n (n_{2x-1}(1 - n_{2x}) + (1 - n_{2x-1})n_{2x}) p_n,\quad (195)$$

while the density of negative quasiparticles $j^- \equiv j_x^-$ is

$$j^- = \frac{1}{Z} \sum_n (n_{2x}(1 - n_{2x+1}) + (1 - n_{2x})n_{2x+1}) p_n.\quad (196)$$

Using the eigenvalue equation for the transfer matrix we get,

$$\begin{aligned}\langle n_{2x} \rangle &= \frac{\langle L | V D_{2x} | R \rangle}{\chi \langle L | R \rangle} = \frac{1}{2}, \\ \langle n_{2x-1} \rangle &= \frac{\langle L | D_{2x-1} W | R \rangle}{\chi \langle L | R \rangle} = \frac{1}{2}.\end{aligned}\quad (186)$$

We can similarly calculate multi-point correlation functions for arbitrary products $n_{2x_1-y_1}, \dots, n_{2x_k-y_k}$, with $x_j = 1, \dots, N$ and $y_j = 0, 1$, for $j = 1, \dots, k$ where $x_0 \equiv 0$ and $x_j \geq x_{j-1}$. Assuming $x_j > x_{j-1}$, we write

and using the decomposition of the transfer matrix T ,

$$T = \sum_{j=1}^2 \chi_j |R_j\rangle \langle L_j|,\quad (190)$$

where the normalized eigenvectors are

$$|R_1\rangle = \frac{1}{\sqrt{2}} \begin{bmatrix} 1 \\ 1 \end{bmatrix} = \langle L_1 |^\dagger, \quad |R_2\rangle = \frac{1}{\sqrt{2}} \begin{bmatrix} 1 \\ -1 \end{bmatrix} = \langle L_2 |^\dagger,$$

and corresponding eigenvalues,

$$\chi_1 = (1 + \xi)(1 + \omega), \quad \chi_2 = (1 - \xi)(1 - \omega),\quad (191)$$

can be rewritten compactly for arbitrary sites as

Computing these expressions, we find that they read

$$j^+ = \frac{\xi}{1 + \xi}, \quad j^- = \frac{\omega}{1 + \omega},\quad (197)$$

which we notice are exactly equivalent to the conditional probabilities of detecting quasiparticles in the NESS, p^+ and p^- , in Eqs. (113) and (114), respectively. Therefore, the ensemble average quasiparticle current,

$$j \equiv j^+ - j^- = \frac{\xi - \omega}{(1 + \xi)(1 + \omega)},\quad (198)$$

which, we remark, is linear in the small parameter regime (i.e., $\xi, \omega \ll 1$), as expected,

$$j \sim \xi - \omega.\quad (199)$$

VI. LARGE DEVIATIONS

A central feature of stochastic KCMs is the existence of *trajectory phase transitions* [46,47] (see also [48–53] and [18] for a review). This refers to the singular change displayed by trajectories with dynamical behavior that is very different from typical. Specifically, the XOR-FA model [19], which has the same constraint as Rule 150, was shown to have an

active-inactive trajectory phase transition, demonstrated by studying the large deviation (LD) statistics of an appropriate trajectory observable (the total number of configuration changes, or dynamical activity [46,48,54]). We now show that the dynamics of the boundary driven Rule 150 also displays such transitions. We do so by computing the exact LD functions that determine the long-time statistics of a large class of trajectory observables.

A. Time integrated observables

We consider general time (and space) additive observables of the form

$$K(N, T) = \sum_{t=0}^{T-1} \sum_{x=1}^{2N-1} (a_x^{2t} + b_x^{2t+1}), \quad (200)$$

where a and b are functions of the occupation on two consecutive sites at given times in a trajectory,

$$a_x^{2t} \equiv a_x(n_x^{2t}, n_{x+1}^{2t}), \quad b_x^{2t+1} \equiv b_x(n_x^{2t+1}, n_{x+1}^{2t+1}). \quad (201)$$

We refer to observables of this type as *dynamical* as they depend on the full time history of the state of the system, namely, the *trajectory* $(\underline{n}^0, \underline{n}^1, \dots, \underline{n}^{2T-1})$. For example, one could consider the time integrated number of excited sites given by $a_x^{2t} = \frac{1}{2}(n_x^{2t} + n_{x+1}^{2t})$ and $b_x^{2t+1} = 0$.

In the long-time limit, $T \rightarrow \infty$, the probability distribution of K has a large deviation (LD) form [55],

$$P_T(K) \asymp \exp[-T\varphi_N(k)], \quad (202)$$

where $\varphi_N(k) \equiv \varphi_N(K/T)$ is the *rate function*. Similarly, it can be shown that the *moment generating function* has a LD form too,

$$M_T(s) \asymp \exp[T\theta_N(s)], \quad (203)$$

where we refer to $\theta_N(s)$ as the *scaled cumulant generating function* (SCGF) as its derivatives at $s=0$ are related to the cumulants of $k \equiv K/T$. The LD functions are connected through a Legendre transform,

$$\theta_N(s) = -\min_k [sk + \varphi_N(k)], \quad (204)$$

which implies that they can intuitively be interpreted as corresponding to the free energy and entropy density of the trajectory ensemble.

To obtain an analytic form for the SCGF, we follow the approach of Refs. [5,13] whereby we deform, or *tilt* the Markov operator [55]. As will be demonstrated, we then have that

$$\theta_N(s) = \ln \tilde{\Lambda}(s), \quad (205)$$

where $\tilde{\Lambda}(s)$ is the eigenvalue of the tilted Markov operator with the largest real part. Finding $\tilde{\Lambda}(s)$, therefore, allows us to study the statistics of K and its cumulants.

B. Tilted Markov operator

The tilted Markov operator $\tilde{\mathbb{M}}(s)$ is defined as

$$\tilde{\mathbb{M}}(s) \equiv \tilde{\mathbb{M}}_O(s)\tilde{\mathbb{M}}_E(s), \quad (206)$$

where $\tilde{\mathbb{M}}_E(s)$ and $\tilde{\mathbb{M}}_O(s)$ are the tilted propagators that act on the even and odd time steps, respectively,

$$\tilde{\mathbb{M}}_E(s) = \mathbb{M}_E A(s), \quad \tilde{\mathbb{M}}_O(s) = \mathbb{M}_O B(s), \quad (207)$$

with $A(s)$ and $B(s)$ the diagonal operators introduced to apply the deformation. It follows that these extensive tilt operators can be expressed as products of local operators acting on pairs of adjacent sites,

$$A(s) = A_{1,2}^{(1)} A_{2,3}^{(2)} \cdots A_{2N-1,2N}^{(2N-1)}, \quad (208)$$

$$B(s) = B_{1,2}^{(1)} B_{2,3}^{(2)} \cdots B_{2N-1,2N}^{(2N-1)},$$

where the subscript index denotes the sites of the lattice on which the operators act nontrivially,

$$A_{x,x+1}^{(x)} = \mathbb{1}^{\otimes(x-1)} \otimes A^{(x)} \otimes \mathbb{1}^{\otimes(2N-x-1)}, \quad (209)$$

$$B_{x,x+1}^{(x)} = \mathbb{1}^{\otimes(x-1)} \otimes B^{(x)} \otimes \mathbb{1}^{\otimes(2N-x-1)},$$

while the superscript index denotes that the matrices are *site dependent*. Specifically, the operators $A^{(x)}$ and $B^{(x)}$ are given by the following local 4×4 diagonal matrices,

$$A^{(x)} = \begin{bmatrix} a_{00}^{(x)} & & & \\ & a_{01}^{(x)} & & \\ & & a_{10}^{(x)} & \\ & & & a_{11}^{(x)} \end{bmatrix}, \quad (210)$$

$$B^{(x)} = \begin{bmatrix} b_{00}^{(x)} & & & \\ & b_{01}^{(x)} & & \\ & & b_{10}^{(x)} & \\ & & & b_{11}^{(x)} \end{bmatrix},$$

where we have introduced the shorthand notations,

$$a_{n_x, n_{x+1}}^{(x)} \equiv \exp[-sa_x(n_x, n_{x+1})], \quad (211)$$

$$b_{n_x, n_{x+1}}^{(x)} \equiv \exp[-sb_x(n_x, n_{x+1})],$$

to denote the exponents of the local functions Eq. (201).

It follows directly from computation that the local tilt operators Eq. (210) can be distributed between the local time evolution operators Eqs. (12) and (90) in such a way that the tilted propagators Eq. (207) can be expressed as

$$\tilde{\mathbb{M}}_E(s) = \tilde{U}_2^{(2)} \tilde{U}_4^{(4)} \cdots \tilde{U}_{2N-2}^{(2N-2)} \tilde{R}_{2N}^{(2N)}, \quad (212)$$

$$\tilde{\mathbb{M}}_O(s) = \tilde{L}_1^{(1)} \tilde{U}_3^{(3)} \cdots \tilde{U}_{2N-3}^{(2N-3)} \tilde{U}_{2N-1}^{(2N-1)},$$

where the tilted bulk matrices read

$$\tilde{U}_{2x}^{(2x)} = U_{2x} A_{2x-1,2x}^{(2x-1)} A_{2x,2x+1}^{(2x)}, \quad (213)$$

$$\tilde{U}_{2x-1}^{(2x-1)} = U_{2x-1} B_{2x-2,2x-1}^{(2x-2)} B_{2x-1,2x}^{(2x-1)},$$

while the tilted boundary matrices are given by

$$\tilde{R}_{2N}^{(2N)} = R_{2N} A_{2N-1,2N}^{(2N-1)}, \quad \tilde{L}_1^{(1)} = L_1 B_{1,2}^{(1)}. \quad (214)$$

C. Dominant eigenvalue

We now look to construct an explicit expression for the leading eigenvector of the tilted Markov operator $\tilde{\mathbb{M}}(s)$, namely, the eigenvector associated to the eigenvalue $\tilde{\Lambda}(s)$ with the largest real part. Specifically, we seek a pair of vectors $\tilde{\rho}$

and \tilde{p}' , that satisfy the coupled equations,

$$\tilde{\mathbb{M}}_E(s)\tilde{p} = \tilde{\Lambda}_R(s)\tilde{p}', \quad \tilde{\mathbb{M}}_O(s)\tilde{p}' = \tilde{\Lambda}_L(s)\tilde{p}, \quad (215)$$

where $\tilde{\Lambda}(s) = \tilde{\Lambda}_R(s)\tilde{\Lambda}_L(s)$, which indeed implies that

$$\tilde{\mathbb{M}}(s)\tilde{p} = \tilde{\Lambda}(s)\tilde{p}. \quad (216)$$

We now postulate a simple staggered MPS ansatz for the components of the eigenvectors similar to the ansatz used for the vectors in Sec. V, that reads

$$\begin{aligned} \tilde{p}_n &= \langle \tilde{L} | \tilde{V}_{n_1}^{(1)} \tilde{W}_{n_2}^{(2)} \dots \tilde{V}_{n_{2N-1}}^{(2N-1)} \tilde{W}_{n_{2N}}^{(2N)} | \tilde{R} \rangle, \\ \tilde{p}'_n &= \langle \tilde{L}' | \tilde{W}_{n_1}^{(1)} \tilde{V}_{n_2}^{(2)} \dots \tilde{W}_{n_{2N-1}}^{(2N-1)} \tilde{V}_{n_{2N}}^{(2N)} | \tilde{R}' \rangle, \end{aligned} \quad (217)$$

where the matrices $\tilde{V}_{n_x}^{(x)}$ and $\tilde{W}_{n_x}^{(x)}$ acting in the auxiliary space \mathbb{C}^2 are now *site dependent*. It then follows that we can efficiently write the pair of vectors, using the compact tensor product notation, as

$$\begin{aligned} \tilde{p} &= \langle \tilde{L} | \tilde{V}_1^{(1)} \tilde{W}_2^{(2)} \dots \tilde{V}_{2N-1}^{(2N-1)} \tilde{W}_{2N}^{(2N)} | \tilde{R} \rangle, \\ \tilde{p}' &= \langle \tilde{L}' | \tilde{W}_1^{(1)} \tilde{V}_2^{(2)} \dots \tilde{W}_{2N-1}^{(2N-1)} \tilde{V}_{2N}^{(2N)} | \tilde{R}' \rangle, \end{aligned} \quad (218)$$

where, explicitly, the vectors of tilted matrices read

$$\tilde{V}_x^{(x)} = \begin{bmatrix} \tilde{v}_0^{(x)} \\ \tilde{v}_1^{(x)} \end{bmatrix}, \quad \tilde{W}_x^{(x)} = \begin{bmatrix} \tilde{w}_0^{(x)} \\ \tilde{w}_1^{(x)} \end{bmatrix}. \quad (219)$$

We demand that these vectors of tilted matrices satisfy the following inhomogeneous bulk relations, that generalizes the homogeneous bulk algebraic cancellation scheme in Eqs. (54) and (59). Explicitly, we require that

$$\begin{aligned} \tilde{U}_{2x}^{(2x)} [\tilde{V}_{2x-1}^{(2x-1)} \tilde{W}_{2x}^{(2x)} \tilde{Z}_{2x+1}^{(2x+1)}] &= \tilde{Z}_{2x-1}^{(2x-1)} \tilde{V}_{2x}^{(2x)} \tilde{W}_{2x+1}^{(2x+1)}, \\ \tilde{U}_{2x+1}^{(2x+1)} [\tilde{Z}_{2x}^{(2x)} \tilde{W}_{2x+1}^{(2x+1)} \tilde{V}_{2x+2}^{(2x+2)}] &= \tilde{W}_{2x}^{(2x)} \tilde{V}_{2x+1}^{(2x+1)} \tilde{Z}_{2x+2}^{(2x+2)}, \end{aligned} \quad (220)$$

which encodes the matrix product equations,

$$\begin{aligned} a_{n_{2x-1}, f_{2x}}^{(2x-1)} a_{f_{2x}, n_{2x+1}}^{(2x)} \tilde{V}_{n_{2x-1}}^{(2x-1)} \tilde{W}_{f_{2x}}^{(2x)} \tilde{Z}_{n_{2x+1}}^{(2x+1)} &= \tilde{Z}_{n_{2x-1}}^{(2x-1)} \tilde{V}_{n_{2x}}^{(2x)} \tilde{W}_{n_{2x+1}}^{(2x+1)}, \\ b_{n_{2x}, f_{2x+1}}^{(2x)} b_{f_{2x+1}, n_{2x+2}}^{(2x+1)} \tilde{Z}_{n_{2x}}^{(2x)} \tilde{W}_{f_{2x+1}}^{(2x+1)} \tilde{V}_{n_{2x+2}}^{(2x+2)} &= \tilde{W}_{n_{2x}}^{(2x)} \tilde{V}_{n_{2x+1}}^{(2x+1)} \tilde{Z}_{n_{2x+2}}^{(2x+2)}, \end{aligned} \quad (221)$$

where, for convenience, we have introduced the *exchange matrices* $\tilde{Z}_{n_x}^{(x)}$ [i.e., site dependent generalizations of the delimiter matrix S (55)], with the associated vector,

$$\tilde{Z}_x^{(x)} = \begin{bmatrix} \tilde{z}_0^{(x)} \\ \tilde{z}_1^{(x)} \end{bmatrix}. \quad (222)$$

We now postulate the following ansatz for the matrices of the inhomogeneous algebra that generalizes Eq. (52),

$$\begin{aligned} \tilde{V}_0^{(x)} &= \begin{bmatrix} 1 & \tilde{v}_{01}^{(x)} \\ 0 & 0 \end{bmatrix}, \quad \tilde{W}_0^{(x)} = \begin{bmatrix} 1 & \tilde{w}_{01}^{(x)} \\ 0 & 0 \end{bmatrix}, \\ \tilde{V}_1^{(x)} &= \begin{bmatrix} 0 & 0 \\ \tilde{v}_{10}^{(x)} & 1 \end{bmatrix}, \quad \tilde{W}_1^{(x)} = \begin{bmatrix} 0 & 0 \\ \tilde{w}_{10}^{(x)} & 1 \end{bmatrix}, \end{aligned} \quad (223)$$

while the ansatz for the exchange matrices reads

$$\tilde{Z}_0^{(x)} = \begin{bmatrix} \tilde{z}_{00}^{(x)} & \tilde{z}_{01}^{(x)} \\ 0 & 0 \end{bmatrix}, \quad \tilde{Z}_1^{(x)} = \begin{bmatrix} 0 & 0 \\ \tilde{z}_{10}^{(x)} & \tilde{z}_{11}^{(x)} \end{bmatrix}. \quad (224)$$

Requiring that the inhomogeneous algebraic relations in Eq. (221) can be exactly solved using the generalized site

dependent matrix ansatz postulated imposes constraints on the tilt operators $A(s)$ and $B(s)$, reminiscent of those placed on the boundary operators R and L in Sec. IV B. A particularly convenient choice of parametrization, that has a remarkably simple physical interpretation, can be obtained by setting

$$\begin{aligned} a_{n_x, n_{x+1}}^{(x)} &= a_{1-n_x, 1-n_{x+1}}^{(x)}, \\ b_{n_x, n_{x+1}}^{(x)} &= b_{1-n_x, 1-n_{x+1}}^{(x)}, \end{aligned} \quad (225)$$

which is nothing but the requirement that $A(s)$ and $B(s)$ obey the *particle-hole* symmetry of the model. Under this set of conditions, the inhomogeneous bulk algebra yields the following two-parameter family of solutions:

$$\begin{aligned} \tilde{v}_{01}^{(2x)} &= \tilde{v}_{10}^{(2x)} = \xi \prod_{j=0}^{x-1} \frac{b_{01}^{(2j)} a_{01}^{(2j+1)}}{b_{00}^{(2j)} a_{00}^{(2j+1)}}, \\ \tilde{w}_{01}^{(2x)} &= \tilde{w}_{10}^{(2x)} = \omega \prod_{j=1}^x \frac{b_{00}^{(2j-1)} a_{00}^{(2j)}}{b_{01}^{(2j-1)} a_{01}^{(2j)}}, \\ \tilde{z}_{00}^{(2x)} &= \tilde{z}_{11}^{(2x)} = \prod_{j=1}^{2x-1} b_{00}^{(j)}, \\ \tilde{z}_{01}^{(2x)} &= \tilde{z}_{10}^{(2x)} = \xi \prod_{j=0}^{x-1} \frac{b_{01}^{(2j)} a_{01}^{(2j+1)} b_{00}^{(2j+1)}}{a_{00}^{(2j+1)}}, \\ \tilde{v}_{01}^{(2x+1)} &= \tilde{v}_{10}^{(2x+1)} = \xi \prod_{j=1}^x \frac{a_{01}^{(2j-1)} b_{01}^{(2j)}}{a_{00}^{(2j-1)} b_{00}^{(2j)}}, \\ \tilde{w}_{01}^{(2x+1)} &= \tilde{w}_{10}^{(2x+1)} = \omega \prod_{j=0}^x \frac{a_{00}^{(2j)} b_{00}^{(2j+1)}}{a_{01}^{(2j)} b_{01}^{(2j+1)}}, \\ \tilde{z}_{00}^{(2x+1)} &= \tilde{z}_{11}^{(2x+1)} = \prod_{j=1}^{2x} \frac{1}{a_{00}^{(j)}}, \\ \tilde{z}_{01}^{(2x+1)} &= \tilde{z}_{10}^{(2x+1)} = \omega \prod_{j=0}^x \frac{b_{00}^{(2j+1)}}{a_{01}^{(2j)} b_{01}^{(2j+1)} a_{00}^{(2j+1)}}, \end{aligned} \quad (226)$$

where we have used the convention that

$$\begin{aligned} a_{n_{-1}, n_0}^{(-1)} &= a_{n_0, n_1}^{(0)} = 1, \\ b_{n_{-1}, n_0}^{(-1)} &= b_{n_0, n_1}^{(0)} = 1. \end{aligned} \quad (227)$$

Analogous to the treatment of the NESS in Sec. V, we additionally require that the tilted row vectors of the left boundary $\langle \tilde{L} |$ and $\langle \tilde{L}' |$ and tilted column vectors of the right boundary $| \tilde{R} \rangle$ and $| \tilde{R}' \rangle$, satisfy inhomogeneous site dependent boundary algebraic relations generalizing the homogeneous identities Eqs. (131), (132), (133), and (134). In particular, we demand the following relations hold,

$$\langle \tilde{L} | \tilde{Z}_1^{(1)} = \langle \tilde{L}' | \tilde{W}_1^{(1)}, \quad (228)$$

$$\tilde{R}_{2N} [\tilde{V}_{2N-1}^{(2N-1)} \tilde{W}_{2N}^{(2N)} | \tilde{R} \rangle] = \tilde{\Lambda}_R \tilde{Z}_{2N-1}^{(2N-1)} \tilde{V}_{2N}^{(2N)} | \tilde{R}' \rangle, \quad (229)$$

$$\tilde{L}_1 [\langle \tilde{L}' | \tilde{W}_1^{(1)} \tilde{V}_2^{(2)}] = \tilde{\Lambda}_L \langle \tilde{L} | \tilde{V}_1^{(1)} \tilde{Z}_2^{(2)}, \quad (230)$$

$$\tilde{Z}_{2N}^{(2N)} | \tilde{R}' \rangle = \tilde{W}_{2N}^{(2N)} | \tilde{R} \rangle, \quad (231)$$

which, in terms of the auxiliary matrices, read

$$\langle \tilde{L} | \tilde{Z}_{n_1}^{(1)} = \langle \tilde{L}' | \tilde{W}_{n_1}^{(1)}, \quad (232)$$

$$\sum_{n_5=0}^1 \phi_{n_3, f_4, n_5} a_{n_3, f_4}^{(3)} \tilde{V}_{n_3}^{(3)} \tilde{W}_{f_4}^{(4)} | \tilde{R} \rangle = \tilde{\Lambda}_R \tilde{Z}_{n_3}^{(3)} \tilde{V}_{n_4}^{(4)} | \tilde{R}' \rangle, \quad (233)$$

$$\sum_{n_0=0}^1 \varphi_{n_0, f_1, n_2} b_{f_1, n_2}^{(1)} \langle \tilde{L}' | \tilde{W}_{f_1}^{(1)} \tilde{V}_{n_2}^{(2)} = \tilde{\Lambda}_L \langle \tilde{L} | \tilde{V}_{n_1}^{(1)} \tilde{Z}_{n_2}^{(2)}, \quad (234)$$

$$\tilde{Z}_{n_4}^{(4)} | \tilde{R}' \rangle = \tilde{W}_{n_4}^{(4)} | \tilde{R} \rangle, \quad (235)$$

where, to save space, we set $N = 2$ at the right boundary. It can be straightforwardly shown by direct computation that if these inhomogeneous bulk and boundary relations are satisfied, then the coupled eigenvalue Eqs. (215) are solved. As an example, for a chain of size $N = 2$, the second relation follows as

$$\begin{aligned} \tilde{\mathbb{M}}_0 \tilde{p}' &= \tilde{L}_1 \tilde{U}_3^{(3)} \langle \tilde{L}' | \tilde{W}_1^{(1)} \tilde{V}_2^{(2)} \tilde{W}_3^{(3)} \tilde{V}_4^{(4)} | \tilde{R}' \rangle \\ &= \tilde{\Lambda}_L \tilde{U}_3^{(3)} \langle \tilde{L} | \tilde{V}_1^{(1)} \tilde{Z}_2^{(2)} \tilde{W}_3^{(3)} \tilde{V}_4^{(4)} | \tilde{R}' \rangle \\ &= \tilde{\Lambda}_L \langle \tilde{L} | \tilde{V}_1^{(1)} \tilde{W}_2^{(2)} \tilde{V}_3^{(3)} \tilde{Z}_4^{(4)} | \tilde{R}' \rangle \\ &= \tilde{\Lambda}_L \langle \tilde{L} | \tilde{V}_1^{(1)} \tilde{W}_2^{(2)} \tilde{V}_3^{(3)} \tilde{W}_4^{(4)} | \tilde{R} \rangle \\ &= \tilde{\Lambda}_L \tilde{p}, \end{aligned} \quad (236)$$

with the first equation of Eq. (215) following analogously. Solving the pair of inhomogeneous algebraic relations for the right boundary, Eqs. (233) and (235), yields a pair of expressions for the spectral parameters,

$$\xi = \sigma \frac{\tilde{\Lambda}_R \tilde{z}_{00}^{(2N+1)} - \tilde{z}_{00}^{(2N)} (1 - \alpha)}{\tilde{z}_{01}^{(2N)} \beta}, \quad (237)$$

$$\omega = \sigma \frac{\tilde{\Lambda}_R \tilde{z}_{00}^{(2N+1)} (1 - \beta) - \tilde{z}_{00}^{(2N)} (1 - \alpha - \beta)}{\tilde{\Lambda}_R \tilde{z}_{01}^{(2N+1)} \beta}, \quad (238)$$

with $\sigma = \pm 1$ and right boundary vectors,

$$| \tilde{R} \rangle = \tilde{r} \begin{bmatrix} 1 \\ \sigma \end{bmatrix}, \quad | \tilde{R}' \rangle = \sigma \frac{\tilde{r}}{\tilde{z}_{00}^{(2N)}} \frac{1 + \sigma \tilde{w}_{01}^{(2N)}}{1 + \sigma \tilde{v}_{01}^{(2N)}} \begin{bmatrix} 1 \\ \sigma \end{bmatrix}, \quad (239)$$

where \tilde{r} is a scalar that determines the normalization of the right boundary vector and with the convention that

$$\begin{aligned} a_{n_{2N}, n_{2N+1}}^{(2N)} &= a_{n_{2N+1}, n_{2N+2}}^{(2N+1)} = 1, \\ b_{n_{2N}, n_{2N+1}}^{(2N)} &= b_{n_{2N+1}, n_{2N+2}}^{(2N+1)} = 1. \end{aligned} \quad (240)$$

Similarly, for the left boundary relations Eqs. (232) and (234), we obtain a pair of solutions for the spectral parameters,

$$\xi = \tau \frac{\tilde{\Lambda}_L (1 - \delta) - (1 - \gamma - \delta)}{\tilde{\Lambda}_L \delta}, \quad (241)$$

$$\omega = \tau \frac{\tilde{\Lambda}_L - (1 - \gamma)}{\delta}, \quad (242)$$

with $\tau = \pm 1$ and left boundary vectors,

$$\langle \tilde{L} | = \tilde{l} [1 \quad \tau], \quad \langle \tilde{L}' | = \tilde{l} [1 \quad \tau], \quad (243)$$

where \tilde{l} is the corresponding scalar that determines the normalization of the left boundary vector. A particularly convenient parametrization for the eigenvector \tilde{p} , that is consistent with the expression for the vector p in Sec. V, is

obtained by setting

$$\tilde{r} = \frac{1}{1 + \sigma \tilde{w}_{01}^{(2N)}}, \quad \tilde{l} = 1. \quad (244)$$

It then follows from the ansatz Eqs. (223) and (224), that the components \tilde{p}_n of the eigenvectors \tilde{p} take the form of a generalized *site dependent* grand canonical ensemble,

$$\tilde{p}_n = \tau^{n_1} \prod_{x^\pm} \tilde{v}_{01}^{(x^+)} \tilde{w}_{01}^{(x^-)} \propto \xi^{N_n^+} \omega^{N_n^-}, \quad (245)$$

where, as before, the τ corresponds to the choice of solution at the left boundary while the sets x^\pm denote the sets of sites which are occupied, respectively, by the positive and negative quasiparticles (e.g., $\tilde{p}_{0010} = \tilde{w}_{01}^{(2)} \tilde{v}_{01}^{(3)} \propto \xi \omega$).

As was done in Sec. V, we now impose equality between the pair of expressions for the spectral parameters at the right and left boundaries. Rearranging and subsequently solving for the eigenvalue $\tilde{\Lambda}(s) = \tilde{\Lambda}_L(s) \tilde{\Lambda}_R(s)$ returns the following pair of quadratic characteristic polynomials,

$$\tilde{\Lambda}^2 - \left(\sum_{j=0}^1 \sum_{k=0}^1 \tau^{j+k} \psi_{j,k} \tilde{Z}_{j,k} \right) \tilde{\Lambda} + \psi \tilde{Z} = 0, \quad (246)$$

where we have introduced

$$\begin{aligned} \tilde{Z}_{00} &= \prod_{j=1}^{2N} a_{00}^{(j)} b_{00}^{(j)}, \\ \tilde{Z}_{01} &= \prod_{j=1}^N a_{00}^{(2j-1)} b_{01}^{(2j-1)} a_{01}^{(2j)} b_{00}^{(2j)}, \\ \tilde{Z}_{10} &= \prod_{j=1}^N a_{01}^{(2j-1)} b_{00}^{(2j-1)} a_{00}^{(2j)} b_{01}^{(2j)}, \\ \tilde{Z}_{11} &= \prod_{j=1}^{2N} a_{01}^{(j)} b_{01}^{(j)}, \end{aligned} \quad (247)$$

which satisfy the following identity:

$$\tilde{Z} \equiv \tilde{Z}_{00} \tilde{Z}_{11} \equiv \tilde{Z}_{01} \tilde{Z}_{10} = \prod_{j=1}^{2N} a_{00}^{(j)} a_{01}^{(j)} b_{00}^{(j)} b_{01}^{(j)}, \quad (248)$$

and the coefficients,

$$\begin{aligned} \psi_{00} &= (1 - \alpha)(1 - \gamma), \\ \psi_{01} &= \alpha \delta, \\ \psi_{10} &= \beta \gamma, \\ \psi_{11} &= (1 - \beta)(1 - \delta), \end{aligned} \quad (249)$$

which satisfy the following equality:

$$\psi \equiv \sum_{j=0}^1 \sum_{k=0}^1 \psi_{j,k} - 1 = (1 - \alpha - \beta)(1 - \gamma - \delta). \quad (250)$$

As a consistency check, when $s = 0$ we recover the quadratic characteristic polynomials Eq. (146) in Sec. V, for which the corresponding dominant eigenvalue $\tilde{\Lambda} = \Lambda = 1$, as expected for a stochastic operator.

D. Dynamical phase transition

We can straightforwardly solve the quadratic equation in Eq. (246) to obtain an explicit expression for $\tilde{\Lambda}(s)$, for any arbitrary observables satisfying the constraint Eq. (225). Specifically, the dominant eigenvalue reads

$$\tilde{\Lambda}(s) = \tilde{\eta}(s) + \sqrt{\tilde{\eta}^2(s) - \tilde{\mu}(s)}, \quad (251)$$

with

$$\tilde{\eta}(s) = \frac{1}{2} \sum_{j=0}^1 \sum_{k=0}^1 \psi_{j,k} \tilde{Z}_{j,k}, \quad \tilde{\mu}(s) = \psi \tilde{Z}. \quad (252)$$

As the observables Eq. (201) are extensive in the system size, we can define the tilting functions as

$$\tilde{Z}_{j,k} = \exp(-Ns\zeta_{j,k}), \quad (253)$$

such that the following limits exist and are finite,

$$\zeta_{j,k} = -\lim_{N \rightarrow \infty} \frac{\ln \tilde{Z}_{j,k}}{Ns}. \quad (254)$$

The SCGF can then be expressed in the scaling form,

$$\theta_N(s) \equiv \vartheta(Ns). \quad (255)$$

Immediately, this scaling form Eq. (255) provides us with the cumulants of K in the long-time limit $T \rightarrow \infty$, namely,

$$\kappa_j \equiv \lim_{T \rightarrow \infty} \frac{1}{T} \langle \langle K^j \rangle \rangle = (-1)^j \left. \frac{d^j}{ds^j} \theta_N(s) \right|_{s=0} \propto N^j, \quad (256)$$

where $\langle \langle K^j \rangle \rangle$ denotes the j th cumulant of the observable K . Note that in the thermodynamic limit (i.e., $N \rightarrow \infty$), the long-time cumulants of K for $j \geq 2$ diverge for $s = 0$, therefore, indicating the existence of a singularity (i.e., a *dynamical phase transition* in the trajectory statistics).

We can construct explicitly the exact form of all cumulants $\langle \langle K^j \rangle \rangle$ for all even system sizes $2N$ in the long-time limit $T \rightarrow \infty$, as detailed in Appendix H. For $j = 1$, we obtain the *mean* of K per unit time,

$$\kappa_1 = -\frac{4\tilde{\eta}' - \tilde{\mu}'}{2(1 - \tilde{\mu})}, \quad (257)$$

while for $j = 2$, we get the *variance* of K per unit time,

$$\kappa_2 = \frac{4\tilde{\eta}'' - \tilde{\mu}''}{2(1 - \tilde{\mu})} + \frac{(4\tilde{\eta}' - \tilde{\mu}')\tilde{\mu}'}{4(1 - \tilde{\mu})^2} - \frac{(4\tilde{\eta}' - \tilde{\mu}')^2}{4(1 - \tilde{\mu})^3}, \quad (258)$$

where the derivatives are given by

$$\tilde{\eta}^{(m)} \equiv \left. \frac{d^m}{ds^m} \tilde{\eta}(s) \right|_{s=0} = \frac{1}{2} \sum_{j=0}^1 \sum_{k=0}^1 \psi_{j,k} (-N\zeta_{j,k})^m, \quad (259)$$

$$\tilde{\mu}^{(m)} \equiv \left. \frac{d^m}{ds^m} \tilde{\mu}(s) \right|_{s=0} = \psi (-N\zeta)^m.$$

We now consider the asymptotic behavior of the scaling function $\vartheta(Ns)$, which under the assumption of positive tilting functions $\zeta_{11} > \dots > \zeta_{00}$, takes the form

$$\vartheta(Ns) = \begin{cases} -Ns\zeta_{11} + \ln \psi_{11} + \dots & Ns \rightarrow \infty, \\ -Ns\zeta_{00} + \ln \psi_{00} + \dots & Ns \rightarrow -\infty. \end{cases} \quad (260)$$

It can then be deduced that the SCGF converges to

$$\lim_{N \rightarrow \infty} \frac{1}{N} \theta_N(s) = \begin{cases} -s\zeta_{11} & s > 0, \\ -s\zeta_{00} & s < 0, \end{cases} \quad (261)$$

where the singularity at $s = 0$ corresponds to a *first-order phase transition*.

In Fig. 7 we plot the SCGF $\theta_N(s)$ and its cumulants, specifically, the mean $-\theta'_N(s)$ and the variance $\theta''_N(s)$, for a particular observable, namely, the current (i.e., the time integrated number of quasiparticles). From inspection, it is clear that the SCGF converges toward the asymptotic form in Eq. (261) as $N \rightarrow \infty$, with the discontinuity (i.e., the critical point) occurring at $s = 0$. Similarly, the mean transitions from being positive for $s < 0$, to negative for $s > 0$ around the critical point at $s = 0$, with the change becoming discontinuous in the thermodynamic limit (i.e., $N \rightarrow \infty$). This transformation in the shape of the mean, characterizing the dynamical phase transition, manifests in the variance as its maximum scales with N , while the corresponding value of s , which indicates the singularity, scales with $1/N$. We also show the rate function $\varphi_N(k)$, which we obtain by taking the Legendre transform of the SCGF Eq. (204),

$$\varphi_N(k) = -\min_s [sk + \theta_N(s)]. \quad (262)$$

As can be seen from inspection, the rate function $\varphi_N(k)$ broadens with increasing finite system size N , indicating large fluctuations in the dynamics. In the limit $N \rightarrow \infty$, $\varphi_N(k)$ converges toward a square well, with the extrema $\max k = \zeta_{00}$ and $\min k = \zeta_{11}$ associated to the coexisting dynamically active phases.

These results are reminiscent of those obtained for the Rule 54 RCA [5]. Dynamics of the Rule 150 RCA sits at the coexistence point between two dynamical phases, one of high activity where K is large, and one of low activity with K vanishing in the large size limit. Fluctuations in each of these phases are highly suppressed with the main source coming from the coexistence (cf. Fig. 7). Much like the case of Rule 54 (i.e., the RCA counterpart to the FA model), we find that the main ingredient facilitating the active-inactive transitions are the kinetic constraints. The simplicity in the form of $\theta_N(s)$, as compared to other KCM, is a consequence of the deterministic dynamics in the bulk, as all fluctuations originate from the stochastic boundaries. Since the probabilistic cost of realizing a rare fluctuation in the boundary (e.g., not emitting any given quasiparticle if doing so yields the empty state) does not scale with the system size, rare trajectories can be easily realized. Boundary control over the bulk is a hallmark of a phase transition, and here, by construction, we have an immediate realization of this phenomenon in space-time.

E. Doob transformation

Having the exact form of the leading eigenstate of the tilted operator also allows us to find the exact *generalized Doob transform* [56–59]. This refers to the construction of a stochastic operator whose trajectories are the atypical trajectories described by the nonstochastic tilted operator. In other words, to derive the operator that gives the optimal dynamics with which to sample the exponentially rare trajectories of the original dynamics associated with counting field s . For long

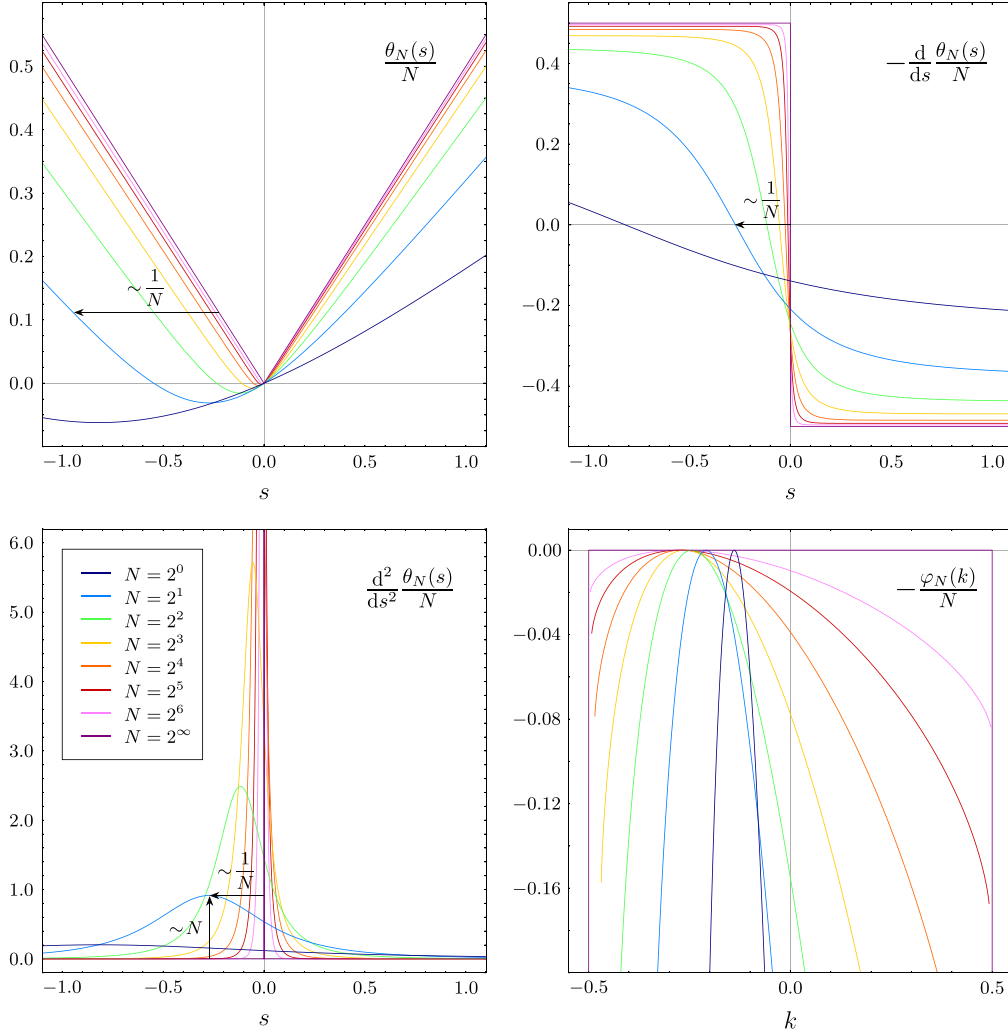


FIG. 7. Dynamical first-order phase transition. SCGF $\theta_N(s)/N$ [top left], mean $-\theta'_N(s)/N$ [top right], variance $\theta''_N(s)/N$ [bottom left], and rate function $\varphi_N(k)/N$ [bottom right] for the current $\zeta_{00} = \zeta_{11} = 0$, $\zeta_{01} = -\zeta_{10} = 1/2$, explicitly, the time integrated number of quasiparticles, for systems of even sizes $2N$ (see legend) with boundary conditional probabilities $\alpha = 3/5$, $\beta = 7/8$, $\gamma = 8/9$, and $\delta = 4/7$. In the thermodynamic limit $N \rightarrow \infty$, the SCGF approaches the asymptotic form in Eq. (261) while the mean exhibits a first-order phase transition about $s = 0$. Correspondingly, the variance diverges as $N \rightarrow \infty$, with the singularity converging toward $s = 0$ as $1/N$. Additionally shown is the rate function which broadens toward a square well in the asymptotic limit.

times, this construction only requires the leading eigenvalue and eigenvector.

We can obtain an explicit expression for the long-time Doob operator from the MPS representation of the leading eigenvector $\tilde{\mathbf{p}}$ of the tilted Markov operator $\tilde{\mathbb{M}}(s)$ through [56–59]

$$\tilde{D}(s) \equiv \frac{1}{\tilde{\Lambda}(s)} \tilde{Q}(s) \tilde{\mathbb{M}}(s) \tilde{Q}^{-1}(s), \quad (263)$$

where $\tilde{\Lambda}(s)$ is the dominant eigenvalue of $\tilde{\mathbb{M}}(s)$ and $\tilde{Q}(s)$ is a diagonal operator defined in terms of the components of the corresponding leading left eigenvector $\tilde{\mathbf{q}}$ of $\tilde{\mathbb{M}}(s)$,

$$\tilde{Q}(s) = \sum_n \mathbf{e}_n \mathbf{e}_n^T \cdot \tilde{\mathbf{q}}, \quad (264)$$

where \mathbf{e}_n denotes a standard basis (column) vector (cf. Sec II) and

$$\tilde{\mathbf{q}} \tilde{\mathbb{M}}(s) = \tilde{\Lambda}(s) \tilde{\mathbf{q}}. \quad (265)$$

To reduce the computation required to obtain an analytic expression for the leading left eigenvector $\tilde{\mathbf{q}}$ we utilize the technique used for Rule 54 in Ref. [5]. Namely, define

$$\tilde{\mathbf{q}} \equiv [A(s) \hat{\mathbf{q}}]^T = \hat{\mathbf{q}}^T A(s), \quad (266)$$

where $\hat{\mathbf{q}}$ can be straightforwardly shown to be the leading right eigenvector of the newly introduced operator $\hat{\mathbb{M}}(s)$, with $\hat{\Lambda}(s) \equiv \tilde{\Lambda}(s)$ the associated eigenvalue. Specifically, taking the transpose of the left eigenvalue Eq. (265), while utilizing the similarity transformation for the left eigenvector Eq. (266),

we have for the left-hand side,

$$\begin{aligned} [\hat{q}^T A(s) \tilde{M}(s)]^T &= [\hat{q}^T A(s) M_O B(s) M_E A(s)]^T \\ &= A^T(s) M_E^T B^T(s) M_O^T A^T(s) \hat{q} \\ &= A(s) M_E^T B(s) M_O^T A(s) \hat{q}, \end{aligned} \quad (267)$$

where, to obtain the final equality, we used the property that the tilt operators $A(s)$ and $B(s)$ are diagonal. The corresponding right-hand side of the equation then reads

$$(\hat{\Lambda}(s) \hat{q}^T A(s))^T = \hat{\Lambda}(s) A^T(s) \hat{q} = \hat{\Lambda}(s) A(s) \hat{q}. \quad (268)$$

Multiplying both sides on the left by $A^{-1}(s)$ then gives

$$\tilde{M}(s) \hat{q} \equiv M_E^T B(s) M_O^T A(s) \hat{q} = \hat{\Lambda}(s) \hat{q}, \quad (269)$$

with the transposed even and odd time step operators,

$$M_E^T = R_{2N}^T \prod_{x=1}^{N-1} U_{2x}, \quad M_O^T = L_1^T \prod_{x=1}^{N-1} U_{2x+1}. \quad (270)$$

As we did for the leading right eigenvector \tilde{p} , we now construct a pair of vectors \hat{q} and \hat{q}' that satisfy the coupled eigenvalue equations,

$$M_O^T A(s) \hat{q} = \hat{\Lambda}_L(s) \hat{q}', \quad M_E^T B(s) \hat{q}' = \hat{\Lambda}_R(s) \hat{q}, \quad (271)$$

where \hat{q} and \hat{q}' take a matrix product form, reminiscent of the ansatz of the vectors \tilde{p}' and \tilde{p} , respectively. More precisely, their components read

$$\begin{aligned} \hat{q}_n &= \langle \hat{L} | \hat{W}_{n_1}^{(1)} \hat{V}_{n_2}^{(2)} \dots \hat{W}_{n_{2N-1}}^{(2N-1)} \hat{V}_{n_{2N}}^{(2N)} | \hat{R} \rangle, \\ \hat{q}'_n &= \langle \hat{L}' | \hat{V}_{n_1}^{(1)} \hat{W}_{n_2}^{(2)} \dots \hat{V}_{n_{2N-1}}^{(2N-1)} \hat{W}_{n_{2N}}^{(2N)} | \hat{R}' \rangle. \end{aligned} \quad (272)$$

Analogous to the right eigenvectors \tilde{p} and \tilde{p}' , the vectors \hat{q} and \hat{q}' satisfy inhomogeneous bulk algebraic relations that can be written as

$$\begin{aligned} b_{n_{2x-1}, f_{2x}}^{(2x-1)} b_{f_{2x}, n_{2x+1}}^{(2x)} \hat{V}_{n_{2x-1}}^{(2x-1)} \hat{W}_{f_{2x}}^{(2x)} \hat{Z}_{n_{2x+1}}^{(2x+1)} &= \hat{Z}_{n_{2x-1}}^{(2x-1)} \hat{V}_{n_{2x}}^{(2x)} \hat{W}_{n_{2x+1}}^{(2x+1)}, \\ a_{n_{2x}, f_{2x+1}}^{(2x)} a_{f_{2x+1}, n_{2x+2}}^{(2x+1)} \hat{Z}_{n_{2x}}^{(2x)} \hat{W}_{f_{2x+1}}^{(2x+1)} \hat{V}_{n_{2x+2}}^{(2x+2)} &= \hat{W}_{n_{2x}}^{(2x)} \hat{V}_{n_{2x+1}}^{(2x+1)} \hat{Z}_{n_{2x+2}}^{(2x+2)}, \end{aligned} \quad (273)$$

which are identical to Eq. (221), but with the local tilting functions exchanged $a_{n_x, n_{x+1}}^{(x)} \leftrightarrow b_{n_x, n_{x+1}}^{(x)}$. It then follows directly that the explicit solutions to these equations are of the same form as Eq. (226), but with

$$\begin{aligned} \hat{V}_{n_x}^{(x)}(a_{n_x, n_{x+1}}^{(x)}, b_{n_x, n_{x+1}}^{(x)}) &\equiv \tilde{V}_{n_x}^{(x)}(b_{n_x, n_{x+1}}^{(x)}, a_{n_x, n_{x+1}}^{(x)}), \\ \hat{W}_{n_x}^{(x)}(a_{n_x, n_{x+1}}^{(x)}, b_{n_x, n_{x+1}}^{(x)}) &\equiv \tilde{W}_{n_x}^{(x)}(b_{n_x, n_{x+1}}^{(x)}, a_{n_x, n_{x+1}}^{(x)}), \\ \hat{Z}_{n_x}^{(x)}(a_{n_x, n_{x+1}}^{(x)}, b_{n_x, n_{x+1}}^{(x)}) &\equiv \tilde{Z}_{n_x}^{(x)}(b_{n_x, n_{x+1}}^{(x)}, a_{n_x, n_{x+1}}^{(x)}). \end{aligned} \quad (274)$$

The corresponding boundary relations then read

$$\begin{aligned} \langle \hat{L}' | \hat{Z}_{n_1}^{(1)} \rangle &= \langle \hat{L} | \hat{W}_{n_1}^{(1)} \rangle, \\ \sum_{n_5=0}^1 \phi_{n_3, n_4, n_5} b_{n_3, f_4}^{(3)} \hat{V}_{n_3}^{(3)} \hat{W}_{f_4}^{(4)} | \hat{R}' \rangle &= \hat{\Lambda}_R \hat{Z}_{n_3}^{(3)} \hat{V}_{n_4}^{(4)} | \hat{R} \rangle, \\ \sum_{n_0=0}^1 \varphi_{n_0, n_1, n_2} a_{f_1, n_2}^{(1)} \langle \hat{L} | \hat{W}_{f_1}^{(1)} \hat{V}_{n_2}^{(2)} \rangle &= \hat{\Lambda}_L \langle \hat{L}' | \hat{V}_{n_1}^{(1)} \hat{Z}_{n_2}^{(2)} \rangle, \\ \hat{Z}_{n_4}^{(4)} | \hat{R} \rangle &= \hat{W}_{n_4}^{(4)} | \hat{R}' \rangle, \end{aligned} \quad (275)$$

which are the same as Eqs. (232), (233), (234), and (235), but the functions $a_{n_x, n_{x+1}}^{(x)}$ and $b_{n_x, n_{x+1}}^{(x)}$ interchanged and with the stochastic boundary matrices R and L replaced by their transposes, which is equivalent to exchanging the elements $\phi_{n_3, f_4, n_5} \leftrightarrow \phi_{n_3, n_4, n_5}$, $\varphi_{n_0, f_1, n_2} \leftrightarrow \varphi_{n_0, n_1, n_2}$. If we solve the right boundary equations, as we did for the right eigenvector, then we obtain the following expressions for the spectral parameters:

$$\begin{aligned} \xi &= \sigma \frac{\hat{\Lambda}_R \hat{z}_{00}^{(2N+1)} - \hat{z}_{00}^{(2N)} (1 - \alpha)}{\hat{z}_{01}^{(2N)} \alpha}, \\ \omega &= \sigma \frac{\hat{\Lambda}_R \hat{z}_{00}^{(2N+1)} (1 - \beta) - \hat{z}_{00}^{(2N)} (1 - \alpha - \beta)}{\hat{\Lambda}_R \hat{z}_{01}^{(2N+1)} \alpha}, \end{aligned} \quad (276)$$

where the right boundary vectors are given by

$$|\hat{R}\rangle = \hat{r} \begin{bmatrix} 1 \\ \sigma \end{bmatrix}, \quad |\hat{R}'\rangle = \sigma \hat{r} \hat{z}_{00}^{(2N)} \frac{1 + \sigma \tilde{v}_{01}^{(2N)}}{1 + \sigma \tilde{w}_{01}^{(2N)}} \begin{bmatrix} 1 \\ \sigma \end{bmatrix}. \quad (277)$$

Similarly solving the left boundary equations gives

$$\begin{aligned} \xi &= \tau \frac{\hat{\Lambda}_L (1 - \delta) - (1 - \gamma - \delta)}{\hat{\Lambda}_L \gamma}, \\ \omega &= \tau \frac{\hat{\Lambda}_L - (1 - \gamma)}{\gamma}, \end{aligned} \quad (278)$$

for the spectral parameters, with the boundary vectors

$$\langle \hat{L} | = \hat{l} [1 \quad \tau], \quad \langle \hat{L}' | = \hat{l} [1 \quad \tau]. \quad (279)$$

It can be easily verified that equating the expressions for the spectral parameters ξ and ω at either boundary and then solving for the eigenvalue $\hat{\Lambda}(s) = \hat{\Lambda}_L \hat{\Lambda}_R$ returns the quadratic characteristic polynomials Eq. (246), as expected. Furthermore, it follows that by setting

$$\hat{r} = \frac{1}{1 + \sigma \hat{v}_{01}^{(2N)}}, \quad \hat{l} = 1, \quad (280)$$

the components \hat{q}_n of the eigenvectors \hat{q} of the operator $\tilde{M}(s)$ take a form reminiscent to that of the vectors \tilde{p} [cf. Eq. (245)]. Specifically,

$$\hat{q}_n = \tau^{n_1} \prod_{x^\pm} \hat{v}_{01}^{(x^\pm)} \hat{w}_{01}^{(x^\pm)} \propto \xi^{N_+} \omega^{N_-}. \quad (281)$$

Explicit expressions for the left eigenvector \tilde{q} of the tilted Markov operator $\tilde{M}(s)$, the diagonal operator $\tilde{Q}(s)$, and, most importantly, the long-time Doob operator $\tilde{D}(s)$ then follow trivially from Eqs. (266), (264), and (263).

VII. CONCLUSIONS

The aim of this paper was to present a comprehensive study into the dynamics of a simple integrable cellular automaton. The model we studied here, the Rule 150 RCA, is integrable [22], but in contrast to other recently studied integrable RCA, its quasiparticles are noninteracting [8]. This allowed us to present within the paper a significant number of exact results, including the stationary states for both closed and open boundaries, the full spectrum of the evolution operator, and the large deviation dynamical phase diagram. Our work here adds to the growing number of exact results on statistical mechanics of

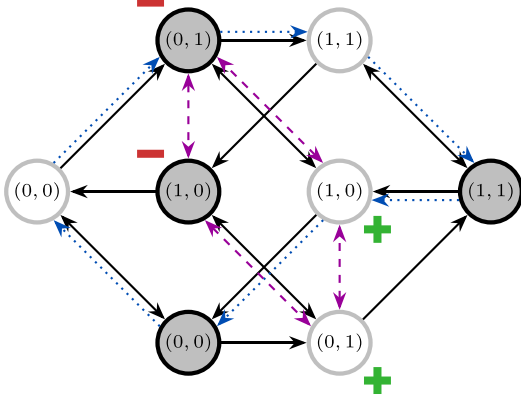


FIG. 8. Quasiparticle constraint. Graph representation of the lattice that illustrates the physical constraint imposed on the numbers of positive and negative quasiparticles by the even size of the system and PBC Eq. (26). Vertices associated to configurations that start on sites with even or odd space-time parity [i.e., $x + t \pmod{2}$] are, respectively, colored black and white; configurations with positive or negative quasiparticles are labeled by pluses and minuses. Black arrows indicate the directed edges which connect vertices obtained by shifting one site in space [i.e., $(n'_x, n'_{x+1}) \leftrightarrow (n'_{x+1}, n'_{x+2})$], or equivalently, one step in time [i.e., $(n'_x, n'_{x+1}) \leftrightarrow (n'_{x+1}, n'_{x+1})$], while purple dashed arrows correspond to the subset of contracted directed edges of the subgraph. To illustrate the basic concepts of this representation, the closed walk associated to the configuration $\underline{n} = (0, 0, 1, 1, 1, 0)$ is mapped by blue dotted arrows.

where the symmetry generator \mathcal{J}_N is trivially given by

$$\mathcal{J}_N = \sum_{n_1, \dots, n_{2N}=0}^1 (-1)^{\sum_x n_x} \mathbf{e}_{n_1, \dots, n_{2N}} \mathbf{e}_{n_1, \dots, n_{2N}}^T. \quad (\text{A14})$$

APPENDIX B: QUASIPARTICLE NUMBER CONSTRAINT

To prove the constraint on the numbers of positive and negative quasiparticles in a given configuration \underline{n} of even size $2N$ with PBC Eq. (26), we introduce a convenient graph theoretic representation for the lattice, shown in Fig. 8. The graph, a *directed bipartite graph*, is composed of two disjoint and independent sets of vertices, that are labeled by binary strings and represent the subconfigurations of adjacent sites with even and odd space and time indices [i.e., $x + t \pmod{2}$], respectively. Vertices of the even or odd set are then connected to vertices of the odd or even set by directed edges that correspond to either shifting one site in space (i.e., $x \leftrightarrow x + 1$) or evolving one step in time (i.e., $t \leftrightarrow t + 1$). We remark that we can simplify the graph significantly by contracting the paths between vertices whose labels represent quasiparticles Eq. (23). Doing so yields a *symmetric directed subgraph* with four vertices [i.e., a pair of vertices from each vertex set corresponding to the subconfigurations $(0, 1)$ and $(1, 0)$], that are each connected to exactly two other vertices. From this, it can be straightforwardly verified that each and every cycle of the subgraph is of even length and so satisfies Eq. (26).

APPENDIX C: MAXIMUM ENTROPY STATE

For the case where $\xi = \omega = 1$, the stationary states, \mathbf{p} and \mathbf{p}' , correspond to the *maximum entropy state*. That is, the state

for which the probabilities for each and every configuration are equal. In this limit, the MPS representation for the state simplifies such that the components of the probability state vectors can be written as

$$\lim_{\xi, \omega \rightarrow 1} p_n = \frac{1}{Z} \text{Tr}(M_{n_1} M_{n_2} \cdots M_{n_{2N-1}} M_{n_{2N}}), \quad (\text{C1})$$

where the auxiliary space matrices,

$$M_0 = \begin{bmatrix} 1 & 1 \\ 0 & 0 \end{bmatrix}, \quad M_1 = \begin{bmatrix} 0 & 0 \\ 1 & 1 \end{bmatrix}. \quad (\text{C2})$$

To prove the stationarity of the maximum entropy state, we introduce a cubic algebraic relation, analog to that in Eq. (54), which reads

$$M_{n_{x-1}} M_{f_x} M_{n_{x+1}} = M_{n_{x-1}} M_{n_x} M_{n_{x+1}}, \quad (\text{C3})$$

where we have utilized the simplifications in Eq. (60) and the fact that, in the limit $\xi, \omega \rightarrow 1$, the auxiliary matrices trivialize, explicitly, $V_{n_x}, W_{n_x} \rightarrow M_{n_x}$. Noting that this identity is solved by the following relation:

$$M_{n_x} M_{n_{x+1}} = M_{n_x}, \quad (\text{C4})$$

which holds for all $n_x = 0, 1$, then proves the invariance of the state. An identical proof holds for the state \mathbf{p}' as, in the limit $\xi, \omega \rightarrow 1$, $\mathbf{p}' \equiv \mathbf{p}$.

APPENDIX D: STATE COUNTING FUNCTION

To show that the state counting function Ω in Eq. (69) really counts the number of states with N^+ positive and N^- negative quasiparticles, we prove that the expressions for the grand canonical partition functions Eqs. (66) and (68) are equivalent. To start, we write the product of transfer matrices as a recursion relation, specifically,

$$T^N = T^{N-1} T, \quad (\text{D1})$$

with elements $T_{ij}^N \equiv (T^N)_{i,j}$ given by

$$T_{ij}^N = \sum_{k=0}^1 T_{ik}^{N-1} T_{kj}. \quad (\text{D2})$$

Substituting this parametrization for the transfer matrix components into Z Eq. (66) admits the following expression for the grand canonical partition function:

$$Z = \sum_{i=0}^1 T_{ii}^N. \quad (\text{D3})$$

Introducing the parametrization of the transfer matrix components,

$$T_{11} = T_{00} = 1 + \xi\omega, \quad T_{10} = T_{01} = \omega + \xi, \quad (\text{D4})$$

then allows us to reduce the system of Eqs. (D2) to just two recursive relations,

$$\begin{aligned} T_{00}^N &= (1 + \xi\omega) T_{00}^{N-1} + (\omega + \xi) T_{01}^{N-1}, \\ T_{01}^N &= (1 + \xi\omega) T_{01}^{N-1} + (\omega + \xi) T_{00}^{N-1}, \end{aligned} \quad (\text{D5})$$

yielding an expression for Z in terms of just one recursive parameter,

$$Z = 2T_{00}^N, \quad (\text{D6})$$

which can subsequently be expressed as a one-parameter second-order recurrence relation,

$$T_{00}^N = 2(1 + \xi\omega)T_{00}^{N-1} - (1 - \xi^2)(1 - \omega^2)T_{00}^{N-2}. \quad (\text{D7})$$

To relate the MPS representation of the grand canonical partition function Eq. (D6) to the expression for Z , obtained by normalizing the thermodynamic ensemble, in Eq. (68), we look for a combinatoric formulation for T_{00}^N . We start by noting that the recursive relations Eqs. (D5) can be rewritten in terms of the following summations:

$$\begin{aligned} T_{00}^N &= \sum_{i=0}^{\lfloor \frac{N}{2} \rfloor} \binom{N}{2i} (1 + \xi\omega)^{N-2i} (\omega + \xi)^{2i}, \\ T_{01}^N &= \sum_{i=0}^{\lfloor \frac{N}{2} \rfloor} \binom{N}{2i} (\omega + \xi)^{N-2i} (1 + \xi\omega)^{2i}. \end{aligned} \quad (\text{D8})$$

Expanding the binomials and rearranging for the spectral parameters then gives the following expression for T_{00}^N ,

$$T_{00}^N = \sum_{i=0}^{\lfloor \frac{N}{2} \rfloor} \binom{N}{2i} \sum_{j=0}^{N-2i} \binom{N-2i}{j} \sum_{k=0}^{2i} \binom{2i}{k} \xi^{2i+j-k} \omega^{j+k}. \quad (\text{D9})$$

To make further progress, we split the expression for T_{00}^N into three separate summations (i.e., $k < i$, $k = i$, $k > i$) which independently count the sets of configurations with $N^+ > N^-$, $N^+ = N^-$, and $N^+ < N^-$ quasiparticles. By proving the equivalence of each of these to the associated part of Eq. (68), we necessarily prove the equivalence of the grand canonical partition functions Eqs. (66) and (68) and the correctness of the state counting function Ω Eq. (69). In what follows, it will prove helpful to refer to the following binomial coefficient identities for increasing or decreasing the integers n and k ,

$$\begin{aligned} \binom{n}{k} &= \frac{k+1}{n-k} \binom{n}{k+1}, \\ \binom{n}{k} &= \frac{n+1-k}{n+1} \binom{n+1}{k}, \end{aligned} \quad (\text{D10})$$

and Vandermonde's identity,

$$\sum_{k=0}^j \binom{m}{k} \binom{n}{j-k} = \binom{m+n}{j}. \quad (\text{D11})$$

To start, we consider the summation for $k < i$,

$$T_{00}^N = \sum_{i=1}^{\lfloor \frac{N}{2} \rfloor} \sum_{j=0}^{N-2i} \sum_{k=0}^{i-1} \binom{N}{2i} \binom{N-2i}{j} \binom{2i}{k} \xi^{2i+j-k} \omega^{j+k}. \quad (\text{D12})$$

To obtain the desired expression, we first shift the summation index $j \mapsto j - k$ and rearrange the order of the summations for j and k such that the expression reads

$$T_{00}^N = \sum_{i=1}^{\lfloor \frac{N}{2} \rfloor} \sum_{k=0}^{i-1} \sum_{j=k}^{N-2i-k} \binom{N}{2i} \binom{N-2i}{j-k} \binom{2i}{k} \xi^{2i+j-2k} \omega^j. \quad (\text{D13})$$

Next, we rearrange the summations for i and k and subsequently shift the index of summation $i \mapsto i + k$ to give

$$\begin{aligned} T_{00}^N &= \sum_{k=0}^{\lfloor \frac{N-2}{2} \rfloor} \sum_{i=1}^{\lfloor \frac{N-2k}{2} \rfloor} \sum_{j=k}^{N-2i-k} \binom{N}{2i+2k} \binom{N-2i-2k}{j-k} \\ &\times \binom{2i+2k}{k} \xi^{2i+j} \omega^j. \end{aligned} \quad (\text{D14})$$

Now, we use the binomial identities in Eq. (D10) to transform the coefficients such that we have

$$\begin{aligned} T_{00}^N &= \sum_{k=0}^{\lfloor \frac{N-2}{2} \rfloor} \sum_{i=1}^{\lfloor \frac{N-2k}{2} \rfloor} \sum_{j=k}^{N-2i-k} \binom{N}{2i+j} \binom{N-2i-j}{k} \\ &\times \binom{2i+j}{j-k} \xi^{2i+j} \omega^j, \end{aligned} \quad (\text{D15})$$

which after rearranging the order of the summations i and k followed by j and k reads

$$T_{00}^N = \sum_{i=1}^{\lfloor \frac{N}{2} \rfloor} \sum_{j=0}^{N-2i} \sum_{k=0}^j \binom{N}{2i+j} \binom{N-2i-j}{k} \binom{2i+j}{j-k} \xi^{2i+j} \omega^j, \quad (\text{D16})$$

where, in the summation over k , we use the identity $\binom{n < k}{k} = 0$. Finally, we apply Vandermonde's identity Eq. (D11) to sum over k to obtain

$$T_{00}^N = \sum_{i=1}^{\lfloor \frac{N}{2} \rfloor} \sum_{j=0}^{N-2i} \binom{N}{2i+j} \binom{N}{j} \xi^{2i+j} \omega^j. \quad (\text{D17})$$

Identifying the numbers of positive and negative quasiparticles as $N^+ \equiv 2i + j$ and $N^- \equiv j$, respectively, it follows directly that this expression is exactly equivalent to Eq. (69) for $N^+ > N^-$, with the constraints in Eqs. (26) and (70) imposed by the bounds of the summations and the factor of 2 from Eq. (D6).

Next, we consider the summation for $k = i$,

$$T_{00}^N = \sum_{i=0}^{\lfloor \frac{N}{2} \rfloor} \sum_{j=0}^{N-2i} \binom{N}{2i} \binom{N-2i}{j} \binom{2i}{i} \xi^{i+j} \omega^{i+j}. \quad (\text{D18})$$

To start, we again shift the summation index $j \mapsto j - i$ to give

$$T_{00}^N = \sum_{i=0}^{\lfloor \frac{N}{2} \rfloor} \sum_{j=i}^{N-i} \binom{N}{2i} \binom{N-2i}{j-i} \binom{2i}{i} \xi^j \omega^j. \quad (\text{D19})$$

Subsequently applying the identities Eq. (D10) yields

$$T_{00}^N = \sum_{i=0}^{\lfloor \frac{N}{2} \rfloor} \sum_{j=i}^{N-i} \binom{N}{j} \binom{N-j}{i} \binom{j}{i} \xi^j \omega^j, \quad (\text{D20})$$

which after rearranging the order of the summations i and j reads

$$T_{00}^N = \sum_{j=0}^N \sum_{i=j}^j \binom{N}{j} \binom{N-j}{i} \binom{j}{i} \xi^j \omega^j, \quad (\text{D21})$$

where again, in the summation over i , we have used the identity $\binom{n < k}{k} = 0$. Further noting the identity $\binom{n}{k} = \binom{n}{n-k}$, then applying Vandermonde’s identity Eq. (D11) to sum over i then gives

$$T_{00}^N = \sum_{j=0}^N \binom{N}{j} \binom{N}{j} \xi^j \omega^j, \quad (\text{D22})$$

which, substituted into Eq. (D6), is exactly equal to Eq. (69) for $N^+ = N^- = j$.

Finally, we consider the summation for $k > i$,

$$T_{00}^N = \sum_{i=1}^{\lfloor \frac{N}{2} \rfloor} \sum_{j=0}^{N-2i} \sum_{k=i+1}^{2i} \binom{N}{2i} \binom{N-2i}{j} \binom{2i}{k} \xi^{2i+j-k} \omega^{j+k}, \quad (\text{D23})$$

which after shifting the summation index $j \mapsto j - 2i + k$ and rearranging the order of the summations j and k reads

$$T_{00}^N = \sum_{i=1}^{\lfloor \frac{N}{2} \rfloor} \sum_{k=i+1}^{2i} \sum_{j=2i-k}^{N-k} \binom{N}{2i} \binom{N-2i}{j-2i+k} \binom{2i}{k} \xi^j \omega^{-2i+j+2k}. \quad (\text{D24})$$

We now shift the index $k \mapsto k + i$,

$$T_{00}^N = \sum_{i=1}^{\lfloor \frac{N}{2} \rfloor} \sum_{k=1}^i \sum_{j=i-k}^{N-i-k} \binom{N}{2i} \binom{N-2i}{j-i+k} \binom{2i}{i+k} \xi^j \omega^{j+2k}, \quad (\text{D25})$$

and subsequently apply Eqs. (D10) to obtain

$$T_{00}^N = \sum_{i=1}^{\lfloor \frac{N}{2} \rfloor} \sum_{k=1}^i \sum_{j=i-k}^{N-i-k} \binom{N}{j+2k} \binom{N-j-2k}{i-k} \times \binom{j+2k}{i+k} \xi^j \omega^{j+2k}. \quad (\text{D26})$$

Last, we rearrange the order of the summations i and k and then i and j , which returns

$$T_{00}^N = \sum_{k=1}^{\lfloor \frac{N}{2} \rfloor} \sum_{j=0}^{N-2k} \sum_{i=k}^j \binom{N}{j+2k} \binom{N-j-2k}{i-k} \times \binom{j+2k}{i+k} \xi^j \omega^{j+2k}, \quad (\text{D27})$$

before applying Vandermonde’s identity Eq. (D11) to sum over i to give

$$T_{00}^N = \sum_{k=1}^{\lfloor \frac{N}{2} \rfloor} \sum_{j=0}^{N-2k} \binom{N}{j+2k} \binom{N}{j} \xi^j \omega^{j+2k}. \quad (\text{D28})$$

Substituted into Eq. (D6), this is precisely equivalent to Eq. (69) for $N^+ < N^-$ with $N^+ = j$ and $N^- = j + 2k$, thus proving the equivalence of Eqs. (66) and (68) and the correctness of Eq. (69).

Remarkably, we can also derive the expression for the counting function Ω directly from physical arguments by recalling the intrinsic properties of the quasiparticles. To start, we note that each and every quasiparticle occupies exactly two adjacent sites of the lattice and is statistically independent

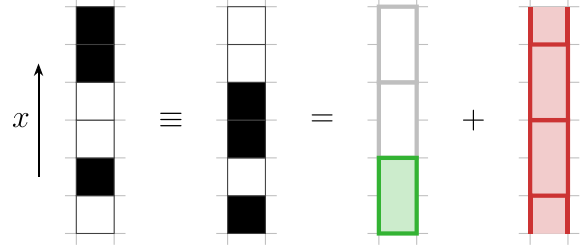


FIG. 9. State counting function. The chain of $2N$ sites can be partitioned into two staggered overlapping lattices of N blocks each. The blocks are composed of adjacent pairs of sites that correspond to either vacua, indicated here by white, or quasiparticles, highlighted green (left) for positive and red (right) for negative. As can be seen with the example configuration $\underline{n} = (0, 1, 0, 0, 1, 1)$, in this picture, configurations are equivalent under the exchange $\square \leftrightarrow \blacksquare$ (i.e., $0 \leftrightarrow 1$), hence the factor of 2 in Eq. (69).

of each and every other quasiparticle. That is, the conditional probability of finding a quasiparticle at a pair of sites, given that the sites do not already contain a quasiparticle of that species does not depend on any of the other quasiparticles positions (see Sec. IV C). It then follows straightforwardly that the binomial coefficients in Eq. (69) can be understood as independently counting the total number of possible ways to arrange N^+ positive and N^- negative statistically independent quasiparticles of size 2 in a system of size $2N$. An illustrative example highlighting the basic concepts of this argument, as well as an explanation for the multiplicative factor of 2 which simply ensures that both subspecies of each quasiparticle are counted is presented in Fig. 9.

APPENDIX E: STOCHASTIC BOUNDARY DRIVING CONSTRAINT

To prove that the stochastic operators R and L must necessarily satisfy the particle-hole symmetry of the model, we show that the constraint Eq. (108) follows directly as a consequence of the boundary consistency condition. Solving separately the pair of Eqs. (96) and (100), yields a unique solution for the spectral parameters ξ and ω in terms of the conditional probabilities ϕ_{001} and ϕ_{011} and the normalization parameter $\Gamma \equiv \Gamma_R/\Gamma_L$. Namely,

$$\xi = \frac{\Gamma - (1 - \phi_{001})}{\phi_{011}}, \quad (\text{E1})$$

$$\omega = \frac{\Gamma(1 - \phi_{011}) - (1 - \phi_{001} - \phi_{011})}{\Gamma\phi_{011}}. \quad (\text{E2})$$

Similarly, solving separately the left boundary equations, Eqs. (95) and (99), returns the following unique solution for ξ and ω in terms of the conditional probabilities ϕ_{100} and ϕ_{110} and normalization parameter Γ ,

$$\xi = \frac{(1 - \phi_{110}) - \Gamma(1 - \phi_{100} - \phi_{110})}{\phi_{110}}, \quad (\text{E3})$$

$$\omega = \frac{1 - \Gamma(1 - \phi_{100})}{\Gamma\phi_{110}}. \quad (\text{E4})$$

We now demand that the expressions for ξ in Eqs. (E1) and (E3) and for ω in Eqs. (E2) and (E4) are equivalent, respectively. Solving these coupled equations then yields a unique expression for the normalization parameter,

$$\Gamma = \frac{\varphi_{110}(1 - \phi_{001}) + (1 - \varphi_{110})\phi_{011}}{\phi_{011}(1 - \varphi_{100}) + (1 - \phi_{011})\varphi_{110}}, \quad (\text{E5})$$

which is equivalent to the expression derived in Eq. (103), where the spectral parameters are given

$$\begin{aligned} \phi_{110} &= \frac{[\varphi_{100}(1 - \phi_{011}) + (1 - \varphi_{100})\phi_{001}] - (1 - \phi_{100})[\phi_{001}(1 - \varphi_{110}) + (1 - \phi_{001})\varphi_{100}]}{\phi_{011}(1 - \varphi_{100}) + (1 - \phi_{011})\varphi_{110}}, \\ \phi_{011} &= \frac{[\phi_{001}(1 - \varphi_{110}) + (1 - \phi_{001})\varphi_{100}] - (1 - \varphi_{001})[\varphi_{100}(1 - \phi_{011}) + (1 - \varphi_{100})\phi_{001}]}{\varphi_{110}(1 - \phi_{001}) + (1 - \varphi_{110})\phi_{011}}. \end{aligned} \quad (\text{E7})$$

Requiring that each and every conditional probability is simultaneously bounded then returns a unique nontrivial solution for the ϕ_{n_3, n_4, n_5} and φ_{n_0, n_1, n_2} , that is

$$\begin{aligned} \phi_{100} &= \phi_{011}, & \phi_{110} &= \phi_{001}, \\ \varphi_{001} &= \varphi_{110}, & \varphi_{011} &= \varphi_{100}, \end{aligned} \quad (\text{E8})$$

which is exactly the constraint in Eq. (108).

$$p_{n_1, \dots, n_{2N}} = \lim_{M \rightarrow \infty} \frac{\text{Tr}(V_{n_1} W_{n_2} \cdots W_{n_{2N}} T^{M-N})}{\text{Tr}(T^M)} = \frac{\langle l | V_{n_1} W_{n_2} \cdots W_{n_{2N}} | r \rangle}{\chi^N \langle l | r \rangle}, \quad (\text{F1})$$

$$p'_{n_1, \dots, n_{2N}} = \lim_{M \rightarrow \infty} \frac{\text{Tr}(W_{n_1} V_{n_2} \cdots V_{n_{2N}} T^{M-N})}{\text{Tr}(T^M)} = \frac{\langle l | W_{n_1} V_{n_2} \cdots V_{n_{2N}} | r \rangle}{\chi^N \langle l | r \rangle}, \quad (\text{F2})$$

$$p_{n_1, \dots, n_{2N-1}} = \lim_{M \rightarrow \infty} \frac{\text{Tr}(V_{n_1} W_{n_2} \cdots V_{n_{2N-1}} (W_0 + W_1) T^{M-N})}{\text{Tr}(T^M)} = \frac{\langle l | V_{n_1} W_{n_2} \cdots V_{n_{2N-1}} | r \rangle}{\chi^{N-1} \langle l | (V_0 + V_1) | r \rangle}, \quad (\text{F3})$$

$$p'_{n_1, \dots, n_{2N-1}} = \lim_{M \rightarrow \infty} \frac{\text{Tr}(W_{n_1} V_{n_2} \cdots W_{n_{2N-1}} (V_0 + V_1) T^{M-N})}{\text{Tr}(T^M)} = \frac{\langle l | W_{n_1} V_{n_2} \cdots W_{n_{2N-1}} | r \rangle}{\chi^{N-1} \langle l | (W_0 + W_1) | r \rangle}, \quad (\text{F4})$$

where we have used the facts that the following products of matrices and vectors hold:

$$\begin{aligned} (W_0 + W_1)|r\rangle &= (1 + \omega)|r\rangle, \\ (V_0 + V_1)|r\rangle &= (1 + \xi)|r\rangle, \end{aligned} \quad (\text{F5})$$

and that both the transfer matrix T and vectors $|r\rangle$ and $\langle l|$ are invariant under the exchange $\xi \leftrightarrow \omega$. That is,

$$T \equiv T', \quad |r\rangle \equiv |r'\rangle, \quad \langle l| \equiv \langle l'|. \quad (\text{F6})$$

To prove the relations in Eqs. (111) and (112), we must show that the following products of vectors and matrices are *linearly dependent*. Explicitly, that for each and every subconfiguration of two sites, there exist scalar coefficients

by

$$\begin{aligned} \xi &= \frac{\phi_{001}(1 - \varphi_{110}) + (1 - \phi_{001})\varphi_{100}}{\phi_{011}(1 - \varphi_{100}) + (1 - \phi_{011})\varphi_{110}}, \\ \omega &= \frac{\varphi_{100}(1 - \phi_{011}) + (1 - \varphi_{100})\phi_{001}}{\varphi_{110}(1 - \phi_{001}) + (1 - \varphi_{110})\phi_{011}}, \end{aligned} \quad (\text{E6})$$

which are precisely the solutions shown in Eq. (110), with $\xi, \omega \in \mathbb{R}^+$ for all $\phi_{001}, \phi_{011}, \varphi_{100}, \varphi_{110} \in [0, 1]$. Moreover, solving the coupled equations for the spectral parameters also imposes a constraint on the conditional probabilities. Specifically, we have that

APPENDIX F: CONDITIONAL PROBABILITY FACTORIZATION

To prove the factorizations in Eqs. (111) and (112), we must first clarify our notation. Specifically, let $p_{n_1, \dots, n_{2N}}$ and $p'_{n_1, \dots, n_{2N}}$ denote the asymptotic probabilities for the configurations of even length $2N$ starting on either even sites at odd times or odd sites at even times, and either even sites at even times or odd sites at odd times. Then, let $p_{n_1, \dots, n_{2N-1}}$ and $p'_{n_1, \dots, n_{2N-1}}$ denote the corresponding asymptotic probabilities for configurations of odd length $2N - 1$. Explicitly, these expressions read

$l_{n_1, n_2}, l'_{n_1, n_2}, r_{n_3, n_4}$, and r'_{n_3, n_4} , such that for the left boundary, the following identities hold:

$$\langle l | V_{n_1} W_{n_2} = l_{n_1, n_2} \langle l | W_{n_2}, \quad (\text{F7})$$

$$\langle l | W_{n_1} V_{n_2} = l'_{n_1, n_2} \langle l | V_{n_2}, \quad (\text{F8})$$

while for the right boundary, the identities read

$$V_{n_3} W_{n_4} |r\rangle = r_{n_3, n_4} V_{n_3} |r\rangle, \quad (\text{F9})$$

$$W_{n_3} V_{n_4} |r\rangle = r'_{n_3, n_4} W_{n_3} |r\rangle. \quad (\text{F10})$$

It can be straightforwardly demonstrated, by checking all four configurations for all four equations, that the scalar

coefficients are given precisely by the tensors of the PSA in Eq. (39) and MPS normalization constant in Eq. (103). Explicitly, for the left boundary,

$$l_{n_1, n_2} = X_{n_1, n_2}, \quad l'_{n_1, n_2} = Y_{n_1, n_2}, \quad (\text{F11})$$

and, similarly, for the right boundary,

$$r_{n_3, n_4} = \frac{1}{\Gamma} X_{n_3, n_4}, \quad r'_{n_3, n_4} = \Gamma Y_{n_3, n_4}. \quad (\text{F12})$$

From here, the factorization identities follow directly. To obtain the relations in Eq. (111), we consecutively apply Eq. (F7) to Eqs. (F1) and (F3) and, similarly, Eq. (F8) to Eqs. (F2) and (F4), while to acquire the equations in Eqs. (112), we instead repeatedly apply (F9) and (F10).

APPENDIX G: EIGENVALUE DEGENERACY CONJECTURE

To check the validity of the conjecture in Eq. (168) for the degeneracy g of the eigenvalue Λ , we perform a simple calculation which counts the total number of eigenvalues. In particular, let $g(N) \equiv 2^{2N}$ denote the total number of eigenvalues of \mathbb{M} for a system of even size $2N$. We argue that we can express this quantity as

$$g(N) = 4 \sum_{p=0}^{N-1} g(N, p), \quad g(N, p) = \sum_{q=0}^{2N-2} g(N, p, q), \quad (\text{G1})$$

which can intuitively be interpreted as counting the total number of degenerate eigenvalues by summing over every angle q , orbital p , and root λ (cf. the multiplicative factor of 4). The degeneracy $g \equiv g(N, p, q)$ then reads

$$g(N, p, q) = \sum_{d|D} \frac{d}{2N-1} \sum_{d'|D'} \mu(d') \binom{\frac{2N-1}{d}}{\frac{p}{d'}}, \quad (\text{G2})$$

where $\mu(\cdot)$ denotes the Möbius function and $j|k$ the set of positive integer divisors j of the integer k , with

$$D = \gcd(2N-1, p, q), \quad D' = \frac{\gcd(2N-1, p)}{q}, \quad (\text{G3})$$

where $\gcd(\cdot)$ denotes the greatest common divisor.

To start, we note that we can eliminate the summation over q by expanding the summations over both q and d , and then collecting terms in d such that

$$g(N, p) = \sum_{d|D''} \sum_{d'|D'} \mu(d') \binom{\frac{2N-1}{d}}{\frac{p}{d'}}, \quad (\text{G4})$$

with the integer

$$D'' = \gcd(2N-1, p). \quad (\text{G5})$$

Expanding the summations over d and d' , and collecting terms with similar binomial coefficients, we then obtain

$$g(N, p) = \sum_{d|D''} \binom{\frac{2N-1}{d}}{\frac{p}{d}} \sum_{d'|d} \mu(d') = \binom{2N-1}{p}, \quad (\text{G6})$$

where, to eliminate the summation over d' , we have used the Möbius summation identity,

$$\sum_{j|k} \mu(j) = \begin{cases} 1, & k = 1, \\ 0, & k > 1. \end{cases} \quad (\text{G7})$$

We now consider the summation over the orbital number p , which we can expand using Pascal's identity to read

$$\begin{aligned} g(N) &= 4 \sum_{p=0}^{N-1} \left[\binom{2N-2}{p-1} + \binom{2N-2}{p} \right] \\ &= 4 \left[2 \sum_{p=0}^{N-2} \binom{2N-2}{p} + \binom{2N-2}{N-1} \right], \end{aligned} \quad (\text{G8})$$

where, to obtain the latter equality, we used the binomial identity $\binom{j}{k < 0} = 0$ to eliminate the term $\binom{2N-1}{-1}$. Finally, we split the first term into two separate summations over $p = 0, \dots, N-2$ and $p = N, \dots, 2N-2$ with the identity $\binom{j}{k} = \binom{j}{j-k}$ to give

$$g(N) = 4 \sum_{p=0}^{2N-2} \binom{2N-2}{p} = 4(2^{2N-2}) = 2^{2N}, \quad (\text{G9})$$

as required where, to acquire the second equality, we used the binomial coefficient summation identity,

$$\sum_{j=0}^k \binom{k}{j} = 2^k. \quad (\text{G10})$$

APPENDIX H: CUMULANTS OF LONG-TIME OBSERVABLES

To construct exact expressions for the cumulants κ_j of the observable K for all even system sizes $2N$ in the long-time T limit, we must first state Faà di Bruno's formula, which generalizes the chain rule for higher derivatives. In particular, it states that if $z(y)$ and $y(x)$ are differentiable functions, then

$$\frac{d^p z}{dx^p} = \sum_{\mathcal{K}} \frac{p!}{k_1! \dots k_p!} \frac{d^q z}{dy^q} \prod_{j=1}^p \left(\frac{1}{j!} \frac{d^j y}{dx^j} \right)^{k_j}, \quad (\text{H1})$$

where the summation is over every p -tuple of nonnegative integers $\mathcal{K} \equiv (k_1, \dots, k_p)$ satisfying the conditions,

$$\sum_{j=1}^p j k_j = p, \quad \sum_{j=1}^p k_j = q. \quad (\text{H2})$$

The exact expressions for the long-time cumulants of the observable K then follow directly from the application of Faà di Bruno's Eq. (H1) to the SCGF Eq. (205). To start, we consider the functions $z(y) = \theta_N(\tilde{\Lambda})$ and $y(x) = \tilde{\Lambda}(s)$, which after applying Eq. (H1) read

$$\frac{d^p \theta_N}{ds^p} = \sum_{\mathcal{K}} \frac{p!}{k_1! \dots k_p!} \frac{d^q \theta_N}{d\tilde{\Lambda}^q} \prod_{j=1}^p \left(\frac{1}{j!} \frac{d^j \tilde{\Lambda}}{ds^j} \right)^{k_j}, \quad (\text{H3})$$

with the intermediate derivative,

$$\frac{d^q \theta_N}{d\tilde{\Lambda}^q} = \frac{(-1)^{q-1} (q-1)!}{\tilde{\Lambda}^q}. \quad (\text{H4})$$

Now, we consider $z(y) = \tilde{\Lambda}(\tilde{\sigma})$ and $y(x) = \tilde{\sigma}(s)$, where we have introduced $\tilde{\sigma}(s) = \tilde{\eta}^2(s) - \tilde{\mu}(s)$, for which

$$\frac{d^p \tilde{\Lambda}}{ds^p} = \frac{d^p \tilde{\eta}}{ds^p} + \sum_{\mathcal{K}} \frac{p!}{k_1! \cdots k_p!} \frac{d^q \tilde{\Lambda}}{d\tilde{\sigma}^q} \prod_{j=1}^p \left(\frac{1}{j!} \frac{d^j \tilde{\sigma}}{ds^j} \right)^{k_j}, \quad (\text{H5})$$

where the intermediate derivative,

$$\frac{d^q \tilde{\Lambda}}{d\tilde{\sigma}^q} = \frac{(-1)^{q-1} (2q)! \tilde{\sigma}^{-(2q-1)/2}}{2^{2q} q!}, \quad (\text{H6})$$

and final derivative,

$$\frac{d^p \tilde{\eta}}{ds^p} = \frac{1}{2} \sum_{k=0}^1 \sum_{j=0}^1 \psi_{j,k} (-N \zeta_{j,k})^p \exp(-Ns \zeta_{j,k}). \quad (\text{H7})$$

Finally, we consider $z = \tilde{\sigma}(\tilde{\eta})$ and $y = \tilde{\eta}(s)$, with

$$\frac{d^p \tilde{\sigma}}{ds^p} = \sum_{\mathcal{K}} \frac{p!}{k_1! \cdots k_p!} \frac{d^q \tilde{\sigma}}{d\tilde{\eta}^q} \prod_{j=1}^p \left(\frac{1}{j!} \frac{d^j \tilde{\eta}}{ds^j} \right)^{k_j} - \frac{d^p \tilde{\mu}}{ds^p}, \quad (\text{H8})$$

where the intermediate derivative,

$$\frac{d\tilde{\sigma}}{d\tilde{\eta}} = 2\tilde{\eta}, \quad \frac{d^2 \tilde{\sigma}}{d\tilde{\eta}^2} = 2, \quad \frac{d^q \tilde{\sigma}}{d\tilde{\eta}^q} = 0, \quad q \geq 3, \quad (\text{H9})$$

and final derivative,

$$\frac{d^p \tilde{\mu}}{ds^p} = \psi(-N\zeta)^p \exp(-Ns\zeta). \quad (\text{H10})$$

For completeness, let us now consider $\mathcal{K} = (k_1, \dots, k_p)$. It can be straightforwardly demonstrated that finding the p -tuples of nonnegative integers satisfying the constraint in Eq. (H2) is equivalent to finding every partition of the positive integer p (i.e., every possible way of writing p as a sum of positive integers, or equivalently, as a sum of p nonnegative integers). The total number of partitions of a nonnegative integer p is given by the partition function $P(p)$ from number theory [61] and exhibits the following convenient recurrence relation,

$$P(p) = \frac{1}{p} \sum_{j=0}^{p-1} \Sigma(p-j) P(j), \quad (\text{H11})$$

where, by convention, $P(0) = 1$ and with $\Sigma(\cdot)$ the sum of divisors function,

$$\Sigma(k) = \sum_{j|k} j, \quad (\text{H12})$$

with $j|k$ denoting the set of positive integer divisors j of the positive integer k . For reference, the integer sequence of the partition functions $P(p)$ can be found on Ref. [62].

-
- [1] A. Bobenko, M. Bordemann, C. Gunn, and U. Pinkall, On two integrable cellular automata, *Commun. Math. Phys.* **158**, 127 (1993).
- [2] T. Prosen and C. Mejía-Monasterio, Integrability of a deterministic cellular automaton driven by stochastic boundaries, *J. Phys. A: Math. Theor.* **49**, 185003 (2016).
- [3] A. Inoue and S. Takesue, Two extensions of exact nonequilibrium steady states of a boundary-driven cellular automaton, *J. Phys. A: Math. Theor.* **51**, 425001 (2018).
- [4] T. Prosen and B. Buča, Exact matrix product decay modes of a boundary driven cellular automaton, *J. Phys. A: Math. Theor.* **50**, 395002 (2017).
- [5] B. Buča, J. P. Garrahan, T. Prosen, and M. Vanicat, Exact large deviation statistics and trajectory phase transition of a deterministic boundary driven cellular automaton, *Phys. Rev. E* **100**, 020103(R) (2019).
- [6] A. J. Friedman, S. Gopalakrishnan, and R. Vasseur, Integrable Many-Body Quantum Floquet-Thouless Pumps, *Phys. Rev. Lett.* **123**, 170603 (2019).
- [7] S. Gopalakrishnan, Operator growth and eigenstate entanglement in an interacting integrable floquet system, *Phys. Rev. B* **98**, 060302(R) (2018).
- [8] S. Gopalakrishnan, D. A. Huse, V. Khemani, and R. Vasseur, Hydrodynamics of operator spreading and quasiparticle diffusion in interacting integrable systems, *Phys. Rev. B* **98**, 220303(R) (2018).
- [9] K. Klobas, M. Medenjak, T. Prosen, and M. Vanicat, Time-dependent matrix product ansatz for interacting reversible dynamics, *Commun. Math. Phys.* **371**, 651 (2019).
- [10] K. Klobas and T. Prosen, Space-like dynamics in a reversible cellular automaton, *SciPost Phys. Core* **2**, 010 (2020).
- [11] V. Alba, J. Dubail, and M. Medenjak, Operator Entanglement in Interacting Integrable Quantum Systems: The Case of the Rule 54 Chain, *Phys. Rev. Lett.* **122**, 250603 (2019).
- [12] V. Alba, Diffusion and operator entanglement spreading, *Phys. Rev. B* **104**, 094410 (2021).
- [13] B. Buča, K. Klobas, and T. Prosen, Rule 54: Exactly solvable model of nonequilibrium statistical mechanics, *J. Stat. Mech.* (2021) 074001.
- [14] T. Iadecola and S. Vijay, Nonergodic quantum dynamics from deformations of classical cellular automata, *Phys. Rev. B* **102**, 180302(R) (2020).
- [15] J. W. P. Wilkinson, K. Klobas, T. Prosen, and J. P. Garrahan, Exact solution of the Floquet-PXP cellular automaton, *Phys. Rev. E* **102**, 062107 (2020).
- [16] F. Ritort and P. Sollich, Glassy dynamics of kinetically constrained models, *Adv. Phys.* **52**, 219 (2003).
- [17] J. P. Garrahan, P. Sollich, and C. Toninelli, Kinetically constrained models, in *Dynamical Heterogeneities in Glasses, Colloids, and Granular Media*, International Series of Monographs on Physics, edited by L. Berthier, G. Biroli, J.-P. Bouchaud, L. Cipelletti, and W. van Saarloos (Oxford University Press, Oxford, UK, 2011), Chap. 10, pp. 341–366.
- [18] J. P. Garrahan, Aspects of nonequilibrium in classical and quantum systems: Slow relaxation and glasses, dynamical large deviations, quantum nonergodicity, and open quantum dynamics, *Physica A* **504**, 130 (2018).

- [19] L. Causser, I. Lesanovsky, M. C. Bañuls, and J. P. Garrahan, Dynamics and large deviation transitions of the XOR-Fredrickson-Andersen kinetically constrained model, *Phys. Rev. E* **102**, 052132 (2020).
- [20] G. H. Fredrickson and H. C. Andersen, Kinetic Ising Model of the Glass Transition, *Phys. Rev. Lett.* **53**, 1244 (1984).
- [21] P. Fendley, K. Sengupta, and S. Sachdev, Competing density-wave orders in a one-dimensional hard-boson model, *Phys. Rev. B* **69**, 075106 (2004).
- [22] T. Gombor and B. Pozsgay, Integrable spin chains and cellular automata with medium-range interaction, *Phys. Rev. E* **104**, 054123 (2021).
- [23] R. G. Palmer, D. L. Stein, E. Abrahams, and P. W. Anderson, Models of Hierarchically Constrained Dynamics for Glassy Relaxation, *Phys. Rev. Lett.* **53**, 958 (1984).
- [24] J. Jäckle and S. Z. Eisinger, A hierarchically constrained kinetic Ising model, *Z. Phys. B* **84**, 115 (1991).
- [25] N. Cancrini, F. Martinelli, C. Roberto, and C. Toninelli, Kinetically constrained spin models, *Probab. Theory Relat. Fields* **140**, 459 (2007).
- [26] A. Nahum, J. Ruhman, S. Vijay, and J. Haah, Quantum Entanglement Growth Under Random Unitary Dynamics, *Phys. Rev. X* **7**, 031016 (2017).
- [27] A. Nahum, S. Vijay, and J. Haah, Operator Spreading in Random Unitary Circuits, *Phys. Rev. X* **8**, 021014 (2018).
- [28] A. Chan, A. De Luca, and J. T. Chalker, Solution of a Minimal Model for Many-Body Quantum Chaos, *Phys. Rev. X* **8**, 041019 (2018).
- [29] B. Bertini, P. Kos, and T. Prosen, Exact Correlation Functions for Dual-Unitary Lattice Models in $1 + 1$ Dimensions, *Phys. Rev. Lett.* **123**, 210601 (2019).
- [30] C. W. von Keyserlingk, T. Rakovszky, F. Pollmann, and S. L. Sondhi, Operator Hydrodynamics, OTOCs, and Entanglement Growth in Systems Without Conservation Laws, *Phys. Rev. X* **8**, 021013 (2018).
- [31] T. Rakovszky, F. Pollmann, and C. W. von Keyserlingk, Diffusive Hydrodynamics of Out-of-Time-Ordered Correlators with Charge Conservation, *Phys. Rev. X* **8**, 031058 (2018).
- [32] C. Sünderhauf, D. Pérez-García, D. A. Huse, N. Schuch, and J. I. Cirac, Localization with random time-periodic quantum circuits, *Phys. Rev. B* **98**, 134204 (2018).
- [33] V. Khemani, A. Vishwanath, and D. A. Huse, Operator Spreading and the Emergence of Dissipative Hydrodynamics Under Unitary Evolution with Conservation Laws, *Phys. Rev. X* **8**, 031057 (2018).
- [34] S. Pai, M. Pretko, and R. M. Nandkishore, Localization in Fractonic Random Circuits, *Phys. Rev. X* **9**, 021003 (2019).
- [35] Ž. Krajnik and T. Prosen, Kardar–Parisi–Zhang physics in integrable rotationally symmetric dynamics on discrete space–time lattice, *J. Stat. Phys.* **179**, 110 (2020).
- [36] K. Klobas, B. Bertini, and L. Piroli, Exact Thermalization Dynamics in the “Rule 54” Quantum Cellular Automaton, *Phys. Rev. Lett.* **126**, 160602 (2021).
- [37] M. van Horssen, E. Levi, and J. P. Garrahan, Dynamics of many-body localization in a translation-invariant quantum glass model, *Phys. Rev. B* **92**, 100305(R) (2015).
- [38] Z. Lan, M. van Horssen, S. Powell, and J. P. Garrahan, Quantum Slow Relaxation and Metastability Due to Dynamical Constraints, *Phys. Rev. Lett.* **121**, 040603 (2018).
- [39] C. J. Turner, A. A. Michailidis, D. A. Abanin, M. Serbyn, and Z. Papić, Quantum scarred eigenstates in a Rydberg atom chain: Entanglement, breakdown of thermalization, and stability to perturbations, *Phys. Rev. B* **98**, 155134 (2018).
- [40] N. Pancotti, G. Giudice, J. I. Cirac, J. P. Garrahan, and M. C. Bañuls, Quantum East Model: Localization, Nonthermal Eigenstates, and Slow Dynamics, *Phys. Rev. X* **10**, 021051 (2020).
- [41] S. Gopalakrishnan and B. Zakirov, Facilitated quantum cellular automata as simple models with nonthermal eigenstates and dynamics, *Quantum Sci. Technol.* **3**, 044004 (2018).
- [42] K. Klobas, M. Vanicat, J. P. Garrahan, and T. Prosen, Matrix product state of multi-time correlations, *J. Phys. A: Math. Theor.* **53**, 335001 (2020).
- [43] R. Serfozo, *Basics of Applied Stochastic Processes* (Springer, Berlin, 2009).
- [44] H. Bethe, On the theory of metals, *Z. Phys.* **71**, 205 (1931).
- [45] G. H. Hardy, *An Introduction to the Theory of Numbers* (Oxford University Press, Oxford, 2008).
- [46] J. P. Garrahan, R. L. Jack, V. Lecomte, E. Pitard, K. van Duijvendijk, and F. van Wijland, Dynamical First-Order Phase Transition in Kinetically Constrained Models of Glasses, *Phys. Rev. Lett.* **98**, 195702 (2007).
- [47] J. P. Garrahan, R. L. Jack, V. Lecomte, E. Pitard, K. van Duijvendijk, and F. van Wijland, First-order dynamical phase transition in models of glasses: an approach based on ensembles of histories, *J. Phys. A: Math. Theor.* **42**, 075007 (2009).
- [48] V. Lecomte, C. Appert-Rolland, and F. van Wijland, Thermodynamic formalism for systems with Markov dynamics, *J. Stat. Phys.* **127**, 51 (2007).
- [49] C. Appert-Rolland, B. Derrida, V. Lecomte, and F. van Wijland, Universal cumulants of the current in diffusive systems on a ring, *Phys. Rev. E* **78**, 021122 (2008).
- [50] C. P. Espigares, P. L. Garrido, and P. I. Hurtado, Dynamical phase transition for current statistics in a simple driven diffusive system, *Phys. Rev. E* **87**, 032115 (2013).
- [51] D. Karevski and G. M. Schütz, Conformal Invariance in Driven Diffusive Systems at High Currents, *Phys. Rev. Lett.* **118**, 030601 (2017).
- [52] P. Helms, U. Ray, and Garnet Kin-Lic Chan, Dynamical phase behavior of the single- and multi-lane asymmetric simple exclusion process via matrix product states, *Phys. Rev. E* **100**, 022101 (2019).
- [53] C. Monthus, Revisiting the Ruelle thermodynamic formalism for markov trajectories with application to the glassy phase of random trap models, *J. Stat. Mech.: Theory Exp.* (2021) 063301.
- [54] C. Maes, Frenesy: Time-symmetric dynamical activity in nonequilibria, *Phys. Rep.* **850**, 1 (2020).
- [55] H. Touchette, The large deviation approach to statistical mechanics, *Phys. Rep.* **478**, 1 (2009).
- [56] V. S. Borkar, S. Juneja, and A. A. Kherani, Performance analysis conditioned on rare events: An adaptive simulation scheme, *Commun. Inf. Syst.* **3**, 259 (2003).
- [57] R. L. Jack and P. Sollich, Large deviations and ensembles of trajectories in stochastic models, *Prog. Theor. Phys. Suppl.* **184**, 304 (2010).

- [58] R. Chetrite and H. Touchette, Nonequilibrium Markov processes conditioned on large deviations, *Ann. Henri Poincaré* **16**, 2005 (2015).
- [59] J. P. Garrahan, Classical stochastic dynamics and continuous matrix product states: Gauge transformations, conditioned and driven processes, and equivalence of trajectory ensembles, *J. Stat. Mech.: Theory Exp* (2016) 073208.
- [60] T. Prosen, Reversible cellular automata as integrable interactions round-a-face: Deterministic, stochastic, and quantized, [arXiv:2106.01292](https://arxiv.org/abs/2106.01292).
- [61] G. E. Andrews, *The Theory of Partitions* (Cambridge University Press, Cambridge, UK, 1976).
- [62] N. J. A. Sloane, The On-Line Encyclopedia of Integer Sequences (2021), <https://oeis.org/A000041>.

Chapter 4

Exact large deviations statistics of the Rule 201 RCA

Exact large deviation statistics of ultralocal observables for the boundary driven “Rule 201” reversible cellular automaton

Joseph W. P. Wilkinson^{1, 2, *} and Juan P. Garrahan^{1, 2}

¹ School of Physics and Astronomy, University of Nottingham, Nottingham, NG7 2RD, United Kingdom

² Centre for the Mathematics and Theoretical Physics of Quantum Non-equilibrium Systems, University of Nottingham, Nottingham, NG7 2RD, United Kingdom

* joseph.wilkinson@nottingham.ac.uk

August 24, 2022

1 Abstract

2 We compute the exact large deviations statistics for a class of dynamical observables of
 3 the boundary driven “Rule 201” reversible cellular automaton. To achieve this, we gen-
 4 eralize the matrix product ansatz used to study the nonequilibrium steady state of the
 5 model, and compute the dominant eigenvalue and associated eigenvector of the tilted
 6 propagator. In order to do so, we solve explicitly the corresponding operator algebra
 7 with finite dimensional matrices of rank four for dynamical observables composed of
 8 space and time additive generic two-body observables. We find that the exact scaled cu-
 9 mulant generating function for this class of observables has a linear response form for
 10 all values of the counting field, indicating that such dynamical observables have cumu-
 11 lants that scale sublinearly with time. In contrast to the homogeneous steady state, the
 12 corresponding dominant eigenvector takes the form of an inhomogeneous generalized
 13 Gibbs state. We briefly discuss the necessary steps that must be taken in order to obtain
 14 nontrivial large deviations for observables with larger support.

15

16 Contents

| | | |
|----|---|-----------|
| 17 | 1 Introduction | 2 |
| 18 | 2 Rule 201 reversible cellular automaton | 3 |
| 19 | 2.1 Definition of the dynamics | 3 |
| 20 | 2.2 Reducibility and ergodicity | 5 |
| 21 | 2.3 Quasiparticle excitations | 7 |
| 22 | 2.4 Statistical states | 8 |
| 23 | 2.5 Compatible boundaries | 10 |
| 24 | 3 Nonequilibrium steady state | 12 |
| 25 | 3.1 Markov propagator | 12 |
| 26 | 3.2 Matrix product ansatz | 12 |
| 27 | 3.3 Bethe equations | 15 |
| 28 | 4 Large deviation statistics | 17 |
| 29 | 4.1 Large deviation principle | 17 |
| 30 | 4.2 Time integrated observables | 18 |

| | | |
|----|--|-----------|
| 31 | 4.3 Tilted Markov propagator | 18 |
| 32 | 4.4 Generalized matrix product ansatz | 19 |
| 33 | 4.5 Inhomogeneous algebraic solutions | 21 |
| 34 | 4.6 Dominant eigenvalue | 26 |
| 35 | 5 Conclusions | 29 |
| 36 | A Nonequilibrium steady state | 30 |
| 37 | B Steady state boundary vectors | 31 |
| 38 | B.1 Homogeneous steady state | 31 |
| 39 | B.2 Inhomogeneous steady state | 33 |
| 40 | References | 35 |
| 41 | <hr/> | |
| 42 | | |

43 1 Introduction

44 Systems that evolve subject to a constrained dynamics often display complex collective be-
 45 haviour, far beyond what is expected based simply on their equilibrium statistical properties.
 46 This rich cooperative dynamics can be found to occur in a variety of many-body systems, in-
 47 cluding systems exhibiting excluding volume interactions, with the paradigmatic example be-
 48 ing simple exclusion processes [1–10], in systems with restrictions in their state spaces, such
 49 as packing and covering problems [11–13], and in systems where the local dynamical rules
 50 impose kinetic constraints, as for example in kinetically constrained models (KCM) [14–21]
 51 (see Refs. [22, 23] for reviews), which were originally introduced to model the slow coopera-
 52 tive relaxation of classical glasses [24] and study the glass transition problem [25]. In recent
 53 decades, interest in KCM has seen a resurgence due to their applicability as tractable models
 54 to study quantum nonequilibrium many-body physics, including problems related to atypical
 55 thermalization [26–28], many-body localization [29–31], and entanglement growth [32–35].

56 In order to capture the complex many-body behaviour of constrained systems, one must
 57 study the statistical properties of dynamical observables far from equilibrium, that depend
 58 on the full time history of the state of the system. For systems in equilibrium, a powerful
 59 framework to deal with such problems is that of linear response theory [36–39], which anal-
 60 yses the fluctuations of thermodynamic quantities through statistical ensembles of configu-
 61 rations. However, the presence of dynamically fluctuating quantities necessarily requires a
 62 nonequilibrium approach, for which the appropriate theoretical framework is that of large de-
 63 viations [24, 40–42]. Here, one studies statistical ensembles of trajectories out of equilibrium,
 64 rather than of configurations in equilibrium, for which the relevant thermodynamic quanti-
 65 ties are the rate function and scaled cumulant generating function, which play the roles of an
 66 entropy and free energy, respectively, for the dynamical ensemble.

67 Obtaining exact results for such dynamical quantities in strongly interacting many-body
 68 systems far from equilibrium is of paramount importance in statistical mechanics and, more-
 69 over, physics in general [43, 44]. Despite this, there are scarce examples of genuine exact large
 70 deviations statistics in interacting models beyond those for the paradigmatic asymmetric sim-
 71 ple exclusion process [6, 45, 46]. In recent years, however, large deviations techniques were
 72 generalized to derive exact results for bulk-deterministic boundary-driven systems, specifi-
 73 cally, for space and time additive ultralocal observables of the now extensively studied “Rule

74 54” reversible cellular automaton [47] (see Ref. [48] for a recent review) and, more currently,
 75 the “Rule 150” reversible cellular automaton [49]. Perhaps more remarkable, is the contem-
 76 porary work, obtained by combining insights from large deviations theory with the powerful
 77 framework of generalized hydrodynamics, that provides a universal method for obtaining the
 78 exact formula for the scaled cumulant generating function of any interacting integrable model
 79 obeying the fundamental hydrodynamics equations [50, 51].

80 In this paper, we further generalize the methods introduced in Ref. [47] to compute the
 81 *exact large deviations statistics* of the “Rule 201” reversible cellular automaton in the boundary-
 82 driven setup. This complements the existing solutions for the repulsively interacting Rule 54
 83 and noninteracting Rule 150, with that of the attractively interacting Rule 201. Via an inhom-
 84 ogeneous matrix product ansatz, we obtain exact analytic expressions for the scaled cumulant
 85 generating functions and corresponding rate functions for a class of space and time extensive
 86 two-site observables. We do so by generalizing the homogeneous matrix product ansatz for the
 87 nonequilibrium steady state, and explicitly compute the leading eigenvalue and eigenvector
 88 of the tilted propagator. In contrast to prior results, we find that the exact scaled cumulant
 89 generating function for this class of observables has a simple linear form for all values of the
 90 counting field, which indicates sublinear scaling of the cumulants with time. We demonstrate,
 91 however, that despite this, the leading eigenvector exhibits a *generalized Gibbs form*, which
 92 contrasts the Gibbs form of the nonequilibrium steady state.

93 2 Rule 201 reversible cellular automaton

94 2.1 Definition of the dynamics

95 The model is defined on a $1 + 1$ dimensional square lattice of even size $2L$ with $L \in \{1, 2, \dots\}$.
 96 The points of the lattice are labelled by coordinates in discrete space and time and are defined
 97 over a finite field that takes only binary values. For simplicity, we will refer to the points of the
 98 lattice as *sites* and the value of the field at each point its *state*. The site at position x and time t
 99 is called *empty* if the state $n_x^t = 0$ and *occupied* if $n_x^t = 1$, with the subscript x and superscript t
 100 respectively denoting the space and time coordinates of the site and n_x^t its state.

101 At discrete time $t \in \{1, 2, \dots\}$, the state of the system is characterized by a *configuration* \underline{n}^t
 102 which we represent by a sequence of $2L$ bits¹,

$$\underline{n}^t \equiv (n_1^t, n_2^t, \dots, n_{2L}^t). \quad (1)$$

103 The time evolution of the state of each site is then determined by,

$$n_x^{t+1} = \begin{cases} f_x^t, & \text{if } x + t = 0 \pmod{2}, \\ n_x^t, & \text{if } x + t = 1 \pmod{2}, \end{cases} \quad (2)$$

104 where we have introduced the convenient shorthand notation,

$$f_x^t = f(n_{x-1}^t, n_x^t, n_{x+1}^t), \quad (3)$$

105 to represent the function f acting on the sites at positions $x - 1$, x , and $x + 1$ at time t that
 106 enacts the discrete, deterministic, and reversible update rule,

$$f_x = 1 + n_{x-1} + n_x + n_{x+1} + n_{x-1}n_{x+1} \pmod{2}, \quad (4)$$

¹The notation for a configuration \underline{n}^t should not be confused with that for the state of a site n_x^t ; the latter will *always* have a subscript x to denote the position of the site in space. Time coordinates, however, will often be omitted (e.g., for a configuration \underline{n} or site n_x).

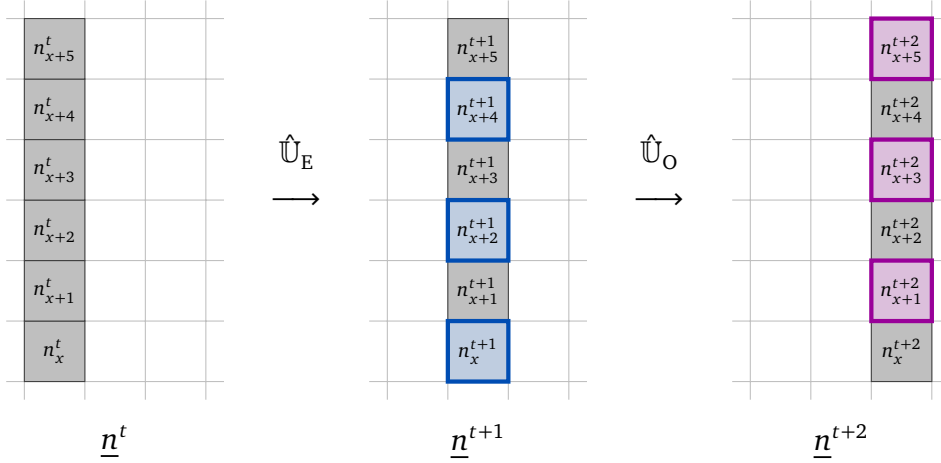


Figure 1: A graphical representation of the discrete time evolution of $2L = 6$ sites under one full step of time evolution (i.e., an even and odd time step). In the first time step, only the sites with even positions are updated by the local dynamical rule f in Eq. (4), while during the second time step, only sites at odd positions are updated. Blue and purple shading indicate which sites have been updated in the even and odd time steps, respectively.

107 given by the *Rule 201 reversible cellular automaton*. Note that the reversibility of Rule 201,
 108 specifically, the invariance of the local dynamics with respect to reflections in space or time,
 109 can be immediately observed by realizing that the update f satisfies the symmetry constraints
 110 imposed by *time-reversibility* and *space-invertibility*, respectively,

$$n_x = f(n_{x-1}, f_x, n_{x+1}), \quad f_x = f(n_{x+1}, n_x, n_{x-1}). \quad (5)$$

111 For sites in the *bulk* (i.e., with positions $x \in \{2, \dots, 2L - 1\}$), the dynamics is deterministic
 112 and reversible and is simply given by the update f in Eq. (4). For sites at the *boundary* (i.e.,
 113 with positions $x \in \{1, 2L\}$), however, there is in general only one adjacent site and, conse-
 114 quently, the dynamics fundamentally depends on the choice of boundary conditions. For the
 115 purposes of this work, we consider a system with *stochastic boundaries*, which we intuitively
 116 interpret as an open subsystem of finite even size $2L$ within a closed system of infinite size with
 117 periodic boundary conditions (cf. Rules 54 [52–54], 150 [49], and 201 [55]). This system can,
 118 therefore, be understood as a chain of finite size coupled to stochastic reservoirs.

119 We can alternatively interpret this dynamical system as a classical model of bits defined
 120 on a one-dimensional square lattice, that we term a *chain*, that evolves subject to a staggered
 121 discrete dynamics composed of two distinct time steps. In the first, which we refer to as the
 122 *even time step*, only the states of sites at even positions are updated by the local dynamical rule
 123 f , whilst during the second, the *odd time step*, only sites with odd positions are updated. This
 124 can be understood intuitively by introducing a simply graphical representation for the lattice
 125 where every site is represented by a cell in a square grid, with the cell colored white if the
 126 site is empty and black if it is occupied (see Figure 1). Using this convention, the local update
 127 rule can be represented geometrically, as demonstrated in Figure 2, by a set of 4 diagrams
 128 which correspond to the time-reversible transitions between the 8 possible combinations of
 129 the 3 binary site values n_{x-1} , n_x , and n_{x+1} . A typical example of the time evolution for an
 130 arbitrary initial configuration is shown in Figure 3.

131 The graphical representation of the discrete time evolution of the lattice in Figures 1 and 2
 132 offers an alternative interpretation of the dynamics, which can be immediately observed by

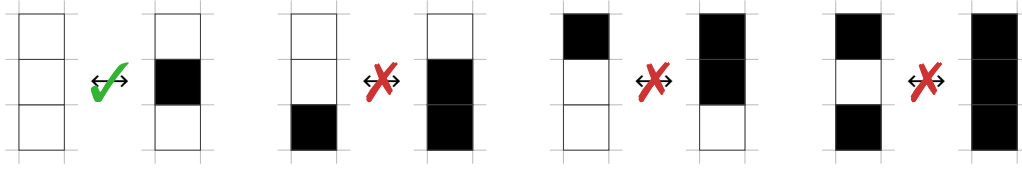


Figure 2: A schematic illustration of the deterministic action of the Rule 201 reversible cellular automaton in Eq. (4) where white and black cells represent empty ($n_x = 0$) and occupied ($n_x = 1$) sites, respectively. Since the local time evolution is reversible, the action of the local update rule on the $2^3 = 8$ possible configurations of 3 sites can be succinctly summarized by just 4 diagrams, with each representing a pair of possible transitions (i.e., one from left to right and one from right to left); allowed transitions are indicated by green ticks, while those prohibited by the dynamics are denoted by red crosses. Notice that only the transition with $n_{x-1} = n_{x+1} = 0$ is allowed, all others are prohibited, hence the alternate names “zero-spin facilitated” FA model and NOR-FA model.

133 inspecting Figure 3. Specifically, by treating pairs of adjacent empty sites² as particles, the
 134 dynamics can be understood as describing a discretized *solitonic gas*. As such, this model can
 135 be considered as perhaps the simplest 1 + 1 dimensional microscopic physical theory exhibit-
 136 ing attractively interacting emergent collective excitations. This complements the extensively
 137 studied Rule 54 [48], which is repulsively interacting, and recently studied Rule 150 [49],
 138 which is noninteracting. However, Rule 201 admits two stark differences, in particular, a dy-
 139 namically disconnected configuration space and a topologically nontrivial vacuum.

140 2.2 Reducibility and ergodicity

141 From a dynamical perspective, the local update rule in Eq. (4) can be understood as a *kinetic*
 142 *constraint* where the state of a site at position x can change if and only if the state of the sites
 143 at positions $x - 1$, x and $x + 1$ satisfy a condition, namely, if both sites $x - 1$ and $x + 1$ are
 144 empty. The Rule 201 reversible cellular automaton can, therefore, be physically interpreted as
 145 a discrete, deterministic, and reversible *kinetically constrained model* (KCM) [22–24]. Explic-
 146 itly, Rule 201 corresponds to a variant of the classic *Fredrickson-Andersen* (FA) model [56, 57],
 147 specifically, the “zero-spin facilitated” FA model³ [55, 58], whereas Rule 54, which has been
 148 studied extensively in recent years (see Ref. [48] for a review) and Rule 150 [49, 59] are respec-
 149 tively associated to the “one-spin facilitated” and “exclusive one-spin facilitated” FA models.
 150 We can explicitly demonstrate this by realizing that the dynamic functions for Rules 54, 150,
 151 and 201 can be written in terms of *Boolean operations* acting on the sites directly adjacent to
 152 the site being updated,

$$f_x = n_x + g_x \pmod{2}, \quad (6)$$

153 where we have again used the shorthand notation $g_x = g(n_{x-1}, n_{x+1})$ to denote the Boolean
 154 function g acting on the sites at positions $x - 1$ and $x + 1$. In the case of Rule 201, the function
 155 g reads,

$$g_x = 1 - n_{x-1} - n_{x+1} + n_{x-1}n_{x+1}, \quad (7)$$

²Explicitly, the particles are identified by collections of four adjacent sites: two empty sites surrounded by two sites for which at least one must be occupied.

³Note that here, we refer to Rule 201 as the “zero-spin facilitated” FA model, in contrast to the “two-spin facilitated” FA model (cf. Ref. [55]), since a state change only occurs if both adjacent sites are in the *empty* state (i.e., “two-spin facilitated” implies the adjacent sites are occupied, as opposed to empty).

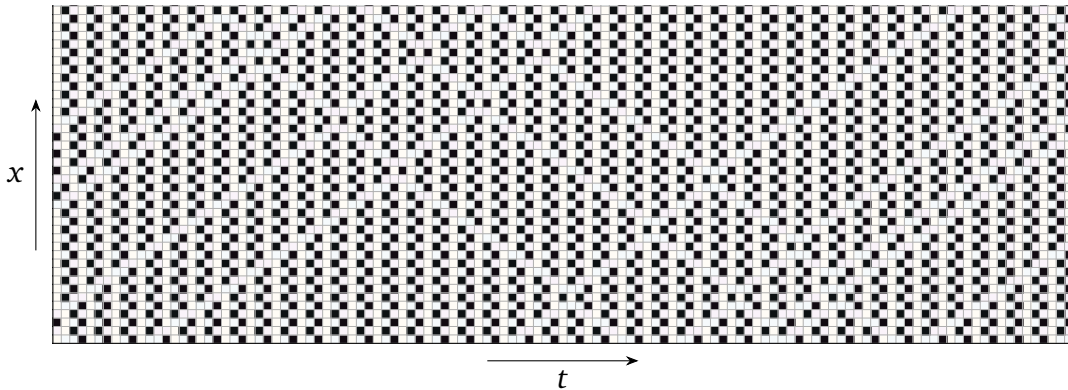


Figure 3: Typical example of the time evolution for a random initial configuration of $2L = 40$ sites. The lattice is evolved according to the local update rule in Eq. (4) across two time steps determined by Eq. (2). Pairs of adjacent empty sites adjacent to at least one occupied site can be understood as particles that move with fixed free velocities of $v^{\pm} = \pm\frac{1}{3}$ and interact via elastic factorized scattering. We interpret the interactions as the particles forming a bound state that decays after one time step, which induces a shift forward by two time steps relative to the paths of the freely moving particles, due to the fractional velocities of $v^{\pm} = \pm\frac{1}{3}$. Note also the nontrivial topological vacuum highlighted by shading the vacuum subconfigurations of repeating 0s, alternating 0s and 1s, and alternating 1s and 0s, respectively, orange, cyan, and magenta. Particles are then identified by the domain walls between these subconfigurations (see Ref. [55] for further details).

156 which is exactly the analytic form of the binary NOR operation. Rule 201 can, therefore,
 157 equivalently be referred to as the NOR-FA model, with Rule 54 the OR-FA model and Rule 150
 158 the XOR-FA model. Furthermore we remark that Rule 201 is also related to the now extensively
 159 studied quantum nonequilibrium many-body PXP model [26, 27, 30, 60–67] since the kinetic
 160 constraint on the classical propagator is identical to that of the energetic constraint on the
 161 quantum Hamiltonian.

162 The dynamical rules of KCM are such that configurational changes occur if and only if a
 163 certain condition—the *kinetic constraint*—is met. As such, the constraint usually manifests in
 164 the dynamics, namely, as a *dynamic constraint*. If the kinetic constraint is “strong” enough,
 165 however, then the local dynamical rule can additionally impose a constraint in the state space,
 166 which we refer to as a *static constraint*. This induces a partitioning of the configurational
 167 space of states into dynamically disconnected subspaces of disjoint subsets of states, each
 168 uniquely characterized by a set of ultralocally conserved quantities which are invariant under
 169 time evolution. This dynamical fragmentation of the state space is known as *reducibility* [22],
 170 a concept intimately related to yet distinct from *nonergodicity* [24]. Precisely, ergodicity is
 171 concerned with the statistical weighting of paths in the state space, specifically in the thermo-
 172 dynamic limit, whereas irreducibility is only concerned with their existence⁴. Of these models,
 173 the kinetic constraints for Rule 54 and Rule 150 are “weak” and, as such, only impose dynamic
 174 constraints, i.e., the state spaces are irreducible. For Rule 201, however, the kinetic constraint
 175 is “strong” enough to enforce a static constraint as well, namely, the spatial localization of ad-
 176 jacent occupied sites (see Ref. [55] for details), which manifests as a fragmentation of the set
 177 of configurations into exponentially many irreducible components that are spanned by con-
 178 figurations with distinct sets of neighbouring occupied sites. For consistency with the other

⁴Reducibility, therefore, implies nonergodicity; the antithesis, however, is not true [22].

179 models, we will only consider the largest of these subspaces which corresponds to the irre-
 180 ducible space of configurations with no adjacent occupied sites, since this allows us to neglect
 181 the invariant quantities characterizing the constraint.

182 The dimensionality of this subspace grows exponentially, according to the well known
 183 Fibonacci sequence,

$$\dim(\mathcal{C}_{2L}) = F_{2L+2} \sim \varphi^{2L+2}, \quad (8)$$

184 where we use the notation \mathcal{C}_L to denote the set of configurations of size L with no adjacent
 185 occupied sites, with F_L the L^{th} Fibonacci number, defined by,

$$F_L = F_{L-1} + F_{L-2}, \quad (9)$$

186 with $F_1 = 1$ and $F_2 = 1$ and $\varphi = \frac{1+\sqrt{5}}{2}$ the Golden ratio. To prove this, we use mathematical
 187 induction. Clearly, the base cases hold since,

$$\dim(\mathcal{C}_1) = |\{0, 1\}| = 2 = F_3, \quad \dim(\mathcal{C}_2) = |\{00, 01, 10\}| = 3 = F_4. \quad (10)$$

188 To prove the induction step, we make the following insightful observation: the set of config-
 189 urations of size L can be obtained by appending a 0 to the end of every configuration of size
 190 $L - 1$, to give the configurations with $n_L = 0$, and a 01 to the configurations of size $L - 2$, to
 191 give the configurations with $n_L = 1$. It then follows straightforwardly that,

$$\dim(\mathcal{C}_L) = \dim(\mathcal{C}_{L-1}) + \dim(\mathcal{C}_{L-2}), \quad (11)$$

192 which is exactly the celebrated Fibonacci recursion relation.

193 2.3 Quasiparticle excitations

194 A remarkable feature of the Rules 54, 150, and 201 is the existence of emergent nondispersive
 195 particle-like collective excitations (i.e., *solitons*), which we refer to simply as particles, that
 196 move with fixed velocities and scatter pairwise. To simplify our analysis of the nonequilibrium
 197 many-body dynamics, we introduce the concept of *quasiparticles* [68]. Effectively, quasipar-
 198 ticles can be understood as virtual particles that are attached to real particles and that jump
 199 between these real particles when they collide, such that the virtual particles “follow” a given
 200 momentum. Clearly, this only holds under certain conditions, since we need to trace a given
 201 momentum. We, therefore, necessarily require *elastic factorized scattering* to ensure momen-
 202 tum conservation which, due to their integrability, these models possess. For Rules 54, 150,
 203 and 201, the concept of quasiparticles is very simple: the quasiparticle with a given momen-
 204 tum is exactly the particle currently with that given momentum. Quasiparticles, therefore, act
 205 simply as velocity tracers. It is worth noting that, generally, the momenta of all particles in a
 206 given system are assumed different, which is not the case here. This is, however, not a problem
 207 since the particles can only have one of two fixed velocities $v^\pm = \pm v$, where v is the free speed
 208 of the particles⁵, and so only particles with different velocities collide.

209 In contrast to Rules 54 and 150, the structure of the quasiparticles in Rule 201, and the
 210 vacuum on which they propagate, are nontrivial. Specifically, the vacuum is a cycle of three
 211 distinct subconfigurations: repeating 0s, alternating 0s and 1s (with the 0s on odd sites), and
 212 alternating 1s and 0s (with the 1s on odd sites) as shown in Figure 3, for example (see Ref. [55]
 213 for details). The particles, and therefore quasiparticles, are then identified as the *domain walls*
 214 between different vacuum subconfigurations. Due to the fact that the particles can only have
 215 either a positive or negative velocity, there are only two distinct types of quasiparticle, which
 216 we appropriately name “positive” and “negative” and label with a “+” and “−”, respectively.

⁵Explicitly, for Rules 54 and 150 $v = 1$ while for Rule 201 $v = \frac{1}{3}$.

217 To determine which quasiparticles are between vacuum subconfigurations we introduce a con-
 218 venient relabelling of the sites, explicitly, we label sites of the vacua composed of repeating
 219 0s by 1, alternating 0s and 1s with 0s on odd sites by 2, and alternating 1s and 0s with 0s
 220 on even sites by 3. It then follows that the identity of the interface between any two sites is
 221 simply given by the Levi-Civita symbol of their labels,

$$\epsilon_{ij} = \begin{cases} +1, & \text{if } (i, j) = (1, 2), (2, 3), (3, 1), \\ 0, & \text{if } (i, j) = (1, 1), (2, 2), (3, 3), \\ -1, & \text{if } (i, j) = (1, 3), (2, 1), (3, 2), \end{cases} \quad (12)$$

222 where $+1, 0, -1$, respectively, denote a positive quasiparticle, the vacuum, and a negative
 223 quasiparticle. An important implication of this reformulation of the model is that, since we
 224 necessarily require the states of two sites of the lattice to identify its vacuum subconfiguration
 225 we, therefore, need to know the states of four sites of the lattice to detect a quasiparticle [55].

226 For Rule 201, when particles with opposite velocity collide they interact *attractively* (which
 227 is in contrast to Rules 54 and 150 which exhibit repulsively interacting and noninteracting
 228 particles), which manifests as a jump forwards two steps in time. Alternatively, and perhaps
 229 more intuitively, we can interpret this interaction as the particles forming a transient bound
 230 state which decays after one full time step. However, due to the fact the velocities of the
 231 particles are $v^\pm = \pm \frac{1}{3}$, this results in the positions of the quasiparticles (i.e., the virtual particles
 232 attached to the real particles) being shifted forwards by two full time steps relative to the
 233 freely propagating paths of the original particles (see, e.g., Figure 3). From a hydrodynamic
 234 perspective the model, therefore, resembles a gas of hard rods with length $\ell = \frac{2}{3}$ [69–71].

235 2.4 Statistical states

236 The macroscopic or *statistical states* of the system are probability distributions over the set
 237 of all configurations and denoted by \mathbf{p}^t . We represent these states as normalized vectors in
 238 $(\mathbb{R}^2)^{\otimes 2L}$ with strictly nonnegative components,

$$\mathbf{p}^t = \sum_{n=0}^{2^{2L}-1} p_n^t \mathbf{n}, \quad p_n^t \geq 0, \quad \sum_{n=0}^{2^{2L}-1} p_n^t = 1. \quad (13)$$

239 where the coefficient p_n^t denotes the probability of the configuration \underline{n} at time t , which is given
 240 by its binary representation,

$$n \equiv \underline{n} = (n_1, \dots, n_{2L}), \quad n = \sum_{x=1}^{2L} 2^{2L-x} n_x, \quad (14)$$

241 and \mathbf{n} the standard basis vector in $(\mathbb{R}^2)^{\otimes 2L}$ associated to \underline{n} ,

$$\mathbf{n} = \bigotimes_{x=1}^{2L} \mathbf{n}_x, \quad \mathbf{n}_x = \begin{bmatrix} \delta_{n_x}^0 \\ \delta_{n_x}^1 \end{bmatrix}, \quad (15)$$

242 with \mathbf{n}_x the elementary basis vector in \mathbb{R}^2 and δ_j^i the Kronecker delta.

243 The time evolution of the statistical states is given locally in terms of an 8×8 permutation
 244 matrix \hat{U} that encodes the local update rule,

$$\hat{U}_{(m_{x-1}, m_x, m_{x+1}), (n_{x-1}, n_x, n_{x+1})} = \delta_{n_{x-1}}^{m_{x-1}} \delta_{f_x}^{m_x} \delta_{n_{x+1}}^{m_{x+1}}, \quad (16)$$

266 2.5 Compatible boundaries

267 Given that we want the system we are considering to be understood as an open subsystem
 268 with stochastic boundaries compatible with the surrounding closed system, which has peri-
 269 odic boundaries, we would like the stochastic boundary operators to possess a particularly
 270 intuitive form. Specifically, we can interpret \hat{L} and \hat{R} as acting deterministically, according to
 271 the local update in Eq. (4), on sites n_0, \dots, n_4 and $n_{2L-3}, \dots, n_{2L+1}$ where n_0 and n_{2L+1} can
 272 be understood as *virtual sites* (i.e., sites inside the closed system, but outside and adjacent to
 273 the open subsystem) with states determined stochastically by the states of the sites n_1, \dots, n_4
 274 and n_{2L-3}, \dots, n_{2L} , respectively, as pictured in Figure 4. The boundary operators \hat{L} and \hat{R}
 275 are accordingly represented by 16×16 stochastic matrices, parameterized in terms of their
 276 components as,

$$\begin{aligned} \hat{L}_{(m_1, m_2, m_3, m_4), (n_1, n_2, n_3, n_4)} &= \sum_{n_0=0}^1 \delta_{f_1}^{m_1} \delta_{n_2}^{m_2} \delta_{f_3}^{m_3} \delta_{n_4}^{m_4} L_{n_0 n_1 n_2 n_3 n_4}, \\ \hat{R}_{(m_1, m_2, m_3, m_4), (n_1, n_2, n_3, n_4)} &= \sum_{n_5=0}^1 \delta_{n_1}^{m_1} \delta_{f_2}^{m_2} \delta_{n_3}^{m_3} \delta_{f_4}^{m_4} R_{n_1 n_2 n_3 n_4 n_5}, \end{aligned} \quad (25)$$

277 where, for readability, we have set $L = 2$ for the right boundary matrix identity. The stochastic
 278 boundary parameters $L_{n_0 n_1 n_2 n_3 n_4}$ and $R_{n_1 n_2 n_3 n_4 n_5}$ correspond to the conditional probabilities
 279 of the virtual sites being in the states n_0 and n_5 , given that the boundary sites are in the
 280 states n_1, n_2, n_3, n_4 , respectively. Since the boundary operators are represented by stochastic
 281 matrices, the columns of \hat{L} and \hat{R} must sum to unity,

$$L_{1 n_1 n_2 n_3 n_4} = 1 - L_{0 n_1 n_2 n_3 n_4}, \quad R_{n_1 n_2 n_3 n_4 1} = 1 - R_{n_1 n_2 n_3 n_4 0}. \quad (26)$$

282 Additionally, given that our discussion is restricted to the irreducible subspace of configura-
 283 tions with no adjacent occupied sites we can set, whilst taking into account the normalization
 284 condition in Eq. (26),

$$L_{0 1 1 n_3 n_4} = L_{0 n_1 1 1 n_4} = L_{0 n_1 n_2 1 1} = 1, \quad (27)$$

$$R_{1 1 n_3 n_4 0} = R_{n_1 1 1 n_4 0} = R_{n_1 n_2 1 1 0} = 1. \quad (28)$$

285 Furthermore, applying the local update in Eq. (4) to the ansatz in Eq. (25), while considering
 286 the normalization in Eq. (26), we immediately realize that we can also set,

$$L_{0 n_1 1 n_3 n_4} = 1, \quad R_{n_1 n_2 1 n_4 0} = 1. \quad (29)$$

287 After imposing these restrictions on the matrix components \hat{L} and \hat{R} , we are left with just
 288 six conditional probabilities per boundary operator. However, we can reduce this number
 289 further by recalling that the entire system, that is, both the finite open subsystem *and* the
 290 surrounding infinite closed system are restricted to the subspace spanned by configurations
 291 with no adjacent occupied sites. It, therefore, follows that the conditional probabilities of the
 292 virtual sites being in the states $n_0 = 1$ and $n_5 = 1$, given the adjacent sites are in the states
 293 $n_1 = 1$ and $n_4 = 1$ must be zero. Together with Eq. (26), this implies that,

$$L_{0 1 n_2 n_3 n_4} = 1, \quad R_{n_1 n_2 n_3 1 0} = 1. \quad (30)$$

294 Hence, we have just three parameters per stochastic boundary operator,

$$L_{0 0 0 0 0}, L_{0 0 0 0 1}, L_{0 0 0 1 0}, \quad R_{0 0 0 0 0}, R_{1 0 0 0 0}, R_{0 1 0 0 0}. \quad (31)$$

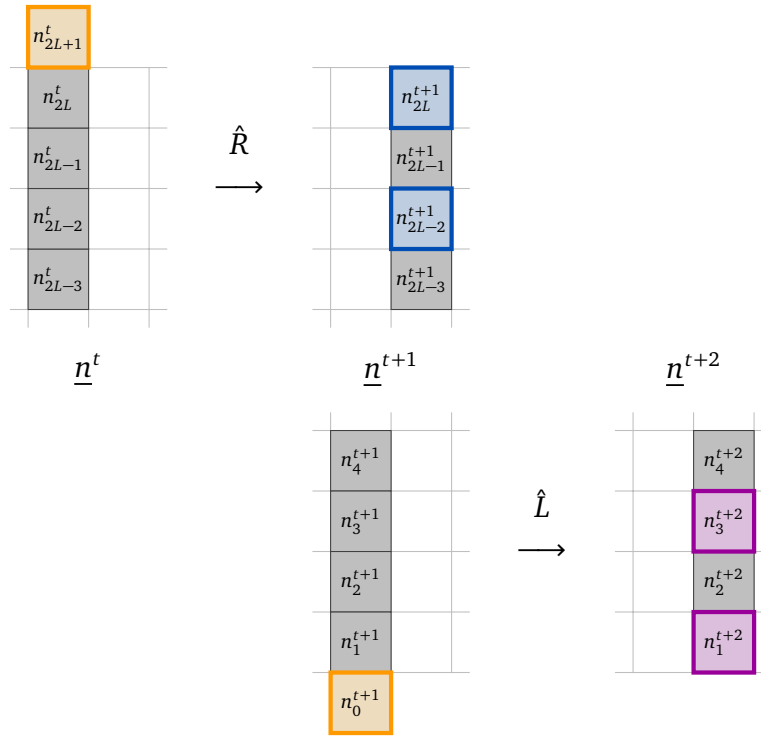


Figure 4: A diagrammatic explanation of the action of the stochastic boundary operators \hat{R} and \hat{L} . They can be intuitively understood as deterministically evolving the boundary and next nearest site according to the local update rule in Eq. (4) using a *virtual site* attached to the boundary, whose state depends on the configuration of the four neighbouring boundary sites and is determined stochastically. Blue and purple coloured squares indicate the sites which have been updated in the even and odd times steps, respectively, with orange shaded squares denoting virtual sites.

295 Before proceeding, it is worth briefly commenting on the choice of boundary operators,
 296 in particular, regarding their support. For Rules 54 and 150, \hat{L} and \hat{R} were represented by
 297 4×4 stochastic matrices (see Refs. [48, 49]), i.e., their support was 2 sites, however, for Rule
 298 201, \hat{L} and \hat{R} have a support of 4 sites and, therefore, are represented by 16×16 matrices.
 299 Mathematically, the necessity for this can be demonstrated by proceeding with the analysis
 300 detailed in the following sections and realizing that there exists no nontrivial solutions for the
 301 NESS, that is, the only possible solution is the *maximum entropy state*. Physically, however, the
 302 need for larger support can be understood in terms of the quasiparticle picture as follows. For
 303 Rule 54, we only required information on the state of 3 adjacent sites of the lattice in order
 304 to determine the existence and species of a quasiparticle. Similarly, for Rule 150, we only
 305 required 2 sites. In either case, since the local stochastic boundary operators have supports of
 306 2 sites inside the lattice, but are additionally dependent on 1 virtual site outside the lattice, they
 307 can “detect” the creation or annihilation of a quasiparticle at the boundary and are, therefore,
 308 compatible with the quasiparticle description of the system, which the algebra explicitly relies
 309 on. In contrast, for Rule 201, we need knowledge of the states of 4 neighbouring sites of the
 310 lattice and hence require \hat{L} and \hat{R} have larger support. We choose 4 sites, as opposed to 3 sites,
 311 so that the local boundary operators are more compatible with the local 3 site bulk operators
 312 (see, e.g., Eq. 24).

313 3 Nonequilibrium steady state

314 3.1 Markov propagator

315 An important set of statistical states are the stationary or *steady states*. These are states that
316 are invariant under the time evolution of the propagator,

$$\hat{\mathbb{U}} = \hat{\mathbb{U}}_O \hat{\mathbb{U}}_E. \quad (32)$$

317 It follows directly from Eq. (20) that the propagator $\hat{\mathbb{U}}$ is a *stochastic matrix*: a nonnegative
318 square matrix whose elements in each and every column sum to unity. Moreover, the propa-
319 gator of the many-body Markov chain is *irreducible* and *aperiodic*⁶ and, therefore, according
320 to the Perron-Frobenius theorem [72] admits a unique steady state, namely, the *nonequilib-*
321 *rium steady state* (NESS), which is the only eigenvector \mathbf{p} of the propagator $\hat{\mathbb{U}}$ with eigenvalue
322 $\Lambda = 1$,

$$\hat{\mathbb{U}}\mathbf{p} = \mathbf{p}. \quad (33)$$

323 while all other eigenvalues are strictly bounded within the unit circle, therefore, guaranteeing
324 the uniqueness of, and exponential relaxation towards, the NESS from an arbitrary initial
325 probability state vector in the asymptotic limit $t \rightarrow \infty$. This also implies that the Markovian
326 dynamics in the irreducible subspace are *ergodic* and *mixing* [23].

327 Due to the staggering of the discrete time evolution, we only require these states to map
328 into themselves after one full time step between *even* time steps. Consequently, we can ad-
329 ditionally define a steady state between *odd* time steps and, therefore, associate two state
330 vectors, denoted by \mathbf{p} and \mathbf{q} , to the NESS, corresponding to steady states on even and odd
331 time steps, respectively. This then allows us to conveniently separate the fixed point condition
332 in Eq. (33) into a pair of coupled eigenvalue-like equations for even and odd times,

$$\hat{\mathbb{U}}_E \mathbf{p} = \Lambda_R \mathbf{q}, \quad \hat{\mathbb{U}}_O \mathbf{q} = \Lambda_L \mathbf{p}, \quad (34)$$

333 with the eigenvalue $\Lambda = \Lambda_L \Lambda_R = 1$ factored into parts. The principal objective of this section
334 is to find exact analytic solutions to these equations, which will prove useful when deriving
335 the exact dynamical large deviation statistics.

336 Prior to proceeding, however, let us clarify our notation. Throughout this chapter, we
337 consider a physical space \mathcal{S} (i.e., the state space) and an auxiliary space \mathcal{A} . The quantities
338 in the physical space are vectors, and are denoted by bold letters or symbols. Additionally,
339 vectors with vector components will be represented using Dirac bracket notation, while vectors
340 with matrix components will be written with a hat. Numeral subscripts on vectors in the
341 physical space then indicate the site position within the tensor product physical space $(\mathbb{R}^2)^{2L}$.
342 Quantities in the auxiliary space are similarly designated using the bracket and hat notations,
343 however, are written in italics instead of bold. Furthermore, the subscripts on quantities in the
344 auxiliary space indicate the state of the site, as opposed to its position. The only exceptions
345 to this convention are the Markov propagator $\hat{\mathbb{U}}$ and local operators \hat{U} , \hat{L} , and \hat{R} , which act
346 nontrivially, both in the physical space \mathcal{S} and auxiliary space \mathcal{A} .

347 3.2 Matrix product ansatz

348 We now postulate a simple ansatz for the NESS \mathbf{p} of the propagator $\hat{\mathbb{U}}$. More precisely, we con-
349 sider a state that can be expressed in a MPS form, reminiscent of the steady state introduced
350 in Ref. [55], which exhibited an efficient MPS representation that can be straightforwardly
351 understood as a *generalized Gibbs state*. The steady state is parameterized by two real *spectral*

⁶The proof is equivalent to that of Rules 54 [48] and 150 [49].

352 parameters ξ and ζ which due to the nonnegativity and normalizability of the probabilities p_n
 353 in Eq. (13) are strictly positive $\xi, \zeta \in \mathbb{R}^+$. The spectral parameters ξ, ζ admit an intuitive in-
 354 terpretation as decaying exponentials of the chemical potentials μ^\pm associated to the numbers
 355 of each species of quasiparticle N^\pm . Explicitly,

$$\xi = \exp(-\mu^+), \quad \zeta = \exp(-\mu^-), \quad (35)$$

356 where the spectral parameters can be understood as the inverse of the absolute activity or
 357 fugacity [73].

358 In order to express the steady state in terms of an efficient MPS, we must necessarily
 359 introduce the matrix components in the physical space \mathcal{S} . We start by defining the following
 360 vector, which constitutes the basis for the algebra,

$$\hat{\mathbf{V}} = \begin{bmatrix} \hat{V}_0 \\ \hat{V}_1 \end{bmatrix}, \quad (36)$$

361 where the components are 4×4 matrices acting on the 4-dimensional auxiliary space \mathcal{A} ,

$$\hat{V}_0 = \begin{bmatrix} 1 & \xi & 0 & 0 \\ 0 & 0 & 1 & 0 \\ 0 & 0 & 0 & 1 \\ 0 & 0 & 0 & 0 \end{bmatrix}, \quad \hat{V}_1 = \begin{bmatrix} 0 & 0 & 0 & 0 \\ 0 & 0 & 0 & 0 \\ 0 & 0 & 0 & 0 \\ \xi & \zeta & 1 & 0 \end{bmatrix}. \quad (37)$$

362 Similarly, we define the physical space vector,

$$\hat{\mathbf{W}} = \begin{bmatrix} \hat{W}_0 \\ \hat{W}_1 \end{bmatrix}, \quad (38)$$

363 which is obtained from $\hat{\mathbf{V}}$ by exchanging the spectral parameters (i.e., $\xi \leftrightarrow \zeta$). Written explic-
 364 itly, $\hat{\mathbf{W}}(\xi, \zeta) = \hat{\mathbf{V}}(\zeta, \xi)$, such that its components,

$$\hat{W}_0 = \begin{bmatrix} 1 & \zeta & 0 & 0 \\ 0 & 0 & 1 & 0 \\ 0 & 0 & 0 & 1 \\ 0 & 0 & 0 & 0 \end{bmatrix}, \quad \hat{W}_1 = \begin{bmatrix} 0 & 0 & 0 & 0 \\ 0 & 0 & 0 & 0 \\ 0 & 0 & 0 & 0 \\ \zeta & \xi & 1 & 0 \end{bmatrix}. \quad (39)$$

365 Akin to the analysis for Rules 54 [48], 150 [49], and 201 [55], these auxiliary space matrices
 366 satisfy a set of *cubic algebraic relations* that provides an explicit cancellation mechanism that
 367 facilitates the exact construction of the NESS of the Markov propagator $\hat{\mathcal{U}}$. In particular,

$$\hat{V}_{n_{x-1}} \hat{W}_{f_x} \hat{V}_{n_{x+1}} \hat{S} = \hat{V}_{n_{x-1}} \hat{S} \hat{V}_{n_x} \hat{W}_{n_{x+1}}, \quad (40)$$

368 where we have introduced the *delimiter matrix* \hat{S} , which is implicitly defined by the algebraic
 369 relations, that reads,

$$\hat{S} = \frac{1}{\xi^2 - \zeta} \begin{bmatrix} \xi\zeta & \xi^2 & 0 & -\zeta \\ -\zeta & -\xi & 0 & \xi \\ 0 & 0 & 1 & 0 \\ 1 & \zeta & 0 & 0 \end{bmatrix}. \quad (41)$$

370 Using the tensor product notation, this relation can be succinctly written as,

$$\hat{U}_x[\hat{\mathbf{V}}_{x-1} \hat{\mathbf{W}}_x \hat{\mathbf{V}}_{x+1} \hat{S}] = \hat{\mathbf{V}}_{x-1} \hat{S} \hat{\mathbf{V}}_x \hat{\mathbf{W}}_{x+1}, \quad (42)$$

371 where each physical component corresponds to one of the possible combinations of the states
 372 n_{x-1} , n_x , and n_{x+1} for the relations in Eq. (40). Remarking that the inverse of the delimiter

373 matrix \hat{S}^{-1} is exactly the delimiter matrix \hat{S} under the exchange of the spectral parameters
 374 $\xi \leftrightarrow \zeta$, that is,

$$\hat{S}^{-1}(\xi, \zeta) = \hat{S}(\zeta, \xi), \quad (43)$$

375 immediately implies a dual relation,

$$\hat{W}_{n_{x-1}} \hat{S}^{-1} \hat{W}_{f_x} \hat{V}_{n_{x+1}} = \hat{W}_{n_{x-1}} \hat{V}_{n_x} \hat{W}_{n_{x+1}} \hat{S}^{-1}, \quad (44)$$

376 which, in the tensor product notation, can be compactly summarized as,

$$\hat{U}_x[\hat{\mathbf{W}}_{x-1} \hat{S}^{-1} \hat{\mathbf{W}}_x \hat{\mathbf{V}}_{x+1}] = \hat{\mathbf{W}}_{x-1} \hat{\mathbf{V}}_x \hat{\mathbf{W}}_{x+1} \hat{S}^{-1}. \quad (45)$$

377 It can be straightforwardly verified that the ansatz for the auxiliary space matrices \hat{V}_0, \hat{V}_1
 378 and \hat{W}_0, \hat{W}_1 in Eqs. (37) and (39), respectively, together with the delimiter matrix \hat{S} in Eq. (41),
 379 satisfy the algebraic relations outlined in Eqs. (40) and (44). For a derivation of the auxiliary
 380 space matrices, albeit in a slightly different form that is equivalent under appropriate row or
 381 column transformations, see Ref. [55].

382 We now propose the simple, yet versatile, ansatz for the NESS vectors, \mathbf{p} and \mathbf{q} , of the
 383 propagator \hat{U} , which takes the form of a staggered MPS⁷,

$$\mathbf{p} = \langle \mathbf{l}_1 | \hat{\mathbf{W}}_2 \hat{\mathbf{V}}_3 \hat{\mathbf{W}}_4 \hat{\mathbf{V}}_5 \cdots \hat{\mathbf{V}}_{2L-3} \hat{\mathbf{W}}_{2L-2} | \mathbf{r}_{2L-1, 2L} \rangle, \quad (46)$$

384 while the associated NESS for the odd time step [cf. Eq. (34)] reads,

$$\mathbf{q} = \langle \mathbf{l}_{1,2} | \hat{\mathbf{W}}_3 \hat{\mathbf{V}}_4 \hat{\mathbf{W}}_5 \hat{\mathbf{V}}_6 \cdots \hat{\mathbf{V}}_{2L-2} \hat{\mathbf{W}}_{2L-1} | \mathbf{r}_{2L} \rangle, \quad (47)$$

385 where we have introduced the following vectors in the physical space \mathcal{S} , for the even time step
 386 steady state,

$$\langle \mathbf{l}_1 | = \begin{bmatrix} \langle l_{01} | \\ \langle l_{11} | \end{bmatrix}, \quad | \mathbf{r}_{2L-1, 2L} \rangle = \begin{bmatrix} | r_{00} \rangle \\ | r_{01} \rangle \\ | r_{10} \rangle \\ | r_{11} \rangle \end{bmatrix}, \quad (48)$$

387 and for the odd time step steady state,

$$\langle \mathbf{l}_{1,2} | = \begin{bmatrix} \langle l_{00} | \\ \langle l_{01} | \\ \langle l_{10} | \\ \langle l_{11} | \end{bmatrix}, \quad | \mathbf{r}_{2L} \rangle = \begin{bmatrix} | r_0 \rangle \\ | r_1 \rangle \end{bmatrix}, \quad (49)$$

388 with components that are row or column vectors in the 4-dimensional auxiliary space \mathcal{A} , such
 389 that the probability components p_n and q_n read,

$$\begin{aligned} p_n &= \langle l_{n_1} | \hat{\mathbf{W}}_{n_2} \hat{\mathbf{V}}_{n_3} \cdots \hat{\mathbf{W}}_{n_{2L-2}} | r_{n_{2L-1} n_{2L}} \rangle, \\ q_n &= \langle l_{n_1 n_2} | \hat{\mathbf{W}}_{n_3} \hat{\mathbf{V}}_{n_4} \cdots \hat{\mathbf{W}}_{n_{2L-1}} | r_{n_{2L}} \rangle. \end{aligned} \quad (50)$$

390 To ensure the coupled equations in Eq. (34) hold for the NESS vectors \mathbf{p} and \mathbf{q} , we neces-
 391 sarily require that the following ‘‘boundary’’ algebraic relations, analog to the ‘‘bulk’’ algebraic
 392 relations in Eqs. (40) and (44), hold,

$$\begin{aligned} \hat{U}_2[\langle \mathbf{l}_1 | \hat{\mathbf{W}}_2 \hat{\mathbf{V}}_3 \hat{S}] &= \langle \mathbf{l}_{1,2} | \hat{\mathbf{W}}_3, \\ \hat{R}_{2L-2, 2L}[\hat{\mathbf{V}}_{2L-3} \hat{\mathbf{W}}_{2L-2} | \mathbf{r}_{2L-1, 2L} \rangle] &= \Lambda_R \hat{\mathbf{V}}_{2L-3} \hat{S} \hat{\mathbf{V}}_{2L-2} \hat{\mathbf{W}}_{2L-1} | \mathbf{r}_{2L} \rangle, \\ \hat{I}_{1,3}[\langle \mathbf{l}_{1,2} | \hat{\mathbf{W}}_3 \hat{\mathbf{V}}_4] &= \Lambda_L \langle \mathbf{l}_1 | \hat{\mathbf{W}}_2 \hat{\mathbf{V}}_3 \hat{\mathbf{W}}_4 \hat{S}^{-1}, \\ \hat{U}_{2L-1}[\hat{\mathbf{W}}_{2L-2} \hat{S}^{-1} \hat{\mathbf{W}}_{2L-1} | \mathbf{r}_{2L} \rangle] &= \hat{\mathbf{W}}_{2L-2} | \mathbf{r}_{2L-1, 2L} \rangle, \end{aligned} \quad (51)$$

⁷Recall that the subscripts denote the tensor product component (i.e., the site position on the lattice) which the vector is an element of. For example, $\hat{\mathbf{W}}_x = \mathbf{1}^{\otimes(x-1)} \otimes \hat{\mathbf{W}} \otimes \mathbf{1}^{\otimes(2L-x)}$, where $\mathbf{1}$ denotes the two-dimensional vector of 2×2 identity matrices $\mathbf{1} = \begin{bmatrix} \hat{\mathbf{1}} & \\ & \hat{\mathbf{1}} \end{bmatrix}^T$ with the product of vectors the *Hadamard product* (i.e., the element-wise vector product).

393 which, in terms of components (i.e., tensors in the auxiliary space), read,

$$\begin{aligned}
& \langle l_{n_1} | \hat{W}_{f_2} \hat{V}_{n_3} \hat{S} = \langle l_{n_1 n_2} | \hat{W}_{n_3}, \\
& \sum_{n_5=0}^1 R_{n_1 f_2 n_3 f_4 n_5} \hat{V}_{n_1} \hat{W}_{f_2} | r_{n_3 f_4} \rangle = \Lambda_R \hat{V}_{n_1} \hat{S} \hat{V}_{n_2} \hat{W}_{n_3} | r_{n_4} \rangle, \\
& \sum_{n_0=0}^1 L_{n_0 f_1 n_2 f_3 n_4} \langle l_{f_1 n_2} | \hat{W}_{f_3} \hat{V}_{n_4} = \Lambda_L \langle l_{n_1} | \hat{W}_{n_2} \hat{V}_{n_3} \hat{W}_{n_4} \hat{S}^{-1}, \\
& \hat{W}_{n_2} \hat{S}^{-1} \hat{W}_{f_3} | r_{n_4} \rangle = \hat{W}_{n_2} | r_{n_3 n_4} \rangle,
\end{aligned} \tag{52}$$

394 where, again, for simplicity, we have set $L = 2$ for the right boundary algebraic relations. We
395 can easily check that, together with the bulk algebraic relations in Eqs. (40) and (44), these
396 boundary algebraic relations solve the coupled equations in Eq. (34). For example, to obtain \mathbf{q}
397 from \mathbf{p} , we first write out $\hat{U}_{\mathbf{E}} \mathbf{p}$ in terms of the matrix product in Eq. (20) and ansatz in Eq. (46).
398 By applying the stochastic boundary operator \hat{R} , while using the second boundary relation in
399 Eq. (52), we introduce the delimiter matrix \hat{S} and parameter Λ_R . Repeatedly applying the
400 deterministic bulk operators \hat{U}_x to the sites with even positions, i.e., sites $n_{2L-4}, n_{2L-6}, \dots, n_2$,
401 utilising the bulk relation in Eq. (40) then shifts the delimiter matrix \hat{S} to the left boundary,
402 where it is eliminated using the first boundary relation in Eq. (52) to return $\Lambda_R \mathbf{q}$. For example,
403 for $L = 4$ we have,

$$\begin{aligned}
\hat{U}_{\mathbf{E}} \mathbf{p} &= \hat{U}_2 \hat{U}_4 \hat{R}_{6,8} \langle \mathbf{1}_1 | \hat{W}_2 \hat{V}_3 \hat{W}_4 \hat{V}_5 \hat{W}_6 | \mathbf{r}_{7,8} \rangle \\
&= \Lambda_R \hat{U}_2 \hat{U}_4 \langle \mathbf{1}_1 | \hat{W}_2 \hat{V}_3 \hat{W}_4 \hat{V}_5 \hat{S} \hat{V}_6 \hat{W}_7 | \mathbf{r}_8 \rangle \\
&= \Lambda_R \hat{U}_2 \langle \mathbf{1}_1 | \hat{W}_2 \hat{V}_3 \hat{S} \hat{V}_4 \hat{W}_5 \hat{V}_6 \hat{W}_7 | \mathbf{r}_8 \rangle \\
&= \Lambda_R \langle \mathbf{1}_{1,2} | \hat{W}_3 \hat{V}_4 \hat{W}_5 \hat{V}_6 \hat{W}_7 | \mathbf{r}_8 \rangle \\
&= \Lambda_R \mathbf{q}.
\end{aligned} \tag{53}$$

404 The coupled equation for the odd time step follows analogously.

405 As before, we pause briefly to comment on the specific choice of boundary vector ansatz.
406 In Ref. [55], we considered site *independent* boundary vectors, that is, all state information
407 was encoded in the bulk vectors \hat{V}_x and \hat{W}_x . For this work, however, we consider site *depen-*
408 *dent* boundary vectors, which is why we have pedagogically presented the preceding analysis,
409 instead of referring to Ref. [55]⁸. The reason for this is reminiscent of the choice made to use
410 4-site, as opposed to 2-site, local stochastic boundary operators \hat{L} and \hat{R} . Specifically, when
411 generalized to analyze the exact dynamical large deviation statistics, the algebra exhibits no
412 nontrivial solutions.

413 3.3 Bethe equations

414 In order to obtain exact analytic expressions for the components of the vectors $\langle \mathbf{1}_1 |, | \mathbf{r}_{2L-1, 2L} \rangle$,
415 $\langle \mathbf{1}_{1,2} |, | \mathbf{r}_{2L} \rangle$, which will return solutions for the components of the NESS, we must solve the
416 boundary algebraic relations in Eq. (52). Doing so, whilst requiring that the spectral param-
417 eters are strictly positive $\xi, \zeta \in \mathbb{R}^+$ and boundary parameters are appropriately bounded con-
418 ditional probabilities $L_{n_0 n_1 n_2 n_3 n_4}, R_{n_{2L-3} n_{2L-2} n_{2L-1} n_{2L} n_{2L+1}} \in [0, 1]$, puts additional constraints on
419 the matrix components of the stochastic boundary operators \hat{L} and \hat{R} . Explicitly,

$$\Lambda_L^3 = \frac{L_{00000} L_{00001} L_{00010}}{L_{00001} + L_{00010} - 1}, \quad \Lambda_R^3 = \frac{R_{00000} R_{10000} R_{01000}}{R_{10000} + R_{01000} - 1}, \tag{54}$$

⁸For completeness, we detail the site independent solutions in Appendix A.

420 which reduces the number of free parameters to just four (i.e., two per stochastic boundary
 421 operator). To simplify the analytic expression for the NESS and, more importantly, guaran-
 422 tee the tractability of the derivation of the dynamical large deviations statistics of the scaled
 423 cumulant generating function, it proves beneficial to introduce the following convenient pa-
 424 rameterization for \hat{L} and \hat{R} , in terms of the probabilities $\alpha, \beta, \gamma, \delta \in [0, 1]$ where for the left
 425 boundary,

$$L_{00000} = \alpha^3, \quad L_{00001} = \beta^3, \quad L_{00010} = \frac{\Lambda_L^3(1-\beta^3)}{\Lambda_L^3 - \alpha^3\beta^3}, \quad (55)$$

426 and similarly for the right boundary,

$$R_{00000} = \gamma^3, \quad R_{10000} = \delta^3, \quad R_{01000} = \frac{\Lambda_R^3(1-\delta^3)}{\Lambda_R^3 - \gamma^3\delta^3}. \quad (56)$$

427 Solving separately for the left boundary (i.e., the first and third equations), we obtain the
 428 following unique solutions for the spectral parameters,

$$\xi = \frac{\Lambda_L^2(1-\beta^3)}{\beta^6}, \quad \zeta = \frac{\Lambda_L(\Lambda_L^3 - \beta^3)}{\beta^6}, \quad (57)$$

429 while the solutions for the left boundary vectors are presented in Appendix B.1. For the right
 430 boundary (i.e., the second and fourth equations) we have,

$$\xi = \frac{\Lambda_R(\Lambda_R^3 - \delta^3)}{\delta^6}, \quad \zeta = \frac{\Lambda_R^2(1-\delta^3)}{\delta^6}, \quad (58)$$

431 with the right boundary vectors, similarly, stated in Appendix B.1. Before we proceed, how-
 432 ever, let us briefly comment on the implications of the constraints in Eq. (54), as the depen-
 433 dence of the boundary parameters on the eigenvalue parameters is problematic. In particular,
 434 it immediately implies that we cannot obtain a general solution for arbitrary choice of condi-
 435 tional probabilities. That is, for $\Lambda \neq 1$, the only solutions for which the conditional probabili-
 436 ties $\alpha, \beta, \gamma, \delta$ are independent of the parameters Λ_L, Λ_R are the nontrivial deterministic limits
 437 $\beta = 0, 1$ and $\delta = 0, 1$, respectively. However, in these limits, there are no valid nontrivial
 438 solutions for the eigenvalues $\Lambda \neq 1$, since,

$$\lim_{\beta \rightarrow 0} \zeta = 0, \quad \lim_{\beta \rightarrow 1} \xi = 0, \quad \lim_{\delta \rightarrow 0} \xi = 0, \quad \lim_{\delta \rightarrow 1} \zeta = 0. \quad (59)$$

439 We are, therefore, restricted to the NESS with $\Lambda = \Lambda_L \Lambda_R = 1$.

440 Pairwise identifying the spectral parameters in Eqs. (57) and (58), we obtain the following
 441 closed set of *Bethe equations* for Λ_L and Λ_R ,

$$\frac{\Lambda_L^2(1-\beta^3)}{\beta^6} = \frac{\Lambda_R(\Lambda_R^3 - \delta^3)}{\delta^6}, \quad \frac{\Lambda_L(\Lambda_L^3 - \beta^3)}{\beta^6} = \frac{\Lambda_R^2(1-\delta^3)}{\delta^6}. \quad (60)$$

442 Eliminating Λ_L , using the identity $\Lambda_L \Lambda_R = 1$, and solving admits the following unique nontrivial
 443 solution⁹,

$$\Lambda_L = \frac{\beta}{\delta} = \frac{1}{\Lambda_R}, \quad (61)$$

444 which subsequently yields the following solutions for the spectral parameters,

$$\xi = \frac{1-\beta^3}{\beta^4\delta^2}, \quad \zeta = \frac{1-\delta^3}{\beta^2\delta^4}. \quad (62)$$

⁹Note that solving the closed pair of equations in Eq. (60) returns six roots for Λ_R and Λ_L (specifically, two roots for Λ_R^3 and Λ_L^3 since the closed pair of equations are quadratic in Λ_R^3 and Λ_L^3). However, pairwise identifying any other pair of solutions requires $\beta, \delta \notin [0, 1]$.

445 and left and right boundary vectors, which are given in Appendix B.1. Notice, the eigenvalue
 446 parameters Λ_L, Λ_R and spectral parameters ξ, ζ only depend on the conditional probabilities
 447 β, δ , that is, they are independent of α, γ .

448 4 Large deviation statistics

449 4.1 Large deviation principle

450 The foundation of large deviation theory (LDT) is the *large deviation principle* (LDP) [42],
 451 which states that the probability distribution of an observable K taking the value tk can be
 452 approximated by a decaying exponential of the form,

$$P(K(t) = tk) \asymp \exp(-tI(k)), \quad (63)$$

453 where $I(k)$ denotes the aptly named *rate function* and t represents an extensive quantity that
 454 is assumed large, specifically, time throughout this thesis. Here, the symbol “ \asymp ” indicates
 455 asymptotic equality, explicitly, that for two extensive quantities $J(t)$ and $K(t)$,

$$J(t) \asymp K(t) \implies \lim_{t \rightarrow \infty} \frac{1}{t} \ln(J(t)) = \lim_{t \rightarrow \infty} \frac{1}{t} \ln(K(t)). \quad (64)$$

456 The rate function $I(k)$ has is central in LDT because it admits a fundamentally important
 457 property. Specifically, there exists a value \bar{k} such that $I(\bar{k}) = 0$ and if $k \neq \bar{k}$ then $I(k) > 0$.
 458 Hence, in the limit $t \rightarrow \infty$, the observable K almost surely takes the value $t\bar{k}$ with fluctuations
 459 about this value that are suppressed exponentially with t as $t \rightarrow \infty$.

460 Taking the Legendre transform of the rate function $I(k)$ returns the *scaled cumulant gener-*
 461 *ating function* (SCGF), denote by $F(s)$, explicitly¹⁰,

$$F(s) = \sup_k (sk - I(k)), \quad (65)$$

462 with s the conjugate parameter to k . To gain some insight into the significance of the SCGF,
 463 we refer to Ref. [42]. Here, it is straightforwardly demonstrated that the rate function $I(k)$
 464 can be interpreted as the negative entropy density. Since in statistical mechanics the Legendre
 465 transform of the entropy is the free energy, the SCGF $F(s)$ can be understood as the negative
 466 free energy density. The validity of the equality in Eq. (65) is guaranteed, if $F(s)$ is differen-
 467 tiable and $K(t)$ satisfies a LDP with rate function $I(k)$, by *Varadhan’s theorem* [42]. The dual
 468 Legendre transform, namely,

$$I(k) = \sup_s (ks - F(s)), \quad (66)$$

469 is correspondingly guaranteed by the *Gartner-Ellis theorem*. By definition, the SCGF can be
 470 equivalently written as a generating functional,

$$F(s) = \lim_{t \rightarrow \infty} \frac{1}{t} \ln(M(s)), \quad (67)$$

471 where $M(s)$ is the *moment generating function* (MGF), defined by,

$$M(s) = \langle \exp(sK(t)) \rangle, \quad (68)$$

472 with $\langle \cdot \rangle$ denoting the expected value. Note that the existence of this limit for the SCGF directly
 473 implies that the MGF also satisfies a LDP

$$M(s) \asymp \exp(tF(s)). \quad (69)$$

¹⁰The symbol “sup” indicates the “supremum of”; for the purposes of this work, however, this can be understood to mean the “maximum of”.

474 Moreover, it is worth stating that the SCGF can, alternatively, be expressed as an infinite series
475 of scaled cumulants,

$$F(s) = \sum_{j=1}^{\infty} \frac{s^j}{j!} c_j, \quad c_j = \lim_{t \rightarrow \infty} \frac{1}{t} C_j \quad (70)$$

476 where C_j denotes the j^{th} cumulant of the observable K , with c_j the associated scaled cumulant.
477 The j^{th} scaled cumulant can, therefore, be obtained by taking the j^{th} derivative of the SCGF
478 with respect to s evaluated at $s = 0$,

$$c_j = \left. \frac{d^j F(s)}{ds^j} \right|_{s=0}. \quad (71)$$

479 4.2 Time integrated observables

480 We consider general space and time extensive observables K of the form,

$$K(L, T) = \sum_{t=0}^{T-1} \sum_{x=1}^{2L-1} (a_{x,x+1}^{2t} + b_{x,x+1}^{2t+1}), \quad (72)$$

481 where we have used the convenient shorthand notation,

$$a_{x,x+1}^t = a_{x,x+1}(n_x^t, n_{x+1}^t), \quad b_{x,x+1}^t = b_{x,x+1}(n_x^t, n_{x+1}^t), \quad (73)$$

482 to denote local two site occupation functions acting on the sites at positions x and $x+1$ at time
483 t . We refer to observables of this form as dynamical, as they depend on the full time history
484 of the state of the system, explicitly, these are *trajectory observables* $K(\omega)$, as opposed to state
485 observables $K(n)$, where,

$$\omega^{2T} = (n^0, n^1, \dots, n^{2T-1}), \quad n^t = (n_1^t, n_2^t, \dots, n_{2L}^t). \quad (74)$$

486 4.3 Tilted Markov propagator

487 In order to obtain an exact analytic expression for the SCGF $F(s)$, we take the approach out-
488 lined in Ref. [47]. Namely, we deform or *tilt* the Markov operator \hat{U} and define the so called
489 *tilted propagator* [42],

$$\hat{U}(s) = \hat{U}_O(s) \hat{U}_E(s), \quad \hat{U}_E(s) = \hat{U}_E \hat{A}(s), \quad \hat{U}_O(s) = \hat{U}_O \hat{B}(s), \quad (75)$$

490 where $\hat{A}(s)$ and $\hat{B}(s)$ are the diagonal operators introduced to apply the tilting. It, therefore,
491 follows, from their diagonal form, that these tilting operators can be expressed as products of
492 local operators acting on adjacent sites,

$$\hat{A}(s) = \prod_{x=1}^{2L-1} \hat{A}_{x,x+1}^{(x,x+1)}, \quad \hat{B}(s) = \prod_{x=1}^{2L-1} \hat{B}_{x,x+1}^{(x,x+1)}, \quad (76)$$

493 where the subscript index denotes the sites of the lattice on which the operators act nontrivially,

$$\begin{aligned} \hat{A}_{x,x+1}^{(x,x+1)} &= \mathbb{1}^{\otimes(x-1)} \otimes \hat{A}^{(x,x+1)} \otimes \mathbb{1}^{\otimes(2N-x-1)}, \\ \hat{B}_{x,x+1}^{(x,x+1)} &= \mathbb{1}^{\otimes(x-1)} \otimes \hat{B}^{(x,x+1)} \otimes \mathbb{1}^{\otimes(2N-x-1)}, \end{aligned} \quad (77)$$

494 while the superscript index indicates that the matrices are now *site dependent*, and, addition-
 495 ally, implicitly implies dependence on the conjugate parameter s . Explicitly, the tilting opera-
 496 tors $\hat{A}^{(x,x+1)}$ and $\hat{B}^{(x,x+1)}$ are given by the following local 4×4 diagonal matrices,

$$\hat{A}^{(x,x+1)} = \begin{bmatrix} a_{00}^{(x,x+1)} & & & \\ & a_{01}^{(x,x+1)} & & \\ & & a_{10}^{(x,x+1)} & \\ & & & a_{11}^{(x,x+1)} \end{bmatrix}, \quad (78)$$

$$\hat{B}^{(x,x+1)} = \begin{bmatrix} b_{00}^{(x,x+1)} & & & \\ & b_{01}^{(x,x+1)} & & \\ & & b_{10}^{(x,x+1)} & \\ & & & b_{11}^{(x,x+1)} \end{bmatrix},$$

497 where we have introduced the convenient shorthand notation,

$$a_{n_x n_{x+1}}^{(x,x+1)} = \exp(-s a_{x,x+1}(n_x, n_{x+1})), \quad (79)$$

$$b_{n_x n_{x+1}}^{(x,x+1)} = \exp(-s b_{x,x+1}(n_x, n_{x+1})),$$

498 to denote the exponents of the local occupation functions in Eq. (73).

499 It follows immediately from direct computation that the tilting operators can be distributed
 500 across the time evolution operators such that we can write,

$$\hat{U}_E(s) = \hat{R}_{2L-2,2L}^{(2L-2,2L)} \prod_{x=1}^{L-2} \hat{U}_{2x}^{(2x)}, \quad \hat{U}_O(s) = \hat{L}_{1,3}^{(1,3)} \prod_{x=2}^{L-1} \hat{U}_{2x+1}^{(2x+1)}, \quad (80)$$

501 where the tilted deterministic bulk matrices read,

$$\hat{U}_{2x}^{(2x)} = \hat{U}_{2x} \hat{A}_{2x-1,2x}^{(2x-1,2x)} \hat{A}_{2x,2x+1}^{(2x,2x+1)}, \quad (81)$$

$$\hat{U}_{2x+1}^{(2x+1)} = \hat{U}_{2x+1} \hat{B}_{2x,2x+1}^{(2x,2x+1)} \hat{B}_{2x+1,2x+2}^{(2x+1,2x+2)},$$

502 while the tilted stochastic boundary matrices are given by,

$$\hat{R}_{2L-2,2L}^{(2L-2,2L)} = \hat{R}_{2L-2,2L} \hat{A}_{2L-3,2L-2}^{(2L-3,2L-2)} \hat{A}_{2L-2,2L-1}^{(2L-2,2L-1)} \hat{A}_{2L-1,2L}^{(2L-1,2L)}, \quad (82)$$

$$\hat{L}_{1,3}^{(1,3)} = \hat{L}_{1,3} \hat{B}_{1,2}^{(1,2)} \hat{B}_{2,3}^{(2,3)} \hat{B}_{3,4}^{(3,4)},$$

503 From here, we make use of the Perron-Frobenius theorem [72], as outlined in Ref. [42]. In
 504 particular, given that the tilting operators, $\hat{A}(s)$ and $\hat{B}(s)$, are diagonal, it follows that the tilted
 505 propagator $\hat{U}(s)$ is irreducible and aperiodic and, as such, similarly admits a unique stationary
 506 distribution probability $\mathbf{p}(s)$ and unique dominant eigenvalue $\Lambda(s)$,

$$\langle \exp(sK(t)) \rangle \asymp (\Lambda(s))^t, \quad (83)$$

507 from which it follows that,

$$F(s) = \ln(\Lambda(s)). \quad (84)$$

508 4.4 Generalized matrix product ansatz

509 We now look to construct an exact analytic form for the dominant eigenvector of the tilted
 510 Markov operator $\hat{U}(s)$, explicitly, the eigenvector associated to the dominant eigenvalue $\Lambda(s)$.
 511 To do so, we employ the methods used in Ref. [47], and later in Ref. [49], that generalizes

512 the MPS ansatz of the NESS. Namely, we seek a pair of vectors, $\mathbf{p}(s)$ and $\mathbf{q}(s)$, satisfying the
513 coupled equations,

$$\hat{U}_E(s)\mathbf{p}(s) = \Lambda_R(s)\mathbf{q}(s), \quad \hat{U}_O(s)\mathbf{q}(s) = \Lambda_L(s)\mathbf{p}(s), \quad (85)$$

514 where $\Lambda_L(s)\Lambda_R(s) = \Lambda(s)$ which, as expected, recovers the eigenvalue equation for the tilted
515 propagator,

$$\hat{U}(s)\mathbf{p}(s) = \Lambda(s)\mathbf{p}(s). \quad (86)$$

516 Following Refs. [47, 49], we now postulate the following simple staggered MPS ansatz for
517 the vectors $\mathbf{p}(s)$ and $\mathbf{q}(s)$,

$$\begin{aligned} \mathbf{p}(s) &= \langle \mathbf{l}_1^{(1)} | \hat{\mathbf{W}}_2^{(2)} \hat{\mathbf{V}}_3^{(3)} \dots \hat{\mathbf{W}}_{2L-2}^{(2L-2)} | \mathbf{r}_{2L-1,2L}^{(2L-1,2L)} \rangle, \\ \mathbf{q}(s) &= \langle \mathbf{l}_{1,2}^{(1,2)} | \hat{\mathbf{W}}_3^{(3)} \hat{\mathbf{V}}_4^{(4)} \dots \hat{\mathbf{W}}_{2L-1}^{(2L-1)} | \mathbf{r}_{2L}^{(2L)} \rangle, \end{aligned} \quad (87)$$

518 where we have introduced generalized physical space vectors of auxiliary space matrices that
519 read,

$$\hat{\mathbf{V}}^{(x)} = \begin{bmatrix} \hat{\mathbf{V}}_0^{(x)} \\ \hat{\mathbf{V}}_1^{(x)} \end{bmatrix}, \quad \hat{\mathbf{W}}^{(x)} = \begin{bmatrix} \hat{\mathbf{W}}_0^{(x)} \\ \hat{\mathbf{W}}_1^{(x)} \end{bmatrix}, \quad (88)$$

520 with, as before, the numeral subscript label on the physical space vectors, $\hat{\mathbf{V}}_x^{(x)}$ and $\hat{\mathbf{W}}_x^{(x)}$, denot-
521 ing the element of the tensor product component (see footnote of Eq. (46) for an explanation)
522 and the associated generalized physical space vectors of auxiliary space vectors for the even
523 time step state vector $\mathbf{p}(s)$,

$$\langle \mathbf{l}^{(1)} | = \begin{bmatrix} \langle l_0^{(1)} | \\ \langle l_1^{(1)} | \end{bmatrix}, \quad | \mathbf{r}^{(2L-1,2L)} \rangle = \begin{bmatrix} |r_{00}^{(2L-1,2L)} \rangle \\ |r_{01}^{(2L-1,2L)} \rangle \\ |r_{10}^{(2L-1,2L)} \rangle \\ |r_{11}^{(2L-1,2L)} \rangle \end{bmatrix}, \quad (89)$$

524 and, likewise, for the odd time step state vector $\mathbf{q}(s)$,

$$\langle \mathbf{l}^{(1,2)} | = \begin{bmatrix} \langle l_{00}^{(1,2)} | \\ \langle l_{01}^{(1,2)} | \\ \langle l_{10}^{(1,2)} | \\ \langle l_{11}^{(1,2)} | \end{bmatrix}, \quad | \mathbf{r}^{(2L)} \rangle = \begin{bmatrix} |r_0^{(2L)} \rangle \\ |r_1^{(2L)} \rangle \end{bmatrix}, \quad (90)$$

525 where we have included the seemingly unnecessary superscript index to denote the explicit
526 dependence on the conjugate parameter s .

527 To ensure Eq. (85) is satisfied, and subsequently recovers the eigenvalue equation of the
528 titled propagator, we demand these vectors satisfy the following algebraic relations that fa-
529 cilitate the efficient cancellation mechanism implying the MPS form of the eigenvectors $\mathbf{p}(s)$
530 and $\mathbf{q}(s)$. Explicitly, the inhomogeneous bulk relations, generalized the NESS bulk relations in
531 Eqs. (40) and (44),

$$\begin{aligned} \hat{U}_{2x}^{(2x)} [\hat{\mathbf{V}}_{2x-1}^{(2x-1)} \hat{\mathbf{W}}_{2x}^{(2x)} \hat{\mathbf{X}}_{2x+1}^{(2x+1)}] &= \hat{\mathbf{X}}_{2x-1}^{(2x-1)} \hat{\mathbf{V}}_{2x}^{(2x)} \hat{\mathbf{W}}_{2x+1}^{(2x+1)}, \\ \hat{U}_{2x+1}^{(2x+1)} [\hat{\mathbf{Y}}_{2x}^{(2x)} \hat{\mathbf{W}}_{2x+1}^{(2x+1)} \hat{\mathbf{V}}_{2x+2}^{(2x+2)}] &= \hat{\mathbf{W}}_{2x}^{(2x)} \hat{\mathbf{V}}_{2x+1}^{(2x+1)} \hat{\mathbf{Y}}_{2x+2}^{(2x+2)}, \end{aligned} \quad (91)$$

532 and the inhomogeneous boundary relations, generalized Eq. (52),

$$\begin{aligned} \hat{U}_2^{(2)} [\langle \mathbf{l}_1^{(1)} | \hat{\mathbf{W}}_2^{(2)} \hat{\mathbf{X}}_3^{(3)}] &= \langle \mathbf{l}_{1,2}^{(1,2)} | \hat{\mathbf{W}}_3^{(3)}, \\ \hat{R}_{2L-2,2L}^{(2L-2,2L)} [\hat{\mathbf{V}}_{2L-3}^{(2L-3)} \hat{\mathbf{W}}_{2L-2}^{(2L-2)} | \mathbf{r}_{2L-1,2L}^{(2L-1,2L)}] &= \Lambda_R(s) \hat{\mathbf{X}}_{2L-3}^{(2L-3)} \hat{\mathbf{V}}_{2L-2}^{(2L-2)} \hat{\mathbf{W}}_{2L-1}^{(2L-1)} | \mathbf{r}_{2L}^{(2L)}, \\ \hat{L}_{1,3}^{(1,3)} [\langle \mathbf{l}_{1,2}^{(1,2)} | \hat{\mathbf{W}}_3^{(3)} \hat{\mathbf{V}}_4^{(4)}] &= \Lambda_L(s) \langle \mathbf{l}_1^{(1)} | \hat{\mathbf{W}}_2^{(2)} \hat{\mathbf{V}}_3^{(3)} \hat{\mathbf{Y}}_4^{(4)}, \\ \hat{U}_{2L-1}^{(2L-1)} [\hat{\mathbf{Y}}_{2L-2}^{(2L-2)} \hat{\mathbf{W}}_{2L-1}^{(2L-1)} | \mathbf{r}_{2L}^{(2L)}] &= \hat{\mathbf{W}}_{2L-2}^{(2L-2)} | \mathbf{r}_{2L-1,2L}^{(2L-1,2L)} \rangle, \end{aligned} \quad (92)$$

533 where to simplify the calculations we have introduced the generalized delimiter matrix vector
534 [cf. Eq. (41)],

$$\hat{\mathbf{X}}^{(x)} = \begin{bmatrix} \hat{X}_0^{(x)} \\ \hat{X}_1^{(x)} \end{bmatrix}, \quad \hat{\mathbf{Y}}^{(x)} = \begin{bmatrix} \hat{Y}_0^{(x)} \\ \hat{Y}_1^{(x)} \end{bmatrix}, \quad (93)$$

535 which are defined as the tilted analogues of the products $\hat{\mathbf{V}}_{2x+1}\hat{\mathbf{S}}$ and $\hat{\mathbf{W}}_{2x}\hat{\mathbf{S}}^{-1}$, specifically,
536 using the definitions in Eqs. (37), (39), and (41),

$$\hat{X}_0 = \hat{V}_0\hat{S}, \quad \hat{X}_1 = \hat{V}_1\hat{S}, \quad \hat{Y}_0 = \hat{W}_0\hat{S}^{-1}, \quad \hat{Y}_1 = \hat{W}_1\hat{S}^{-1}. \quad (94)$$

537 For clarity, we will refer to these auxiliary space matrices as *exchange matrices*.

538 Whilst the compact tensor product notation is efficient, it is ultimately the relations in
539 terms of their components that we explicitly solve. Therefore, let us present these now. First,
540 the matrix product ansatz in Eq. (87),

$$\begin{aligned} p_n(s) &= \langle l_{n_1}^{(1)} | \hat{W}_{n_2}^{(2)} \hat{V}_{n_3}^{(3)} \dots \hat{W}_{n_{2L-2}}^{(2L-2)} | r_{n_{2L-1}n_{2L}}^{(2L-1,2L)} \rangle, \\ q_n(s) &= \langle l_{n_1n_2}^{(1,2)} | \hat{W}_{n_3}^{(3)} \hat{V}_{n_4}^{(4)} \dots \hat{W}_{n_{2L-1}}^{(2L-1)} | r_{n_{2L}}^{(2L)} \rangle, \end{aligned} \quad (95)$$

541 next, the inhomogeneous bulk algebraic relations in Eq. (91),

$$\begin{aligned} a_{n_{2x-1}f_{2x}}^{(2x-1,2x)} a_{f_{2x}n_{2x+1}}^{(2x,2x+1)} \hat{V}_{n_{2x-1}}^{(2x-1)} \hat{W}_{f_{2x}}^{(2x)} \hat{X}_{n_{2x+1}}^{(2x+1)} &= \hat{X}_{n_{2x-1}}^{(2x-1)} \hat{V}_{n_{2x}}^{(2x)} \hat{W}_{n_{2x+1}}^{(2x+1)}, \\ b_{n_{2x}f_{2x+1}}^{(2x,2x+1)} b_{f_{2x+1}n_{2x+2}}^{(2x+1,2x+2)} \hat{Y}_{n_{2x}}^{(2x)} \hat{W}_{f_{2x+1}}^{(2x+1)} \hat{V}_{n_{2x+2}}^{(2x+2)} &= \hat{W}_{n_{2x}}^{(2x)} \hat{V}_{n_{2x+1}}^{(2x+1)} \hat{Y}_{n_{2x+2}}^{(2x+2)}, \end{aligned} \quad (96)$$

542 and, finally, the inhomogeneous boundary algebraic relations in Eq. (92),

$$\begin{aligned} a_{n_1f_2}^{(1,2)} a_{f_2n_3}^{(2,3)} \langle l_{n_1}^{(1)} | \hat{W}_{f_2}^{(2)} \hat{X}_{n_3}^{(3)} &= \langle l_{n_1n_2}^{(1,2)} | \hat{W}_{n_3}^{(3)} \rangle, \\ \sum_{n_5=0}^1 R_{n_1f_2n_3f_4n_5} a_{n_1f_2}^{(1,2)} a_{f_2n_3}^{(2,3)} a_{n_3f_4}^{(3,4)} \hat{V}_{n_1}^{(1)} \hat{W}_{f_2}^{(2)} | r_{n_3f_4}^{(3,4)} \rangle &= \Lambda_R(s) \hat{X}_{n_1}^{(1)} \hat{V}_{n_2}^{(2)} \hat{W}_{n_3}^{(3)} | r_{n_4}^{(4)} \rangle, \\ \sum_{n_0=0}^1 L_{n_0f_1n_2f_3n_4} b_{f_1n_2}^{(1,2)} b_{n_2f_3}^{(2,3)} b_{f_3n_4}^{(3,4)} \langle l_{f_1n_2}^{(1,2)} | \hat{W}_{f_3}^{(3)} \hat{V}_{n_4}^{(4)} &= \Lambda_L(s) \langle l_{n_1}^{(1)} | \hat{W}_{n_2}^{(2)} \hat{V}_{n_3}^{(3)} \hat{Y}_{n_4}^{(4)} \rangle, \\ b_{n_2f_3}^{(2,3)} b_{f_3n_4}^{(3,4)} \hat{Y}_{n_2}^{(2)} \hat{W}_{f_3}^{(3)} | r_{n_4}^{(4)} \rangle &= \hat{W}_{n_2}^{(2)} | r_{n_3n_4}^{(3,4)} \rangle, \end{aligned} \quad (97)$$

543 where, again, for readability we have set $L = 2$ for the right boundary relations.

544 4.5 Inhomogeneous algebraic solutions

545 In order to proceed with the explicit calculations to derive the dominant eigenvalue $\Lambda(s)$ and
546 the corresponding eigenvector $\mathbf{p}(s)$ of the titled propagator $\hat{\mathbf{U}}(s)$ we must propose an ansatz for
547 the auxiliary space components of the physical space vectors in Eqs. (91) and (92), reminiscent
548 of the methods introduced to study the exact large deviation statistics of Rules 54 [47] and

549 150 [49]. In particular, we employ the following transformations for the bulk matrices,

$$\begin{aligned}
\hat{V}_0 &= \begin{bmatrix} 1 & \xi & 0 & 0 \\ 0 & 0 & 1 & 0 \\ 0 & 0 & 0 & 1 \\ 0 & 0 & 0 & 0 \end{bmatrix} \rightarrow \hat{V}_0^{(x)} = \begin{bmatrix} 1 & \xi v_1^{(x)} & 0 & 0 \\ 0 & 0 & 1 & 0 \\ 0 & 0 & 0 & 1 \\ 0 & 0 & 0 & 0 \end{bmatrix}, \\
\hat{V}_1 &= \begin{bmatrix} 0 & 0 & 0 & 0 \\ 0 & 0 & 0 & 0 \\ 0 & 0 & 0 & 0 \\ \xi & \zeta & 1 & 0 \end{bmatrix} \rightarrow \hat{V}_1^{(x)} = \begin{bmatrix} 0 & 0 & 0 & 0 \\ 0 & 0 & 0 & 0 \\ 0 & 0 & 0 & 0 \\ \xi v_2^{(x)} & \zeta v_3^{(x)} & 1 & 0 \end{bmatrix}, \\
\hat{W}_0 &= \begin{bmatrix} 1 & \zeta & 0 & 0 \\ 0 & 0 & 1 & 0 \\ 0 & 0 & 0 & 1 \\ 0 & 0 & 0 & 0 \end{bmatrix} \rightarrow \hat{W}_0^{(x)} = \begin{bmatrix} 1 & \zeta w_1^{(x)} & 0 & 0 \\ 0 & 0 & 1 & 0 \\ 0 & 0 & 0 & 1 \\ 0 & 0 & 0 & 0 \end{bmatrix}, \\
\hat{W}_1 &= \begin{bmatrix} 0 & 0 & 0 & 0 \\ 0 & 0 & 0 & 0 \\ 0 & 0 & 0 & 0 \\ \zeta & \xi & 1 & 0 \end{bmatrix} \rightarrow \hat{W}_1^{(x)} = \begin{bmatrix} 0 & 0 & 0 & 0 \\ 0 & 0 & 0 & 0 \\ 0 & 0 & 0 & 0 \\ \zeta w_2^{(x)} & \xi w_3^{(x)} & 1 & 0 \end{bmatrix},
\end{aligned} \tag{98}$$

550 which, we remark, satisfy a similar relation to the homogeneous bulk matrices, explicitly,
551 $\hat{V}_{n_x}(\xi, \zeta, v_j^{(x)}) = \hat{W}_{n_x}(\zeta, \xi, w_j^{(x)})$, while for the exchange matrices,

$$\begin{aligned}
\hat{X}_0 &= \begin{bmatrix} 0 & 0 & 0 & 1 \\ 0 & 0 & 1 & 0 \\ 1 & \zeta & 0 & 0 \\ 0 & 0 & 0 & 0 \end{bmatrix} \rightarrow \hat{X}_0^{(x)} = \begin{bmatrix} 0 & 0 & 0 & x_1^{(x)} \\ 0 & 0 & x_2^{(x)} & 0 \\ x_3^{(x)} & \zeta x_4^{(x)} & 0 & 0 \\ 0 & 0 & 0 & 0 \end{bmatrix}, \\
\hat{X}_1 &= \begin{bmatrix} 0 & 0 & 0 & 0 \\ 0 & 0 & 0 & 0 \\ 0 & 0 & 0 & 0 \\ \zeta & \xi & 1 & 0 \end{bmatrix} \rightarrow \hat{X}_1^{(x)} = \begin{bmatrix} 0 & 0 & 0 & 0 \\ 0 & 0 & 0 & 0 \\ 0 & 0 & 0 & 0 \\ \zeta x_5^{(x)} & \xi x_6^{(x)} & x_7^{(x)} & 0 \end{bmatrix}, \\
\hat{Y}_0 &= \begin{bmatrix} 0 & 0 & 0 & 1 \\ 0 & 0 & 1 & 0 \\ 1 & \xi & 0 & 0 \\ 0 & 0 & 0 & 0 \end{bmatrix} \rightarrow \hat{Y}_0^{(x)} = \begin{bmatrix} 0 & 0 & 0 & y_1^{(x)} \\ 0 & 0 & y_2^{(x)} & 0 \\ y_3^{(x)} & \xi y_4^{(x)} & 0 & 0 \\ 0 & 0 & 0 & 0 \end{bmatrix}, \\
\hat{Y}_1 &= \begin{bmatrix} 0 & 0 & 0 & 0 \\ 0 & 0 & 0 & 0 \\ 0 & 0 & 0 & 0 \\ \xi & \zeta & 1 & 0 \end{bmatrix} \rightarrow \hat{Y}_1^{(x)} = \begin{bmatrix} 0 & 0 & 0 & 0 \\ 0 & 0 & 0 & 0 \\ 0 & 0 & 0 & 0 \\ \xi y_5^{(x)} & \zeta y_6^{(x)} & y_7^{(x)} & 0 \end{bmatrix},
\end{aligned} \tag{99}$$

552 which similarly satisfy an equivalent relation, $\hat{X}_{n_x}(\xi, \zeta, x_j^{(x)}) = \hat{Y}_{n_x}(\zeta, \xi, y_j^{(x)})$.

553 Substituting these ansätze into the inhomogeneous bulk algebraic relations in Eq. (91)
554 we obtain the following recursive solutions for the components of the tilted auxiliary space

555 exchange matrices,

$$\begin{aligned}
x_1^{(2x+1)} &= \frac{1}{a_{00}^{(2x-1,2x)} a_{00}^{(2x,2x+1)}} x_1^{(2x-1)}, & y_1^{(2x)} &= b_{01}^{(2x-2,2x-1)} b_{10}^{(2x-1,2x)} y_1^{(2x-2)}, \\
x_3^{(2x+1)} &= \frac{1}{a_{01}^{(2x-1,2x)} a_{10}^{(2x,2x+1)}} x_3^{(2x-1)}, & y_3^{(2x)} &= b_{00}^{(2x-2,2x-1)} b_{00}^{(2x-1,2x)} y_3^{(2x-2)}, \\
x_7^{(2x+1)} &= \frac{1}{a_{10}^{(2x-1,2x)} a_{01}^{(2x,2x+1)}} x_7^{(2x-1)}, & y_7^{(2x)} &= b_{10}^{(2x-2,2x-1)} b_{01}^{(2x-1,2x)} y_7^{(2x-2)},
\end{aligned} \tag{100}$$

556 and the following simplifying relations for the remaining components,

$$\begin{aligned}
x_2^{(2x+1)} &= \frac{a_{00}^{(2x+1,2x+2)}}{a_{10}^{(2x+1,2x+2)}} x_7^{(2x+1)}, & y_2^{(2x)} &= \frac{b_{10}^{(2x,2x+1)}}{b_{00}^{(2x,2x+1)}} y_7^{(2x)}, \\
x_4^{(2x+1)} &= w_1^{(2x+1)} x_3^{(2x+1)}, & y_4^{(2x)} &= v_1^{(2x)} y_3^{(2x)}, \\
x_5^{(2x+1)} &= w_2^{(2x+1)} x_7^{(2x+1)}, & y_5^{(2x)} &= v_2^{(2x)} y_7^{(2x)}, \\
x_6^{(2x+1)} &= w_3^{(2x+1)} x_7^{(2x+1)}, & y_6^{(2x)} &= v_3^{(2x)} y_7^{(2x)}.
\end{aligned} \tag{101}$$

557 Employing the convention, introduced in Ref. [47], that assumes that the left boundary con-
558 ditions imply that,

$$a_{n_{-1}n_0}^{(-1,0)} = a_{n_0n_1}^{(0,1)} = 1, \quad b_{n_{-1}n_0}^{(-1,0)} = b_{n_0n_1}^{(0,1)} = 1, \tag{102}$$

559 we can rewrite the recursion relations in Eq. (100) succinctly as,

$$\begin{aligned}
x_1^{(2x+1)} &= \prod_{j=1}^x \frac{1}{a_{00}^{(2j-1,2j)} a_{00}^{(2j,2j+1)}}, & y_1^{(2x)} &= \prod_{j=1}^x b_{01}^{(2j-2,2j-1)} b_{10}^{(2j-1,2j)}, \\
x_3^{(2x+1)} &= \prod_{j=1}^x \frac{1}{a_{01}^{(2j-1,2j)} a_{10}^{(2j,2j+1)}}, & y_3^{(2x)} &= \prod_{j=1}^x b_{00}^{(2j-2,2j-1)} b_{00}^{(2j-1,2j)}, \\
x_7^{(2x+1)} &= \prod_{j=1}^x \frac{1}{a_{10}^{(2j-1,2j)} a_{01}^{(2j,2j+1)}}, & y_7^{(2x)} &= \prod_{j=1}^x b_{10}^{(2j-2,2j-1)} b_{01}^{(2j-1,2j)},
\end{aligned} \tag{103}$$

560 It is worth noting that whilst the tilted local operators commute [cf. Eqs. (23) and (24)], due to
561 the inhomogeneity of the algebraic relations and irreversibility of the dynamics, their order is
562 *fixed*. Particularly, on the even time step the boundary operator $\hat{R}^{(2L-2,2L)}$ must be applied first
563 so as to create the exchange matrix $\hat{X}^{(2L-3)}$, which is then sequentially shifted *down* the lattice
564 by the bulk operators $\hat{U}^{(2L-4)}, \hat{U}^{(2L-6)}, \dots, \hat{U}^{(4)}$ before being annihilated by $\hat{U}^{(2)}$. Similarly, on
565 the odd time step, the boundary operator $\hat{L}^{(1,3)}$ is applied first creating $\hat{Y}^{(4)}$, which is moved
566 *up* the lattice by the bulk operators $\hat{U}^{(5)}, \hat{U}^{(7)}, \dots, \hat{U}^{(2L-3)}$ and then annihilated by $\hat{U}^{(2L-1)}$.
567 However, the relations derived in Eq. (100) hold indefinitely and so we choose the convention
568 used in Refs. [47, 49].

569 For the components of the titled auxiliary space bulk matrices, Eq. (91) returns the follow-

570 ing recursive solutions, for the odd indexed components,

$$\begin{aligned}
v_1^{(2x+1)} &= \frac{a_{10}^{(2x+1,2x+2)} b_{00}^{(2x+2,2x+3)} x_1^{(2x+1)} y_3^{(2x+2)}}{a_{00}^{(2x+1,2x+2)} b_{10}^{(2x+2,2x+3)} x_7^{(2x+1)} y_7^{(2x+2)}} v_1^{(2x)}, \\
v_2^{(2x+1)} &= \frac{a_{00}^{(2x+1,2x+2)} b_{00}^{(2x+1,2x+2)} x_7^{(2x+1)} y_7^{(2x+2)}}{a_{10}^{(2x+1,2x+2)} b_{01}^{(2x+1,2x+2)} x_3^{(2x+1)} y_1^{(2x+2)}} v_2^{(2x)}, \\
v_3^{(2x+1)} &= \frac{b_{00}^{(2x+1,2x+2)} b_{00}^{(2x+2,2x+3)} x_1^{(2x+1)} y_3^{(2x+2)}}{b_{01}^{(2x+1,2x+2)} b_{10}^{(2x+2,2x+3)} x_3^{(2x+1)} y_1^{(2x+2)}} v_3^{(2x)}, \\
w_1^{(2x+1)} &= \frac{a_{00}^{(2x+1,2x+2)} b_{00}^{(2x+1,2x+2)} x_7^{(2x+1)} y_7^{(2x+2)}}{a_{10}^{(2x+1,2x+2)} b_{01}^{(2x+1,2x+2)} x_3^{(2x+1)} y_1^{(2x+2)}} w_1^{(2x)}, \\
w_2^{(2x+1)} &= \frac{a_{10}^{(2x+1,2x+2)} b_{01}^{(2x+1,2x+2)} x_1^{(2x+1)} y_3^{(2x+2)}}{a_{00}^{(2x+1,2x+2)} b_{00}^{(2x+1,2x+2)} x_7^{(2x+1)} y_7^{(2x+2)}} w_2^{(2x)}, \\
w_3^{(2x+1)} &= \frac{x_1^{(2x+1)} y_3^{(2x+2)}}{x_3^{(2x+1)} x_1^{(2x+2)}} w_3^{(2x)},
\end{aligned} \tag{104}$$

571 and, similarly, for the even indexed components,

$$\begin{aligned}
v_1^{(2x)} &= \frac{b_{10}^{(2x,2x+1)} a_{00}^{(2x+1,2x+2)} y_7^{(2x)} x_7^{(2x+1)}}{b_{00}^{(2x,2x+1)} a_{10}^{(2x+1,2x+2)} y_3^{(2x)} y_1^{(2x+1)}} v_1^{(2x-1)}, \\
v_2^{(2x)} &= \frac{b_{00}^{(2x,2x+1)} a_{00}^{(2x,2x+1)} y_1^{(2x)} x_3^{(2x+1)}}{b_{10}^{(2x,2x+1)} a_{01}^{(2x,2x+1)} y_7^{(2x)} x_7^{(2x+1)}} v_2^{(2x-1)}, \\
v_3^{(2x)} &= \frac{a_{00}^{(2x,2x+1)} a_{00}^{(2x+1,2x+2)} y_1^{(2x)} x_3^{(2x+1)}}{a_{01}^{(2x,2x+1)} a_{10}^{(2x+1,2x+2)} y_3^{(2x)} x_1^{(2x+1)}} v_3^{(2x-1)}, \\
w_1^{(2x)} &= \frac{b_{00}^{(2x,2x+1)} a_{00}^{(2x,2x+1)} y_1^{(2x)} x_3^{(2x+1)}}{b_{10}^{(2x,2x+1)} a_{01}^{(2x,2x+1)} y_7^{(2x)} x_7^{(2x+1)}} w_1^{(2x-1)}, \\
w_2^{(2x)} &= \frac{b_{10}^{(2x,2x+1)} a_{01}^{(2x,2x+1)} y_7^{(2x)} x_7^{(2x+1)}}{b_{00}^{(2x,2x+1)} a_{00}^{(2x,2x+1)} y_3^{(2x)} x_1^{(2x+1)}} w_2^{(2x-1)}, \\
w_3^{(2x)} &= \frac{y_1^{(2x)} x_3^{(2x+1)}}{y_3^{(2x)} x_1^{(2x+1)}} w_3^{(2x-1)}.
\end{aligned} \tag{105}$$

572 We can drastically simplify these relations by recursive self-substitution, which produces a
573 telescoping product, that can be subsequently reduced using the so called method of quo-
574 tients cancellation technique. Enacting this simplification, whilst utilising the aforementioned

575 boundary conditions, we obtain,

$$\begin{aligned}
v_1^{(2x+1)} &= \prod_{j=1}^{x+1} \frac{b_{00}^{(2j-1,2j)} b_{00}^{(2j,2j+1)}}{b_{01}^{(2j-1,2j)} b_{10}^{(2j,2j+1)}}, & v_1^{(2x)} &= \prod_{j=1}^{x+1} \frac{a_{00}^{(2j-2,2j-1)} a_{00}^{(2j-1,2j)}}{a_{01}^{(2j-2,2j-1)} a_{10}^{(2j-1,2j)}}, \\
v_2^{(2x+1)} &= 1, & v_2^{(2x)} &= 1, \\
v_3^{(2x+1)} &= \prod_{j=1}^{x+1} \frac{b_{00}^{(2j-1,2j)} b_{00}^{(2j,2j+1)}}{b_{01}^{(2j-1,2j)} b_{10}^{(2j,2j+1)}}, & v_3^{(2x)} &= \prod_{j=1}^{x+1} \frac{a_{00}^{(2j-2,2j-1)} a_{00}^{(2j-1,2j)}}{a_{01}^{(2j-2,2j-1)} a_{10}^{(2j-1,2j)}}, \\
w_1^{(2x+1)} &= 1, & w_1^{(2x)} &= 1, \\
w_2^{(2x+1)} &= \prod_{j=1}^{x+1} \frac{a_{01}^{(2j-2,2j-1)} a_{10}^{(2j-1,2j)}}{a_{00}^{(2j-2,2j-1)} a_{00}^{(2j-1,2j)}}, & w_2^{(2x)} &= \prod_{j=1}^x \frac{b_{01}^{(2j-1,2j)} b_{10}^{(2j,2j+1)}}{b_{00}^{(2j-1,2j)} b_{00}^{(2j,2j+1)}}, \\
w_3^{(2x+1)} &= \prod_{j=1}^{x+1} \frac{a_{01}^{(2j-2,2j-1)} a_{10}^{(2j-1,2j)}}{a_{00}^{(2j-2,2j-1)} a_{00}^{(2j-1,2j)}}, & w_3^{(2x)} &= \prod_{j=1}^x \frac{b_{01}^{(2j-1,2j)} b_{10}^{(2j,2j+1)}}{b_{00}^{(2j-1,2j)} b_{00}^{(2j,2j+1)}}.
\end{aligned} \tag{106}$$

576 These solutions are, however, *not* unique, as solving the relations additionally requires that
577 the following constraint on the tilting functions holds for all x ,

$$\frac{a_{00}^{(x-1,x)} a_{00}^{(x,x+1)}}{a_{01}^{(x-1,x)} a_{10}^{(x,x+1)}} = \frac{b_{01}^{(x-1,x)} b_{10}^{(x,x+1)}}{b_{00}^{(x-1,x)} b_{00}^{(x,x+1)}}, \tag{107}$$

578 which is reminiscent of the constraint imposed for Rule 150 [49]. Rather than applying this
579 constraint explicitly, we recall that the matrix product ansatz in Eq. (87) for $\mathbf{p}(s)$ and $\mathbf{q}(s)$
580 is independent of the exchange matrices $\hat{\mathbf{X}}^{(x)}$ and $\hat{\mathbf{Y}}^{(x)}$ and, since the recursive solutions for
581 the components of the bulk matrices only depend on the fractions in the expression for the
582 constraints, we can freely introduce a parameter $\eta^{(x)}$, defined by the constraint,

$$\eta^{(x)} = \frac{a_{00}^{(x-1,x)} a_{00}^{(x,x+1)}}{a_{01}^{(x-1,x)} a_{10}^{(x,x+1)}} = \frac{b_{01}^{(x-1,x)} b_{10}^{(x,x+1)}}{b_{00}^{(x-1,x)} b_{00}^{(x,x+1)}}. \tag{108}$$

583 Hence, we can succinctly parameterize the solutions for the components of the nontrivial aux-
584 iliary space bulk matrices as,

$$\begin{aligned}
v_1^{(2x+1)} &= v_3^{(2x+1)} = \prod_{j=1}^{x+1} \frac{1}{\eta^{(2j)}}, & v_1^{(2x)} &= v_3^{(2x)} = \prod_{j=1}^{x+1} \eta^{(2j-1)}, \\
w_2^{(2x+1)} &= w_3^{(2x+1)} = \prod_{j=1}^{x+1} \frac{1}{\eta^{(2j-1)}}, & w_2^{(2x)} &= w_3^{(2x)} = \prod_{j=1}^x \eta^{(2j)},
\end{aligned} \tag{109}$$

585 Before proceeding to the inhomogeneous boundary algebraic relations, we momentarily
586 comment on the form of the bulk algebraic solutions. For Rule 54, the recursive solutions
587 for the components of the vectors of matrices equivalent to $\hat{\mathbf{X}}^{(x)}$ and $\hat{\mathbf{Y}}^{(x)}$ could be written
588 in terms of just one free parameter, namely, $x_1^{(2x+1)}$ and $y_1^{(2x+2)}$, respectively. While these
589 were subsequently determined by the boundary conditions, it is interesting to compare this
590 result with Rule 150 and Rule 201. In particular, we make two important realizations. The
591 first is with respect to the ‘‘vacuum’’ of the models, specifically, the states of sites on which the
592 quasiparticle excitations move whereas the second is associated with the recursive relations for
593 the components of the exchange matrices, obtained by explicitly solving the inhomogeneous

594 bulk algebraic relations. Starting with the former, we recall the form of the vacua of Rules 54,
595 150, and 201. For Rule 54, the vacuum is characterized by the following configuration,

$$\dots 0000 \dots, \quad (110)$$

596 while for Rule 150, it is either of the following configurations,

$$\dots 0000 \dots \quad \dots 1111 \dots, \quad (111)$$

597 and, finally, for Rule 201 it is all of the following configurations,

$$\dots 0000 \dots \quad \dots 0101 \dots \quad \dots 1010 \dots \quad (112)$$

598 Now, we consider the latter observation¹¹. For Rule 54, the recursive relations for the compo-
599 nents of the exchange matrices $\hat{X}_{n_x}^{(x)}$ are resolved in terms of just one parameter, which takes
600 the form of the following product,

$$\prod_x a_{00}^{(x-1,x)} a_{00}^{(x,x+1)}. \quad (113)$$

601 For Rule 150, the equivalent relations depend on two parameters of the form,

$$\prod_x a_{00}^{(x-1,x)} a_{00}^{(x,x+1)}, \quad \prod_x a_{11}^{(x-1,x)} a_{11}^{(x,x+1)}, \quad (114)$$

602 while those for Rule 201 are functions of three parameters, given by,

$$\prod_x a_{00}^{(x-1,x)} a_{00}^{(x,x+1)}, \quad \prod_x a_{01}^{(x-1,x)} a_{10}^{(x,x+1)}, \quad \prod_x a_{10}^{(x-1,x)} a_{01}^{(x,x+1)}. \quad (115)$$

603 Comparing these observations, we immediately realize that there is an intimate relation be-
604 tween the quasiparticle interpretation of these models and the exact MPS representations of
605 their states constructed using this formalism. Moreover the auxiliary space can be understood
606 as attempting to detect or measure the quasiparticle content in a given state. We use the word
607 “attempting” since, as was detailed previously, in order to identify a quasiparticle we need
608 knowledge of four adjacent sites of the lattice. However, when measuring the states of the
609 sites, the auxiliary space only stores information about the content of the last site, therefore,
610 prohibiting the detection of the quasiparticles, or at least, their species. Hence, the matrices
611 can be understood as indiscriminately associating a factor to each and every quasiparticle irre-
612 spective of its species, that depends only on its position in the lattice. Naively, one would think
613 that extending the support of the tilting functions would resolve this complication, however,
614 this is not possible, at least not within the current formulation, since the algebra is funda-
615 mentally limited by the range of the local time evolution operators. For now, we omit further
616 discussion of this nontrivial problem and refer the reader to the concluding remarks in Chap-
617 ter 5.

618 4.6 Dominant eigenvalue

619 With the inhomogeneous bulk algebraic relations solved, we now look to solve the correspond-
620 ing boundary algebra in Eq. (92). Resolving the identities for the left boundary, we obtain the
621 following solutions for the spectral parameters,

$$\xi = \frac{\Lambda_L^2(1-\beta^3)}{\beta^6}, \quad \zeta = \frac{\Lambda_L(\Lambda_L^3-\beta^3)}{\beta^6}, \quad (116)$$

¹¹For simplicity, we only consider the components of the matrices of the vector $\hat{\mathbf{X}}^{(x)}$, since the same argument follows for $\hat{\mathbf{Y}}^{(x)}$.

622 which we remark are identical to the solutions in Eq. (57)¹². Additionally, we find that the con-
 623 straint remains enforced by the boundary relations, presented in terms of the parameterization
 624 as,

$$L_{00000} = \alpha^3, \quad L_{00001} = \beta^3, \quad L_{00010} = \frac{\Lambda_L^3(1-\beta^3)}{\Lambda_L^3 - \alpha^3\beta^3}. \quad (117)$$

625 The corresponding explicit expressions for the left boundary vectors are given in Appendix B.2.
 626 Resolving the right boundary identities, we get,

$$\xi = \frac{\Lambda_R(\Lambda_R^3 - \chi^3\delta^3)}{\chi^4\delta^6}, \quad \zeta = \frac{\Lambda_R^2(1-\delta^3)}{\chi^2\delta^6}, \quad (118)$$

627 where, for convenience, we introduce the compact shorthand notations,

$$\chi(s) = \prod_{x=1}^L \chi^{(2x-1)} = \prod_{x=1}^L \chi^{(2x)}, \quad (119)$$

628 with the parameter $\chi^{(x)}$, similar to $\eta^{(x)}$, defined by the constraint,

$$\chi^{(x)} = a_{00}^{(x-1,x)} a_{00}^{(x,x+1)} b_{00}^{(x-1,x)} b_{00}^{(x,x+1)} = a_{01}^{(x-1,x)} a_{10}^{(x,x+1)} b_{01}^{(x-1,x)} b_{10}^{(x,x+1)}. \quad (120)$$

629 and the convention (cf. Ref. [47]) which assumes the right boundary conditions impose,

$$a_{n_{2L}n_{2L+1}}^{(2L,2L+1)} = a_{n_{2L+1}n_{2L+2}}^{(2L+1,2L+2)} = 1, \quad b_{n_{2L}n_{2L+1}}^{(2L,2L+1)} = b_{n_{2L+1}n_{2L+2}}^{(2L+1,2L+2)} = 1. \quad (121)$$

630 As expected, we also find that the right boundary relations dictate the following constraint,
 631 again, given in terms of the convenient parameterization introduced for the NESS as,

$$R_{00000} = \gamma^3, \quad R_{10000} = \delta^3, \quad R_{01000} = \frac{\Lambda_R^3(1-\delta^3)}{\Lambda_R^3 - \chi^3\gamma^3\delta^3}. \quad (122)$$

632 Note here, however, the additional factor of χ . Pairwise equating the solutions for the spectral
 633 parameters, we obtain a closed set of Bethe equations for $\Lambda_L(s)$ and $\Lambda_R(s)$, that read,

$$\frac{\Lambda_L^2(1-\beta^3)}{\beta^6} = \frac{\Lambda_R(\Lambda_R^3 - \chi^3\delta^3)}{\chi^4\delta^6}, \quad \frac{\Lambda_L(\Lambda_L^3 - \beta^3)}{\beta^6} = \frac{\Lambda_R^2(1-\delta^3)}{\chi^2\delta^6}, \quad (123)$$

634 which, after substituting $\Lambda_L(s)$ with $\Lambda_L(s)\Lambda_R(s) = \Lambda(s)$, can be written as a pair of quadratics
 635 in $(\Lambda_R(s))^3$,

$$\begin{aligned} \beta^6\Lambda_R^6 - \chi^3\beta^6\delta^3\Lambda_R^3 - \chi^4(1-\beta^3)\delta^6\Lambda^2 &= 0, \\ \beta^6(1-\delta^3)\Lambda_R^6 + \chi^2\beta^3\delta^6\Lambda\Lambda_R^3 - \chi^2\delta^6\Lambda^4 &= 0, \end{aligned} \quad (124)$$

636 the solutions of which are given by,

$$\begin{aligned} \Lambda_R^3 &= \frac{\chi^3\beta^3\delta^3 \pm \chi^2\delta^3\sqrt{\chi^2\beta^6 + 4(1-\beta^3)\Lambda^2}}{2\beta^3}, \\ \Lambda_R^3 &= -\frac{\chi^2\delta^6\Lambda \pm \chi\delta^3\Lambda\sqrt{\chi^2\delta^6 + 4(1-\delta^3)\Lambda^2}}{2\beta^3(1-\delta^3)}. \end{aligned} \quad (125)$$

¹²Note that to ensure readability, we omit the explicit dependence of the parameters $\Lambda_L(s)$ and $\Lambda_R(s)$ on the conjugate parameter s in these equations.

637 Identifying and solving these equations is nontrivial and, therefore, we employ the method of
 638 radical isolation, which after a few relatively simple calculations, returns an octic characteristic
 639 polynomial that admits the following remarkable factorization,

$$\Lambda^3(\Lambda - \chi) \sum_{j=0}^4 \phi_j \chi^{4-j} \Lambda^j = 0, \quad (126)$$

640 where the coefficients are simply,

$$\begin{aligned} \phi_0 &= 1, \\ \phi_1 &= 1, \\ \phi_2 &= 1 - 2(1 - \beta^3)(1 - \delta^3), \\ \phi_3 &= 1 - 2(1 - \beta^3)(1 - \delta^3) - \beta^3 \delta^3, \\ \phi_4 &= \beta^3 \delta^3 (1 - \beta^3)(1 - \delta^3). \end{aligned} \quad (127)$$

641 Immediately, we realize that in the limit $s = 0$, which sets $\chi = 1$, the dominant eigenvalue
 642 $\Lambda(0) = 1$ associated to the NESS is recovered and, therefore, we are able to straightforwardly
 643 identify the dominant eigenvalue for all s as,

$$\Lambda(s) = \chi(s) = \exp\left(-s \sum_{x=1}^{2L-1} (a_{x,x+1}(0,0) + b_{x,x+1}(0,0))\right), \quad (128)$$

644 where to obtain the final equality we used the definitions in Eqs. (79), (119), and (120), from
 645 which we recall that the constraint in Eq. (120) must hold. As anticipated in the discussion
 646 in the previous subsection, the support of the large deviation tilting functions $a_{x,x+1}(n_x, n_{x+1})$
 647 and $b_{x,x+1}(n_x, n_{x+1})$ is simply too small to “measure” any quantity of interest (e.g., the quasi-
 648 particles), and just “weights” the vacuum (i.e., the absence of quasiparticles). Further analysis
 649 is, therefore, unnecessary since the dynamical behaviour of the SCGF is linear in the conjugate
 650 parameter and independent of the conditional probabilities,

$$F(s) = \ln(\Lambda(s)) = -s \sum_{x=1}^{2L-1} (a_{x,x+1}(0,0) + b_{x,x+1}(0,0)), \quad (129)$$

651 and, therefore, all cumulants other than the first (i.e., the mean) are zero.

652 A notable feature of these results, however, is the resultant expression for the dominant
 653 eigenvector, which takes the form of an inhomogeneous *generalized Gibbs ensemble*, with each
 654 and every quasiparticle statistically weighted by the two-body tilting functions [cf. Eq. (98)].
 655 This is in contrast to the NESS, which models a homogeneous Gibbs ensemble, for which each
 656 and every quasiparticle of the same species are indistinguishably weighted by the spectral pa-
 657 rameters ξ and ζ . Whilst we are currently unable to comment in more detail on this particular
 658 result, we will further investigate this connection, namely, between the local conserved quan-
 659 tities of the model (i.e., the quasiparticles), and the exact finite-dimensional matrix product
 660 form of its dominant eigenvector (i.e., a generalized Gibbs ensemble) in future work. For com-
 661 pleteness, we present the explicit expressions for the solutions for the parameters relevant to
 662 the dominant eigenvector $\mathbf{p}(s)$. First, the eigenvalue parameters $\Lambda_L(s)$ and $\Lambda_R(s)$,

$$\Lambda_L = \frac{\beta}{\delta}, \quad \Lambda_R = \chi \frac{\delta}{\beta}, \quad (130)$$

663 which we note are identical (up to a factor χ for Λ_R) to the untilted solutions, as are the
 664 resultant expressions for the spectral parameters ξ and ζ ,

$$\xi = \frac{1 - \beta^3}{\beta^4 \delta^2}, \quad \zeta = \frac{1 - \delta^3}{\beta^2 \delta^4}. \quad (131)$$

665 The associated conditional probabilities for the stochastic boundary operators \hat{L} and \hat{R} are then
 666 given by, for the left boundary,

$$L_{00000} = \alpha^3, \quad L_{00001} = \beta^3, \quad L_{00010} = \frac{1 - \beta^3}{1 - \alpha^3 \delta^3}, \quad (132)$$

667 while for the right boundary, they are,

$$R_{00000} = \gamma^3, \quad R_{10000} = \delta^3, \quad R_{01000} = \frac{1 - \delta^3}{1 - \beta^3 \gamma^3}, \quad (133)$$

668 which we note are also independent of the large deviation tilting functions. The explicit ex-
 669 pressions for the boundary vectors can be found in Appendix B.2.

670 5 Conclusions

671 In this paper, we studied the large deviations statistics of a general class of space and time
 672 additive two-body dynamical observables in the “Rule 201” reversible cellular automaton with
 673 stochastic boundary driving. We computed their exact scaled cumulant generating function via
 674 an inhomogeneous matrix product ansatz for the dominant eigenvalue and associated eigen-
 675 vector of the tilted Markov propagator. We explicitly demonstrated that the exact scaled cu-
 676 mulant generating function exhibits a simple linear response form for this class of extensive
 677 observables for all values of the tilting field, thus, indicating that the cumulants of these dynam-
 678 ical observables scale sublinearly with time. We also showed that the corresponding dominant
 679 eigenvector displays an inhomogeneous generalized Gibbs ensemble form, therefore general-
 680 izing the Gibbs state of the NESS. By this, we mean that if one restricts to trajectories with
 681 an atypical value of the dynamical observables, as controlled by the counting field, then the
 682 associated steady state is of the generalized Gibbs ensemble form.

683 An obvious question is how this framework can be generalized to study additive observ-
 684 ables with larger spatial support. As explained, the simplicity of the result above derives from
 685 the restriction imposed on the analytic methods used to obtain the exact expressions for the
 686 dominant eigenvalues, specifically, from the support of the tilting functions, which are upper
 687 bounded by the interaction range of the local time evolution operators. The limiting factor is
 688 the three site algebraic relations, which restrict the support of the local observables. There-
 689 fore, perhaps the most obvious approach is to construct algebraic relations that are solved
 690 recursively as opposed to independently. By this, we refer to a set of relations that are solved:
 691 first for an “opening” boundary, with a minimally sufficient set of bulk sites; then recursively
 692 through the system, each time adding additional bulk sites to the “opening” relation; and lastly
 693 for a “closing” boundary, thus returning the alternate dominant eigenvector. Furthermore, the
 694 results here can also be used to address related questions in models with more complex dy-
 695 namics, such as cellular automata with asymmetric local update rules or with irreversible bulk
 696 dynamics. We hope to report on progress in these directions in the future.

697 Acknowledgements

698 We thank Katja Klobas and Tomaž Prosen for collaboration on closely related projects and in-
 699 sightful comments and suggestions. We acknowledge support of The Leverhulme Trust through
 700 Grant number RPG-2018-181.

701 A Nonequilibrium steady state

702 In this Appendix, we briefly derive the exact MPS representation of the NESS, specifically, for
 703 specialized (i.e., site independent) boundary vectors. Here, the matrix product ansatz for the
 704 steady state vector components p_n, q_n reads,

$$\begin{aligned} p_n &= \langle l | \hat{V}_{n_1} \hat{W}_{n_2} \cdots \hat{V}_{n_{2L-1}} \hat{W}_{n_{2L}} | r \rangle, \\ q_n &= \langle l' | \hat{W}_{n_1} \hat{V}_{n_2} \cdots \hat{W}_{n_{2L-1}} \hat{V}_{n_{2L}} | r' \rangle. \end{aligned} \quad (134)$$

705 The bulk algebraic relations are identical to those in Eqs. (40) and (44),

$$\begin{aligned} \hat{V}_{n_{x-1}} \hat{W}_{f_x} \hat{V}_{n_{x+1}} \hat{S} &= \hat{V}_{n_{x-1}} \hat{S} \hat{V}_{n_x} \hat{W}_{n_{x+1}}, \\ \hat{W}_{n_{x-1}} \hat{S}^{-1} \hat{W}_{f_x} \hat{V}_{n_{x+1}} &= \hat{W}_{n_{x-1}} \hat{V}_{n_x} \hat{W}_{n_{x+1}} \hat{S}^{-1}, \end{aligned} \quad (135)$$

706 and, therefore, return precisely the bulk and delimiter matrices in Eqs. (37), (39), and (41).
 707 However, in contrast, the boundary algebraic relations are now given by (cf. Ref. [55]),

$$\begin{aligned} \langle l | \hat{V}_{n_1} \hat{S} &= \langle l' | \hat{W}_{n_1}, \\ \sum_{n_5=0}^1 R_{n_1 f_2 n_3 f_4 n_5} \hat{V}_{n_1} \hat{W}_{f_2} \hat{V}_{n_3} \hat{W}_{f_4} | r \rangle &= \Lambda_R \hat{V}_{n_1} \hat{S} \hat{V}_{n_2} \hat{W}_{n_3} \hat{V}_{n_4} | r' \rangle, \\ \sum_{n_0=0}^1 L_{n_0 f_1 n_2 f_3 n_4} \langle l' | \hat{W}_{f_1} \hat{V}_{n_2} \hat{W}_{f_3} \hat{V}_{n_4} &= \Lambda_L \langle l | \hat{V}_{n_1} \hat{W}_{n_2} \hat{V}_{n_3} \hat{W}_{n_4} \hat{S}^{-1}, \\ \hat{W}_{n_4} \hat{S}^{-1} | r' \rangle &= \hat{W}_{n_4} | r \rangle, \end{aligned} \quad (136)$$

708 where, as before, we set $L = 2$ for the right boundary identities.

709 As was the case for the generalized boundary algebraic relations (i.e., the site dependent
 710 boundary relations), solving these relations puts constraints on the matrix components of the
 711 stochastic boundary operators \hat{L} and \hat{R} ,

$$\Lambda_L^3 = \frac{L_{00000} L_{00001} L_{00010}}{L_{00001} + L_{00010} - 1}, \quad \Lambda_R^3 = \frac{R_{00000} R_{10000} R_{01000}}{R_{10000} + R_{01000} - 1}, \quad (137)$$

712 however, additionally imposes that,

$$L_{00001} = L_{00000}, \quad R_{10000} = R_{00000}. \quad (138)$$

713 Reintroducing the parameterization in terms of $\alpha, \beta, \gamma, \delta \in [0, 1]$, we have¹³,

$$L_{00000} = L_{00001} = \beta^3, \quad L_{00010} = \frac{\Lambda_L^3 (1 - \beta^3)}{\Lambda_L^3 - \beta^6}, \quad (139)$$

714 and, likewise, for the right boundary,

$$R_{00000} = R_{10000} = \delta^3, \quad R_{01000} = \frac{\Lambda_R^3 (1 - \delta^3)}{\Lambda_R^3 - \delta^6}, \quad (140)$$

715 which, clearly, are independent of α, γ .

716 Solving for the left boundary relations yields the following expressions for the spectral
 717 parameters,

$$\xi = \frac{\Lambda_L^2 (1 - \beta^3)}{\beta^6}, \quad \zeta = \frac{\Lambda_L (\Lambda_L^3 - \beta^3)}{\beta^6}, \quad (141)$$

¹³Note that we could equivalently parameterize the conditional probabilities $L_{n_0 n_1 n_2 n_3 n_4}$ and $R_{n_1 n_2 n_3 n_4 n_5}$ in terms of α, γ instead of β, δ , since $\alpha = \beta$ and $\gamma = \delta$.

718 while solving the right boundary relations gives,

$$\xi = \frac{\Lambda_R(\Lambda_R^3 - \delta^3)}{\delta^6}, \quad \zeta = \frac{\Lambda_R^2(1 - \delta^3)}{\delta^6}, \quad (142)$$

719 which we note are identical to those obtained for the site dependent boundary vector NESS.

720 The corresponding left boundary vectors are,

$$\langle l| = \left[1 \quad \frac{\Lambda_L^3 - \beta^6}{\Lambda_L^2 \beta^3} \quad \frac{1}{\Lambda_L} \quad \frac{\beta^3}{\Lambda_L^2} \right], \quad \langle l'| = \left[1 \quad \frac{\Lambda_L^3 - \beta^6}{\Lambda_L \beta^3} \quad \Lambda_L \quad \frac{\beta^3}{\Lambda_L} \right], \quad (143)$$

721 with the right boundary vectors given by,

$$|r\rangle = \begin{bmatrix} 1 \\ \delta^3 \\ \Lambda_R^2 \\ 1 \\ \Lambda_R \\ \Lambda_R \\ \delta^3 \end{bmatrix}, \quad |r'\rangle = \begin{bmatrix} 1 \\ \delta^3 \\ \Lambda_R \\ \Lambda_R \\ \Lambda_R^2 \\ \delta^3 \end{bmatrix}, \quad (144)$$

722 Given that the expressions for the spectral parameters ξ, ζ are exactly equal to those obtained
723 for the generalized NESS, the solutions are equivalent,

$$\Lambda_L = \frac{\beta}{\delta} = \frac{1}{\Lambda_R}. \quad (145)$$

724 Substituting these into the solutions for the spectral parameters yields,

$$\xi = \frac{1 - \beta^3}{\beta^4 \delta^2}, \quad \zeta = \frac{1 - \delta^3}{\beta^2 \delta^4}, \quad (146)$$

725 as expected, while for the left boundary vectors we have,

$$\langle l| = \left[1 \quad \frac{1 - \beta^3 \delta^3}{\beta^2 \delta} \quad \frac{\delta}{\beta} \quad \beta \delta^2 \right], \quad \langle l'| = \left[1 \quad \frac{1 - \beta^3 \delta^3}{\beta \delta^2} \quad \frac{\beta}{\delta} \quad \beta^2 \delta \right], \quad (147)$$

726 and, similarly, for the right boundary vectors,

$$|r\rangle = \begin{bmatrix} 1 \\ \beta^2 \delta \\ \beta \\ \delta \\ 1 \\ \beta \delta^2 \end{bmatrix}, \quad |r'\rangle = \begin{bmatrix} 1 \\ \beta \delta^2 \\ \delta \\ \beta \\ 1 \\ \beta^2 \delta \end{bmatrix}. \quad (148)$$

727 B Steady state boundary vectors

728 B.1 Homogeneous steady state

729 In this Appendix, we state the site dependent boundary vectors that solve the boundary algebraic relations (cf. Ref. [55]) in Eq. (52). Prior to solving for the NESS, the components of the
730 left boundary vectors $\langle l_1|$ and $\langle l_{1,2}|$ read,
731

$$\begin{aligned} \langle l_0| &= \left[1 \quad \frac{\Lambda_L^2(1 - \beta^3)}{\beta^6} \quad \frac{\Lambda_L^3 - \alpha^3 \beta^3}{\Lambda_L^2 \beta^3} \quad \frac{1}{\Lambda_L} \right], \\ \langle l_1| &= \left[\frac{1 - \beta^3}{\beta^3} \quad \frac{\Lambda_L^3 - \beta^3}{\Lambda_L \beta^3} \quad \frac{\alpha^3}{\Lambda_L^2} \quad 0 \right], \end{aligned} \quad (149)$$

732

$$\begin{aligned}
\langle l_{00}| &= \left[\frac{1}{\Lambda_L} \quad \frac{\Lambda_L(1-\beta^3)}{\beta^6} \quad \frac{\Lambda_L^3-\beta^3}{\beta^6} \quad \frac{\Lambda_L^3-\alpha^3\beta^3}{\Lambda_L^2\beta^3} \right], \\
\langle l_{01}| &= \left[\frac{\Lambda_L^2(1-\beta^3)}{\beta^6} \quad \frac{\Lambda_L(\Lambda_L^3-\beta^3)}{\beta^6} \quad 1 \quad 0 \right], \\
\langle l_{10}| &= \left[\frac{\Lambda_L^3-\beta^3}{\Lambda_L\beta^3} \quad \frac{\Lambda_L(\Lambda_L^3-\beta^3)(1-\beta^3)}{\beta^9} \quad \frac{1-\beta^3}{\beta^3} \quad \frac{\alpha^3}{\Lambda_L^2} \right], \\
\langle l_{11}| &= [0 \quad 0 \quad 0 \quad 0].
\end{aligned} \tag{150}$$

733 while the components of the right boundary vectors $|r_{2L-1,2L}\rangle$ and $|r_{2L}\rangle$ are,

$$\begin{aligned}
|r_{00}\rangle &= \begin{bmatrix} \frac{\Lambda_R^2((\Lambda_R^3-2\Lambda_R^3\delta^3+\gamma^3\delta^6)+\delta^3(\delta^3-\gamma^3))}{\delta^3(\Lambda_R^3-2\Lambda_R^3\delta^3+\gamma^3\delta^6)} \\ 1 \\ 0 \\ 0 \end{bmatrix}, \\
|r_{01}\rangle &= \begin{bmatrix} \frac{\Lambda_R^2(1-\delta^3)(\delta^3-\gamma^3)}{(\Lambda_R^3-2\Lambda_R^3\delta^3+\gamma^3\delta^6)\delta^6(\delta^3-\gamma^3)} \\ \frac{(\Lambda_R^3-2\Lambda_R^3\delta^3+\gamma^3\delta^6)}{\Lambda_R(\Lambda_R^3-2\Lambda_R^3\delta^3+\delta^9)} \\ \frac{\Lambda_R(\Lambda_R^3-2\Lambda_R^3\delta^3+\delta^9)}{\delta^3(\Lambda_R^3-2\Lambda_R^3\delta^3+\gamma^3\delta^6)} \\ 0 \end{bmatrix}, \\
|r_{10}\rangle &= \begin{bmatrix} 0 \\ 0 \\ 0 \\ \frac{\Lambda_R^3(\Lambda_R^3-2\Lambda_R^3\delta^3+\delta^9)}{\delta^6(\Lambda_R^3-2\Lambda_R^3\delta^3+\gamma^3\delta^6)} \end{bmatrix}, \\
|r_{11}\rangle &= \begin{bmatrix} 0 \\ 0 \\ 0 \\ 0 \end{bmatrix},
\end{aligned} \tag{151}$$

734

$$\begin{aligned}
|r_0\rangle &= \begin{bmatrix} 1 \\ \frac{\delta^3((\Lambda_R^6-2\Lambda_R^3\delta^3+\delta^9)(\Lambda_R^3-2\Lambda_R^3\delta^3+\gamma^3\delta^6)+\delta^3(\delta^3-\gamma^3)(\Lambda_R^3-\delta^3-\delta^6))}{\frac{\Lambda_R^2(\Lambda_R^6-2\Lambda_R^3\delta^3+\delta^9)(\Lambda_R^3-2\Lambda_R^3\delta^3+\gamma^3\delta^6)}{(\Lambda_R^6-2\Lambda_R^3\delta^3+\gamma^3\delta^6)(\Lambda_R^3-2\Lambda_R^3\delta^3+\delta^9)}} \\ 0 \end{bmatrix}, \\
|r_1\rangle &= \begin{bmatrix} \frac{\delta^6(\delta^3-\gamma^3)}{\Lambda_R^3(1-\delta^3)-\delta^3(\Lambda_R^3-\gamma^3\delta^3)} \\ \frac{\delta^6(\delta^3-\gamma^3)\delta^3((\Lambda_R^6-2\Lambda_R^3\delta^3+\delta^9)-\Lambda_R^3(\Lambda_R^3-\delta^3-\delta^6))}{\Lambda_R^2(\Lambda_R^6-2\Lambda_R^3\delta^3+\delta^9)(\Lambda_R^3-2\Lambda_R^3\delta^3+\gamma^3\delta^6)} \\ \frac{\delta^6(\delta^3-\gamma^3)(\Lambda_R^3-2\Lambda_R^3\delta^3+\delta^9)}{\Lambda_R(\Lambda_R^6-2\Lambda_R^3\delta^3+\delta^9)(\Lambda_R^3-2\Lambda_R^3\delta^3+\gamma^3\delta^6)} \\ \frac{\Lambda_R(\Lambda_R^3-2\Lambda_R^3\delta^3+\delta^9)}{\delta^3(\Lambda_R^3-2\Lambda_R^3\delta^3+\gamma^3\delta^6)} \end{bmatrix}.
\end{aligned} \tag{152}$$

735 We can drastically simplify these expressions by making a simple observation, specifically, that
736 the unique solutions for the spectral parameters ξ and ζ and, therefore, eigenvalue paramete-
737 rs Λ_L and Λ_R are independent of the conditional probabilities α and γ , that is, they explicitly
738 depend on β and δ . Consequently, we can, for simplicity and without loss of significant gen-
739 erality, set $\alpha = \beta$ and $\gamma = \delta$ to obtain the following expressions for the left boundary vectors,

$$\begin{aligned}
\langle l_0| &= \left[1 \quad \frac{1-\beta^3}{\beta^4\delta^2} \quad \frac{1-\beta^3\delta^3}{\beta^2\delta} \quad \frac{\delta}{\beta} \right], \\
\langle l_1| &= \left[\frac{1-\beta^3}{\beta^3} \quad \frac{1-\delta^3}{\beta\delta^2} \quad \frac{\beta^5}{\delta^2} \quad 0 \right],
\end{aligned} \tag{153}$$

740

$$\begin{aligned}
\langle l_{00} | &= \left[\frac{\delta}{\beta} \quad \frac{1-\beta^3}{\beta^5 \delta} \quad \frac{1-\delta^3}{\beta^3 \delta^3} \quad \frac{1-\beta^3 \delta^3}{\beta^2 \delta} \right], \\
\langle l_{01} | &= \left[\frac{1-\beta^3}{\beta^4 \delta^2} \quad \frac{1-\delta^3}{\beta^2 \delta^4} \quad 1 \quad 0 \right], \\
\langle l_{10} | &= \left[\frac{1-\delta^3}{\beta \delta^2} \quad \frac{(1-\beta^3)(1-\delta^3)}{\beta^5 \delta^4} \quad \frac{1-\beta^3}{\beta^3} \quad \beta \delta^2 \right], \\
\langle l_{11} | &= [0 \quad 0 \quad 0 \quad 0],
\end{aligned} \tag{154}$$

741 and simplified right boundary vectors,

$$\begin{aligned}
|r_{00}\rangle &= \begin{bmatrix} \frac{1}{\beta^2 \delta} \\ 1 \\ 0 \\ 0 \end{bmatrix}, & |r_{01}\rangle &= \begin{bmatrix} 0 \\ 0 \\ \frac{1}{\beta \delta^2} \\ 0 \end{bmatrix}, \\
|r_{10}\rangle &= \begin{bmatrix} 0 \\ 0 \\ 0 \\ \frac{1}{\beta^3 \delta^3} \end{bmatrix}, & |r_{11}\rangle &= \begin{bmatrix} 0 \\ 0 \\ 0 \\ 0 \end{bmatrix},
\end{aligned} \tag{155}$$

742

$$|r_0\rangle = \begin{bmatrix} 1 \\ \beta^2 \delta \\ \frac{\beta}{\delta} \\ 0 \end{bmatrix}, \quad |r_1\rangle = \begin{bmatrix} 0 \\ 0 \\ 0 \\ \frac{1}{\beta \delta^2} \end{bmatrix}, \tag{156}$$

743 where we have additionally set Λ_L and Λ_R according to Eq. (61).744 **B.2 Inhomogeneous steady state**

745 As was done for the NESS, we present here the boundary vectors that resolve the inhomogeneous boundary relations in Eq. (92). For the left boundary,

746

$$\begin{aligned}
\langle l_0^{(1)} | &= \left[1 \quad \frac{\Lambda_L^2(1-\beta^3)}{\beta^6} \frac{1}{\eta^{(2)}} \quad \frac{\Lambda_L^3 - \alpha^3 \beta^3}{\Lambda_L^2 \beta^3} \quad \frac{1}{\Lambda_L} \right], \\
\langle l_1^{(1)} | &= \left[\frac{1-\beta^3}{\beta^3} \quad \frac{\Lambda_L^3 - \beta^3}{\Lambda_L \beta^3} \frac{1}{\eta^{(2)}} \quad \frac{\alpha^3}{\Lambda_L^2} \quad 0 \right],
\end{aligned} \tag{157}$$

747

$$\begin{aligned}
\langle l_{00}^{(1,2)} | &= \left[\frac{1}{\Lambda_L} \quad \frac{\Lambda_L(1-\beta^3)}{\beta^6} \eta^{(1)} \eta^{(3)} \quad \frac{\Lambda_L^3 - \beta^3}{\beta^6} \quad \frac{\Lambda_L^3 - \alpha^3 \beta^3}{\Lambda_L^2 \beta^3} \eta^{(1)} \right], \\
\langle l_{01}^{(1,2)} | &= \left[\frac{\Lambda_L^2(1-\beta^3)}{\beta^6} \quad \frac{\Lambda_L^3(\Lambda_L^3 - \beta^3)}{\beta^6} \eta^{(1)} \eta^{(3)} \quad 1 \quad 0 \right], \\
\langle l_{10}^{(1,2)} | &= \left[\frac{\Lambda_L^3 - \beta^3}{\Lambda_L \beta^3} \frac{1}{\eta^{(1)}} \quad \frac{\Lambda_L(\Lambda_L^3 - \beta^3)(1-\beta^3)}{\beta^9} \eta^{(3)} \quad \frac{1-\beta^3}{\beta^3} \frac{1}{\eta^{(1)}} \quad \frac{\alpha^3}{\Lambda_L^2} \right], \\
\langle l_{11}^{(1,2)} | &= [0 \quad 0 \quad 0 \quad 0].
\end{aligned} \tag{158}$$

748 Similarly, for the right boundary,

$$\begin{aligned}
 |r_{00}^{(2L-2,2L)}\rangle &= \begin{bmatrix} \frac{\Lambda_R^2((\Lambda_R^3-2\Lambda_R^3\delta^3+\chi^3\gamma^3\delta^6)+\chi^3\delta^3(\delta^3-\gamma^3))}{\chi\delta^3(\Lambda_R^3-2\Lambda_R^3\delta^3+\chi^3\gamma^3\delta^6)}\chi_1^{(2L+1)} \\ \chi\chi_1^{(2L+1)} \\ 0 \\ 0 \end{bmatrix}, \\
 |r_{01}^{(2L-2,2L)}\rangle &= \begin{bmatrix} -\frac{\Lambda_R^2\chi^2(1-\delta^3)(\delta^3-\gamma^3)}{(\Lambda_R^3-2\Lambda_R^3\delta^3+\chi^3\gamma^3\delta^6)}\chi_1^{(2L+1)} \\ \frac{\delta^6(\delta^3-\gamma^3)}{(\Lambda_R^3-2\Lambda_R^3\delta^3+\chi^3\gamma^3\delta^6)}\chi_1^{(2L+1)}\eta^{(2L)} \\ \frac{\Lambda_R(\Lambda_R^3-2\Lambda_R^3\delta^3+\chi^3\delta^9)}{\delta^3(\Lambda_R^3-2\Lambda_R^3\delta^3+\chi^3\gamma^3\delta^6)}\chi_1^{(2L+1)}\prod_{x=1}^L\eta^{(2x)} \\ 0 \end{bmatrix}, \\
 |r_{10}^{(2L-2,2L)}\rangle &= \begin{bmatrix} 0 \\ 0 \\ 0 \\ \frac{\Lambda_R^3(\Lambda_R^3-2\Lambda_R^3\delta^3+\chi^3\delta^9)}{\chi^2\delta^6(\Lambda_R^3-2\Lambda_R^3\delta^3+\chi^3\gamma^3\delta^6)}\chi_1^{(2L+1)} \end{bmatrix}, \\
 |r_{11}^{(2L-2,2L)}\rangle &= \begin{bmatrix} 0 \\ 0 \\ 0 \\ 0 \end{bmatrix},
 \end{aligned} \tag{159}$$

749

$$\begin{aligned}
 |r_0^{(2L)}\rangle &= \begin{bmatrix} 1 \\ \frac{\chi^2\delta^3((\Lambda_R^3-2\Lambda_R^3\delta^3+\chi^3\gamma^3\delta^6)(\Lambda_R^6-2\Lambda_R^3\chi^3\delta^3+\chi^6\delta^9)+\Lambda_R^3\chi^3\delta^3(\delta^3-\gamma^3)(\Lambda_R^3-\chi^3\delta^3-\chi^3\delta^6))}{\Lambda_R^2(\Lambda_R^3-2\Lambda_R^3\delta^3+\chi^3\gamma^3\delta^6)(\Lambda_R^6-2\Lambda_R^3\chi^3\delta^3+\chi^6\delta^9)} \\ \frac{\chi(\Lambda_R^3-2\Lambda_R^3\delta^3+\chi^3\delta^9)(\Lambda_R^6-2\Lambda_R^3\chi^3\delta^3+\chi^6\gamma^3\delta^6)}{\Lambda_R(\Lambda_R^3-2\Lambda_R^3\delta^3+\chi^3\gamma^3\delta^6)(\Lambda_R^6-2\Lambda_R^3\chi^3\delta^3+\chi^6\delta^9)}\prod_{x=1}^L\frac{1}{\eta^{(2x-1)}} \\ 0 \end{bmatrix}, \\
 |r_1^{(2L)}\rangle &= \begin{bmatrix} \frac{\chi^3\delta^6(\delta^3-\gamma^3)}{\Lambda_R^3-2\Lambda_R^3\delta^3+\chi^3\gamma^3\delta^6} \\ \frac{\chi^5\delta^6(\delta^3-\gamma^3)(\delta^3(\Lambda_R^6-2\Lambda_R^3\chi^3\delta^3+\chi^6\delta^9)-\Lambda_R^3(\Lambda_R^3-\chi^3\delta^3-\chi^3\delta^6))}{\Lambda_R^2(\Lambda_R^3-2\Lambda_R^3\delta^3+\chi^3\gamma^3\delta^6)(\Lambda_R^6-2\Lambda_R^3\chi^3\delta^3+\chi^6\delta^9)} \\ \frac{\chi^7\delta^6(\delta^3-\gamma^3)(\Lambda_R^3-2\Lambda_R^3\delta^3+\chi^3\delta^9)}{\Lambda_R(\Lambda_R^3-2\Lambda_R^3\delta^3-\chi^3\gamma^3\delta^6)(\Lambda_R^6-2\Lambda_R^3\chi^3\delta^3+\chi^6\delta^9)}\prod_{x=1}^L\frac{1}{\eta^{(2x-1)}} \\ \frac{\Lambda_R(\Lambda_R^3-2\Lambda_R^3\delta^3+\chi^3\delta^9)}{\delta^3(\Lambda_R^3-2\Lambda_R^3\delta^3+\chi^3\gamma^3\delta^6)} \end{bmatrix}.
 \end{aligned} \tag{160}$$

750 For the simple case introduced for the NESS, where we set $\gamma = \delta$ and $\alpha = \beta$ and fix Λ_L and
 751 Λ_R as in Eq. (130), we have for the left boundary vectors,

$$\begin{aligned}
 \langle l_0^{(1)}| &= \left[1 \quad \frac{1-\beta^3}{\beta^4\delta^2}\frac{1}{\eta^{(2)}} \quad \frac{1-\beta^3\delta^3}{\beta^2\delta} \quad \frac{\delta}{\beta} \right], \\
 \langle l_1^{(1)}| &= \left[\frac{1-\beta^3}{\beta^3} \quad \frac{1-\delta^3}{\beta\delta^2}\frac{1}{\eta^{(2)}} \quad \beta\delta^2 \quad 0 \right],
 \end{aligned} \tag{161}$$

752

$$\begin{aligned}
 \langle l_{00}^{(1,2)}| &= \left[\frac{\delta}{\beta} \quad \frac{1-\beta^3}{\beta^5\delta}\eta^{(1)}\eta^{(3)} \quad \frac{1-\delta^3}{\beta^3\delta^3} \quad \frac{1-\beta^3\delta^3}{\beta^2\delta}\eta^{(1)} \right], \\
 \langle l_{01}^{(1,2)}| &= \left[\frac{1-\beta^3}{\beta^4\delta^2} \quad \frac{1-\delta^3}{\delta^6}\eta^{(1)}\eta^{(3)} \quad 1 \quad 0 \right], \\
 \langle l_{10}^{(1,2)}| &= \left[\frac{1-\delta^3}{\beta\delta^2}\frac{1}{\eta^{(1)}} \quad \frac{(1-\beta^3)(1-\delta^3)}{\beta^5\delta^4}\eta^{(3)} \quad \frac{1-\beta^3}{\beta^3}\frac{1}{\eta^{(1)}} \quad \beta\delta^2 \right], \\
 \langle l_{11}^{(1,2)}| &= [0 \quad 0 \quad 0 \quad 0],
 \end{aligned} \tag{162}$$

753 and, likewise, for the right boundary vectors,

$$\begin{aligned}
 |r_{00}^{(2L-2,2L)}\rangle &= \begin{bmatrix} \frac{\chi}{\beta^2\delta} x_1^{(2L+1)} \\ \chi x_1^{(2L+1)} \\ 0 \\ 0 \end{bmatrix}, & |r_{01}^{(2L-2,2L)}\rangle &= \begin{bmatrix} 0 \\ 0 \\ \frac{1}{\beta\delta^2} x_1^{(2L+1)} \prod_{x=1}^L \eta^{(2x)} \\ 0 \end{bmatrix}, \\
 |r_{10}^{(2L-2,2L)}\rangle &= \begin{bmatrix} 0 \\ 0 \\ 0 \\ \frac{\chi}{\beta^3\delta^3} x_1^{(2L+1)} \end{bmatrix}, & |r_{11}^{(2L-2,2L)}\rangle &= \begin{bmatrix} 0 \\ 0 \\ 0 \\ 0 \end{bmatrix},
 \end{aligned} \tag{163}$$

754

$$|r_0^{(2L)}\rangle = \begin{bmatrix} 1 \\ \beta^2\delta \\ \frac{\beta}{\delta} \prod_{x=1}^L \frac{1}{\eta^{(2x-1)}} \\ 0 \end{bmatrix}, \quad |r_1^{(2L)}\rangle = \begin{bmatrix} 0 \\ 0 \\ 0 \\ \frac{\chi}{\beta\delta^2} \end{bmatrix}. \tag{164}$$

755

756 References

- 757 [1] B. Derrida, E. Domany and D. Mukamel, *An exact solution of a one-dimensional*
 758 *asymmetric exclusion model with open boundaries*, J. Stat. Phys. **69**, 667 (1992),
 759 doi:[10.1007/BF01050430](https://doi.org/10.1007/BF01050430).
- 760 [2] B. Derrida, M. R. Evans, V. Hakim and V. Pasquier, *Exact solution of a 1D asymmet-*
 761 *ric exclusion model using a matrix formulation*, J. Phys.: Math. Gen. **26**, 1493 (1993),
 762 doi:[10.1088/0305-4470/26/7/011](https://doi.org/10.1088/0305-4470/26/7/011).
- 763 [3] B. Derrida, S. A. Janowsky, J. L. Lebowitz and E. R. Speer, *Exact solution of the to-*
 764 *tally asymmetric simple exclusion process: shock profiles*, J. Stat. Phys. **73**, 813 (1993),
 765 doi:[10.1007/BF01052811](https://doi.org/10.1007/BF01052811).
- 766 [4] B. Derrida, M. R. Evans and D. Mukamel, *Exact diffusion constant for one-dimensional*
 767 *asymmetric exclusion models*, J. Phys. A: Math. Gen. **26**, 4911 (1993), doi:[10.1088/0305-](https://doi.org/10.1088/0305-4470/26/19/023)
 768 [4470/26/19/023](https://doi.org/10.1088/0305-4470/26/19/023).
- 769 [5] B. Derrida, *An exactly soluble non-equilibrium system: the asymmetric simple exclusion*
 770 *process*, Phys. Rep. **301**, 65 (1998), doi:[10.1016/S0370-1573\(98\)00006-4](https://doi.org/10.1016/S0370-1573(98)00006-4).
- 771 [6] B. Derrida and J. L. Lebowitz, *Exact large deviation function in the asymmetric exclusion*
 772 *process*, Phys. Rev. Lett. **80**, 209 (1998), doi:[10.1103/PhysRevLett.80.209](https://doi.org/10.1103/PhysRevLett.80.209).
- 773 [7] G. M. Schütz and E. Domany, *Phase transitions in an exactly soluble one-dimensional*
 774 *exclusion process*, J. Stat. Phys. **72**, 277 (1993), doi:[10.1007/BF01048050](https://doi.org/10.1007/BF01048050).
- 775 [8] G. M. Schütz, *Exact solution of the master equation for the asymmetric exclusion process*,
 776 J. Stat. Phys. **88**, 427 (1997), doi:[10.1007/BF02508478](https://doi.org/10.1007/BF02508478).
- 777 [9] J. de Gier and F. H. L. Essler, *Bethe ansatz solution of the asymmetric exclusion*
 778 *process with open boundaries*, Phys. Rev. Lett. **95**, 240601 (2005),
 779 doi:[10.1103/PhysRevLett.95.240601](https://doi.org/10.1103/PhysRevLett.95.240601).

- 780 [10] J. de Gier and F. H. L. Essler, *Exact spectral gaps of the asymmetric exclusion process with*
781 *open boundaries*, J. Stat. Mech.: Theory Exp. **2006**, P12011 (2006), doi:[10.1088/1742-](https://doi.org/10.1088/1742-5468/2006/12/p12011)
782 [5468/2006/12/p12011](https://doi.org/10.1088/1742-5468/2006/12/p12011).
- 783 [11] M. E. Fisher, *Statistical mechanics of dimers on a plane lattice*, Phys. Rev. **124**, 1664
784 (1961), doi:[10.1103/PhysRev.124.1664](https://doi.org/10.1103/PhysRev.124.1664).
- 785 [12] L. Balents, *Spin liquids in frustrated magnets*, Nature **464**, 199 (2010),
786 doi:[10.1038/nature08917](https://doi.org/10.1038/nature08917).
- 787 [13] R. Moessner and K. S. Raman, *Quantum Dimer Models*, In C. Lacroix, P. Mendels and
788 F. Mila, eds., *Introduction to Frustrated Magnetism: Materials, Experiments, Theory*, vol.
789 164 of *Springer Series in Solid-State Sciences*, chap. 17, pp. 437–479. Springer, Berlin,
790 doi:[10.1007/978-3-642-10589-0_17](https://doi.org/10.1007/978-3-642-10589-0_17) (2011).
- 791 [14] R. G. Palmer, D. L. Stein, E. Abrahams and P. W. Anderson, *Models of hierarchi-*
792 *cally constrained dynamics for glassy relaxation*, Phys. Rev. Lett. **53**, 958 (1984),
793 doi:[10.1103/PhysRevLett.53.958](https://doi.org/10.1103/PhysRevLett.53.958).
- 794 [15] J. Jäckle, *Models of the glass transition*, Rep. Prog. Phys. **49**, 171 (1986),
795 doi:[10.1088/0034-4885/49/2/002](https://doi.org/10.1088/0034-4885/49/2/002).
- 796 [16] G. H. Fredrickson, *Recent developments in dynamical theories of the liquid-glass transition*,
797 Ann. Rev. Phys. Chem. **39**, 149 (1988), doi:[10.1146/annurev.pc.39.100188.001053](https://doi.org/10.1146/annurev.pc.39.100188.001053).
- 798 [17] J. Jäckle and S. Eisinger, *A hierarchically constrained kinetic Ising model*, Z. Physik B
799 Cond. Matt. **84**, 115 (1991), doi:[10.1007/BF01453764](https://doi.org/10.1007/BF01453764).
- 800 [18] S. Eisinger and J. Jäckle, *Analytical approximations for the hierarchically constrained*
801 *kinetic Ising chain*, J. Stat. Phys. **73**, 643 (1993), doi:[10.1007/BF01054344](https://doi.org/10.1007/BF01054344).
- 802 [19] R. L. Jack, J. P. Garrahan and D. Chandler, *Space-time thermodynamics and subsystem*
803 *observables in a kinetically constrained model of glassy materials*, J. Chem. Phys. **125**,
804 184509 (2006), doi:[10.1063/1.2374885](https://doi.org/10.1063/1.2374885).
- 805 [20] I. Lesanovsky and J. P. Garrahan, *Kinetic constraints, hierarchical relaxation, and onset*
806 *of glassiness in strongly interacting and dissipative Rydberg gases*, Phys. Rev. Lett. **111**,
807 215305 (2013), doi:[10.1103/PhysRevLett.111.215305](https://doi.org/10.1103/PhysRevLett.111.215305).
- 808 [21] M. C. Bañuls and J. P. Garrahan, *Using matrix product states to study the dynamical*
809 *large deviations of kinetically constrained models*, Phys. Rev. Lett. **123**, 200601 (2019),
810 doi:[10.1103/PhysRevLett.123.200601](https://doi.org/10.1103/PhysRevLett.123.200601).
- 811 [22] F. Ritort and P. Sollich, *Glassy dynamics of kinetically constrained models*, Adv. Phys. **52**,
812 219 (2003), doi:[10.1080/0001873031000093582](https://doi.org/10.1080/0001873031000093582).
- 813 [23] J. P. Garrahan, P. Sollich and C. Toninelli, *Kinetically Constrained Models*, In L. Berthier,
814 G. Biroli, J.-P. Bouchaud, L. Cipelletti and W. van Saarloos, eds., *Dynamical Heterogeneities*
815 *in Glasses, Colloids, and Granular Media*, International Series of Monographs on Physics,
816 chap. 10, pp. 341–366. Oxford University Press (2011).
- 817 [24] J. P. Garrahan, *Aspects of non-equilibrium in classical and quantum systems: slow relaxation*
818 *and glasses, dynamical large deviations, quantum no-ergodicity, and open quantum dynam-*
819 *ics*, Physica A: Stat. Mech. Appl. **504**, 130 (2018), doi:[10.1016/j.physa.2017.12.149](https://doi.org/10.1016/j.physa.2017.12.149).

- 820 [25] G. Biroli and J. P. Garrahan, *Perspective: the glass transition*, J. Chem. Phys. **138**, 12A301
821 (2013), doi:[10.1063/1.4795539](https://doi.org/10.1063/1.4795539).
- 822 [26] C. J. Turner, A. A. Michailidis, D. A. Abanin, M. Serbyn and Z. Papić, *Weak er-*
823 *godicity breaking from quantum many-body scars*, Nature Physics **14**, 745 (2018),
824 doi:[10.1038/s41567-018-0137-5](https://doi.org/10.1038/s41567-018-0137-5).
- 825 [27] C. J. Turner, A. A. Michailidis, D. A. Abanin, M. Serbyn and Z. Papić, *Quan-*
826 *tum scarred eigenstates in a Rydberg atom chain: entanglement, breakdown of ther-*
827 *malization, and stability to perturbations*, Phys. Rev. B **98**, 155134 (2018),
828 doi:[10.1103/PhysRevB.98.155134](https://doi.org/10.1103/PhysRevB.98.155134).
- 829 [28] W. W. Ho, S. Choi, H. Pichler and M. D. Lukin, *Periodic orbits, entanglement, and quantum*
830 *many-body scars in constrained models: matrix product state approach*, Phys. Rev. Lett.
831 **122**, 040603 (2019), doi:[10.1103/PhysRevLett.122.040603](https://doi.org/10.1103/PhysRevLett.122.040603).
- 832 [29] M. van Horssen, E. Levi and J. P. Garrahan, *Dynamics of many-body localization*
833 *in a translation-invariant quantum glass model*, Phys. Rev. B **92**, 100305 (2015),
834 doi:[10.1103/PhysRevB.92.100305](https://doi.org/10.1103/PhysRevB.92.100305).
- 835 [30] Z. Lan, M. van Horssen, S. Powell and J. P. Garrahan, *Quantum slow relaxation*
836 *and metastability due to dynamical constraints*, Phys. Rev. Lett. **121**, 040603 (2018),
837 doi:[10.1103/PhysRevLett.121.040603](https://doi.org/10.1103/PhysRevLett.121.040603).
- 838 [31] N. Pancotti, G. Giudice, J. I. Cirac, J. P. Garrahan and M. C. Bañuls, *Quantum East model:*
839 *localization, nonthermal eigenstates, and slow dynamics*, Phys. Rev. X **10**, 021051 (2020),
840 doi:[10.1103/PhysRevX.10.021051](https://doi.org/10.1103/PhysRevX.10.021051).
- 841 [32] J. G. Bohnet, B. C. Sawyer, J. W. Britton, M. L. Wall, A. M. Rey, M. Foss-Feig and J. J.
842 Bollinger, *Quantum spin dynamics and entanglement generation with hundreds of trapped*
843 *ions*, Science **352**, 1297 (2016), doi:[10.1126/science.aad9958](https://doi.org/10.1126/science.aad9958).
- 844 [33] A. Nahum, J. Ruhman, S. Vijay and J. Haah, *Quantum entanglement growth under random*
845 *unitary dynamics*, Phys. Rev. X **7**, 031016 (2017), doi:[10.1103/PhysRevX.7.031016](https://doi.org/10.1103/PhysRevX.7.031016).
- 846 [34] C. W. von Keyserlingk, T. Rakovszky, F. Pollman and S. L. Sondhi, *Operator hydrodynam-*
847 *ics, OTOCs, and entanglement growth in systems with conservation laws*, Phys. Rev. X **8**,
848 021013 (2018), doi:[10.1103/PhysRevX.8.021013](https://doi.org/10.1103/PhysRevX.8.021013).
- 849 [35] S. Gopalakrishnan, *Operator growth and eigenstate entanglement in an*
850 *interacting integrable Floquet system*, Phys. Rev. B **98**, 060302 (2018),
851 doi:[10.1103/PhysRevB.98.060302](https://doi.org/10.1103/PhysRevB.98.060302).
- 852 [36] R. Kubo, *Statistical-mechanical theory of irreversible processes. I. General theory and simple*
853 *applications to magnetic and conduction problems*, J. Phys. Soc. Jap. **12**, 570 (1957),
854 doi:[10.1143/JPSJ.12.570](https://doi.org/10.1143/JPSJ.12.570).
- 855 [37] M. Toda, R. Kubo and N. Saitô, *Statistical Physics I: Equilibrium Statistical Mechanics*,
856 Springer, 2 edn. (2012).
- 857 [38] R. Kubo, M. Toda and N. Hashitsume, *Statistical Physics II: Nonequilibrium Statistical*
858 *Mechanics*, Springer, 2 edn. (2012).
- 859 [39] G. Gallavotti and E. G. D. Cohen, *Dynamical ensembles in nonequilibrium statistical me-*
860 *chanics*, Phys. Rev. Lett. **74**, 2694 (1995), doi:[10.1103/PhysRevLett.74.2694](https://doi.org/10.1103/PhysRevLett.74.2694).

- 861 [40] R. S. Ellis, *An overview of the theory of large deviations and applications to statistical*
862 *mechanics*, Scand. Actuar. J. **1995**, 97 (1995), doi:[10.1080/03461238.1995.10413952](https://doi.org/10.1080/03461238.1995.10413952).
- 863 [41] J. P. Garrahan, R. L. Jack, V. Lecomte, E. Pitard, K. van Duijvendijk and F. van Wijland,
864 *Dynamical first-order phase transition in kinetically constrained models of glasses*, Phys.
865 Rev. Lett. **98**, 195702 (2007), doi:[10.1103/PhysRevLett.98.195702](https://doi.org/10.1103/PhysRevLett.98.195702).
- 866 [42] H. Touchette, *The large deviation approach to statistical mechanics*, Phys. Rep. **478**, 1
867 (2009), doi:[10.1016/j.physrep.2009.05.002](https://doi.org/10.1016/j.physrep.2009.05.002).
- 868 [43] R. J. Baxter, *Exactly Solved Models in Statistical Mechanics*, Elsevier (1989).
- 869 [44] M. Takahashi, *Thermodynamics of One-Dimensional Solvable Models*, Cambridge Univer-
870 sity Press (1999).
- 871 [45] J. de Gier and F. H. L. Essler, *Large deviation function for the current in the*
872 *open asymmetric simple exclusion process*, Phys. Rev. Lett. **107**, 010602 (2011),
873 doi:[10.1103/PhysRevLett.107.010602](https://doi.org/10.1103/PhysRevLett.107.010602).
- 874 [46] M. Gorissen, A. Lazarescu, K. Mallick and C. Vanderzande, *Exact current statistics of the*
875 *asymmetric simple exclusion process with open boundaries*, Phys. Rev. Lett. **109**, 170601
876 (2012), doi:[10.1103/PhysRevLett.109.170601](https://doi.org/10.1103/PhysRevLett.109.170601).
- 877 [47] B. Buča, J. P. Garrahan, T. Prosen and M. Vanicat, *Exact large deviation statistics and*
878 *trajectory phase transition of a deterministic boundary driven cellular automaton*, Phys.
879 Rev. E **100**, 020103 (2019), doi:[10.1103/PhysRevE.100.020103](https://doi.org/10.1103/PhysRevE.100.020103).
- 880 [48] B. Buča, K. Klobas and T. Prosen, *Rule 54: exactly solvable model of nonequilibrium statis-*
881 *tical mechanics*, J. Stat. Mech.: Theory Exp. **2021**, 074001 (2021), doi:[10.1088/1742-](https://doi.org/10.1088/1742-5468/ac096b)
882 [5468/ac096b](https://doi.org/10.1088/1742-5468/ac096b).
- 883 [49] J. W. P. Wilkinson, T. Prosen and J. P. Garrahan, *Exact solution of the*
884 *“Rule 150” reversible cellular automaton*, Phys. Rev. E **105**, 034124 (2022),
885 doi:[10.1103/PhysRevE.105.034124](https://doi.org/10.1103/PhysRevE.105.034124).
- 886 [50] J. Myers, M. J. Bhaseen, R. J. Harris and B. Doyon, *Transport fluctua-*
887 *tions in integrable models out of equilibrium*, SciPost Phys. **8**, 007 (2020),
888 doi:[10.21468/SciPostPhys.8.1.007](https://doi.org/10.21468/SciPostPhys.8.1.007).
- 889 [51] G. Perfetto and B. Doyon, *Euler-scale dynamical fluctuations in non-equilibrium interacting*
890 *integrable systems*, SciPost Phys. **10**, 116 (2021), doi:[10.21468/SciPostPhys.10.5.116](https://doi.org/10.21468/SciPostPhys.10.5.116).
- 891 [52] T. Prosen and C. Mejía-Monasterio, *Integrability of a deterministic cellular automa-*
892 *ton driven by stochastic boundaries*, J. Phys. A: Math. Theor. **49**, 185003 (2016),
893 doi:[10.1088/1751-8113/49/18/185003](https://doi.org/10.1088/1751-8113/49/18/185003).
- 894 [53] T. Prosen and B. Buča, *Exact matrix product decay modes of a boundary driven cellular au-*
895 *tomaton*, J. Phys. A: Math. Theor. **50**, 395002 (2017), doi:[10.1088/1751-8121/aa85a3](https://doi.org/10.1088/1751-8121/aa85a3).
- 896 [54] A. Inoue and S. Takesue, *Two extensions of exact nonequilibrium steady states of a*
897 *boundary-driven cellular automaton*, J. Phys. A: Math. Theor. **51**, 425001 (2018),
898 doi:[10.1088/1751-8121/aadc29](https://doi.org/10.1088/1751-8121/aadc29).
- 899 [55] J. W. P. Wilkinson, K. Klobas, T. Prosen and J. P. Garrahan, *Exact solu-*
900 *tion of the Floquet-PXP cellular automaton*, Phys. Rev. E **102**, 062107 (2020),
901 doi:[10.1103/PhysRevE.102.062107](https://doi.org/10.1103/PhysRevE.102.062107).

- 902 [56] G. H. Fredrickson and H. C. Andersen, *Kinetic Ising model of the glass transition*, Phys.
903 Rev. Lett. **53**, 1244 (1984), doi:[10.1103/PhysRevLett.53.1244](https://doi.org/10.1103/PhysRevLett.53.1244).
- 904 [57] G. H. Fredrickson and H. C. Andersen, *Facilitated kinetic Ising models and the glass tran-*
905 *sition*, J. Chem. Phys. **83**, 5822 (1985), doi:[10.1063/1.449662](https://doi.org/10.1063/1.449662).
- 906 [58] T. Iadecola and S. Vijay, *Nonergodic quantum dynamics from deformations of classical cel-*
907 *lular automata*, Phys. Rev. B **102**, 180302 (2020), doi:[10.1103/PhysRevB.102.180302](https://doi.org/10.1103/PhysRevB.102.180302).
- 908 [59] L. Causer, I. Lesanovsky, M. C. Bañuls and J. P. Garrahan, *Dynamics and large deviation*
909 *transitions of the XOR-Fredrickson-Andersen kinetically constrained model*, Phys. Rev. E
910 **102**, 052132 (2020), doi:[10.1103/PhysRevE.102.052132](https://doi.org/10.1103/PhysRevE.102.052132).
- 911 [60] B. Olmos, R. González-Férez and I. Lesanovsky, *Collective Rydberg excitations*
912 *of an atomic gas confined in a ring lattice*, Phys. Rev. A **79**, 043419 (2009),
913 doi:[10.1103/PhysRevA.79.043419](https://doi.org/10.1103/PhysRevA.79.043419).
- 914 [61] I. Lesanovsky, *Many-body spin interactions and the ground state of a dense Rydberg lattice*
915 *gas*, Phys. Rev. Lett. **106**, 025301 (2011), doi:[10.1103/PhysRevLett.106.025301](https://doi.org/10.1103/PhysRevLett.106.025301).
- 916 [62] B. Olmos, R. González-Férez, I. Lesanovsky and L. Velázquez, *Universal time evolution of*
917 *a Rydberg lattice gas with perfect blockade*, J. Phys. A: Math. Theor. **45**, 325301 (2012),
918 doi:[10.1088/1751-8113/45/32/325301](https://doi.org/10.1088/1751-8113/45/32/325301).
- 919 [63] I. Lesanovsky and H. Katsure, *Interacting Fibonacci anyons in a Rydberg gas*, Phys. Rev.
920 A **86**, 041601 (2012), doi:[10.1103/PhysRevA.86.041601](https://doi.org/10.1103/PhysRevA.86.041601).
- 921 [64] C.-J. Lin and O. I. Motrunich, *Exact quantum many-body scar states in*
922 *the Rydberg-blockaded atom chain*, Phys. Rev. Lett. **122**, 173401 (2019),
923 doi:[10.1103/PhysRevLett.122.173401](https://doi.org/10.1103/PhysRevLett.122.173401).
- 924 [65] K. Bull, I. Martin and Z. Papić, *Systematic construction of scarred many-*
925 *body dynamics in 1D lattice models*, Phys. Rev. Lett. **123**, 030601 (2019),
926 doi:[10.1103/PhysRevLett.123.030601](https://doi.org/10.1103/PhysRevLett.123.030601).
- 927 [66] D. K. Mark, C.-J. Lin and O. I. Motrunich, *Exact eigenstates in the Lesanovsky model,*
928 *proximity to integrability and the PXP model, and approximate scar states*, Phys. Rev. B
929 **101**, 094308 (2020), doi:[10.1103/PhysRevB.101.094308](https://doi.org/10.1103/PhysRevB.101.094308).
- 930 [67] K. Bull, J.-Y. Desaulles and Z. Papić, *Quantum scars as embeddings of weakly*
931 *broken Lie algebra representations*, Phys. Rev. B **101**, 165139 (2020),
932 doi:[10.1103/PhysRevB.101.165139](https://doi.org/10.1103/PhysRevB.101.165139).
- 933 [68] B. Doyon, *Lecture notes on generalised hydrodynamics*, SciPost Phys. Lect. Notes p. 18
934 (2020), doi:[10.21468/SciPostPhysLectNotes.18](https://doi.org/10.21468/SciPostPhysLectNotes.18).
- 935 [69] H. Spohn, *Large Scale Dynamics of Interacting Particles*, Springer (1991).
- 936 [70] B. Doyon and H. Spohn, *Dynamics of hard rods with initial domain wall state*, J. Stat.
937 Mech.: Theor. Exp. **2017**, 073210 (2017), doi:[10.1088/1742-5468/aa7abf](https://doi.org/10.1088/1742-5468/aa7abf).
- 938 [71] B. Doyon, T. Yoshimura and J.-S. Caux, *Soliton gases and generalized hydrodynamics*,
939 Phys. Rev. Lett. **120**, 045301 (2018), doi:[10.1103/PhysRevLett.120.045301](https://doi.org/10.1103/PhysRevLett.120.045301).
- 940 [72] R. Serfozo, *Basics of Applied Stochastic Processes*, Springer, doi:[10.1007/978-3-540-](https://doi.org/10.1007/978-3-540-89332-5)
941 [89332-5](https://doi.org/10.1007/978-3-540-89332-5) (2009).

- 942 [73] P. W. Atkins, J. de Paula and J. Keeler, *Atkins' Physical Chemistry*, Oxford University Press,
943 11 edn. (2017).

Chapter 5

Conclusion

The main objective of this thesis was to generalize the mathematical methods and theoretical techniques used to study a simple model displaying interacting nonequilibrium many-body physics, specifically, the Rule 54 reversible cellular automaton (RCA54), to other similar, yet distinct, systems, with the ambitious goal of gaining insight towards a general theoretical framework for nonequilibrium statistical mechanics. In particular, we considered two reversible cellular automata, explicitly, the attractively interacting Rule 201 (RCA201) and the noninteracting Rule 150 (RCA150), which complement the extensively studied repulsively interacting RCA54.

The key motivation behind the investigation of these simple models is that they admit exact solutions, which derives from their integrability. Particularly, the models exhibit asymptotically freely propagating emergent excitations that interact via perfectly elastic factorized scattering. Consequently, the dynamics can be recast in terms of quasiparticles possessing solitonic degrees of freedom, implying the existence of an extensive number of local conserved charges. This insight is the cornerstone to the solvability of these models, as is demonstrated throughout the three publication-style chapters, which we now summarise.

In the first publication-style chapter, we studied the dynamics of RCA201 and informally established the integrability of the model by means of a precise physical derivation of its conserved charges. From the integrability, specifically, the quasiparticle interpretation of the dynamics, we obtained the exact analytic expressions for the steady states, for systems with closed and open boundaries, in terms of a generalization of the simple staggered matrix product ansatz used to solve RCA54. Moreover, we showed that, despite the additional complexities of the model, that is, the nontrivial topological vacuum and ergodicity-breaking invariant quantities, the family of steady states exhibited an instructive generalized Gibbs ensemble form, from which useful thermodynamics properties can be obtained, such as the partition function, which we exactly derive.

The study of interacting models is at the core of nonequilibrium statistical mechanics, however, valuable insight can also be acquired from noninteracting models, which are often easier to solve. In the second publication-style chapter, we do exactly this and explore the dynamical properties of the simple RCA150, whereby the motivation was to present a comprehensive review of the dynamics of the model, and provide a pedagogical introduction to this remarkably useful

and rapidly developing field. Due to the dynamical simplicity, arising from the noninteracting nature of the quasiparticles, we were able to obtain a significant number of exact results, mostly in terms of the versatile matrix product ansatz, including the steady states for closed and open systems, the complete spectra of the deterministic and stochastic propagators, therefore, facilitating the study of the full relaxation dynamics, and the large deviations statistics of extensive observables, which we showed exhibits a dynamical first order phase transition. We expect the results detailed in this manuscript [344] to be straightforwardly extendable and generalizable, thus, allowing many more results to be obtained exactly, including, but not limited to, those found for RCA54 [338].

Large deviations theory is an outstanding theoretical framework that has provided significant insight into the understanding of nonequilibrium statistical physics and, as such, is of the utmost importance in this thesis. Hence, in the third and final publication-style chapter we study the large deviation statistics of RCA201. Whilst we were able to explicitly construct an exact expression for the dominant eigenvalue, the analytic solution obtained was trivial and, hence, did not provide any insight into the atypical dynamical behaviour of the model. We proceeded to demonstrate that the simplicity of this result arose due to the limitations of the theoretical framework, specifically, the restricted support of the local tilting functions, which is upper bounded by the ultralocal interaction range of the time evolution operators. At the moment, it is not entirely obvious how to remedy this, however, a few potentially promising resolutions have been considered. Perhaps, the most obvious, is to construct a set of algebraic relations that are solved sequentially, from boundary to boundary, that would eliminate entirely the aforementioned support limitations and could potentially facilitate the development of novel methods for studying one-dimensional lattice models. Indeed, initial efforts towards progress in this direction are being made, which we hope to report on soon.

Arguably, the most prominent open question is whether the mathematical framework utilised throughout this work can be formulated for generic discrete one-dimensional lattice systems displaying similar emergent phenomena. From the work presented here, one might be inclined to think that the results appear to depend almost entirely on the particularities of the model, and that there is no clear intuition as to what exactly enables this solvability in general, however, we report this is not the case. Indeed, meaningful progress in this direction has recently been made. In Ref. [331] an algebraic framework was proposed, which generalized known methods from integrability and interacting lattice systems, to study spin chains and cellular automata with “medium range” interactions. They demonstrated that the two families of models were intimately related via Trotterization, specifically of the spin chain Hamiltonian to obtain the cellular automata propagator, and further proved that RCA150 is indeed Yang-Baxter integrable with three site interactions. However, they were unable to prove the integrability of RCA54 and RCA201, but suggested that Hamiltonians with larger interaction ranges could prove beneficial to investigate. This insight was later confirmed in Ref. [346], where the Yang-Baxter integrability of RCA54 was proven using a generalization of the Hamiltonian deformation with six-site interactions originally introduced in Ref. [329]. Furthermore, we expect to publish promising research on this topic soon generalizing many of the

results obtained for RCA54, including the Bethe ansatz integrability [329] and generalized hydrodynamics [278], in addition to a collection of new results, such as the exact periodic spectral and large deviations statistics of RCA.

This potentially valid theoretical framework for studying one-dimensional RCA immediately grants us many interesting directions for future research. Of particular note are the extensions of the matrix product ansatz used to obtain other exact results for the classical model, such as those of RCA54 outlined in Ref. [334]. Perhaps a more ambitious, yet rewarding, prospect would be to try extend these generalizations to the quantum versions of the models, where the bits at the sites of the lattice are replaced by *qubits*, such that the state space and time evolution are governed by quantum mechanics. This would provide an ideal platform to study problems relating to the complexity of the dynamics of quantum nonequilibrium systems, including entanglement growth [320, 323, 324], atypical thermalization [220, 312, 313], and many-body localization [158, 347].

Bibliography

- [1] E. H. von Zeipel, [Mon. Not. R. Astron. Soc.](#) **84**, 665 (1924).
- [2] A. Boulares and D. P. Cox, [Astrophys. J.](#) **365**, 544 (1990).
- [3] V. Biffi, S. Borgani, G. Murante, E. Rasia, S. Planelles, G. L. Granato, C. Ragone-Figueroa, A. M. Beck, M. Gaspari, and K. Dolag, [Astrophys. J.](#) **827**, 112 (2016).
- [4] B. Cannon, Walter, [Physiol. Rev.](#) **9**, 399 (1929).
- [5] H. Levene, [Am. Nat.](#) **87**, 331 (1953).
- [6] D. Thiessen and B. Gregg, [Ethol. Sociobiol.](#) **1**, 111 (1980).
- [7] C. J. G. Gersick, [Acad. Manag. Rev.](#) **16**, 10 (1991).
- [8] P. Bak and K. Sneppen, [Phys. Rev. Lett.](#) **71**, 4083 (1993).
- [9] W. B. White, S. M. Johnson, and G. B. Dantzig, [J. Chem. Phys.](#) **28**, 751 (1958).
- [10] K. G. Denbigh, *The Principles of Chemical Equilibrium*, 4th ed. (Cambridge University Press, 1981).
- [11] P. W. Atkins, J. de Paula, and J. Keeler, *Atkins' Physical Chemistry*, 11th ed. (Oxford University Press, 2017).
- [12] R. J. Silbey, R. A. Alberty, M. G. Bawendi, and G. A. Papadantonakis, *Physical Chemistry*, 5th ed. (Wiley, 2021).
- [13] J. von Neumann, [Rev. Econ. Stud.](#) **13**, 1 (1945).
- [14] G. Debreu, *Theory of Value: An Axiomatic Analysis of Economic Equilibrium*, 4th ed. (Yale University Press, 1977).
- [15] K. J. Arrow, [Am. Econ. Rev.](#) **64**, 253 (1974).
- [16] A. Mas-Colell, *The Theory of General Economic Equilibrium: A Differentiable Approach*, 2nd ed. (Cambridge University Press, 1990).
- [17] H. R. Varian, *Microeconomic Analysis*, 3rd ed. (W. W. Norton & Company, 1992).
- [18] J. T. Hack, [Am. J. Sci.](#) **258-A**, 80 (1960).

- [19] F. S. Spear, *Metamorphic Phase Equilibria and Pressure-Temperature-Time Paths*, 2nd ed. (Mineralogical Society of America, 1994).
- [20] D. Knighton, *Fluvial Forms and Processes: A New Perspective*, 2nd ed. (Routledge, 1998).
- [21] J. F. Nash, *Proc. Natl. Acad. Sci.* **36**, 48 (1950).
- [22] J. F. Nash, *Ann. Math.* **54**, 286 (1951).
- [23] R. J. Aumann, *J. Math. Econ.* **1**, 67 (1974).
- [24] R. J. Aumann, *Econometrica* **55**, 1 (1987).
- [25] J. von Neumann and O. Morgenstern, *Theory of Games and Economic Behaviour*, anniv. ed. (Princeton University Press, 2007).
- [26] N. Daniels, *J. Philos.* **76**, 256 (1979).
- [27] N. Daniels, *Justice and Justification: Reflective Equilibrium in Theory and Practice*, new ed. (Cambridge University Press, 2008).
- [28] R. Cummins, in *Rethinking Intuition: The Psychology of Intuition and its Role in Philosophical Inquiry*, edited by M. R. DePaul and W. Ramsey (Rowman & Littlefield Publishers, Inc, 1998) Chap. 7, pp. 113–127.
- [29] G. H. Kramer, *J. Econ. Theory* **16**, 310 (1977).
- [30] A. Lindbeck and J. W. Weibull, *J. Public Econ.* **51**, 195 (1993).
- [31] R. Perotti, *Rev. Econ. Stud.* **60**, 755 (1993).
- [32] G. Debreu, *Proc. Natl. Acad. Sci.* **38**, 886 (1952).
- [33] I. Gilboa and A. Matsui, *Econometrica* **59**, 859 (1991).
- [34] C. Kittel and H. Kroemer, *Thermal Physics*, 2nd ed. (W. H. Freeman, 1980).
- [35] R. K. Pathria and P. D. Beale, *Statistical Mechanics*, 4th ed. (Academic Press, 2021).
- [36] D. V. Schroeder, *An Introduction to Thermal Physics*, 2nd ed. (Oxford University Press, 2021).
- [37] F. Schwabl, *Statistical Mechanics*, 2nd ed. (Springer, 2006).
- [38] R. C. Tolman, *The Principles of Statistical Mechanics*, new ed. (Dover Publications Inc., 2003).
- [39] F. Reif, *Fundamentals of Statistical and Thermal Physics*, new ed. (Waveland Press, Inc., 2009).
- [40] E. T. Jaynes, *Phys. Rev.* **106**, 620 (1957).

- [41] E. T. Jaynes, *Phys. Rev.* **108**, 171 (1957).
- [42] V. Vedral, *Rev. Mod. Phys.* **74**, 197 (2002).
- [43] F. Troiani and M. Affronte, *Chem. Soc. Rev.* **40**, 3119 (2011).
- [44] J. Goold, M. Huber, A. Riera, L. del Rio, and P. Skrzypczyk, *J. Phys. A: Math. Theor.* **49**, 143001 (2016).
- [45] R. C. Tolman, *Proc. Natl. Acad. Sci.* **11**, 436 (1925).
- [46] G. N. Lewis, *Proc. Natl. Acad. Sci.* **11**, 179 (1925).
- [47] G. E. Crooks, *J. Stat. Mech.: Theory Exp.* **2011**, P07008.
- [48] E. H. Lieb and J. Yngvason, *Phys. Today* **53**, 32 (2000).
- [49] J. J. Loschmidt, *Wien. Ber.* **73**, 128 (1876).
- [50] L. Boltzmann, *Lectures on Gas Theory* (J. A. Barth, 1896).
- [51] F. Spitzer, *Adv. Math.* **5**, 246 (1970).
- [52] T. M. Liggett, *Interacting Particle Systems*, Classics in Mathematics (Springer, New York, USA, 1985).
- [53] H. Spohn, *Large Scale Dynamics of Interacting Particles* (Springer, 1991).
- [54] N. Singh, *Mod. Phys. Lett. B* **27**, 1330003 (2013).
- [55] A. V. Andreev, O. Agam, B. D. Simons, and B. L. Altshuler, *Phys. Rev. Lett.* **76**, 3947 (1996).
- [56] L. D'Alessio, Y. Kafri, A. Polkovnikov, and M. Rigol, *Adv. Phys.* **65**, 239 (2016).
- [57] J. M. Deutsch, *Phys. Rev. B* **43**, 2046 (1991).
- [58] M. Srednicki, *Phys. Rev. E* **50**, 888 (1994).
- [59] M. Rigol, V. Dunjko, and M. Olshanii, *Nature* **452**, 854 (2008).
- [60] D. Bernoulli, *Hydrodynamica* (Johannis Reinholdi Dulseckeri, 1738).
- [61] L. Euler, *Mémoires de l'académie des sciences de Berlin* **11**, 274 (1757).
- [62] J. J.-B. Fourier, *Théorie Analytique de la Chaleur* (Firmin Didot, 1822).
- [63] J. C. Maxwell, *Theory of Heat* (Longmans, Green & Co., 1871).
- [64] J. W. Gibbs, *Am. J. Sci.* **16**, 441 (1878).
- [65] J. W. Gibbs, *Elementary Principles in Statistical Mechanics* (Charles Scribner's Sons, 1902).

-
- [66] M. Planck, *Treatise on Thermodynamics*, reprint ed. (Dover Publications Inc, 2010).
- [67] S. Carnot, *Reflections on the Motive Power of Fire* (Bachelier, 1824).
- [68] R. Clausius, *Philos. Mag.* **2**, 1 (1851).
- [69] R. Clausius, *Philos. Mag.* **2**, 102 (1851).
- [70] R. Clausius, *Philos. Mag.* **12**, 81 (1856).
- [71] W. Thomson, *Trans. R. Soc. Edinb.* **21**, 123 (1857).
- [72] R. Clausius, *The Mechanical Theory of Heat* (Macmillan, 1879).
- [73] T. Matsubara, *Prog. Theor. Phys.* **14**, 351 (1995).
- [74] R. Alicki, *J. Phys. A: Math. Gen.* **12**, L103 (1979).
- [75] N. N. Bogolubov and N. N. Bogolubov, Jr., *Introduction to Quantum Statistical Mechanics*, 2nd ed. (World Scientific Publishing Company, 2010).
- [76] S. Vinjanampathy and J. Anders, *Contemp. Phys.* **57**, 545 (2016).
- [77] F. Binder, L. A. Correa, C. Gogolin, J. Anders, and G. Adesso, *Thermodynamics in the Quantum Regime*, 1st ed. (Springer, 2018).
- [78] S. Deffner and S. Campbell, *Quantum Thermodynamics*, 1st ed. (Morgan & Claypool Publishers, 2019).
- [79] S. R. de Groot and P. Mazur, *Non-equilibrium Thermodynamics*, new ed. (Dover Publications Inc., 2011).
- [80] I. Prigogine, *Non-equilibrium Statistical Mechanics*, illus. ed. (Dover Publications Inc., 2017).
- [81] H. J. Kreuzer, *Nonequilibrium Thermodynamics and its Statistical Foundations*, new ed. (Oxford University Press, 1983).
- [82] M. Toda, R. Kubo, and N. Saitô, *Statistical Physics I: Equilibrium Statistical Mechanics*, 2nd ed. (Springer, 2012).
- [83] R. Kubo, M. Toda, and N. Hashitsume, *Statistical Physics II: Nonequilibrium Statistical Mechanics*, 2nd ed. (Springer, 2012).
- [84] R. Zwanzig, *Nonequilibrium Statistical Mechanics*, illust. ed. (Oxford University Press, 2001).
- [85] A. Fick, *Ann. Phys.* **170**, 59 (1855).
- [86] A. Fick, *Lond. Edinb. Dublin Philos. Mag. J. Sci.* **10**, 30 (1855).
- [87] J. Weber, *Phys. Rev.* **101**, 1620 (1956).

-
- [88] R. Kubo, *Rep. Prog. Phys.* **29**, 255 (1966).
- [89] D. Chandler, *Introduction to Modern Statistical Mechanics* (Oxford University Press, Oxford, UK, 1987).
- [90] W. Sutherland, *Lond. Edinb. Dublin Philos. Mag. J. Sci.* **9**, 781 (1905).
- [91] A. Einstein, *Ann. Phys.* **322**, 549 (1905).
- [92] M. v. Smoluchowski, *Ann. Phys.* **326**, 756 (1906).
- [93] J. B. Johnson, *Phys. Rev.* **32**, 97 (1928).
- [94] H. Nyquist, *Phys. Rev.* **32**, 110 (1928).
- [95] H. B. Callen and T. A. Welton, *Phys. Rev.* **83**, 34 (1951).
- [96] M. S. Green, *J. Chem. Phys.* **20**, 1281 (1952).
- [97] M. S. Green, *J. Chem. Phys.* **22**, 398 (1954).
- [98] R. Kubo, *J. Phys. Soc. Jap.* **12**, 570 (1957).
- [99] L. Onsager, *Phys. Rev.* **37**, 405 (1931).
- [100] L. Onsager, *Phys. Rev.* **38**, 2265 (1931).
- [101] H. B. G. Casimir, *Rev. Mod. Phys.* **17**, 343 (1945).
- [102] D. J. Searles and D. J. Evans, *J. Chem. Phys.* **112**, 9727 (2000).
- [103] D. J. Evans, D. J. Searles, and S. R. Williams, *J. Chem. Phys.* **128**, 014504 (2008).
- [104] D. J. Evans, E. G. D. Cohen, and G. P. Morriss, *Phys. Rev. Lett.* **71**, 2401 (1993).
- [105] G. Gallavotti and E. G. D. Cohen, *Phys. Rev. Lett.* **74**, 2694 (1995).
- [106] D. J. Evans and D. J. Searles, *Adv. Phys.* **51**, 1529 (2002).
- [107] D. J. Evans and D. J. Searles, *Phys. Rev. E* **53**, 5808 (1996).
- [108] C. Jarzynski, *Phys. Rev. Lett.* **78**, 2690 (1997).
- [109] C. Jarzynski, *Phys. Rev. E* **56**, 5018 (1997).
- [110] G. E. Crooks, *Phys. Rev. E* **60**, 2721 (1999).
- [111] P. Vladimirov, *Nonequilibrium statistical mechanics in one dimension* (Cambridge University Press, 1997).
- [112] T. Giamarchi, *Quantum physics in one dimension* (Clarendon Press, 2003).
- [113] E. H. Lieb and D. C. Mattis, *Mathematical physics in one dimension: exactly solvable models of interacting particles* (Academic Press, 2013).

-
- [114] M. Cramer, J. Eisert, M. B. Plenio, Plenio, and J. Dreißig, [Phys. Rev. A](#) **73**, 012309 (2006).
- [115] M. B. Hastings, [J. Stat. Mech.: Theory Exp.](#) **2007**, p08024.
- [116] M. M. Wolf, F. Verstraete, M. B. Hastings, and J. I. Cirac, [Phys. Rev. Lett.](#) **100**, 070502 (2008).
- [117] F. Verstraete, V. Murg, and J. I. Cirac, [Adv. Phys.](#) **57**, 143 (2008).
- [118] M. C. Bañuls, M. B. Hastings, F. Verstraete, and J. I. Cirac, [Phys. Rev. Lett.](#) **102**, 240603 (2009).
- [119] U. Schollwöck, [Ann. Phys.](#) **326**, 96 (2011).
- [120] R. Orús, [Ann. Phys.](#) **349**, 117 (2014).
- [121] J. Cui, J. I. Cirac, and M. C. Bañuls, [Phys. Rev. Lett.](#) **114**, 220601 (2015).
- [122] S. Paeckel, T. Köhler, A. Swoboda, S. R. Manmana, U. Schollwöck, and C. Hubig, [Ann. Phys.](#) **411**, 167998 (2019).
- [123] J. I. Cirac, D. Pérez-García, N. Schuch, and F. Verstraete, [Rev. Mod. Phys.](#) **93**, 045003 (2021).
- [124] M. C. Bañuls, [Tensor network algorithms: a route map](#) (2022), [arXiv:2205.10345](#) .
- [125] R. J. Baxter, *Exactly Solved Models in Statistical Mechanics* (Elsevier, 1989).
- [126] M. Takahashi, *Thermodynamics of One-Dimensional Solvable Models* (Cambridge University Press, 1999).
- [127] N. J. Zabusky and M. D. Kruskal, [Phys. Rev. Lett.](#) **15**, 240 (1965).
- [128] E. Fermi, J. Pasta, S. Ulam, and M. Tsingou, *Studies of non-linear problems*, Technical Report (Los Alamos National Labs, Los Alamos, NM, United States, 1955).
- [129] C. S. Gardner, J. M. Greene, M. D. Kruskal, and R. M. Miura, [Phys. Rev. Lett](#) **19**, 1095 (1967).
- [130] A. Shabat and V. Zakharov, [Sov. Phys. J. Exp. Theor. Phys.](#) **34**, 62 (1972).
- [131] A. B. Zamolodchikov and A. B. Zamolodchikov, [Nucl. Phys. B](#) **133**, 525 (1978).
- [132] L. D. Faddeev and V. E. Korepin, [Phys. Rep.](#) **42**, 1 (1978).
- [133] M. Toda, [J. Phys. Soc. Jpn](#) **22**, 431 (1967).
- [134] M. Toda, *Theory of Nonlinear Lattices* (Springer, 1989).

- [135] W. Heisenberg, *Z. Physik* **49**, 619 (1928).
- [136] H. Bethe, *Z. Physik* **71**, 205 (1931).
- [137] R. L. Orbach, *Pys. Rev.* **112**, 309 (1958).
- [138] E. H. Lieb and W. Liniger, *Phys. Rev.* **130**, 1605 (1963).
- [139] E. H. Lieb, *Phys. Rev.* **130**, 1616 (1963).
- [140] E. H. Lieb and F.-Y. Wu, *Phys. Rev. Lett.* **20**, 1445 (1968).
- [141] C. N. Yang and C. P., *J. Math. Phys.* **10**, 1115 (1969).
- [142] P. Calabrese, F. H. L. Essler, and G. Mussardo, *J. Stat. Mech.: Theory Exp.* **2016**, 064001.
- [143] L. D. Faddeev, *J. Sov. Math.* **5**, 334 (1976).
- [144] L. A. Takhtadzhan and L. D. Faddeev, *Russ. Math. Surv.* **34**, 11 (1979).
- [145] E. K. Sklyanin, L. A. Takhtadzhan, and L. D. Faddeev, *Theor. Math. Phys.* **40**, 688 (1979).
- [146] P. P. Kulish and E. K. Sklyanin, *Phys. Lett. A* **70**, 461 (1979).
- [147] L. D. Faddeev, *Acta Appl. Math.* **39**, 69 (1995).
- [148] L. D. Faddeev, *Int. J. Mod. Phys. A* **10**, 1845 (1995).
- [149] L. D. Faddeev, *How algebraic Bethe ansatz works for integrable model* (1996), [arXiv:hep-th/9605187](https://arxiv.org/abs/hep-th/9605187) .
- [150] L. E. Reichl, *A Modern Course in Statistical Physics*, 4th ed. (Wiley, 2016).
- [151] M. Rigol, V. Dunjko, V. Yurovsky, and M. Olshanii, *Phys. Rev. Lett.* **98**, 050405 (2007).
- [152] J. Eisert, M. Friesdorf, and C. Gogolin, *Nature Physics* **11**, 124 (2015).
- [153] T. Langen, S. Erne, R. Geiger, B. Rauer, T. Schweigler, M. Kuhnert, W. Rohringer, I. E. Mazets, T. Gasenzer, and J. Schmiedmayer, *Science* **348**, 207 (2015).
- [154] F. H. L. Essler and M. Fagotti, *J. Stat. Mech.: Theory Exp.* **2016**, 064002.
- [155] L. Vidmar and M. Rigol, *J. Stat. Mech.: Theory Exp.* **2016**, 064007.
- [156] E. Ilievski, M. Medenjak, and T. Prosen, *Phys. Rev. Lett.* **115**, 120601 (2015).
- [157] E. Ilievski, J. De Nardis, B. Wouters, J.-S. Caux, F. H. L. Essler, and T. Prosen, *Phys. Rev. Lett.* **115**, 157201 (2015).

- [158] R. Vassuer and J. E. Moore, *J. Stat. Mech.: Theory Exp.* **2016**, 064010.
- [159] P. Calabrese, *SciPost Phys. Lect. Notes* , 20 (2020).
- [160] F. Göhmann, *SciPost Phys. Lect. Notes* , 16 (2020).
- [161] D. Chen, M. White, C. Borries, and B. DeMarco, *Phys. Rev. Lett.* **106**, 235304 (2011).
- [162] F. Meinert, M. J. Mark, E. Kirilov, K. Lauber, P. Weinmann, A. J. Daley, and H.-C. Nägerl, *Phys. Rev. Lett.* **111**, 053003 (2013).
- [163] F. Meinert, M. J. Mark, E. Kirilov, K. Lauber, P. Weinmann, M. Gröbner, A. J. Daley, and H.-C. Nägerl, *Science* **344**, 1259 (2014).
- [164] P. Calabrese and J. Cardy, *Phys. Rev. Lett.* **96**, 136801 (2006).
- [165] P. Calabrese, F. H. L. Essler, and M. Fagotti, *Phys. Rev. Lett.* **106**, 227203 (2011).
- [166] P. Calabrese, F. H. L. Essler, and M. Fagotti, *J. Stat. Mech.: Theory Exp.* **2012**, P07016.
- [167] P. Calabrese, F. H. L. Essler, and M. Fagotti, *J. Stat. Mech.: Theory Exp.* **2012**, P07022.
- [168] F. H. L. Essler, S. Evangelisti, and M. Fagotti, *Phys. Rev. Lett.* **109**, 247206 (2012).
- [169] M. Fagotti and F. H. L. Essler, *Phys. Rev. B* **87**, 245107 (2013).
- [170] V. Alba and P. Calabrese, *Proc. Nat. Acad. Sci.* **114**, 7947 (2017).
- [171] V. Alba, B. Bertini, M. Fagotti, L. Piroli, and P. Ruggiero, *J. Stat. Mech.: Theory Exp.* **2021**, 114004.
- [172] O. A. Castro-Alvaredo, B. Doyon, and T. Yoshimura, *Phys. Rev. X* **6**, 041065 (2016).
- [173] B. Bertini, M. Collura, J. De Nardis, and M. Fagotti, *Phys. Rev. Lett.* **117**, 207201 (2016).
- [174] C. Gogolin and J. Eisert, *Rep. Prog. Phys.* **79**, 056001 (2016).
- [175] B. Doyon, *Comm. Math. Phys.* **351**, 155 (2017).
- [176] E. Ilievski and J. De Nardis, *Phys. Rev. B* **96**, 081118 (2017).
- [177] B. Doyon, *SciPost Phys.* **5**, 54 (2018).
- [178] A. Bastianello, B. Bertini, B. Doyon, and R. Vasseur, *J. Stat. Mech.: Theory Exp.* **2022**, 014001.
- [179] B. Doyon, *SciPost Phys. Lect. Notes* , 18 (2020).

- [180] H. Touchette, *Phys. Rep.* **478**, 1 (2009).
- [181] H. Cramér, in *Colloque consacré à la théorie des probabilités*, Vol. 736 (Hermann, Paris, 1938) pp. 2–23.
- [182] S. R. S. Varadhan, *Commun. Pure Appl. Math.* **19**, 261 (1966).
- [183] M. D. Donsker and S. R. S. Varadhan, *Commun. Pure App. Math.* **28**, 1 (1975).
- [184] M. D. Donsker and S. R. S. Varadhan, *Commun. Pure App. Math.* **28**, 279 (1975).
- [185] M. D. Donsker and S. R. S. Varadhan, *Commun. Pure App. Math.* **29**, 389 (1976).
- [186] M. D. Donsker and S. R. S. Varadhan, *Commun. Pure App. Math.* **36**, 183 (1983).
- [187] A. D. Wentzell and M. I. Freidlin, *Russ. Math. Surv.* **25**, 1 (1970).
- [188] O. E. Lanford, in *Statistical Mechanics and Mathematical Problems*, Lecture Notes in Physics, Vol. 20, edited by A. Lenard (Springer, Berlin, 1973) pp. 1–113.
- [189] R. S. Ellis, *Entropy, Large Deviations, and Statistical Mechanics* (Springer, New York, 1985).
- [190] Y. Oono, *Prog. Theor. Phys. Suppl.* **99**, 165 (1989).
- [191] R. S. Ellis, *Scand. Actuar. J.* **1995**, 97 (1995).
- [192] R. S. Ellis, *Physica D* **133**, 106 (1999).
- [193] J. G. Papastavridis, *Analytical mechanics: a comprehensive treatise on the dynamics of constrained systems; for engineers, physicists, and mathematicians*, 1st ed. (Oxford University Press, 2002).
- [194] M. E. Fisher, *Phys. Rev.* **124**, 1664 (1961).
- [195] G. Misguich, D. Serban, and V. Pasquier, *Phys. Rev. Lett.* **89**, 137202 (2002).
- [196] L. Balents, *Nature* **464**, 199 (2010).
- [197] R. Moessner and K. S. Raman, in *Introduction to Frustrated Magnetism: Materials, Experiments, Theory*, Springer Series in Solid-State Sciences, Vol. 164, edited by C. Lacroix, P. Mendels, and F. Mila (Springer, Berlin, 2011) Chap. 17, pp. 437–479.
- [198] G. H. Fredrickson and H. C. Andersen, *Phys. Rev. Lett.* **53**, 1244 (1984).
- [199] R. G. Palmer, D. L. Stein, E. Abrahams, and P. W. Anderson, *Phys. Rev. Lett.* **53**, 958 (1984).

- [200] G. H. Fredrickson and H. C. Andersen, *J. Chem. Phys.* **83**, 5822 (1985).
- [201] J. Jäckle, *Rep. Prog. Phys.* **49**, 171 (1986).
- [202] G. H. Fredrickson, *Ann. Rev. Phys. Chem.* **39**, 149 (1988).
- [203] J. Jäckle and S. Eisinger, *Z. Physik B Cond. Matt.* **84**, 115 (1991).
- [204] S. Eisinger and J. Jäckle, *J. Stat. Phys.* **73**, 643 (1993).
- [205] F. Ritort and P. Sollich, *Adv. Phys.* **52**, 219 (2003).
- [206] C. Toninelli, G. Biroli, and D. S. Fisher, *Phys. Rev. Lett.* **92**, 185504 (2004).
- [207] S. Whitelam, L. Berthier, and J. P. Garrahan, *Phys. Rev. E* **71**, 026128 (2005).
- [208] A. C. Pan, J. P. Garrahan, and D. Chandler, *Phys. Rev. E* **72**, 041106 (2005).
- [209] R. L. Jack, J. P. Garrahan, and D. Chandler, *J. Chem. Phys.* **125**, 184509 (2006).
- [210] J. P. Garrahan, R. L. Jack, V. Lecomte, E. Pitard, K. van Duijvendijk, and F. van Wijland, *Phys. Rev. Lett.* **98**, 195702 (2007).
- [211] N. Cancrini, F. Martinelli, C. Roberto, and C. Toninelli, *Probab. Theor. Relat. Fields* **140**, 459 (2008).
- [212] J. P. Garrahan, P. Sollich, and C. Toninelli, in *Dynamical Heterogeneities in Glasses, Colloids, and Granular Media*, International Series of Monographs on Physics, edited by L. Berthier, G. Biroli, J.-P. Bouchaud, L. Cipelletti, and W. van Saarloos (Oxford University Press, 2011) Chap. 10, pp. 341–366.
- [213] I. Lesanovsky and J. P. Garrahan, *Phys. Rev. Lett.* **111**, 215305 (2013).
- [214] J. P. Garrahan, *Physica A: Stat. Mech. Appl.* **504**, 130 (2018).
- [215] M. C. Bañuls and J. P. Garrahan, *Phys. Rev. Lett.* **123**, 200601 (2019).
- [216] S. F. Swallen, P. A. Bonvallet, R. J. McMahon, and M. D. Ediger, *Phys. Rev. Lett.* **90**, 015901 (2003).
- [217] M. van Horssen, E. Levi, and J. P. Garrahan, *Phys. Rev. B* **92**, 100305 (2015).
- [218] Z. Lan, M. van Horssen, S. Powell, and J. P. Garrahan, *Phys. Rev. Lett.* **121**, 040603 (2018).
- [219] C. J. Turner, A. A. Michailidis, D. A. Abanin, M. Serbyn, and Z. Papić, *Nature Physics* **14**, 745 (2018).

- [220] C. J. Turner, A. A. Michailidis, D. A. Abanin, M. Serbyn, and Z. Papić, *Phys. Rev. B* **98**, 155134 (2018).
- [221] W. W. Ho, S. Choi, H. Pichler, and M. D. Lukin, *Phys. Rev. Lett.* **122**, 040603 (2019).
- [222] T. Cristina and G. Biroli, *J. Stat. Phys.* **130**, 83 (2008).
- [223] B. Derrida, *Phys. Rep.* **301**, 65 (1998).
- [224] B. Derrida, E. Domany, and D. Mukamel, *J. Stat. Phys.* **69**, 667 (1992).
- [225] G. M. Schütz and E. Domany, *J. Stat. Phys.* **72**, 277 (1993).
- [226] B. Derrida, M. R. Evans, V. Hakim, and V. Pasquier, *J. Phys.: Math. Gen.* **26**, 1493 (1993).
- [227] B. Derrida, S. A. Janowsky, J. L. Lebowitz, and E. R. Speer, *J. Stat. Phys.* **73**, 813 (1993).
- [228] B. Derrida, M. R. Evans, and D. Mukamel, *J. Phys. A: Math. Gen.* **26**, 4911 (1993).
- [229] M. R. Evans, D. P. Foster, C. Godrèche, and D. Mukamel, *J. Stat. Phys.* **80**, 69 (1995).
- [230] G. M. Schütz, *J. Stat. Phys.* **88**, 427 (1997).
- [231] B. Derrida and J. L. Lebowitz, *Phys. Rev. Lett.* **80**, 209 (1998).
- [232] J. de Gier and F. H. L. Essler, *Phys. Rev. Lett.* **95**, 240601 (2005).
- [233] J. de Gier and F. H. L. Essler, *J. Stat. Mech.: Theory Exp.* **2006**, P12011.
- [234] M. Schulz and S. Trimper, *Int. J. Mod. Phys. B* **11**, 2927 (1997).
- [235] O. Blondel, N. Cancrini, F. Martinelli, C. Roberto, and C. Toninelli, *Fredrickson-Andersen one spin facilitated model out of equilibrium* (2012), [arXiv:1205.4584](https://arxiv.org/abs/1205.4584) .
- [236] R. L. Jack, T. Nemoto, and V. Lecomte, *J. Stat. Mech.: Theory Exp.* **2020**, 053204.
- [237] I. Hartarsky, F. Martinelli, and C. Toninelli, *Fredrickson–Andersen model in two dimensions* (2022), [arXiv:2205.02297](https://arxiv.org/abs/2205.02297) .
- [238] J. von Neumann, in *Cerebral Mechanisms in Behaviour: The Hixon Symposium*, edited by L. A. Jeffress (John Wiley & Sons, 1951) Chap. 1, pp. 1–31.
- [239] J. von Neumann, *Theory of Self-Reproducing Automata* (University of Illinois Press, 1966).
- [240] M. Gardner, *Sci. Am.* **223**, 120 (1970).

- [241] A. Adamatzky, *Game of Life Cellular Automata* (Springer, 2010).
- [242] T. Toffoli and N. Margolus, *Cellular Automata Machines: A New Environment for Modeling* (MIT Press, 1987).
- [243] S. Wolfram, *Rev. Mod. Phys.* **55**, 601 (1983).
- [244] S. Wolfram, *Cellular Automata and Complexity* (CRC Press, 1994).
- [245] S. Wolfram, *A New Kind of Science* (Wolfram Media, 2002).
- [246] P. Kos, B. Bertini, and T. Prosen, *Phys. Rev. X* **11**, 011022 (2021).
- [247] A. Chan, A. De Luca, and J. T. Chalker, *Phys. Rev. Lett.* **121**, 060601 (2018).
- [248] A. J. Friedman, A. Chan, A. De Luca, and J. T. Chalker, *Phys. Rev. Lett.* **123**, 210603 (2019).
- [249] B. Skinner, J. Ruhman, and A. Nahum, *Phys. Rev. X* **9**, 031009 (2019).
- [250] A. Zabalo, M. J. Gullans, J. H. Wilson, S. Gopalakrishnan, D. A. Huse, and J. H. Pixley, *Phys. Rev. B* **101**, 060301 (2020).
- [251] Y. Bao, S. Choi, and E. Altman, *Phys. Rev. B* **101**, 104301 (2020).
- [252] S. Choi, Y. Bao, X.-L. Qi, and E. Altman, *Phys. Rev. Lett.* **125**, 030505 (2020).
- [253] P. Kos, B. Bertini, and T. Prosen, *Phys. Rev. Lett.* **126**, 190601 (2021).
- [254] T. Rakovszky, F. Pollman, and C. W. von Keyserlingk, *Phys. Rev. Lett.* **122**, 250602 (2019).
- [255] B. Bertini, P. Kos, and T. Prosen, *Phys. Rev. X* **9**, 021033 (2019).
- [256] S. Gopalakrishnan and A. Lamacraft, *Phys. Rev. B* **100**, 064309 (2019).
- [257] B. Bertini, P. Kos, and T. Prosen, *SciPost Phys.* **8**, 67 (2020).
- [258] B. Bertini, P. Kos, and T. Prosen, *SciPost Phys.* **8**, 68 (2020).
- [259] B. Bertini and L. Piroli, *Phys. Rev. B* **102**, 064305 (2020).
- [260] L. Piroli, B. Bertini, J. I. Cirac, and T. Prosen, *Phys. Rev. B* **101**, 094304 (2020).
- [261] H. F. Trotter, *Proc. Am. Math. Soc.* **10**, 545 (1959).
- [262] M. Suzuki, *Commun. Math. Phys.* **51**, 183 (1976).
- [263] M. Suzuki, *Prog. Theor. Phys.* **56**, 1454 (1976).
- [264] M. Suzuki, *Commun. Math. Phys.* **57**, 193 (1977).
- [265] M. Suzuki, *J. Math. Phys.* **26**, 601 (1985).

- [266] G. Vidal, *Phys. Rev. Lett.* **91**, 147902 (2003).
- [267] F. Verstraete, J. J. García-Ripoll, and J. I. Cirac, *Phys. Rev. Lett.* **93**, 207204 (2004).
- [268] G. Vidal, *Phys. Rev. Lett.* **93**, 040502 (2004).
- [269] M. Zwolak and G. Vidal, *Phys. Rev. Lett.* **93**, 207205 (2004).
- [270] N. Hatano and M. Suzuki, in *Quantum Annealing and Other Optimization Methods*, edited by A. Das and B. K. Chakrabarti (Springer, 2005) pp. 37–68.
- [271] A. Klümper, *Z. Phys., B Condens. Matter* **91**, 507 (1993).
- [272] A. Klümper, in *Quantum Magnetism*, edited by U. Schollwöck, J. Richter, D. J. J. Farnell, and R. F. Bishop (Springer, 2008) pp. 349–379.
- [273] F. Göhmann, M. Karbach, A. Klümper, K. K. Kozłowski, and J. Suzuki, *J. Stat. Mech.: Theor. Exp.* **2017**, 113106 (2017).
- [274] M. Vanicat, L. Zadnik, and T. Prosen, *Phys. Rev. Lett.* **121**, 030606 (2018).
- [275] C. S. Lent, P. D. Tougaw, W. Porod, and G. H. Bernstein, *Nanotechnology* **4**, 49 (1993).
- [276] K. Wiesner, in *Encyclopedia of Complexity and Systems Science*, edited by R. A. Meyers (Springer, 2009) pp. 7154–7164.
- [277] J. I. Cirac, D. Pérez-García, N. Schuch, and F. Verstraete, *J. Stat. Mech.: Theor. Exp.* **2017**, 083105 (2017).
- [278] S. Gopalakrishnan, D. A. Huse, V. Khemani, and R. Vasseur, *Phys. Rev. B* **98**, 220303 (2018).
- [279] P. Arrighi, *Nat. Comput.* **18**, 885 (2019).
- [280] I. Lesanovsky, K. Macieszczak, and J. P. Garrahan, *Quantum Sci. Technol.* **4**, 02LT02 (2019).
- [281] T. M. Wintermantel, Y. Wang, G. Lochead, S. Shevate, G. K. Brennen, and S. Whitlock, *Phys. Rev. Lett.* **124**, 070503 (2020).
- [282] L. Piroli and J. I. Cirac, *Phys. Rev. Lett.* **125**, 190402 (2020).
- [283] E. Gillman, F. Carollo, and I. Lesanovsky, *Phys. Rev. Lett.* **125**, 100403 (2020).
- [284] T. Iadecola and S. Vijay, *Phys. Rev. B* **102**, 180302 (2020).
- [285] T. Farrelly, *Quantum* **4**, 368 (2020).

- [286] E. Gillman, F. Carollo, and I. Lesanovsky, *Phys. Rev. Lett.* **127**, 230502 (2021).
- [287] J. I. Cirac and P. Zoller, *Phys. Rev. Lett.* **74**, 4091 (1995).
- [288] L.-M. Duan, J. I. Cirac, and P. Zoller, *Science* **292**, 1695 (2001).
- [289] D. Leibfried, R. Blatt, C. Monroe, and D. Wineland, *Rev. Mod. Phys.* **75**, 281 (2003).
- [290] D. Porras and J. I. Cirac, *Phys. Rev. Lett.* **92**, 207901 (2004).
- [291] H. Häffner, C. F. Roos, and R. Blatt, *Phys. Rep.* **469**, 155 (2008).
- [292] N. Syassen, D. M. Bauer, M. Lettner, T. Volz, D. Dietze, J. J. García-Ripoll, J. I. Cirac, G. Rempe, and S. Dürr, *Science* **320**, 1329 (2008).
- [293] I. Bloch, J. Dalibard, and W. Zwerger, *Rev. Mod. Phys.* **80**, 885 (2008).
- [294] C. Chin, R. Grimm, P. Julienne, and E. Tiesinga, *Rev. Mod. Phys.* **82**, 1225 (2010).
- [295] C.-C. Chien, S. Peotta, and M. Di Ventra, *Nat. Phys.* **11**, 998 (2015).
- [296] J. G. Bohnet, B. C. Sawyer, J. W. Britton, M. L. Wall, A. M. Rey, M. Foss-Feig, and J. J. Bollinger, *Science* **352**, 1297 (2016).
- [297] I. Buluta and F. Nori, *Science* **326**, 108 (2009).
- [298] K. Kim, M.-S. Chang, S. Korenblit, R. Islam, E. E. Edwards, J. K. Freericks, G.-D. Lin, L.-M. Duan, and C. Monroe, *Nature* **465**, 590 (2010).
- [299] J. T. Barreiro, M. Müller, P. Schindler, D. Nigg, T. Monz, M. Chwalla, M. Hennrich, C. F. Roos, P. Zoller, and R. Blatt, *Nature* **470**, 486 (2011).
- [300] I. Bloch, J. Dalibard, and S. Nascimbene, *Nat. Phys.* **8**, 267 (2012).
- [301] R. Blatt and C. F. Roos, *Nat. Phys.* **8**, 277 (2012).
- [302] I. M. Georgescu, S. Ashhab, and F. Nori, *Rev. Mod. Phys.* **86**, 153 (2014).
- [303] H. Weimer, R. Löw, T. Pfau, and H. P. Büchler, *Phys. Rev. Lett.* **101**, 250601 (2008).
- [304] R. Löw, H. Weimer, J. Nipper, J. B. Balewski, B. Butscher, H. P. Büchler, and T. Pfau, *J. Phys. B: At. Mol. Opt.* **45**, 113001 (2012).
- [305] I. Lesanovsky and J. P. Garrahan, *Phys. Rev. A* **90**, 011603 (2014).
- [306] M. Marcuzzi, E. Levi, S. Diehl, J. P. Garrahan, and I. Lesanovsky, *Phys. Rev. Lett.* **113**, 210401 (2014).
- [307] H. Bernien, S. Schwartz, A. Keesling, H. Levine, A. Omran, H. Pichler, S. Choi, A. S. Zibrov, M. Endres, M. Greiner, V. Vuletić, and M. D. Lukin, *Nature* **551**, 579 (2017).

- [308] R. Gutiérrez, C. Simonelli, M. Archimi, F. Castellucci, E. Arimondo, C. Donatella, M. Marcuzzi, I. Lesanovsky, and O. Morsch, [Phys. Rev. A **96**, 041602 \(2017\)](#).
- [309] V. Lienhard, S. de Léséleuc, D. Barredo, T. Lahaye, A. Browaeys, M. Schuler, L.-P. Henry, and A. M. Läuchli, [Phys. Rev. X **8**, 021070 \(2018\)](#).
- [310] C. G. Wade, M. Marcuzzi, E. Levi, J. M. Kondo, I. Lesanovsky, C. S. Adams, and K. J. Weatherill, [Nature Communications **9**, 1 \(2018\)](#).
- [311] T. Rakovszky, F. Pollman, and C. W. von Keyserlingk, [Phys. Rev. X **8**, 031058 \(2018\)](#).
- [312] K. Klobas, B. Bertini, and L. Piroli, [Phys. Rev. Lett. **126**, 160602 \(2021\)](#).
- [313] K. Klobas and B. Bertini, [SciPost Phys. **11**, 106 \(2021\)](#).
- [314] I. Lesanovsky, [Phys. Rev. Lett. **106**, 025301 \(2011\)](#).
- [315] C. Sünderhauf, D. Pérez-García, D. A. Huse, N. Schuch, and J. I. Cirac, [Phys. Rev. B **98**, 134204 \(2018\)](#).
- [316] S. Pai, M. Pretko, and R. M. Nandkishore, [Phys. Rev. X **9**, 021003 \(2019\)](#).
- [317] A. Nahum, J. Ruhman, S. Vijay, and J. Haah, [Phys. Rev. X **7**, 031016 \(2017\)](#).
- [318] S. Gopalakrishnan, [Phys. Rev. B **98**, 060302 \(2018\)](#).
- [319] C. W. von Keyserlingk, T. Rakovszky, F. Pollman, and S. L. Sondhi, [Phys. Rev. X **8**, 021013 \(2018\)](#).
- [320] K. Klobas and B. Bertini, [SciPost Phys. **11**, 107 \(2021\)](#).
- [321] A. Nahum, S. Vijay, and J. Haah, [Phys. Rev. X **8**, 021014 \(2018\)](#).
- [322] V. Khemani, A. Vishwanath, and D. A. Huse, [Phys. Rev. X **8**, 031057 \(2018\)](#).
- [323] V. Alba, J. Dubail, and M. Medenjak, [Phys. Rev. Lett. **122**, 250603 \(2019\)](#).
- [324] V. Alba, [Phys. Rev. B **104**, 094410 \(2021\)](#).
- [325] S. Gopalakrishnan and B. Zakirov, [Quantum Sci. Technol. **3**, 044004 \(2018\)](#).
- [326] N. Pancotti, G. Giudice, J. I. Cirac, J. P. Garrahan, and M. C. Bañuls, [Phys. Rev. X **10**, 021051 \(2020\)](#).
- [327] B. Bertini, P. Kos, and T. Prosen, [Phys. Rev. Lett. **123**, 210601 \(2019\)](#).
- [328] A. Chan, A. De Luca, and J. T. Chalker, [Phys. Rev. X **8**, 041019 \(2018\)](#).

-
- [329] A. J. Friedman, S. Gopalakrishnan, and R. Vasseur, *Phys. Rev. Lett.* **123**, 170603 (2019).
- [330] B. Pozsgay, *J. Phys. A: Math. Theor.* **54**, 384001 (2021).
- [331] T. Gombor and B. Pozsgay, *Phys. Rev. E* **104**, 054123 (2021).
- [332] T. Gombor and B. Pozsgay, *SciPost Phys.* **12**, 102 (2022).
- [333] A. Bobenko, M. Bordemann, C. Gunn, and U. Pinkall, *Commun. Math. Phys.* **158**, 127 (1993).
- [334] B. Buča, K. Klobas, and T. Prosen, *J. Stat. Mech.: Theory Exp.* **2021**, 074001.
- [335] T. Prosen and C. Mejía-Monasterio, *J. Phys. A: Math. Theor.* **49**, 185003 (2016).
- [336] T. Prosen and B. Buča, *J. Phys. A: Math. Theor.* **50**, 395002 (2017).
- [337] A. Inoue and S. Takesue, *J. Phys. A: Math. Theor.* **51**, 425001 (2018).
- [338] B. Buča, J. P. Garrahan, T. Prosen, and M. Vanicat, *Phys. Rev. E* **100**, 020103 (2019).
- [339] K. Klobas, M. Medenjak, T. Prosen, and M. Vanicat, *Commun. Math. Phys.* **371**, 651 (2019).
- [340] K. Klobas and T. Prosen, *SciPost Phys. Core* **2**, 10 (2020).
- [341] K. Klobas, M. Vanicat, J. P. Garrahan, and T. Prosen, *J. Phys. A: Math. Theor.* **53**, 335001 (2020).
- [342] K. Klobas and T. Prosen, *J. Phys. A: Math. Theor.* **55**, 094003 (2022).
- [343] J. Lopez-Piqueres, S. Gopalakrishnan, and R. Vasseur, *J. Phys. A: Math. Theor.* **55**, 234005 (2022).
- [344] J. W. P. Wilkinson, T. Prosen, and J. P. Garrahan, *Phys. Rev. E* **105**, 034124 (2022).
- [345] J. W. P. Wilkinson, K. Klobas, T. Prosen, and J. P. Garrahan, *Phys. Rev. E* **102**, 062107 (2020).
- [346] T. Gombor and B. Pozsgay, *Integrable deformations of superintegrable quantum circuits* (2022), [arXiv:2205.02038](https://arxiv.org/abs/2205.02038) .
- [347] D. A. Abanin and Z. Papić, *Ann. Phys.* **529**, 1700169 (2017).